THE EFFECTS OF HYPEROSMOTIC CULTURE CONDITIONS ON THE GS-NS0 ANTIBODY PRODUCTION PROCESS: A COMBINED EXPERIMENTAL AND MODELLING STUDY

by

Yingswan HO

October 2006

A thesis submitted in partial fulfillment of the degree of Doctor of Philosophy of the University of London and for the Diploma of Membership of Imperial College

Department of Chemical Engineering and Chemical Technology

Imperial College London

London SW7 2AZ

Abstract

Mammalian cells are widely used today in the large-scale production of recombinant proteins for therapeutic and diagnostic applications. In particular, the Glutamine Synthetase-NS0 (GS-NS0) system under study is an industrially significant cell line that has been used to produce several important therapeutic antibody products currently available in the market. With continually increasing demand for monoclonal antibodies, the study of environmental variables such as culture pH, temperature and medium osmolarity plays a key role in the improvement of antibody production yields. In particular, hyperosmolarity is an economically viable factor that has been previously reported to enhance both specific antibody productivity and overall antibody production in GS-NS0 cells. The central goal of this study is therefore to develop an understanding of the intracellular effects of hyperosmotic conditions on the GS-NS0 antibody production process; so as to improve antibody production yields.

A new 'hybrid' model describing the GS-NS0 antibody production process is first developed using GS-NS0 data available in literature. The model, constructed using both unstructured and structured elements, describes the growth, metabolism and extracellular antibody production characteristics of GS-NS0 cells. A global sensitivity analysis (GSA) of the model is subsequently carried out, leading to the identification of parameters that significantly influenced antibody production rates, including the specific mRNA transcription rates, specific polypeptide translation rates and the mRNA degradation rates, thereby providing part of the basis for the experimental study.

The experimental study on GS-NS0 cells under normal and hyperosmotic conditions is focused on two key areas: firstly, based on the GSA findings, the intracellular behaviour of IgG mRNA and polypeptide chains are analysed. Secondly, to obtain a clearer understanding of the underlying mechanism of hyperosmolarity, the cell cycle trends and energy levels of the cells have also been monitored. Experimental results show that hyperosmotic conditions induce G0/G1 cycle arrest in GS-NS0 cells, but do not increase intracellular energy levels despite an increase in glucose uptake rates. Additionally, estimates of the key parameters identified by GSA are derived successfully from the intracellular mRNA and polypeptide chain analyses. The estimated parameter values also indicate that the enhancement of mRNA specific transcription rates is the key reason for the higher specific antibody productivities observed under hyperosmotic conditions. The hybrid model is subsequently updated by the estimated values of key parameters and is validated by both intracellular and extracellular

experimental data. Finally, the model successfully predicts the optimal hyperosmotic induction time for a biphasic culture (as verified by experimental data), thereby demonstrating its potential applicability in product optimisation strategies.

Acknowledgements

There are a number of people who I must thank for their support and assistance in various forms throughout the course of this work.

Thanks go to my supervisor, Dr Athanasios Mantalaris, for kindly taking me on as his student mid-term through the work, and for his advice and encouragement over the past few years. I am also grateful for the various skills that I have learnt from him, which has helped me become a better researcher.

Special thanks also go to Dr Julie Varley, who started me on this adventure and who generously continued to provide helpful suggestions and intellectual support throughout my project.

The Agency for Science, Technology And Research (ASTAR) in Singapore provided me with the opportunity of studying overseas by sponsoring my Ph.D. studies, for which I am extremely grateful. I would also like to thank my ASTAR mentor, Professor Miranda Yap, for her useful advice and support over the years.

A number of individuals from other departments have provided me with invaluable technical expertise in different areas of my project. These include Dr David Mann from the Biochemistry department, who guided me through the intricacies of Western blotting and generously offered me the use of his equipment, as well as Mr Ian Moss, who taught me the principles of capillary electrophoresis and assisted me in the development of a protocol for intracellular nucleotide measurement. Additionally, I must also thank Dr Mark Smales for providing me with the IgG mRNA probe sequences, Dr Sergei Kucherenko for providing me with the global sensitivity analysis code and Dr Cathy Ye for her kind assistance in flow cytometry.

I have been very fortunate to share my office with a great group of people, who provided many a stimulating lunchtime conversation: Laleh Safinia, Joan Ma, Maya Lim, and Teresa Mortera Blanca, Yunyi Kang, Iliana Fauzi, Siti Ismail and Jae Min Cha. Also, I would like to thank the "cell culture bunch" within our research group: Fabio Sidoli, Mon-Han Wu, Cleo Kontoravdi and Carolyn Lam, for all the fruitful discussions we had and the

helpful comments they provided me with. Special thanks also go to Carolyn, who gave me lots of useful advice in the preparation of this thesis.

I would now like to give a special mention to Dr Robin Kumar, the pioneering member of our group and a veritable "fountain of wisdom". He has been a constant source of support and encouragement through the highs and lows, and I am truly indebted to him for the incredible generosity and patience he has shown me over the years.

I would also like to acknowledge the support of my friends in London, in particular, Wern Sze Teo, Philip See and Victor Lim, for keeping my feet on the ground and providing me with a listening ear whenever I needed one.

Finally and most importantly, my heartfelt gratitude goes to my family – my parents and my brother Ying Chiat, for their unstinting support and belief in me. The completion of this work would not have been possible without their love and encouragement, and I dedicate this thesis to them.

Publications

Conference presentations and journal publications:

Ho, Y. and Varley, J. (2003) Development of an antibody production model for GS-NS0 cells in response to changes in osmotic pressure. *Poster presented at Asia-Pacific Conference on Biochemical Engineering 2003*, Brisbane, Australia.

Ho, Y.; Varley, J.; Mantalaris, A.M. (2006). Antibody production in the GS-NS0 system under normal and hyperosmotic culture conditions: a combined modelling and experimental study. *Oral presentation at 2006 AIChE Annual Meeting*, San Francisco, USA.

Ho, Y.; Varley J. and Mantalaris, A.M. (2006). Development and analysis of a mathematical model for antibody-producing GS-NS0 cells under normal and hyperosmotic culture conditions. *Biotechnol. Prog.* **22**: 1560-1569.

Contents

List of Figures

List of Tables

Chapter 1

Introduction

1.1 Background and motivation

The production of monoclonal antibodies for therapeutic and diagnostic purposes constitutes a significant part of the current biotechnology industry, with worldwide sales projected to reach US$22.5 billion in 2009 [b2b conference flyer., 2004]. Industrial production of monoclonal antibodies is currently carried out mainly in mammalian cell culture systems, including the Chinese Hamster Ovary (CHO), SP2/0, and NS0 cell lines [Chu and Robinson, 2001]. This is due to their ability to carry out complex post-translational modifications and protein folding in an authentic manner [Hauser, 1997], which is essential for retaining the biological activity of the product in contrast to other expression systems, such as bacteria or yeast cells. As a result of this unique characteristic, products in development have been reported to lean towards being mammalian cell culture-based in the near future [Ransohoff et al., 2004], further highlighting their importance in the biopharmaceutical industry.

Among the mammalian cell culture systems used in large-scale antibody production, the Glutamine Synthetase-NS0 (GS-NS0) system, utilised in this study, is an industrially significant cell line that has been used in recent years for the production of many important therapeutic antibodies, including *Synagis*™, *Zenapax*® [Lonza Press Release., 1998a, 1998b] and *Mylotarg*™ [Wyeth Pharmaceuticals Inc., 2005]. One of the key advantages of the GS-NS0 cell system is its ability to synthesise glutamine, an amino acid essential for cell growth,

intracellularly, thus negating the need for an exogenous glutamine supply. The resulting reduction in ammonia accumulation thus alleviates the inhibitory effects of ammonium ions on cell growth and antibody production.

Hyperosmotic culture conditions

The antibody production process in mammalian cells tends to be affected by changes in the environmental conditions of the culture. Such environmental factors include culture pH, temperature and osmolarity. In particular, hyperosmotic culture conditions have been reported to show a significant positive effect on the antibody production rate of GS-NS0 cells [Duncan et al., 1997; Wu et al., 2004]. Being easily induced by the addition of salts such as sodium chloride or potassium chloride also increases the economic potential of its use to improve antibody production rates. However, the reduction in cell growth caused by hyperosmotic pressure often leads to a dilution of its positive effect on antibody productivity. The trade-off between growth and productivity is therefore an important consideration for the implementation of hyperosmotic culture conditions in product optimisation strategies.

Potential advantages of a modelling approach

The continual increase in demand for recombinant therapeutic products has also led to predictions of a shortage in plant manufacturing capacity in the biopharmaceutical industry within the next five years [Ransohoff et al., 2004]. In order to reduce the discrepancy between supply and demand, key aims of the industry are focused on improving efficiency of the antibody production process in mammalian cells, as well as the reduction of the time-to-market [Zhou and Titchener-Hooker, 1999]. At present, cell culture experimentation is the main means of improving antibody production yields industrially. It generally involves trial and error optimisation of culture parameters, which result in large numbers of experiments that tends to be expensive and time-consuming [Jacquez, 1998]. In view of the situation, the utilisation of mathematical models is proposed as a means of presenting preliminary experimental information in a logical and systematic manner, thereby allowing for the identification of any key relationships between process parameters, variables and product output rates [Bailey, 1998]. In-depth analyses of these models can help identify parameters

with significant effects on antibody production that can then be singled out for more detailed studies, thus guiding the design of experiments. This approach would therefore lead to a possible reduction in the required number of experiments with time- and cost-saving implications.

In this study, the effects of hyperosmotic conditions on the GS-NS0 antibody production process will be evaluated through modelling and experimental means. The study involves first developing a mathematical model capable of predicting antibody production in GS-NS0 cells and then conducting an experimental study on cells cultivated under normal and hyperosmotic conditions. The main objectives of the study are outlined in the next section.

1.2 Thesis Objectives

The central goal of this thesis is to undertake a combined experimental and modelling approach in understanding and improving the antibody production process in GS-NS0 cells under normal and hyperosmotic culture conditions. Within the central goal, there are four main objectives. Firstly, a model capable of describing the mechanism of antibody production in GS-NS0 cells is to be developed. Secondly, a global sensitivity analysis is to be carried out on the model in order to identify key parameters affecting the antibody production rate. The third objective is to investigate the intracellular antibody production process through an experimental study on the cells at normal and hyperosmotic culture conditions. Design of the experimental study will be guided by the global sensitivity analysis findings obtained from the second objective. Results derived from the experiments will subsequently be incorporated into the model. Finally, the practical applicability of the model is to be demonstrated by its use in the development of an antibody production optimisation strategy based on the use of hyperosmotic conditions.

1.3 Thesis Outline

In Chapter 2 of this thesis, a review of antibody production in mammalian cells is provided. This includes an overview of the industrially important cell systems used for large-scale therapeutic monoclonal antibody production, a brief introduction to the development process of the GS-NS0 cell line, a detailed description of the antibody production mechanism in GS-NS0 cells, as well as a summary of the findings on the effects of hyperosmotic pressure on various cell culture systems. Pertinent developments in the types of mathematical models used to represent cell growth and antibody production and model analysis techniques will also be discussed in this chapter. In Chapter 3, the mathematical model developed for describing antibody production in GS-NS0 cells and its underlying assumptions is presented. The results obtained from the developed model is compared to existing experimental data and output from a single-cell model originally developed for hybridoma cells. Details of the global sensitivity analysis (GSA) used for in-depth study of the GS-NS0 antibody production model and its subsequent role in extension of the model to hyperosmotic culture conditions are discussed. In Chapters 4 and 5, the experimental study conducted on GS-NS0 cells under both normal and hyperosmotic conditions is described. Chapter 4 will focus on growth, metabolism and antibody production processes in GS-NS0 cells under both osmotic conditions. The chapter also includes a study of the cell cycle and cellular energy trends for normal and hyperosmotic cultures. Based on the findings of GSA, transcription and translation processes are identified as being key to antibody production. Chapter 5 will therefore describe the behaviour of mRNA molecules and intracellular IgG polypeptide concentrations with respect to culture time and medium osmolarity. Chapter 6 consists of the incorporation of the experimental findings into the antibody production model. The incorporated model is then used to develop a strategy involving the use of hyperosmotic culture conditions, based on the trade-off between decreased cell growth and increased antibody productivity. The proposed strategy is then assessed through experimental validation. Finally, the conclusions obtained from this study and recommendations of potential areas for future research in this field are summarised in Chapter 7.

Chapter 2

Literature Review

The major role that mammalian cell systems play in the industrial production of monoclonal antibodies today has been highlighted in Chapter 1. In this chapter, an overview of the different mammalian cell systems currently used for recombinant antibody production industrially will first be given, with particular focus on the GS-NS0 cell system (Section 2.1). Additionally, in order to improve antibody production yields in mammalian cells, having an insight to the antibody production mechanism within these cells is also an important consideration. Section 2.2 will therefore provide a detailed description of the intracellular antibody production pathway, as well as a discussion of the observations and results derived from literature about each individual step in the pathway. Section 2.3 summarises briefly the main product optimisation approaches currently employed before focusing specifically on the reported effects of hyperosmolarity on cell growth, metabolism and antibody production in various mammalian cell culture systems. Finally, Section 2.4 includes a review on the major cell culture models that currently exist in literature and a brief discussion on the relevant analysis techniques adopted to study them in more detail.

2.1 Industrial monoclonal antibody production – mammalian cell culture systems

Three principal mammalian cell lines are currently being used for the production of nearly all commercially available recombinant monoclonal antibody products: CHO and the myeloma cell lines: SP2/0 and NS0 [Chu and Robinson, 2001]. This is evident from Table 2.1, which

summarises the Food and Drug Administration (FDA) and European Union (EU) approved therapeutic monoclonal antibody products as of 2005 [Reichert et al., 2005]. In particular, the NS0 cell line, transfected with the glutamine-synthetase (GS) gene has been used to produce a number of recent antibody therapeutic products (*Synagis*™, *Zenapax*® [Lonza Press Release., 1998a, 1998b] and *Mylotarg*™ [Wyeth Pharmaceuticals Inc., 2005]), highlighting its importance in the biopharmaceutical industry.

2.1.1 The GS-NS0 cell system

Development of the NS0 expression system

A detailed description of how the NS0 cell line was derived can be found in Barnes et al. [2000]. This section provides a brief summary of the NS0 developmental process. The development of the NS0 cell line began in 1962 with the discovery that injection of mineral oil into BALB/c mice induced tumours [Potter and Boyce, 1962]. It was found that one of the tumours, MOPC21, secreted IgG1 [Potter et al., 1965], which became the basis for the establishment of a continuous tissue culture line by Horibata and Harris [1970]. After a series of transplantations in mice, the cells were grown *in vitro* in suspension cultures and known as P3K cells [Barnes et al., 2000]. Subsequent cloning and re-cloning of these cells resulted in two cell lines which were then further developed. One of the cell lines, termed 289-16, only synthesised light antibody chains [Ramasamy et al., 1974], and was subsequently renamed NSI/1 [Cowan et al., 1974]. The cells were further cloned and selected for resistance to 8-azaguanine. The resultant cell line, P3/NSI/1-Ag4-1, only expressed intracellular κ light chains [Kohler and Milstein, 1976]. Finally, the cells were cloned again to generate a sub-line known as NS0/1 (Non-Secreting), which did not secrete or produce any heavy or light Ig chains naturally [Galfre and Milstein, 1981]. This cell line was able to produce Ig molecules only when the desired foreign Ig genes were transfected into the cell. Hence, the desired Ig product would be the only Ig species present in the extracellular medium.

Due to their origins as immunoglobulin-producing tumour cells, NS0 cells have a high efficiency in the production and secretion of proteins. In addition, NS0 cells are grown in suspension cultures, hence making the adaptation process from serum to serum-free, and

subsequently protein-free medium much easier. This is particularly crucial in large-scale antibody production, as it reduces both the costs of the downstream purification process and of the growth medium [Barnes et al., 2000].

Product	Brand Name	Cell Line	Year Approved
Abciximab	ReoPro	SP2/0	1994
Adalimumab*	Humira	Unspecified	2002
Alemtuzumab*	Campath-1H	CHO	2001
Basiliximab	Simulect	Myeloma	1998
Bevacizumab*	Avastin	CHO	2004
Cetuximab	Erbitux	Myeloma	2004
Daclizumab*	Zenapax	GS-NS0	1997
Efalizumab	Raptiva	CHO	2003
Gemtuzumab ozogamicin*	Mylotarg	GS-NS0	2000
Ibritumomab tiuxetan*	Zevalin	CHO	2002
Infliximab	Remicade	SP2/0	1998
Muromonab-CR3*	Orthoclone OKT3	Ascites	1986
Omalizumab*	Xolair	CHO	2003
Palivizumab	Synagis	GS-NS0	1998
Rituximab	Rituxan	CHO	1997
Tositumomab*	Bexxar	Unspecified	2003
Trastuzumab	Herceptin	CHO	1998

Table 2.1. List of FDA and EU-approved therapeutic monoclonal antibody products as of 2005. (Adapted from Reichert et al., 2005 with additional information from the FDA website, 2006 and drug prescription sheets of products with (*) in table)

Glutamine and glutamine-synthetase (GS)

Glutamine is an amino acid whose cellular metabolism and function is crucial to mammalian cells. It participates in a significant number of metabolic pathways, including protein synthesis, purine and pyrimidine biosynthesis, ammonia formation, the biosynthesis and degradation of amino acids, amino sugars and certain co-factors [Barnes et al., 2000]. In addition, glutamine has been reported to be a source of energy for mammalian cells [Reitzer et al., 1979]. *In vivo*, glutamine is synthesised by a large number of cells that contain the enzyme glutamine synthetase (GS). GS catalyses the reversible synthesis of glutamine from glutamate and ammonia, in a reaction that requires the hydrolysis of ATP [Elliott, 1951]. However, most mammalian cells *in vitro* contain extremely low levels of endogenous GS, which results in their inability to produce glutamine [Barnes et al., 2000]. As a result, glutamine has to be added to the culture medium for cell growth to occur, hence causing the production and accumulation of ammonia in the culture. Free ammonium ions formed during the catabolic breakdown of glutamine can inhibit growth and production of cell cultures [Butler and Spier, 1984], often resulting in lower antibody productivity.

Principles of the GS-NS0 system

As explained previously, mammalian cells in culture require an exogenous source of glutamine or exogenous GS in order to survive. However, by incorporating a GS gene in a plasmid vector containing the gene of a heterologous protein (usually the desired antibody product), and subsequent transfection into the NS0 cells, the need for an external glutamine source can be eliminated. The selection of cells which have successfully taken up the plasmid and are stably expressing the GS gene (and thus also the heterologous protein) can be made in glutamine-free medium, as only cells with the GS gene will be able to survive [Barnes et al., 2000]. The growth of GS-NS0 cells in glutamine-free medium results in a much lower accumulation of free ammonia, as shown by Zhou et al. [1997]. In addition, a recent report has indicated that GS-NS0 systems can produce up to 5.1 g/L of total monoclonal antibody product [Birch, 2005], making it one of the more prominent systems for the large-scale production of recombinant antibodies at present. As the number of studies into this cell line are relatively limited in comparison to other cell systems such as hybridoma and CHO systems, more insight into the GS-NS0 system will contribute towards an overall better understanding of the antibody production mechanism, as well as provide useful information which may lead to a better optimised production process.

2.2 Antibody Production in Mammalian Cells

2.2.1 The Antibody Production Pathway

In mammalian cells, the antibody production process consists of two main parts: synthesis of the antibody molecule in the endoplasmic reticulum (ER), and its transport to the extracellular medium. Antibody synthesis in mammalian cells takes place mainly in the ER. The process begins in the nucleus, where the DNA sequences for the heavy (H) and light (L) IgG polypeptide species are transcribed onto messenger RNA (mRNA). The correctly transcribed mRNA will be translated in association with membrane-bound polyribosomes in the rough ER [Bibila and Flickinger, 1991a]. The growing polypeptide chain is co-translationally translocated via a protein translocation channel across the ER [Sakaguchi, 1997]. Initial glycosylation of the polypeptide chain occurs, where a number of oligosaccharides are covalently attached to the polypeptide. Further modifications of these oligosaccharides take place subsequently. The polypeptide chains are then folded and the assembly of the antibody molecule, consisting of two identical H and L chains follows. This process is shown schematically in Figure 2.1.

Subsequently, only correctly assembled antibody molecules are transported out of the ER and into the Golgi complex, where further glycosylation reactions take place. These reactions convert the molecules into functional proteins [Savage, 1997]. The functional antibodies are finally packed into secretory vesicles and secreted to the extracellular medium (Figure 2.2).

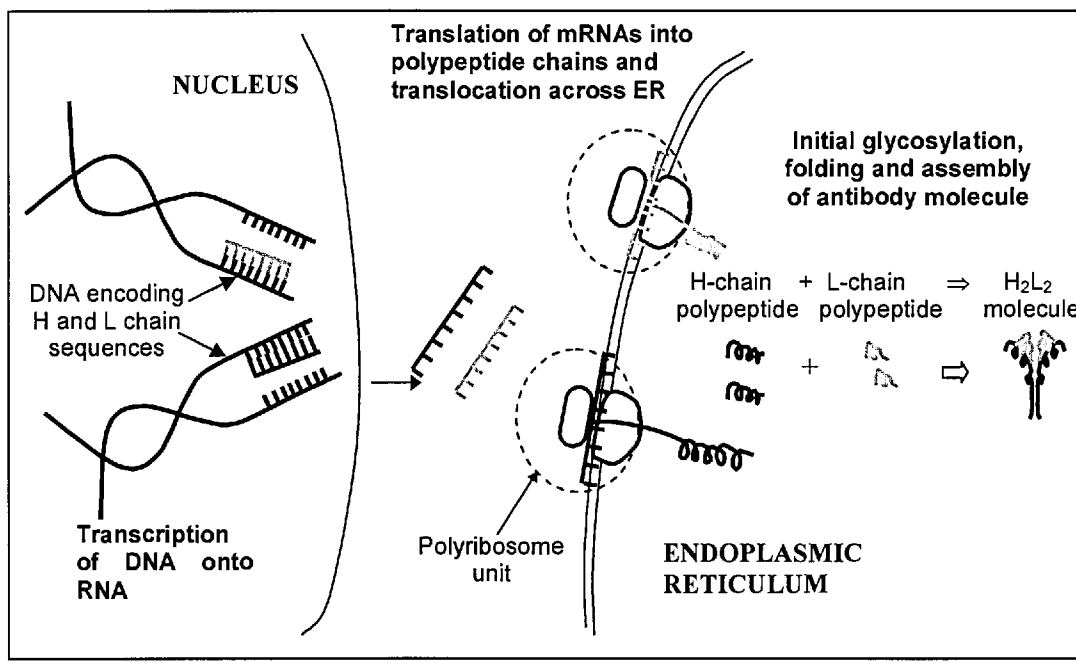

Figure 2.1. Intracellular antibody synthesis process. (Adapted from Oh et al., 1993)

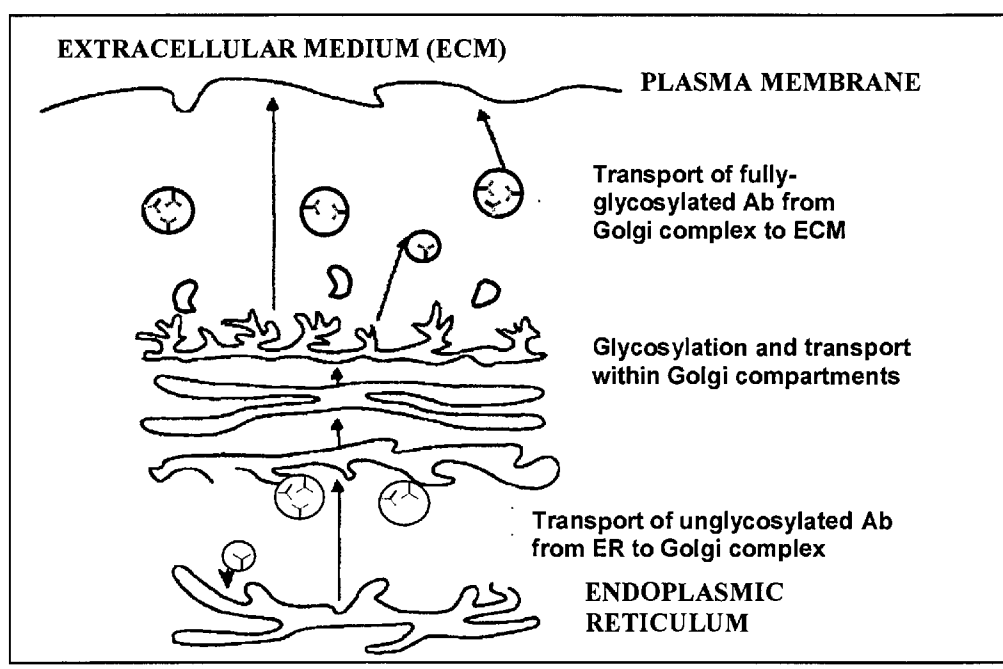

Figure 2.2. Intracellular antibody transport and secretion to medium. (Adapted from McKinney et al., 1995)

2.2.2 Individual Pathway Steps and the Antibody Production Rate

The relationships between the various steps in the antibody production pathway and the antibody production rate are crucial for the identification of the rate-limiting step(s) in the pathway. The following sub-sections provide a summary of the observations and results obtained from literature about each individual step.

Transcription

In a study of CHO cells, Pendse et al. [1992] found a limited correlation between transfected mRNA transcript abundance and the rate of protein secretion. It was also found that while there was a positive relationship between the level of transcription and specific protein production rates, the increase in the production rate did not correlate with the high level of gene transcription attainable [Dorner and Kaufman, 1990; Merten et al., 1994]. Similar observations were also made in a study on hybridoma cells carried out by Lee and Lee [2000], where it was found that specific antibody production rates increased by a much smaller factor than the increase in transcription levels as the osmotic pressure was increased. However, Leno et al. [1992] (hybridoma cells) could not identify any correlation between the specific antibody production rate, q_{Ab}, and the amounts of H and L chains mRNAs at any stage of the culture. These observations imply that while an increase in transcription rates may correlate with increased antibody production, transcription is unlikely to be the rate-limiting step in the process.

Translation and translocation

Translation is a relatively high energy-consuming step as compared to transcription. As a result, feeding strategies aimed at increasing energy production in cells tend to lead to increased translation of H and L chain mRNAs into polypeptide chains. This is therefore likely to lead to an increase in specific antibody production rate. Bibila and Flickinger [1992a; 1992b] stated that translation was likely to be the controlling step for antibody secretion rates in slow growing hybridoma cells, based on simulations carried out using their structured kinetic model for antibody production. McKinney et al. [1995] made the same

postulate in another study on a hybridoma cell line. Lee and Lee [2000] also found experimentally that the increase in q_{Ab} during the exponential phase of the culture agreed more closely with the increase in H and L chain translation rates.

The translocation process occurs co-translationally in mammalian cells. As a result, translocation rates are often based on translation rates [Gonzalez et al., 2001]. However, the current literature search has not revealed any significant studies into the translocation of H and L polypeptides across the ER membrane.

Folding and assembly

The folding and assembly process is also a high energy-consuming step. This is due to the interaction of incompletely folded H and L chains with molecular chaperones such as GRP 78 and GRP94, which prevent incorrectly folded and assembled antibody molecules from leaving the ER. Consequently, energy (in the form of ATP) is required to dissociate the completely folded and assembled antibody molecules from the molecular chaperones [Dorner and Kaufman, 1994; Gething and Sambrook, 1992]. Bibila and Flickinger [1992b] predicted that the folding and assembly of H and L chains are likely to be rate-controlling under fast growth conditions, based on simulations using their kinetic model. While there has not been a substantial amount of data on the folding and assembly rates in antibody production, many studies have hypothesised that it is one of the controlling steps in the production pathway [Gonzalez et al., 2001; McKinney et al., 1995; Oh et al., 1993].

Transport from ER to Golgi

The antibody transport rate from the ER to the Golgi complex appears to correlate with the folding and assembly rate, giving rise to the possibility that antibody transport is in fact governed by its rate of assembly [McKinney et al., 1995]. However, in general, antibody transport from the ER to the Golgi has been assumed to follow the bulk flow mechanism [Bibila and Flickinger, 1991b; Wieland et al., 1987], in which the rate of transport is dependent on the antibody concentration in the ER. In addition, model simulations by Bibila and Flickinger [1992a; 1992b] seem to suggest that the antibody production rate does not vary by a substantial amount when the transport rate constant changes. Based on the above

observations, it appears that transport of antibody molecules from the ER to the Golgi is not a rate-limiting step in the antibody production process.

Golgi processing (further glycosylation)

There has been little experimental data concerning further processing in the Golgi complex. This may be attributed to the fact that different glycosylation reactions are required for the production of different antibodies. Moreover, the use of different cell lines for the production of the same antibody also results in a variation in the glycosylation patterns. However, it has been found that the time required for processing in the Golgi remains more or less constant, at 20 minutes for the production of different proteins [Bibila and Flickinger, 1991b]. In addition, it appears that the inhibition of sialylation (a glycosylation reaction) has no significant effect on the kinetics of immunoglobulin secretion [Thorens and Vassalli, 1986]. Furthermore, in a review on glycosylation, Goochee and Monica [1990] stated, "aberrant glycosylation does not prevent secretion of IgG".

While glycosylation in the Golgi complex is responsible for the correct functioning of the antibody molecule, it is unlikely to be a rate-limiting process. This is based on the observation that the Golgi processing time for different proteins is approximately constant. In addition, as dissimilar antibody molecules are glycosylated differently across various cell lines, it is difficult to generalise the processing steps involved.

Transport from Golgi to extracellular medium (ECM)

The transport from the Golgi to the ECM also does not appear to significantly affect the specific antibody secretion rate [Bibila and Flickinger, 1992a], based on the assumption that transport occurs by the bulk flow mechanism.

In summary, the above observations suggest that the most likely candidates for the rate-limiting steps in antibody production are: i) translation and ii) the folding and assembly step. It is possible that both steps may be responsible for the determination of q_{Ab}, as both processes require substantial amounts of energy (in the form of ATP), which is a likely limiting factor in the antibody production process.

2.3 Optimisation of Antibody Production and Hyperosmolarity

2.3.1 Current Product Optimisation Approaches

Many different approaches have been proposed to improve antibody production yields from mammalian cells. These approaches aim to accomplish two main objectives: (i) to improve specific growth rates and thus viable cell density in the culture, as well as extend its longevity and (ii) to increase specific antibody productivity (q_{Ab}). Cell cultures possessing a combination of both of these features will usually achieve high volumetric production rates [Birch and Racher, 2006], which are then likely to result in larger final antibody titres.

Maximisation of cell density and culture longevity

A key research area in cell culture product optimisation is the study of using different culture configurations to increase cell density and extend culture longevity, with an aim to maximising the "cumulative volumetric cell hours" [Dutton et al., 1998]. The authors defined "cumulative volumetric cell hour" as the accumulated amount of time that viable cells spend in the culture medium, during which they are actively producing the antibody product. Three culture configurations that have been used to maximise the "cumulative volumetric cell hour" are the fed-batch, perfusion and cell immobilisation cultures [Sun, 2000]. These configurations will be further described below.

A fed-batch culture is primarily a batch process in which cells are inoculated in culture medium and the antibody product is either periodically harvested or harvested at the end of the culture. However, nutrients and other ingredients are continuously or intermittently fed into the system throughout the various stages of the culture to improve cell growth and prolong the culture. In addition, a proportion of culture medium is removed constantly or at specific time points to delay the accumulation of metabolites such as lactate and ammonia thus leading to increased culture longevity.

In a perfusion culture, culture medium is fed continuously into the bioreactor containing the cells while the same amount of cell-free culture supernatant is removed from the system. This results in a higher cell density, as well as an increased productivity.

However, the culture conditions must be well controlled so that the culture environment can be kept optimal.

The immobilisation of cells can help prevent mechanical damage of cells in large-scale suspension cultures, thereby leading to sustained cell viabilities and subsequently improved antibody productivity [Seifert and Phillips, 1999]. This technique can also be used effectively to separate the cells from the culture medium in perfusion cultures. However, a key disadvantage of the immobilised culture system lies in the difficulty in directly monitoring of viable cell concentration in the culture. Instead, the cell density has to be estimated indirectly through the measurement of other parameters, such as the glucose uptake rate [Rodrigues et al., 1999].

There have also been many studies on optimal nutrient feeding strategies and the minimisation of metabolites that restrict cell growth and productivity. The supplementation of nutrients, such as glucose and glutamine, in fed-batch culture has extended culture longevity and improved cell growth, as limiting nutrients are replenished continuously [Bibila and Robinson, 1995]. In addition, step increases in the amount of glucose and glutamine in a continuous system has also been reported to increase cell growth [Miller et al., 1989a, , 1989b].

Attempts to increase culture longevity are focused on the inhibition of apoptosis in cell cultures. This can be achieved through the over-expression of anti-apoptotic genes [Mercille and Massie, 1998; Simpson et al., 1998], as well as the supplementation of specific factors (Interleukin-6) to the culture medium [Chung et al., 1997].

Maximisation of specific antibody productivity, q_{Ab}

To improve q_{Ab}, several factors have been added into the culture medium, including autocrine factors [Pendse and Bailey, 1990] and monocyclic nucleotides [Dalili and Ollis, 1988]. The adaptation of cells to serum- and protein-free media has also been proven to increase q_{Ab} [Lambert and Merten, 1997].

However, while it has been found that serum- and protein-free media improves q_{Ab}, the reason behind the change remains unknown. Moreover, the addition of factors is comparatively more expensive than implementation of environmental stresses, by changing, for example, temperature, pH or osmolarity [Zhou, 2002]. Deviation from normal

physiological conditions (usually 37°C, pH 7.0 and osmolarity of 290-310 mOsm/kg [Bogner et al., 2004]) in cell cultures tends to elicit regulatory responses from cells, as they attempt to 're-normalise' their intracellular environment. This allows the change in environmental conditions to act as a form of stress to the cells, causing them to activate various metabolic and signalling pathways, which may in turn result in different protein production rates. Environmental stresses have been previously utilised in product optimisation strategies as a means of improving antibody productivity [Kaufmann et al., 1999; Yoon et al., 2004] and represents another major research area in cell culture-based antibody production. In this study, the focus will be on evaluating the effects of hyperosmotic culture conditions on the antibody production process in GS-NS0 cells. Subsequently, a biphasic culture strategy based on hyperosmotic conditions will also be explored, which will aim to combine enhanced specific antibody productivities with an improvement in viable cell density values.

2.3.2 Osmolarity

Osmolarity is an important environmental variable and one that is easily altered by the addition of readily available and economical salts such as sodium chloride (NaCl) into the culture. Various studies have been carried out to assess the potential of osmotic stress in improving antibody production rates. In general, it has been found that hyperosmotic stress leads to an increase in q_{Ab}, but results in a simultaneous decrease in cell growth rate [Zhou, 2002]. The actual extent of change differs for different cell lines - in some cell lines, the increase in q_{Ab} offsets the detrimental effect on cell growth at hyperosmotic pressure, hence leading to increased antibody production levels. Conversely, in other cell lines, this trend is inversed - the decline in cell growth erodes any improvement in q_{Ab}, thereby leading to an unchanged or lower antibody production level.

This inverse relationship between q_{Ab} and cell growth rate presents one of the major obstacles involved in manipulating osmotic pressure to improve antibody production levels. To overcome this conflict, supplementary methods have been suggested, including the use of osmoprotectants and the gradual adaptation of cells to hyperosmotic pressure by step increases. These strategies have been successful to a certain extent: osmoprotectants such as glycine betaine have improved cell growth but resulted in a smaller increase in q_{Ab}, while

gradual adaptation of cells to hyperosmotic pressure has reduced the detrimental effect on cell growth. In the next subsection, detailed effects of hyperosmolarity on the various aspects of mammalian cell cultures will be further described so as to provide a clearer picture of the possible mechanisms through which antibody productivity is improved.

Effects of osmotic pressure on cellular functions

Cell growth and antibody production

Hyperosmotic pressure appears to have a general effect across many mammalian cell lines in terms of cell growth and specific antibody productivity (q_{Ab}). Cell growth is suppressed; the specific growth rate and maximum cell viable concentration decreases with increasing osmolarity, while q_{Ab} is increased. For example, in a study on hybridoma cells, Ozturk and Palsson [1991b] found that the specific growth rate decreased by a factor of about 2 when the culture osmolarity was increased from 290 (control osmolarity) to 435 mOsm/kg. Conversely, q_{Ab} increased by more than 2-fold over the same rise in osmotic pressure. Similarly, Ryu et al. [2001] carried out osmolarity experiments on Chinese Hamster Ovary (CHO) cells and found that specific growth rate was halved when the osmotic pressure was raised from 302 mOsm/kg (control) to 469 mOsm/kg. In addition, q_{Ab} was increased by more than 2-fold as osmolarity increased. The same trend was observed in a study on GS-NS0 cells [Duncan et al., 1997], when the osmolarity was increased from 275 (control) to 400 mOsm/kg.

As a result of the decrease in growth rate, the increase in q_{Ab} does not necessarily lead to an increase in total antibody production. Hence, hyperosmotic pressure may have a positive, unchanged or negative effect on total antibody titre (see Table 2.2). To reduce the negative effect of reduced cell growth, cells have been adapted gradually to hyperosmotic medium. Oh et al. [1993] compared the specific growth rate between cells that are subjected to osmotic shock and cells which have been adapted to hyperosmotic pressure for hybridoma cells. The results showed that the fall in specific growth rate was reduced by 20% for adapted cells as compared to unadapted cells when osmolarity was increased from 300 to 350 mOsm/kg. The maximum cell concentration also vastly improved. These changes

enabled the maximum antibody titre, at 350 mOsm/kg, to increase by 76% for adapted cells. This example highlights the potential of hyperosmotic pressure as a cost-effective measure in improving antibody production yields.

Cell metabolism

Glucose and glutamine are the main energy sources in mammalian cell cultures and are most commonly analysed in literature. Cellular metabolism rates are analysed based on the uptake of these nutrients, as well as the specific production rate of lactate (by-product of glucose metabolism) and ammonia (by-product of glutamine metabolism).

Glucose metabolism

It has been widely reported that the specific uptake rate of glucose, q_{glc}, increased with increasing osmotic pressure for hybridoma, CHO and GS-NS0 cells [Duncan et al., 1997; Oh et al., 1995; Ozturk and Palsson, 1991b; Takagi et al., 2000]. Consequently, the specific production of lactate, q_{lac}, also increased. However, in contrast to the above observations, experiments carried out on hybridoma cells by Oyaas et al. [1994] on hybridoma cells reveal no changes in either q_{glc} or q_{lac} with increasing osmolarities, despite the increase in q_{Ab}.

Glutamine metabolism

For hybridoma cells, Oh et al. [1995] reported an increase in specific glutamine utilisation rate, q_{gln}, with increasing osmolarity. Similar trends in q_{gln} have been reported by Ozturk and Palsson [1991b] and Lin et al. [1999a]. Additionally, the specific ammonia production rate, q_{NH4}, increased correspondingly with q_{gln} [Lin et al., 1999a; Ozturk and Palsson, 1991b]. It was postulated that the increase in cell metabolic rates results in an increase in the amount of ATP produced, which was then channelled into the production of antibody [Lin et al., 1999a]. Ozturk and Palsson [1991b] also proposed that the increase in cellular metabolism rates could be partially attributed to increase in cell volume resulting from hyperosmotic pressure.

Cell size

It has been observed that the cell sizes in hyperosmotic cultures tend to be larger than those in standard osmotic medium [Ozturk and Palsson, 1991b]. In fact, in a study on KR12H-2 transfectomas, Lee and Lee [2000] observed a 50% increase in cell volume and cell mass when the osmotic pressure was raised from 285 to 425 mOsm/kg. In addition, the dry cell weight and total cellular RNA also increased in hyperosmotic cultures [Lee and Lee, 2000; Oh et al., 1995]. These findings could have been a result of improved transport of nutrients, including amino acids, into the cell, due to the stimulation of Na^+-amino acid symports during cell regulatory volume increase (RVI). The accumulation of nutrients would have caused cell volume to increase, while the increased amino acids uptake would increase the biosynthesis rate of protein in the cell [Oh et al., 1993]. In addition, the increase in total cellular RNA may also be partially responsible for the increase in antibody production rate.

Cell cycle

Introduction to the cell cycle

The cell cycle refers to the process by which DNA is replicated and segregated in order to form two genetically identical daughter cells [Alberts et al., 1994]. The cycle can be divided into four distinct phases [Faraday et al., 2001]:

(i) G0/G1 (GAP 1): a period between cytokinesis and the beginning of DNA synthesis
(ii) S: the DNA synthesis phase
(iii) G2 (GAP 2): a period between the end of DNA synthesis and the start of mitosis
(iv) M: the mitosis phase, where cell division occurs.

The cycle can be viewed as a repetitive sequence of events in which each event has to be completed before the next event can occur. In order to ensure that a cell does not divide before the DNA has been replicated, the subcellular organelles have been duplicated and the cell has grown to a critical size [Fussenegger and Bailey, 1998] two main 'checkpoints' exist within the four cycle phases. These include: a commitment to chromosome replication in the G1 phase and a commitment to mitotic cell division at the end of G2 phase. However, for animal cell cultures, the latter (G2/M) control checkpoint is subsidiary compared to the former, as cells spend the longest part of their cycle in G1 [Lewin, 2000], therefore the focus here will be on the G1 phase control checkpoint.

At the G1 phase checkpoint, the cells make a decision on whether to proceed past the G1 phase towards completion of the S phase and progression through the G2 phase. The decision is made based on two main criteria: firstly, the existence of a favourable extracellular environment in terms of nutrient supply, conditions such as temperature, pH and osmolarity, as well as the availability of growth factors and hormones in the extracellular medium. The second criterion is an assessment of whether the cell mass is sufficient to support a division cycle [Lewin, 2000]. Cells not meeting the above criteria due to, for instance, DNA damage as a result of extracellular conditions, will be arrested in the G1 phase so as to allow time for DNA repair to occur [Nyberg, 2002].

Effects of osmotic culture conditions on cell cycle

There is a significant difference in the cell cycle distribution when cultures are subjected to hyperosmotic culture conditions. Hyperosmolarity appears to induce cell cycle arrest in the $G0/G_1$ phase [Ryu et al., 2001] for CHO cells – 84% of cells at an osmolarity of 502 mOsm/kg were in the $G0/G_1$ phase, compared to 45% of cells at the standard osmolarity of 302 mOsm/kg. Cherlet and Marc [1999] also reported increasing proportion of cells in the $G0/G_1$ phase with increasing osmolarity, up to 425 mOsm/kg, for OKT3 mouse hybridoma cells. However, there have also been contradicting observations; for instance, Sun [2000] reported that the proportion of cells in the $G0/G_1$ phase decreased with increasing osmolarity in hybridoma cells (167.4G5.3), while the fraction of cells in the DNA synthesis (S) phase increased.

In addition, there have been various attempts to link the cell cycle to antibody production rates. Hayter et al. [1992] stated that q_{Ab} was higher in the $G0/G_1$ and G_2 phases (preparation phases for cell division) as compared to the S and M (mitotic cell division phase) phases in a mouse hybridoma line. However, Lloyd et al. [2000] conducted a study on CHO cells and found contradictory results: q_{Ab} was reported to be lowest when the majority of cells were in the $G0/G_1$ phase, intermediate when the majority of cells were in the S phase and greatest when the majority of cells were in the G_2/M phases. Cherlet et al. [1995] also reported maximum q_{Ab} when cells were in the G_2/M phases for a murine hybridoma cell line.

In the light of differing observations, no general consensus has been reached in relation to the optimal cell cycle phase for antibody production. It appears that cell cycle effects on q_{Ab} may be cell-line specific and the relationship between antibody production and cell cycle progression cannot be generalised at present [Zhou, 2002].

Intracellular mRNA and IgG heavy and light chain concentrations

There have been few studies focusing on the intracellular concentrations of mRNA and IgG polypeptide species at hyperosmotic culture conditions, perhaps due to the difficulties in obtaining these values as compared to extracellular concentrations. The findings from two major studies currently available in literature today will be described in detail here. It should be noted that both studies are based on different hybridoma cell lines. In the first study on KR12H-2 transfectoma cells, Lee and Lee [2000] reported substantial increases in the levels of heavy (322% increase) and light chain (340% increase) mRNA as the culture osmolarity is increased from 285 mOsm/kg to 425 mOsm/kg during the mid-exponential phase. While the ratio of light (L) to heavy (H) chain mRNA remained relatively constant at 2.3, the half-lives of H and L chain mRNA at 485 mOsm/kg (5 hrs for H mRNA, 5.6 hours for L mRNA) were lower than at 285 mOsm/kg (8 hrs for H mRNA, 8.7 hrs for L mRNA). These observations led to estimated specific transcription rate increases of 476% and 484% for H and L mRNA respectively. The authors also estimated that the specific translation rates for H and L chains increased by 172% and 240% respectively when the osmolarity of the culture was raised from 285 to 425 mOsm/kg. The authors hence concluded that the key reason for the increase in q_{Ab} at hyperosmotic culture conditions was the enhanced transcription rates of H and L mRNA.

In the second study on the hybridoma cell line 167.4G5.3, Sun et.al. [2004] conducted osmotic shock experiments by changing the culture osmolarity from 290 to 400 mOsm/kg at the mid-exponential phase of the culture. Measurements of the mRNA levels of both control and osmotic shock cultures showed that H and L mRNA levels per cell were higher in the latter cultures, particularly 72-84 hours after the induction of osmotic shock. However, the authors did not see a corresponding increase in antibody production rate, protein synthesis or antibody secretion rate. Conversely, they observed an increase in the

immunoglobulin translation rate for cultures subjected to osmotic shock, which was commensurate with an increase in antibody production. They therefore concluded that the increase in translation rate was likely to play a key role in improving antibody production rates.

Based on the above observations, it could be noted that the H and L mRNA levels increased under hyperosmotic culture conditions for both studies. Similarly, immunoglobulin translation rates were reportedly higher for hyperosmotic cultures relative to normal osmotic cultures. However, both studies derived different conclusions with respect to the improvement of antibody production rates – the former study concluded that increased transcription rates were responsible for the increase in production while the latter postulated that transcription rates were not correlated to increased antibody production. Instead, increased translation rates were the main reason of antibody production increase. As such, there are still differing opinions regarding the mechanism through which hyperosmolarity improves antibody production. In the next section, a summary of the possible mechanisms proposed in literature will be presented and discussed. The effects of hyperosmotic culture conditions on the cell growth and antibody production aspects of a number of different cell culture systems can be found in Table 2.2. In addition, the general effects of osmotic pressure on the various aspects of cell physiology for mammalian cells that have been discussed are summarised in Table 2.3.

Cell line	Observations/findings	Reference
CHO (CS13-0.02 cell line)	• Unspecified decrease in μ as osmolarity increases from 305 to 537 mOsm/kg • q_{Ab} increased by approximately 400% over same increase in osmolarity • Final Ab titer decreased by approximately 60%.	[Ryu et al., 2001]
GS-NS0	• Decrease in μ as osmolarity increases from 275 to 400 mOsm/kg. • 1.8-fold increase in q_{Ab} over same increase in osmolarity. • No mention of final Ab titer.	[Duncan et al., 1997]
Hybridoma	• 2-fold decrease in μ as osmolarity increases from 290 to 435 mOsm/kg. • q_{Ab} increased by more than 2-fold over same increase in osmolarity. • Final Ab titer relatively unchanged.	[Ozturk and Palsson, 1991b]
Hybridoma (KR12H-2 Transfectoma)	• μ decreased by 20% as osmolarity increases from 285 to 425 mOsm/kg. • q_{Ab} increased by 376% over the same increase in osmolarity. • Final Ab titer increased by about 60% over same increase in osmolarity.	[Lee and Lee, 2000]

Table 2.2. Summary of hyperosmotic effects on cell growth and antibody production in various cell systems.

Physiology aspect	Response to hyperosmotic pressure
Cell growth	Decrease
Specific antibody productivity	Increase
Cell metabolism	Increase
Cell size	Increase
Cell cycle distribution	Cell line-dependent: G_1 phase arrest or increase in S phase
Total cellular RNA levels	Increase
H and L mRNA levels	Increase
H and L translation rates	Increase

Table 2.3. Summary of effects of hyperosmotic pressure on cell physiology

Hyperosmotic effects on antibody production – proposed mechanisms

As the detailed mechanism of enhanced q_{Ab} as a consequence of hyperosmotic pressure is still not clearly understood at the basic cellular level, there have been a number of hypotheses proposed regarding this phenomenon [Ryu et al., 2001] in literature, including the following:

Increase in transcription rates

Hyperosmotic pressure induces the transcriptional activation because of the change of chromatin structure, as in the case of treatment with sodium butyrate, which is also known for enhancing the production of proteins while suppressing growth rates [Oh et al., 1993]. The chromatin becomes dispersed due to the unbinding of histones from DNA and made more accessible to RNA polymerase for transcription [Lee and Lee, 2000]. This leads subsequently to an increase in transcription rates and hence improved antibody production rates.

Stimulation of assembly rates

Hyperosmotic pressure may also stimulate the expression of assembly step catalysts and chaperone-like proteins in the ER, such as PDI or GRP78 and other similar molecular chaperones, which has been reported to increase the assembly rate of a single-chain antibody fragment in eukaryotic cells [Shusta et al., 1998]. However, it must be noted that overproduction of GRP78 may instead result in a decreased antibody assembly rate, as excessive binding of heavy and light chain to the chaperone occurs [Dorner et al., 1992; Gonzalez et al., 2001]. In a study on three chaperone-like ER proteins (GRP78, GRP94, ERp72) on batch cultures of GS-NS0 cells, Downham et.al. [1996] observed an increase in the expressions of all three ER proteins as the culture progressed towards the stationary and decline phases, which corresponded to a halt in the uptake of glucose and glutamate by cells. However, the authors also found that increased productivity due to glutamate feeding during the batch culture did not relate to enhanced induction of the ER proteins and concluded that a more detailed study was required to discern any likely relationship between ER chaperone protein expression and antibody productivity. Based on the above contradictory observations

with regards to this hypothesis, it may be likely that the extent of stimulation of the above proteins is cell-line dependent.

Increased amino acid uptake rates leading to enhanced antibody productivities

Hyperosmotic pressure has been reported to enhance the transport of a number of amino acids into cells [Oh et al., 1995; Oh et al., 1993; Pastor-Anglada; et al., 1996]. The increase in amino acid uptake rates resulted in a larger available pool of amino acids for biosynthesis, thus leading to improved specific antibody productivities [Oh et al., 1995; Oh et al., 1993].

Increased energy levels due to enhanced uptake of nutrients

Hyperosmotic pressure enhances the uptake of nutrients such as glucose, hence resulting in an increase in ATP production rates. This increase, coupled with the lower growth rate, implies that there is a larger amount of ATP being channelled into the antibody production process [Lin et al., 1999a]. As the antibody translation process is highly energy-dependent, this mechanism is likely to improve the translation rates of heavy and light IgG chains.

Cell cycle phase-associated antibody production

Hyperosmotic pressure induces G_1 phase arrest. It has been observed in CHO cells that higher productivity is obtained when the majority of cells are in the G_1 phase. It has been suggested that this is due to the fact that cells in that phase do not need to devote cellular resources to biomass production, hence enhancing q_{Ab}. However, this observation does not seem to be universal – a number of other studies found that antibody productivity is highest during the G_2/M phase [Cherlet et al., 1995; Lloyd et al., 2000].

The aim of the combined modelling and experimental approach undertaken in this study is to ascertain the degree of applicability of some of the proposed mechanisms of hyperosmolarity to the GS-NS0 cell line, as well as establish the possible rate-limiting step(s) in the GS-NS0 antibody production process.

2.4 Modelling and mathematical analysis of cell culture processes

2.4.1 Importance of mathematical models

Incomplete understanding of mammalian cell culture kinetics often hinders the design and development of control strategies for antibody production systems [DiMasi and Swartz, 1995]. With the increasing demand for antibody products from mammalian cell lines, process optimisation has become a matter of extreme importance in the biopharmaceuticals industry [Mainwaring et al., 2002]. While the use of experiments to optimise the values of various culture parameters (such as nutrient feeding rates and environmental conditions) is the current preferred means of improving antibody production rates, this approach often results in large numbers of experiments that are expensive and time-consuming [Jacquez, 1998]. An alternative approach to the above method is the use of mathematical models, which allows for the organization of preliminary experimental information in a logical and systematic manner, thereby facilitating the identification and quantification of key relationships between process parameters, variables and product output rates [Bailey, 1998]. Additionally, a thorough and systematic analysis of these models will help to identify key parameters affecting antibody production rates, which can then be studied in more detail experimentally. This approach is therefore likely to lead to a reduction in the required number of experiments for product optimisation, leading to savings both in terms of time and costs.

2.4.2 Cell growth and metabolism models

Cell growth and metabolism models constitute the largest proportion of mathematical models describing the mammalian antibody production process. One of the earliest cell growth models was developed by Monod, which relates bacterial growth rates to the availability of a substrate required for growth [Monod, 1949]. The kinetics in this model was based on the 'Michaelis-Menten' kinetics equation, which has been used extensively in the current, more sophisticated models of cell growth and metabolism.

Structured and unstructured models

Most cell culture models can be divided into two categories, namely unstructured and structured. Unstructured models are empirical and disregard intrinsic intracellular processes, while structured models aim to incorporate such features [Portner and Schafer, 1996]. Fully structured models are ideal for capturing the true nature of cellular functions; an example of an up-to-date structured model is the single-cell model developed by Sanderson [Sanderson, 1997]. This model accounts for some 50 components in three distinct regions (medium, cytoplasm and mitochondria) and includes descriptions of major metabolic pathways, competitive trans-membrane transport, product formation, and cell growth and death. However, incorporation of biological detail has also contributed towards model complexity resulting in high computational costs and rendering model analysis particularly difficult [Sidoli et al., 2005]. In contrast, the simpler unstructured models utilise mainly extracellular data while treating intracellular processes as a "black box". Although this approach does not allow for the in-depth study of cellular processes, such models have been reported to be of great importance in aiding the design of monitoring and optimisation strategies [Provost and Bastin, 2004]. Additionally, they may be a good starting point for relatively new cell systems where data are limited.

Unstructured models – a summary

Many existing unstructured models are based on empirical correlations between the specific monoclonal antibody production rate, q_{Ab} and other variables, such as the specific growth rate [de Tremblay et al., 1992; Frame and Hu, 1991; Linardos et al., 1991] or the concentrations of nutrients like glucose and glutamine [Dalili et al., 1990; Jang and Barford, 2000]. Suzuki and Ollis [1989] also incorporated the characteristics of the cell cycle into a model by correlating the fraction of cells in each phase of the cell cycle to q_{Ab}. In general, these empirical correlations consisted of a growth-independent term and a growth-dependent term, which were determined experimentally.

The development of structured models

One of the first structured models was developed by Batt and Kompala [1989], which consisted of defined 'metabolic pools' for amino acids, proteins, nucleotides and lipids. The antibodies produced were regarded as part of the protein pool and the interactions between different pools and the extracellular environment were described by Michaelis-Menten equations [Portner and Schafer, 1996]. Subsequently, Wu et al. [1992] derived a single-cell model for the growth and metabolism of Chinese Hamster Ovary (CHO) cells. In their model, glucose and glutamine were substitutable precursors of intracellular metabolites, and their respective contributions were determined by a 'dominance factor', which in turn was a function of their relative intracellular concentrations.

In 1995, DiMasi and Swartz formulated an energetically structured (ES) model applicable to steady-state hybridoma cell growth in continuous culture. The model was based on the amount of energy (in the form of ATP) produced and consumed during catabolic and anabolic (biosynthesis) processes respectively. The predictions of specific nutrient utilisation rates, specific metabolite production rates with respect to specific growth rate were shown to agree well with the experimental results reported by Miller et al. [1987; 1988a; 1988b; 1989a; 1989b] on hybridoma cells.

As mentioned briefly in the previous subsection, the most recent structured model was developed by Sanderson et al. [1999], involving detailed descriptions of major metabolic pathways, competitive trans-membrane transport, product formation and cell growth and death. It has been applied to a variety of cell cultures, including hybridoma and baculovirus/insect cell systems. The rates of cell growth and antibody production in this model were represented by Michaelis-Menten type equations, which were in turn modulated by the availability of energy and the necessary precursor molecules, as well as the concentration of inhibitory products (such as lactate and ammonia) in the cell. Trans-membrane transport was described by a modified version of the diffusion equation while the reactions in the major metabolic pathways were described using Michaelis-Menten kinetics. [Sanderson et al., 1999]. The combination of equations was able to provide a detailed description of intracellular metabolic events with respect to time. The model was

subsequently applied to a variety of cell culture systems, including two types of hybridoma cells and a baculovirus/insect cell system.

The survey of the metabolism models in the literature seems to suggest that there is a trend towards the generalisation of models to various mammalian cell culture systems and beyond. While the models are extremely useful in the optimisation of antibody production based on metabolic factors (nutrient feeding), they do not consider the detailed steps in antibody production, and hence cannot be used to identify the rate-controlling step(s) in the antibody production pathway. The lack of detailed information leads to an incomplete understanding of the actual process of antibody production, which may hamper further improvements in antibody production rates.

Antibody synthesis and secretion models

There have been very few models that depict the antibody synthesis and secretion process as described in Section 2.2. The first key model describing this process was a basic structured kinetic model constructed by Bibila and Flickinger [1991a] for the description of antibody production in hybridoma cells. The model consisted of three main steps used to describe antibody synthesis:

- Transcription of the heavy (H) and light (L) chain mRNAs
- Translation of H and L mRNAs into H and L polypeptide chains
- Assembly of the H and L polypeptide chains in the ER to form the antibody molecule

This basic model was subsequently incorporated in a three-compartment model [Bibila and Flickinger, 1991b] describing the inter-organelle transport of the assembled antibody molecule. The three main steps in this larger model consisted of:

- Transport of assembled antibody from the ER to the Golgi
- Further processing of the molecule in the Golgi complex (glycosylation) and transport of the antibody from the Golgi to the extracellular medium (ECM)

The model was structured with respect to the process of antibody synthesis and secretion alone, instead of at the whole cell level, in order to develop a modelling framework that was useful in identifying possibly rate-limiting steps in the antibody production process. Based on steady-state and transient model simulations carried out by Bibila and Flickinger

[1992a; 1992b] on the antibody secretory pathway in response to blocks in each key process step, the study concluded that the main rate-limiting steps were: the assembly rate of the antibody in the ER under fast growth conditions and the H and L chain translation rates under slow growth conditions.

The second key model for monoclonal antibody synthesis was developed by Gonzalez et al. [2001] and consisted of the following key steps:

- Production of nucleotides from a pool of precursors (consisting of amino acids used for biosynthesis)
- Transcription
- Translation and polypeptide translocation across the ER membrane
- Primary glycosylation (catalysed by oligosaccharide transferase [OST])
- Folding and assembly (including the involvement of protein disulphide isomerase [PDI], a catalyst for disulphide bond formation and GRP78, a molecular chaperone binding to incompletely assembled molecules)

The model was analysed using metabolic control analysis, a technique which attempted to relate the overall properties of a metabolic system to the properties of its component parts [Gonzalez et al., 2001]. The technique used flux control coefficients, which gave an understanding of the control of each step on the pathway. It was found that the control structure of antibody synthesis was shared between transcription and post-translational steps, including folding, glycosylation and the synthesis of nucleotides from precursors. The actual controlling step would depend on the concentration of the precursor pool, as well as the levels of OST, GRP78 and PDI.

The conflicting point between the two models was the fact that while translation was considered to be a possible rate-limiting step in the first model, in the second model, it was stressed that translation was not a rate-controlling step 'under all conditions' [Gonzalez et al., 2001]. This might be due to differences in the approaches of the two models. The first model is based on mass balances for transcription and translation, with a number of empirical correlations derived from experimental data, as well as reaction kinetics for the assembly and interorganelle transport steps. In contrast, the second model is based purely on reaction kinetics. This resulted in the involvement of a large number of variables, including

the concentrations of DNA, various enzymes involved in each of the reaction steps, as well as the intermediate complexes formed (such as the mRNA-Ribosome complex). This latter approach requires a large amount of data relating to the kinetic parameters of each enzymes and the concentration of reaction intermediates with respect to time, which is not easily obtainable or available in literature. Many of the parameter values used in the model have therefore been derived for bacteria and yeast cell lines rather than mammalian cell lines, and this may lead to inaccuracies in the actual model.

In addition to the two models above, there have also been a number of models that concentrated on certain steps in the antibody production pathway. Schroder et al. [1999] came up with a kinetic model for transcription and translation of recombinant protein in gene amplified CHO cells and used it to determine that neither of the two processes was rate-limiting for recombinant protein production. Percy et al. [1975] devised a theoretical model for the covalent assembly of immunoglobulins which was based on the probabilities of the formation of a disulphide bond between two heavy chains, as well as, between a heavy and a light chain. The model successfully predicted the assembly rate for both IgG1 and IgG4 molecules, based on the experimental results of Petersen and Dorrington [1974]. Robinson and Lauffenburger [1996] developed a model describing the interactions between the molecular chaperone GRP78 and foreign proteins in general in the folding process. Gonzalez et al. [2002] also derived a kinetic model for the folding and assembly of recombinant proteins in eukaryotic cells. This model incorporates the interactions of the chaperone GRP78, as well as PDI, which as mentioned above, is a catalyst for the formation of disulphide bonds.

Umana and Bailey [1997] created a model that described the N-glycosylation process of recombinant glycoproteins passing through the Golgi complex, consisting of mass balances for 33 different oligosaccharide species which can be linked to the specific protein. Monica et al. [1997] also developed a model depicting sialylation of N-linked oligosaccharides in the trans-Golgi network. This model was based on Michaelis-Menten-type dependency of reaction rates. The model was used to predict the heterogeneous outcome of a post-translational oligosaccharide biosynthesis step, which would lead to the production of proteins of varying quality.

The above models all contributed to the characterisation of the antibody production pathway. It is through such models that more insight into the intracellular mechanisms that govern antibody synthesis and secretion can be gained.

Antibody production models and osmolarity effects

At present, there appears to be no publication regarding an antibody production model that takes into account the effects of hyperosmotic culture conditions, although there have been a considerable number of experimental studies on osmotic effects on hybridoma and CHO cell lines (see Section 2.3.2). The closest resemblance of a model being used to describe the process is the study on transfectoma cells and their response to hyperosmotic pressure by Lee and Lee [2000], which has been described in Section 2.3.2. Based on their experimental results, the authors derived a correlation for the relative transcription rates at different osmotic pressures during exponential growth, which was subsequently used to quantify the relative mRNA transcription rates at different osmolarities. The correlation was derived from the H and L mRNA mass balances found in the model developed by Bibila and Flickinger [1991a]:

$$\frac{S}{S_o} = \left[\frac{(k+\mu)}{(k_o+\mu_o)}\right]\left[\frac{[mRNA]}{[mRNA]_o}\right] \qquad (2.1)$$

where S is the transcription rate, k is the decay rate constant, μ represents the specific growth rate and [mRNA] is the intracellular mRNA concentration. The subscript 'o' refers to the original (control) osmolarity state.

The lack of a model that is able to describe antibody production in hyperosmotic cultures may be another reason why hyperosmolarity is rarely used as a means of improving antibody production rates. As such, the construction of such a model will be beneficial in gaining an improved insight into hyperosmotic pressure mechanisms and contribute towards the developing of optimisation strategies for antibody production.

2.4.3 Mathematical analysis of cell culture models

Having developed a mathematical model based on known experimental information, it is important to determine the robustness of the model structure and its validity under different environmental conditions. As such, an in-depth analysis of the model should be carried out to increase confidence in the model predictions [Saltelli, 2000], by evaluating existing relationships between model inputs (parameters) as well as how changes in the values of these inputs affect model outputs.

Identifiability and sensitivity analysis mtehods

Information on model parameters can be gathered through either a parameter identifiability or a sensitivity analysis approach [Kontoravdi et al., 2005]. An identifiability study is used to determine whether a unique solution can be derived for each parameter from measured experimental values [Sidoli et al., 2005]. While established methods have been derived for identifiability studies on simple models [Jacquez, 1998], carrying out such an analysis on highly non-linear and dynamic models has been reported to be extremely difficult computationally [Ljung and Glad, 1994; Sidoli et al., 2005]. In contrast, sensitivity analysis (SA) is defined as the study of how a variation in model output (antibody production) can be allocated among different sources of variation in the inputs (changes in parameter values) [Saltelli et al., 2004]. SA tends to have a lower computational cost as the derivation of unique solutions for each parameter is not required. As such, the SA approach tends to be more widely used in a variety of biological modelling applications, as summarised in the next subsection.

Use of SA in various biological modelling applications

Different sensitivity analysis techniques have been used to evaluate the structure and test the validity of mathematical models developed for a wide range of biological applications, including drug delivery [Rullmann et al., 2005; Tzafriri et al., 2005] tissue engineering [Malda et al., 2004; Radisic et al., 2005; Schiek and May, 2005] and signalling pathway modelling [Babu et al., 2004; Mutalik et al., 2004; Waters et al., 1990]. In the area of cell culture modelling, SA has been implemented in plant cell culture [Zhang and Su, 2002], insect/retrovirus

cell culture [Cruz et al., 2000; Enden et al., 2005] and hybridoma cell culture models [Dhir et al., 2000; Kontoravdi et al., 2005; Lavric et al., 2005, , 2006; Sidoli et al., 2004].

Types of Sensitivity Analysis

Sensitivity analysis methods can be generally classified into three different groups: screening, local sensitivity analysis and global sensitivity analysis methods. Screening methods provide a qualitative measure of the relative importance of each model parameter and are particularly useful for the evaluation of large-scale models, which tend to have a high computational cost of analysis [Saltelli, 2000]. Local sensitivity analysis techniques involve the determination of changes in model output as parameter values are altered within the close vicinity of their nominal value. However, local sensitivity analysis data is by definition *local* as it is related only to a single point in the parameter space. Such data is not able to provide useful information on effects resulting from significant changes in parameter values, which might occur, for instance, in a cell culture model under different feeding regimes or environmental conditions [Turanyi and Rabitz, 2000]. In contrast, global sensitivity analysis (GSA) methods take into consideration the entire possible ranges of parameter values while apportioning the changes in the output to changes in input factors [Saltelli, 2000]. This characteristic is important in cell culture models as it allows for the analysis of how model parameters behave over their entire known physiological ranges. Additionally, in a GSA study, simultaneous changes in multiple parameter values are usually carried out, hence providing more information about both first- and higher- order sensitivities.

In this study, GSA has been chosen to evaluate the relative impacts of model parameters on antibody production, as well as the possible interactive effects between different parameters. This decision is based on the fact that GSA provides the most detailed quantitative information on model parameters, which subsequently aids in the identification of key parameters crucial to the antibody production process which are then studied experimentally.

Chapter 3

Development and Analysis of a 'Hybrid' Model

3.1 Introduction

It has been mentioned briefly in Chapter 2 that while a fully structured cell culture model is ideal for capturing the true nature of intracellular processes, there are difficulties involved, both in the obtaining of the required experimental data for the determination of model parameters, as well as conducting a detailed analysis of such a model [Sidoli et al., 2005]. For example, in a highly structured model such as the single cell model developed by Sanderson [1997], there are over 350 parameters, many of which can only be determined accurately with intracellular metabolism data. As such data are still currently rather scarce (and non-dynamic), most of the parameters had to be estimated with existing extracellular metabolism data, utilising a set of heuristics and trial and error techniques [Sanderson, 1997]. Additionally, the large number of equations and parameters involved in the single cell model poses a big challenge in terms of conducting an accurate analysis of the model. The problems faced in assessing the effects of individual parameter value changes for the single cell model are highlighted in a parameter estimability study conducted by Sidoli et.al. [2005]. Based on the above issues, the development of a fully structured model to describe antibody production in GS-NS0 cells is likely to have limited model flexibility at present and therefore impractical as a first step. However, adopting a wholly unstructured model

approach will not allow for accurate representation of the intracellular antibody production process in GS-NS0 cells, which is a main focus of this study.

In view of these limitations, a combined unstructured and structured modelling approach has instead been undertaken for the development of the hybrid model presented in this chapter. As dynamic intracellular metabolic data for the GS-NS0 cell system is not currently available in literature, to the best of the author's knowledge, an unstructured approach is used to describe cell growth, death and metabolic processes. The processes of antibody synthesis and transport are described through a structured model approach so as to gain greater insight into the individual production steps and aid identification of possible rate-limiting steps. The model thus allows for a detailed description of the antibody production process without the need for intracellular metabolic data.

3.2 Model structure

As mentioned in Section 3.1, the model comprises of an unstructured description of cell growth and death kinetics, nutrient uptake and metabolite production, as well as a structured description of the intracellular antibody synthesis and secretion process. The unstructured elements of the model utilises Michaelis-Menten kinetic type expressions as the basis for description of cellular growth, death and metabolic processes. The structured element of the model is based on the antibody production pathway model developed by Bibila [1991] for hybridoma cells and consists of the following main steps: transcription of heavy (H) and light (L) mRNA molecules, translation of the H and L mRNA into H and L polypeptide chains, assembly of two H and L chains to form the H_2L_2 antibody structure, transport of the fully formed antibody molecule from the endoplasmic reticulum to the Golgi complex and subsequently to the extracellular medium. A graphic representation of the hybrid model is shown in Figure 3.1.

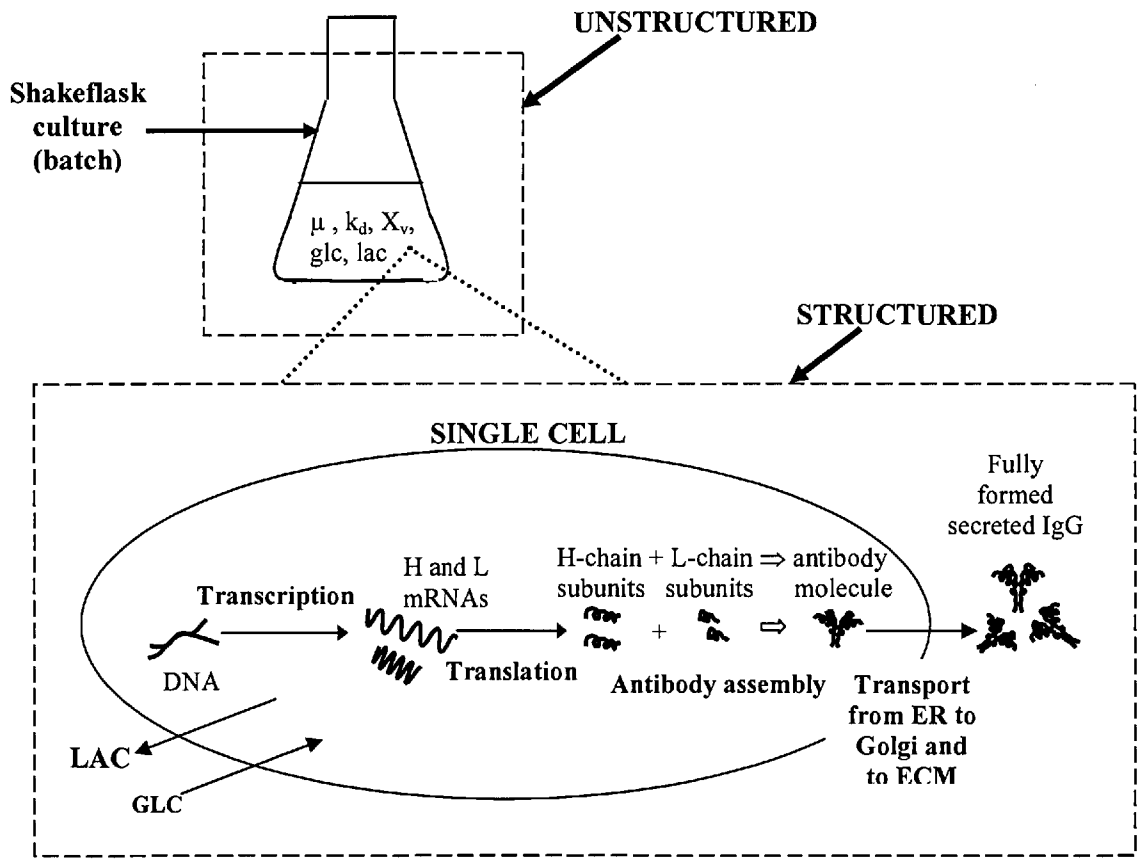

Figure 3.1. Schematic representation of hybrid model, showing both unstructured elements (cell growth, death and metabolism) and structured elements (antibody production pathway)

3.2.1 Assumptions

The proposed model operates under a number of assumptions: firstly, it is assumed that a well-mixed system exist in the shake flask cultures, hence any spatial variation in cell numbers and metabolite concentrations has been ignored. The cell culture is also assumed to be homogenous, as elements of the cell cycle has not been incorporated into the model. This implies that the nutrient uptake, metabolic production and antibody production behaviour of each cell is averaged over all viable cells in the whole culture. It should also be noted that the kinetic expressions have been developed for a batch culture.

3.2.2 Mathematical formulation

The unstructured part of the model comprises of the following expressions based on a combination of Michaelis-Menten kinetics and the mass conservation equations.

Cell growth and death

Equations (3.1) to (3.3) are continuity equations that describe the total (X_T), viable (X_v) and non-viable (X_d) cell numbers present in the shake flask culture.

$$\frac{dX_T}{dt} = \mu X_v - k_{lys} X_d \tag{3.1}$$

$$\frac{dX_v}{dt} = (\mu - k_d) X_v \tag{3.2}$$

$$\frac{dX_d}{dt} = k_d X_v - k_{lys} X_d \tag{3.3}$$

where μ refers to the specific growth rate, k_d is the specific death rate and k_{lys} represents the specific lysis rate of GS-NS0 cells.

The specific growth rate is assumed to be dependent on the concentration of glucose, as the main nutrient in the culture. The influence of lactate as the main inhibitor of cell growth in this expression was found to be negligible based on the experimental data obtained from our laboratory [personal communication, Wu, 2005]. Therefore, the specific growth

rate, μ, can be represented by a Michaelis-Menten type expression dependent on the extracellular glucose concentration [*GLC*]:

$$\mu = \mu_{\max}\left(\frac{[GLC]-[GLC]_{\min}}{K_{glc}+([GLC]-[GLC]_{\min})}\right) \tag{3.4}$$

where μ_{max} is the maximum possible specific growth rate, $[GLC]_{\min}$ is the minimum threshold glucose concentration and K_{glc} is the Monod constant for glucose consumption. The $[GLC]_{\min}$ term implies that the cells have an inability to absorb glucose once it falls below a certain minimum concentration.

In addition, the specific death rate, k_d, has been described using an expression adapted from de Tremblay et al. [1992]. This expression once again involves the accumulation of lactate, [LAC], as the main instigator of cell death:

$$k_d = \frac{K_{d,1}}{\mu_{\max} - K_{d,T}[LAC]} \tag{3.5}$$

where $K_{d,1}/\mu_{max}$ is equivalent to the minimum specific death rate (when no lactate is present in the medium) and $K_{d,T}$ is a death rate constant associated with the toxicity of lactate in the medium.

The specific lysis rate, k_{lys}, of cells has been linearly correlated with the specific death rate,k_d, as shown in the following expression:

$$k_{lys} = k_{l,1}k_d - k_{l,2} \tag{3.6}$$

where $k_{l,1}$ is the rate constant related to k_d and $k_{l,2}$ represents the threshold rate below which cell lysis is assumed to be negligible.

Cell metabolism

Cellular metabolism expressions have been derived to describe glucose uptake and lactate production. Expressions for glutamine and ammonia, which are found in most unstructured models, have been omitted since the GS-NS0 cell line used in this study does not require exogenous glutamine. In addition, the accumulation of ammonia in the GS-NS0 cultures has been shown to be less than 1 mM [Wu, 2006], and hence it is not expected to reach toxic

proportions based on the concentrations reported in the literature (approximately 2-3 mM, [Schneider et al., 1996]). The glucose uptake rate is described as follows:

$$\frac{d[GLC]}{dt} = -q_{glc} X_v \tag{3.7}$$

where $[GLC]$ is the glucose concentration and q_{glc} refers to the specific glucose consumption rate of the cells.

The specific glucose consumption rate, q_{glc}, comprises of two terms: a "maintenance energy" term, m_{glc} [Jang and Barford, 2000], which describes consumption at zero cell growth, as well as a Michaelis-Menten type term that is dependent on the glucose concentration in the extracellular medium:

$$q_{glc} = m_{glc} + K_{glc,\max} \frac{[GLC]-[GLC]_{\min}}{K_{glc,1} - \left([GLC]-[GLC]_{\min}\right)} \tag{3.8}$$

where $K_{glc,max}$ is the maximum uptake rate of glucose by the cells and $K_{glc,1}$ is the Monod constant for glucose consumption.

The accumulation of lactate in the extracellular medium, $[LAC]$, is given by:

$$\frac{d[LAC]}{dt} = q_{lac} X_v \tag{3.9}$$

where q_{lac} is the specific production rate of lactate by the cells.

The specific production rate of lactate, q_{lac}, includes a minimum lactate production term, m_{lac}, as well as a glucose uptake dependent term:

$$q_{lac} = q_{glc} Y_{lac,glc} + m_{lac} \tag{3.10}$$

where $Y_{lac,glc}$ refers to the yield of lactate from glucose.

Antibody production

This section describes the structured part of the hybrid model, which is based on the antibody synthesis and secretion pathway model proposed by Bibila [1991]. Expressions represent the intracellular mass balances for heavy and light chain mRNA species, heavy and light polypeptide chains, as well as the fully formed antibody molecule in a single cell. The

accumulation of heavy (H) and light (L) chain messenger RNA molecules, m_H and m_L, within a cell are represented by equations (3.11) and (3.12):

$$\frac{dm_H}{dt} = S_H - k_H m_H - \mu\, m_H \tag{3.11}$$

$$\frac{dm_L}{dt} = S_L - k_L m_L - \mu\, m_L \tag{3.12}$$

where S_H and S_L are the transcription rates of H and L messenger RNA molecules respectively. The specific decay rates of the H and L messenger RNA molecules, k_H and k_L, are assumed to be equal and can be derived from the half-life of the molecules, $t_{1/2}$:

$$k_H = k_L = \frac{\ln 2}{t_{1/2}} \tag{3.13}$$

Similarly, continuity equations can be written for the H and L polypeptide chain concentrations, $[H]$ and $[L]$, as well as the concentration of the antibody assembly intermediate, the half-molecule, HL ($[HL]$):

$$\frac{d[H]}{dt} = T_H m_H - \mu\, m_H - R_H \tag{3.14}$$

$$\frac{d[L]}{dt} = T_L m_L - \mu\, m_L - R_L \tag{3.15}$$

$$\frac{d[HL]}{dt} = R_{HL} - 2R_{Ab} - \mu[HL] \tag{3.16}$$

where T_H and T_L are the specific translation rates of the H and L polypeptide chains, R_H and R_L are the rate of consumption of the H and L chains in antibody assembly, R_{HL} is the rate of formation of the HL half-molecule and R_{Ab} is the rate of formation of the full H_2L_2 molecule.

The cB72.3 antibody produced belongs to the IgG_4 subclass and its main assembly pathway can be summarized by the following reaction scheme proposed by Percy et al. [1975]:

$$H + L \overset{k_{HL}}{\Rightarrow} HL \tag{3.17}$$

$$HL + HL \overset{k_{HH}}{\Rightarrow} H_2L_2 \tag{3.18}$$

Assuming that mass action kinetics applies in the above reaction pathway, the reaction rates can therefore be represented by the following equations:

$$R_H = R_L = R_{HL} = k_{HL}[H]\ [L] \tag{3.19}$$

$$R_{Ab} = k_{HH}[HL][HL] \tag{3.20}$$

where k_{HL} and k_{HH} are the assembly rate constants for the reactions depicted by Equations 3.17 and 3.18 respectively.

The mass balance of the fully formed antibody molecule in the endoplasmic reticulum (ER), $[H_2L_2]_{ER}$ is hence given by:

$$\frac{d[H_2L_2]_{ER}}{dt} = R_{Ab} - k_{ER}[H_2L_2]_{ER} - \mu[H_2L_2]_{ER} \tag{3.21}$$

where k_{ER} is the rate constant for antibody transport from the ER to the Golgi complex and can be determined by the time required for transportation of half the number of total H_2L_2 molecules from the ER to the Golgi complex, $t_{1/2,ER}$:

$$k_{ER} = \frac{\ln 2}{t_{1/2,ER}} \tag{3.22}$$

A similar mass balance can be derived for the antibody molecule in the Golgi complex:

$$\frac{d[H_2L_2]_G}{dt} = k_{ER}[H_2L_2]_{ER} - k_G[H_2L_2]_G - \mu[H_2L_2]_G \tag{3.23}$$

where k_G is the rate constant for antibody transport from the Golgi complex to the extracellular medium (ECM) and can be determined by the time required for transportation of half the number of total H_2L_2 molecules from the Golgi complex to the ECM, $t_{1/2,G}$:

$$k_G = \frac{\ln 2}{t_{1/2,G}} \tag{3.24}$$

Finally, the accumulation of antibody in the medium, $[H_2L_2]_{ECM}$ is derived from the following expression:

$$\frac{d[H_2L_2]_{ECM}}{dt} = X_V \, k_G [H_2L_2]_G \tag{3.25}$$

Initial parameter values for the hybrid model were determined using both existing literature data for the intracellular antibody production process, as well as currently available data on the GS-NS0 cell system, based on a series of shake flask batch cultures carried out by Wu et al. [2004]. These parameter values can be found in Appendix A.

3.2.3 Modelling environment

The mathematical simulation of the proposed antibody production model has been carried out using a commercially available dynamic modelling software called gPROMS [Process Systems Enterprise Ltd., 2002]. gPROMS is a well established simulation and optimisation engine, originally developed for the design of chemical plants. The ability of the software to carry out dynamic simulations allows for the tracking of changes in the concentration of intracellular intermediates with time. In addition, the program has a parameter estimation module that can be used for the estimation of parameters from the experimental data generated.

3.2.4 Adaptation of the single cell model (Sanderson)

Description of the single cell model

The single cell model (SCM) first developed for hybridoma cells by Sanderson [1997], has been adapted in this study to test the validity of the hybrid model and to provide a basis for comparison of the model outputs. The single cell model takes into consideration the major intracellular metabolic processes of glycolysis, tri-carboxylic acid (TCA) cycle, basic amino acid and fatty acid metabolism, as well as the external process of glutaminolysis. The types of mathematical expressions used in the model will be briefly described in this section. A complete description of these expressions can be found in [Sanderson, 1997].

Firstly, the reaction rates for the intracellular metabolic processes are described using an adapted form of Michaelis-Menten kinetics, which takes into consideration the effects of multiple reactants as well as any feedback inhibition effects caused by products or other components. The adapted Michaelis-Menten kinetics has also been used to represent the incorporation of various media components into cells (specific growth rate) and antibody product (q_{Ab}). In this way, the antibody production rate is directly linked to the concentration of the individual amino acids and nutrients available in the cell. Additionally, the rate of cell death is presented as a function of the specific growth rate of the cells. Transport of components into and out of the cell is modelled using another form of the Michaelis-Menten expression, in which the difference in extracellular and intracellular concentrations of each component is the driving force for transport. Finally, each of the different nutrient or metabolite species present in the cell are represented by general mass conservation equations in the form:

$$\begin{matrix} \textit{Accumulation} \\ \textit{Rate} \end{matrix} = \begin{matrix} \textit{Inflow} \\ \textit{Rate} \end{matrix} - \begin{matrix} \textit{Outflow} \\ \textit{Rate} \end{matrix} + \begin{matrix} \textit{Generation} \\ \textit{Rate} \end{matrix} - \begin{matrix} \textit{Consumption} \\ \textit{Rate} \end{matrix} \tag{3.26}$$

Hence, the accumulation of the species inside the cell is given by the combination of the rates of reaction, the dilution rate caused by cell growth and the consumption of the species as it is incorporated into new cells or used in the production of antibody.

Application of the SCM to GS-NS0 cell system

In the adaptation of the SCM for the GS-NS0 cell system, a number of modifications had to be made in order to accommodate for differences in the characteristics of hybridoma and GS-NS0 cells. A key change was in the removal of the extracellular description of glutaminolysis, based on the fact that GS-NS0 cells do not require an exogenous glutamine supply. Additionally, some model parameters values were changed based on existing data for the GS-NS0 cell system [Wu et al., 2004]. Firstly, parameters related to the glutamine to glutamate conversion pathway ($V_{M,GLN}$ and $K_{I,ATP4}$) have been dampened due to the ability of GS-NS0 cells to synthesise glutamine intracellularly. Alterations in parameter values relating to the specific growth, death and antibody production, as well as glucose and lactate metabolism, have been made to take into consideration differences between the metabolic

usage and growth behaviour of the GS-NS0 and hybridoma cell lines. The parameters whose values have been changed are shown in Table 3.1.

Parameter [a]	Units	Values used [b]
V_{CELL}	μL	1.72×10^{-6}
$V_{M,CELL}$	μmol L(cell)$^{-1}$ hr^{-1}	0.045
$K_{I,\ LAC}$	μmol L(cell)$^{-1}$	1.8×10^{4}
K_{SDR}	hr^{-1}	1.5×10^{-3}
$K_{D,XD}$	hr^{-1}	5×10^{-4}
MW_{AB}	-	150
$V_{M,\ AB}$	μmol L(cell)$^{-1}$ hr^{-1}	3
$V_{M,GL}$	μmol L(cell)$^{-1}$ hr^{-1}	2×10^{5}
K_{GL}	μmol L(cell)$^{-1}$	3.5×10^{3}
$V_{M1,PY}$	μmol L(cell)$^{-1}$ hr^{-1}	1.20×10^{7}
$K_{I,ATP4}$	μmol L(cell)$^{-1}$	2.25×10^{3}
$V_{M,GLN}$	μmol L(cell)$^{-1}$ hr^{-1}	7.65×10^{2}
$V_{M1,SER}$	μmol L(cell)$^{-1}$ hr^{-1}	5.00×10^{3}

[a] For parameter descriptions, refer to [Sanderson, 1997]

[b] Parameters are based on [Sanderson, 1997] and fitted to GS-NS0 data from [Wu et.al., 2004].

Table 3.1. Summary of key parameter changes for the SCM.

3.3 Global sensitivity analysis of the hybrid model

The importance of carrying out a detailed analysis on a model after it has been developed has been discussed in Section 2.4.3. As mentioned previously, a global sensitivity analysis (GSA) has been conducted on the hybrid model as it is able to provide detailed quantitative information on each model parameter, thereby facilitating the identification of key parameters crucial to the antibody production process.

There are a number of GSA techniques that can be used to evaluate the sensitivity of parameters in a model. These include correlation ratios, the Fourier amplitude sensitivity test (FAST) [Saltelli, 2000] and the Sobol' method [Sobol', 2001]. For this study, the Sobol' GSA method has been chosen as its number generator, known as a low discrepancy sequence, is able to sample the defined parameter space more uniformly than random number generators (for example, those used in Monte-Carlo methods), hence leading to more efficient coverage of the space [Sidoli et al., 2005]. The Sobol' GSA is a variance-based Monte-Carlo method which evaluates the effect of each parameter on model output by the computation of sensitivity indices (SI), whose values range from 0 to 1. Two SI values are calculated for each parameter - the individual SI (SI_{ind}), which represents the main effect of the parameter on model output and the total SI (SI_{tot}), which includes both the main effect of the parameter as well as the additional effects caused by interaction of the parameter with other parameters. Parameters with high SI values are considered to have a larger impact on the model output.

3.3.1 Derivation of sensitivity indices

Sobol' [2001] considers an integrable function, $f(x)$, which is written in the form:

$$f(x) = f_o + \sum_{s=1}^{n} \sum_{i_1 < \ldots < i_s}^{n} f_{i_1 \ldots i_s}\left(x_{i_1}, \ldots, x_{i_s}\right) \tag{3.27}$$

where $1 \le i_1 < \ldots < i_S < n$.

The function represented by Equation 3.27 implies that *f(x)* can be broken down into terms of different orders:

$$f(x) = f_o + \underbrace{\sum_i f_i(x_i)}_{1^{st}\text{ order term}} + \underbrace{\sum_{i<j} f_{ij}(x_i, x_j)}_{2^{nd}\text{ order term}} + \ldots + \underbrace{f_{12\ldots n}(x_1, x_2, \ldots, x_n)}_{n^{th}\text{ order term}} \tag{3.28}$$

Equation 3.27 can then be defined as an Analysis of Variances (ANOVA)-representation of *f(x)* if

$$\int_0^1 f_{i_1\ldots i_s}(x_{i_1}, \ldots, x_{i_s})\, dx_k = 0 \qquad \text{for} \qquad k = i_1, \ldots, i_s . \tag{3.29}$$

If *f(x)* is square integrable, the total variance, *D*, can then be calculated by squaring Equation 3.27 and integrating over n dimensions:

$$D = \int f^2(x)dx - f_o^2 = \sum_{s=1}^{n} \sum_{i_1<\ldots<i_s}^{n} \int f_{i_1\ldots i_s}^2 dx_{i_1\ldots i_s} \tag{3.30}$$

Therefore, if

$$D_{i_1\ldots i_s} = \int f_{i_1\ldots i_s}^2 dx_{i_1}\ldots dx_{i_s} \tag{3.31}$$

then

$$D = \sum_{s=1}^{n} \sum_{i_1<\ldots<i_s}^{n} D_{i_1\ldots i_s} \tag{3.32}$$

where $D_{i_1\ldots i_s}$ represents the partial variances in the value of *f(x)* as a result of simultaneous changes in the values of factors i_1 to i_S. Equation 3.32 thus states that the sum of all partial variances associated with factors i_1 to i_S is equal to the total variance of the function. The global sensitivity indices can therefore be defined as:

$$S_{i_1\ldots i_s} = \frac{D_{i_1\ldots i_s}}{D} \tag{3.33}$$

In this study, the function *f(x)* is equivalent to the extracellular antibody concentration, which is the key output from the hybrid model. In addition, the parameters in the model are represented by the factors i_1 to i_S. The individual SI of each parameter is given by the first order indices $S_{i_1}, S_{i_2}, \ldots, S_{i_S}$ while the total SI of a parameter is given by the sum

of first order and all higher order indices associated with that parameter. For instance, the individual SI of parameter i_1 is S_{i_1} while its total SI, assuming there are n parameters in the model, is given by:

$$SI_{tot} = S_{i_1} + \sum_{1<j}^{n} S_{i_1 i_j} + \sum_{1<j<k}^{n} S_{i_1 i_j i_k} + \ldots + S_{i_1 i_2 \ldots i_n} \tag{3.34}$$

3.4 Results and analyses

3.4.1 Normal osmotic conditions – hybrid model and SCM outputs

In this section, the hybrid model and adapted SCM simulation outputs are compared to the experimental data obtained by Wu et al. [2004] for GS-NS0 cells. Figures 3.2 a to 3.2 f show the experimental and predicted trends in cell number, growth and death rates, metabolism and antibody production for the hybrid and SCM. The viable cell number is well predicted by both the hybrid and SCM (Figure 3.2 a). In the case of the total cell number, while the hybrid model has a tendency to overestimate the total cell number at the stationary and early decline culture phases, it is able to capture the experimental trend more closely than the SCM (Figure 3.2 b). The agreement of both models with experimental data for the dead cell number appears quite satisfactory (Figure 3.2 b). Although both models are able to predict specific cell growth rates reasonably well, however, it can be seen that the SCM predicted cell death rate deviates from experimental data as the culture enters the decline phase (Figure 3.2 c). The differences in trends at this late culture phase may be attributed to the different death rate expressions used in both models. Specifically, the hybrid model utilizes an expression that takes into account the maximum specific cell growth rate and the detrimental effects of lactate accumulation while the death rate expression in the SCM is a correlation based primarily on the specific cell growth rate. The results also indicate that the hybrid model simulations for glucose consumption (Figure 3.2 d) and lactate production (Figure 3.2 e) are in better agreement than those produced by the SCM particularly beyond the mid-exponential phase of the culture (>48 hrs). Finally, the antibody accumulation profile (Figure 3.2 f) indicates that the predicted final antibody titer for both models is within 7% of the

experimental value, which is well within the proposed experimental error margin of 10% normally associated with cell culture data [Sanderson, 1997]. The above results confirm the predictive ability of the hybrid model for the GS-NS0 system, which in certain cases performs better than the complex SCM.

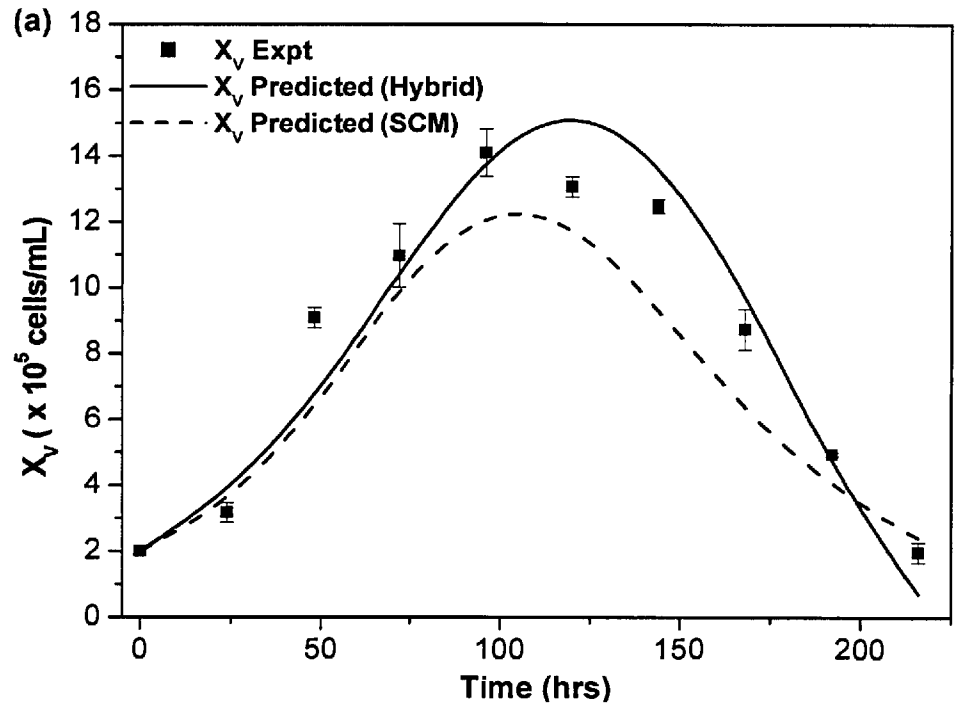
(a)
X_V Expt
X_V Predicted (Hybrid)
X_V Predicted (SCM)
X_V (x 10^5 cells/mL)
Time (hrs)

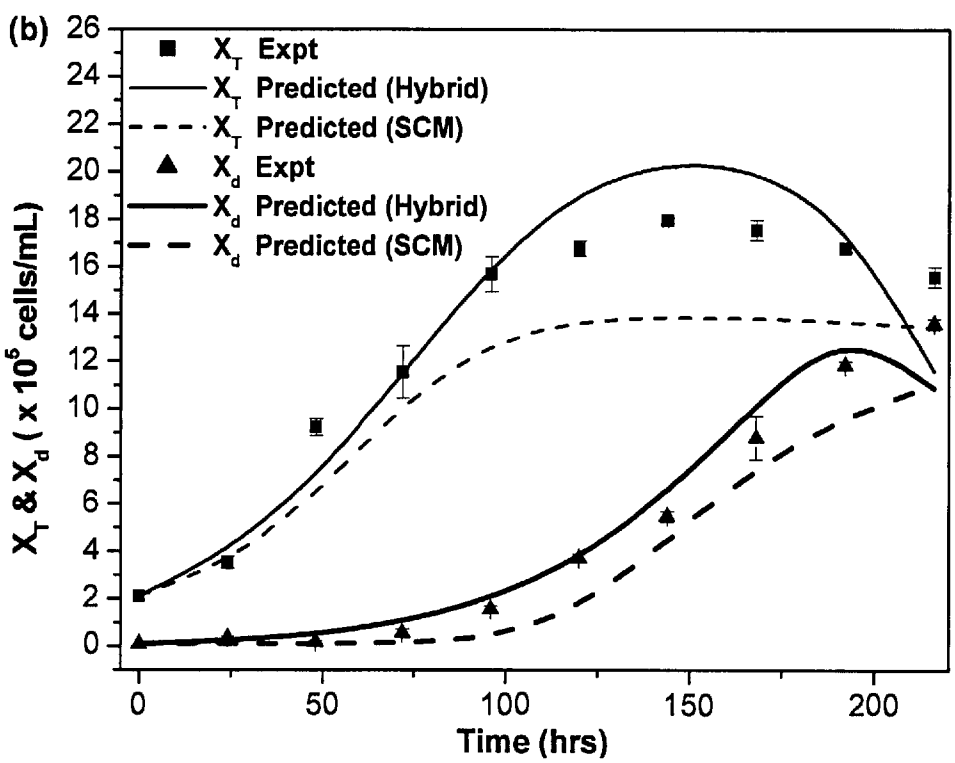
(b)
X_T Expt
X_T Predicted (Hybrid)
X_T Predicted (SCM)
X_d Expt
X_d Predicted (Hybrid)
X_d Predicted (SCM)
X_T & X_d (x 10^5 cells/mL)
Time (hrs)

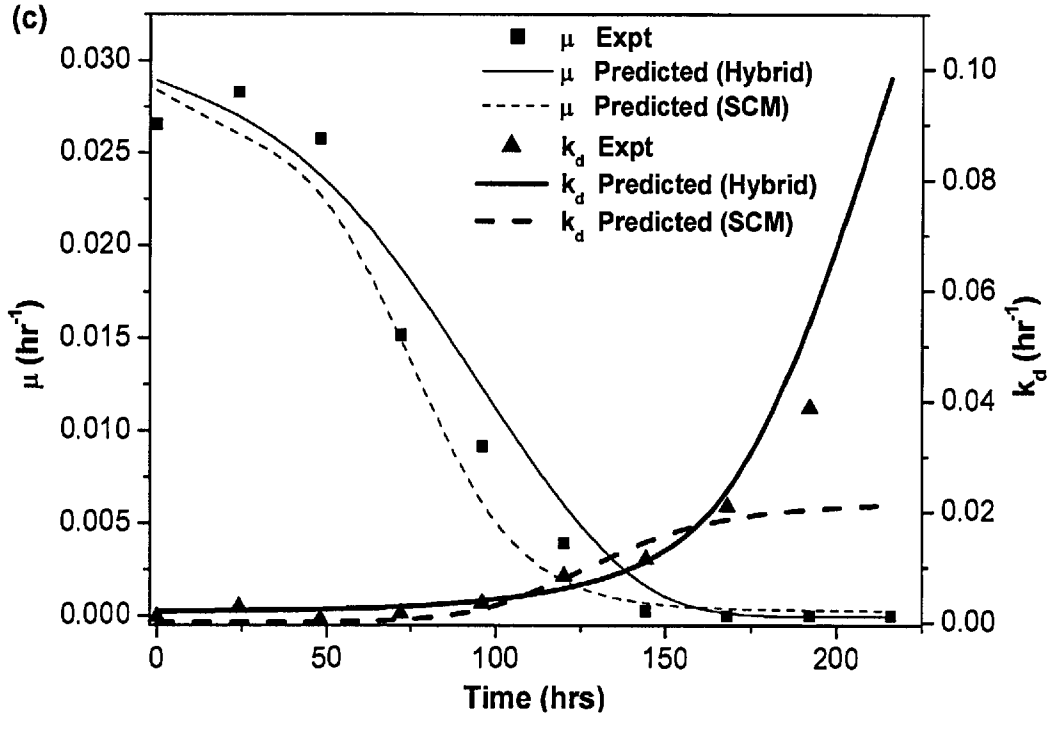
(c)
μ Expt
μ Predicted (Hybrid)
μ Predicted (SCM)
k_d Expt
k_d Predicted (Hybrid)
k_d Predicted (SCM)
μ (hr^{-1})
k_d (hr^{-1})
Time (hrs)

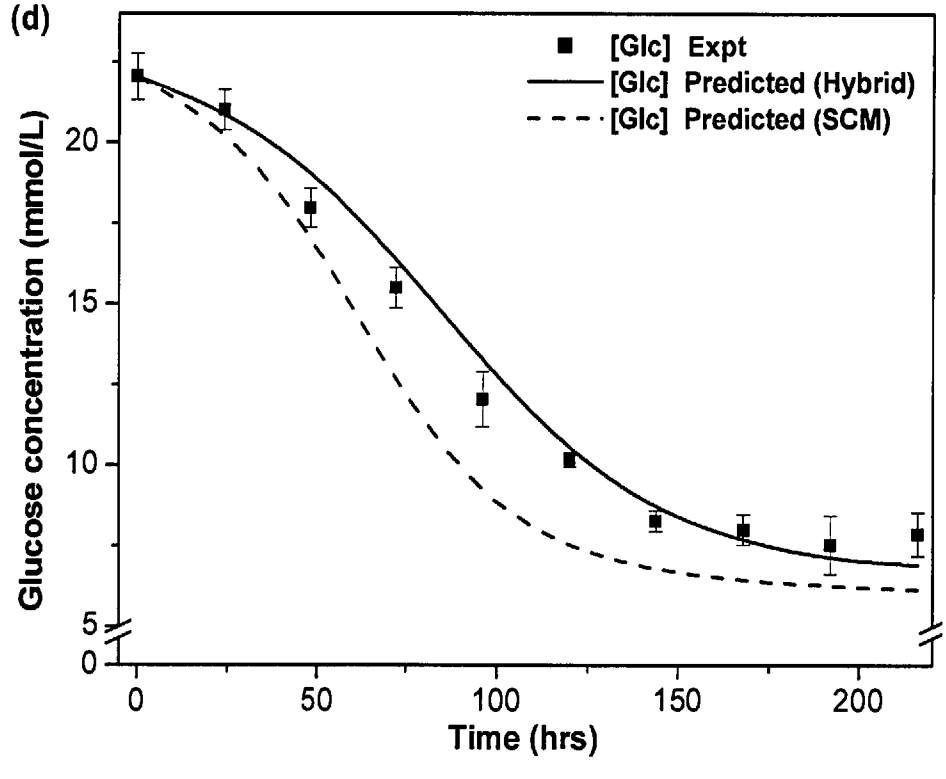
(d)
[Glc] Expt
[Glc] Predicted (Hybrid)
[Glc] Predicted (SCM)
Glucose concentration (mmol/L)
Time (hrs)

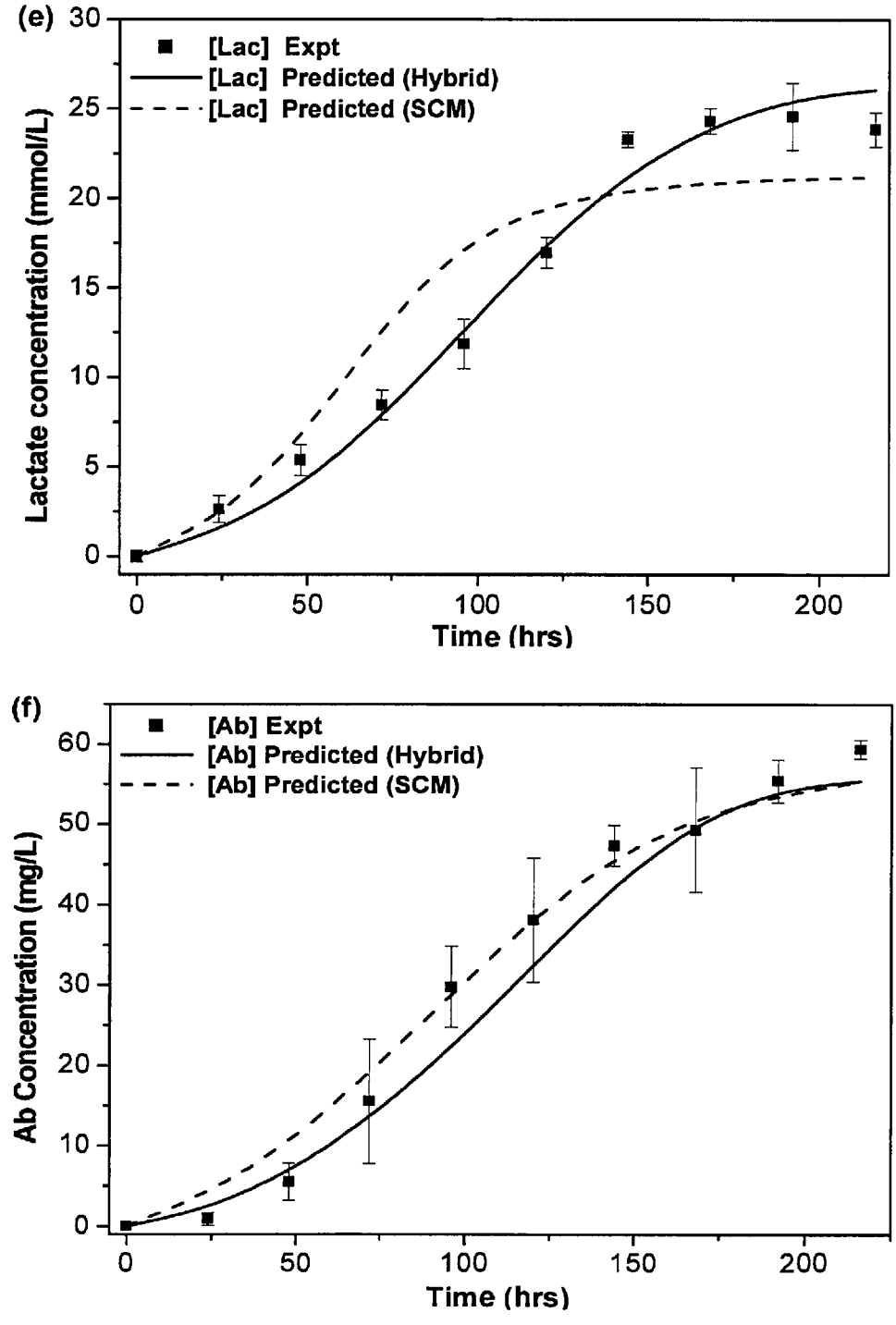

Figure 3.2. Comparison of single-cell model (SCM) and hybrid model (Hybrid) simulation results with experimental data (Expt) for the GS-NS0 system under normal culture conditions (290 mOsm/kg), as obtained from reference [Wu et al., 2004]: (a) viable cell number (X_v), (b) total (X_T) and dead (X_d) cell numbers, (c) specific growth (μ) and death (k_d) rates, (d) glucose concentration in the medium ([Glc]), (e) lactate concentration in the medium ([Lac]), and (f) antibody concentration in the medium ([Ab]).

3.4.2 Results and analysis of GSA

The Sobol' GSA method used here to analyse the hybrid model has been described in Section 3.3. The key advantage of the Sobol' method is that it provides detailed quantitative data regarding the relative importance of each parameter on the antibody production process by the computation of the sensitivity indices, SI_{ind} and SI_{tot}. In this study, GSA has been focused mainly on parameters specifically related to the antibody production mechanism, whose initial values have been largely obtained from literature. To capture possible dynamic variations in the impact of the parameters on antibody production at different culture phases, the analysis is conducted at 24-hour intervals from the mid-exponential phase (48 hrs) to the decline phase (192 hours). Parameter behaviour in the early exponential phase (24 hrs) has been omitted as the antibody produced during this time period was relatively insignificant in comparison to later culture phases.

Figure 3.3 a shows the SI_{ind} and SI_{tot} for the model parameters averaged over all time points. It can be observed that the individual sensitivity indices for the specific heavy and light chain transcription (S_H, S_L) and translation (T_H, T_L) rates are significant. Figure 3.3 b, which presents SI_{ind} for all parameters under study at different time points, further reveals that the SI values of the specific transcription and translation rates remain consistently high throughout the entire culture. Differences in the individual impact of each parameter as the culture progresses are also highlighted by Figure 3.3 b, where it can be seen that a number of parameters increase while others decrease in importance with respect to their effects on antibody production. The GSA confirms the importance of transcriptional and translational processes within the antibody production mechanism. Furthermore, the sensitivity of certain parameters varies with culture time, which is in agreement with their biological function. Specifically, Figure 3.3 c shows that the initial intracellular amounts of heavy and light chains appear to be important at an early culture stage. Their impact on antibody production decline rapidly at later culture stages as reflected by the decrease in SI_{ind} and SI_{tot}. Conversely, the impact of the half-life of heavy and light mRNA molecules on the antibody production titer is predicted to be larger in the stationary and decline phases (Figure 3.3 d) based on the increasing SI_{ind} and SI_{tot} values.

Additionally, the interaction effects, given by the difference between SI_{tot} and SI_{ind} for the significant parameters have been assessed by further GSA, for which the key parameters, S_H, S_L, T_{H0} and T_{L0}, are grouped as a single parameter and the sensitivity indices recalculated. Consequently, the SI_{ind} of the grouped parameters is found to constitute more than 90% of the SI_{tot}, indicating that any key interactive effects are likely to be among the significant parameters, rather than with other less significant parameters.

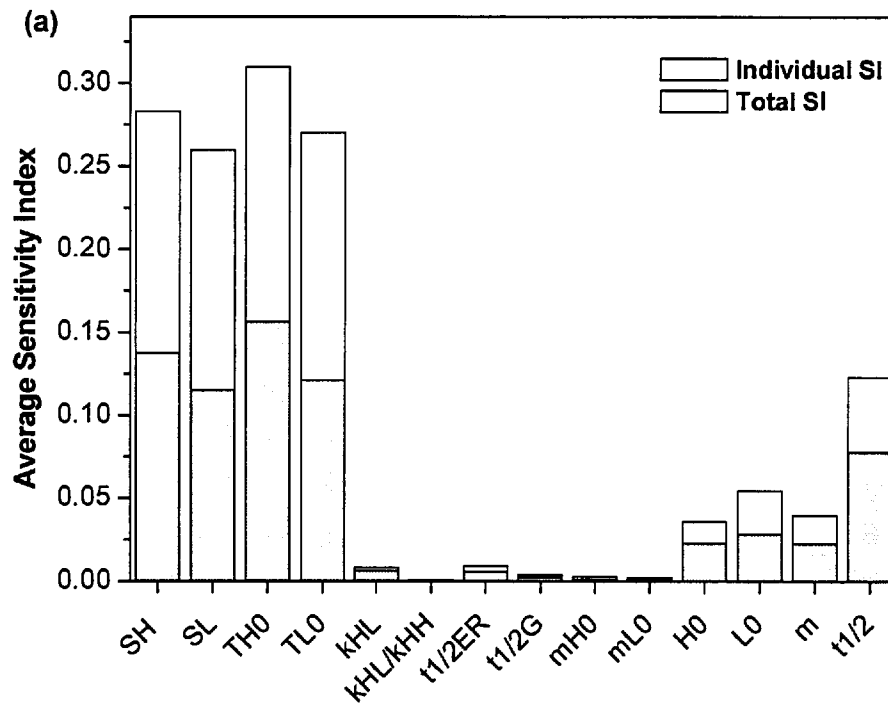
(a)
Individual SI
Total SI
Average Sensitivity Index
0.00
0.05
0.10
0.15
0.20
0.25
0.30
SH
SL
TH0
TL0
kHL
kHL/kHH
t1/2ER
t1/2G
mH0
mL0
H0
L0
m
t1/2

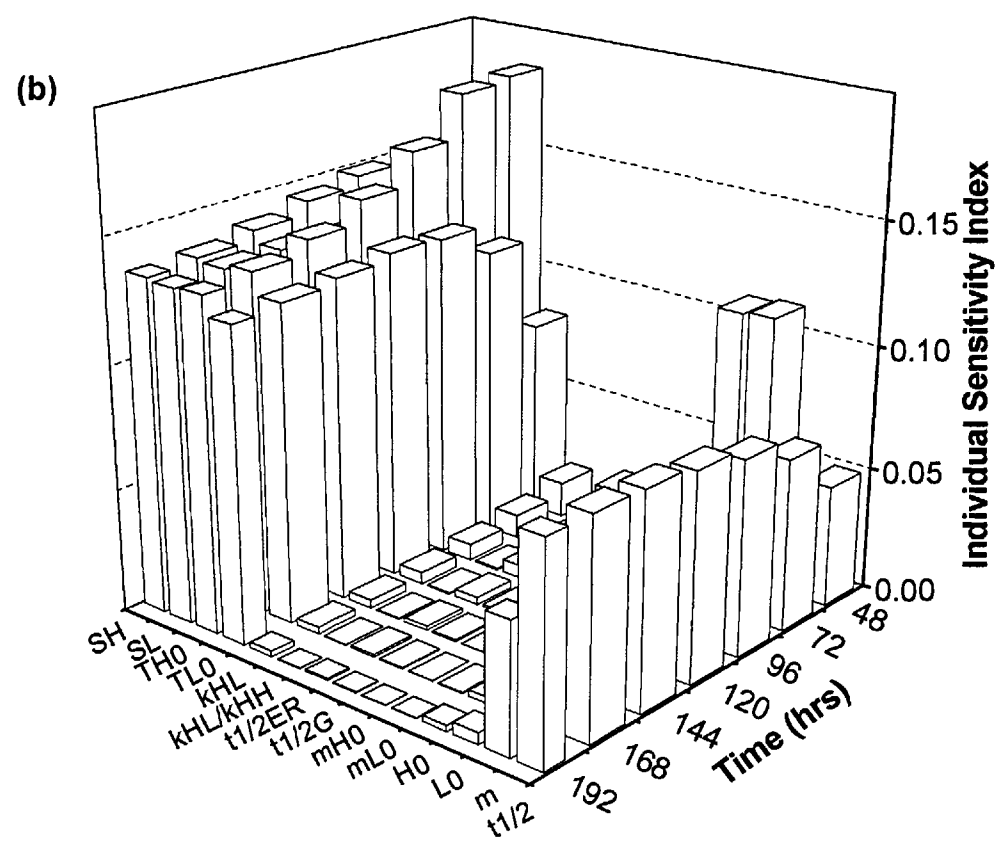
(b)
Individual Sensitivity Index
0.00
0.05
0.10
0.15
Time (hrs)
48
72
96
120
144
168
192
SH
SL
TH0
TL0
kHL
kHL/kHH
t1/2ER
t1/2G
mH0
mL0
H0
L0
m
t1/2

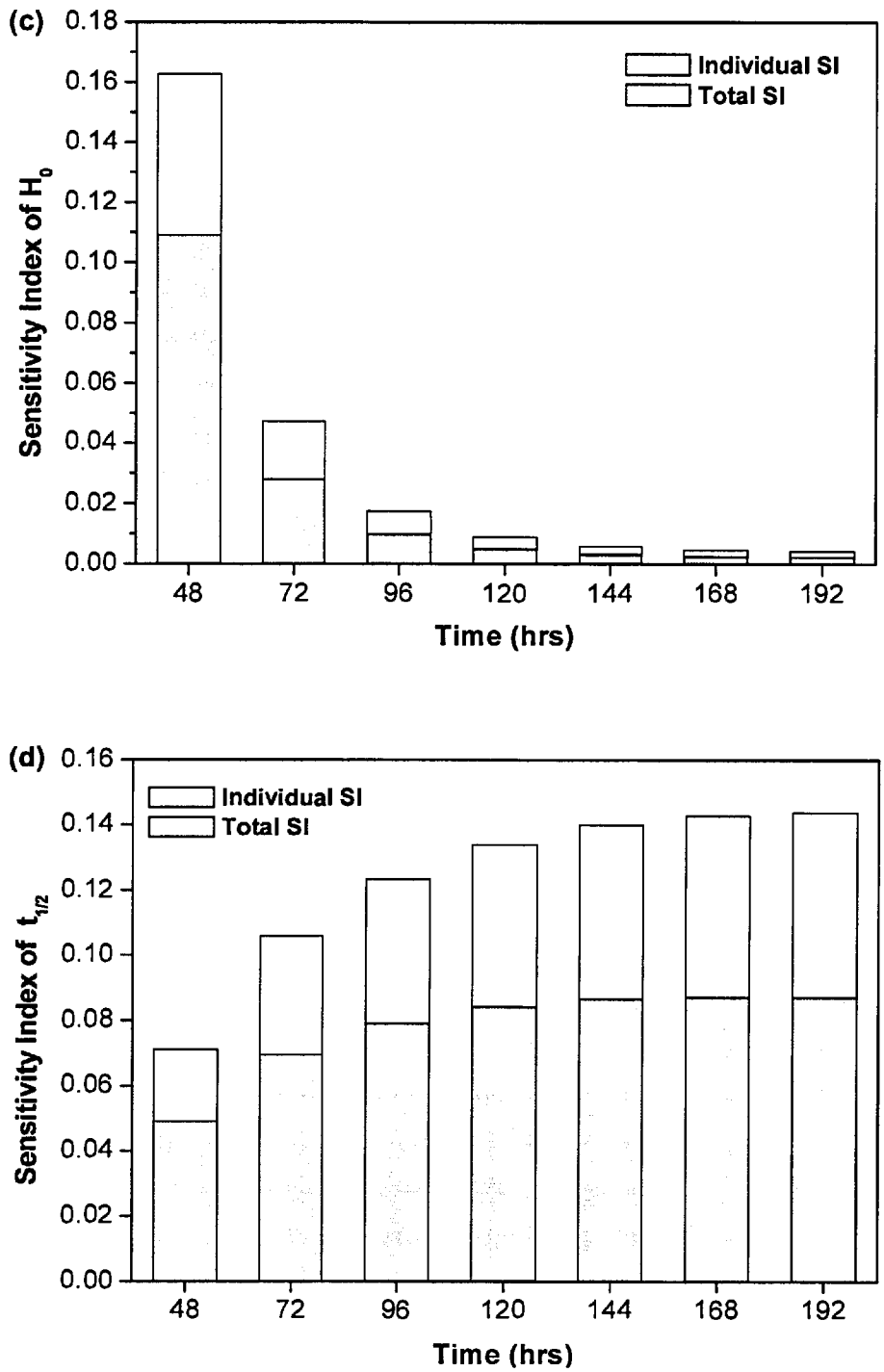

Figure 3.3. (a) Average individual and total sensitivity indices of all parameters, (b) Individual sensitivity indices of parameters over all time points, (c) Individual and total sensitivity indices of initial heavy chain concentration, H0, over culture time, (d) Individual and total sensitivity indices of half-lives of mRNA, t1/2, over culture time.

GSA at hyperosmotic conditions

In order to ascertain that the GSA results at normal osmotic conditions are still applicable with changes in the unstructured model parameters (particularly the cell growth, death and metabolism parameters) at hyperosmotic culture conditions, the GSA has been repeated for hyperosmotic culture simulations at 24-hour time points from the mid-exponential phase (72 hrs) to the decline phase (288 hrs) of the culture. The SI_{ind} and SI_{tot} values averaged over all time points for both normal and hyperosmotic culture conditions are summarised in Table 3.2. It can be observed that the SI values in both cases are relatively similar in terms of parameter importance and therefore verify that the results of the GSA are valid under both sets of culture conditions.

Parameter	Av SI_{ind} (290)	Av SI_{ind} (450)	Av SI_{tot} (290)	Av SI_{tot} (450)
S_H	0.138	0.143	0.283	0.288
S_L	0.115	0.116	0.260	0.258
T_{H0}	0.156	0.136	0.310	0.278
T_{L0}	0.121	0.102	0.270	0.237
k_{HL}	0.006	0.005	0.008	0.006
k_{HL}/k_{HH}	4.29E-04	3.20E-04	0.001	0.001
$t_{1/2,ER}$	0.006	0.007	0.009	0.010
$t_{1/2,G}$	0.002	0.003	0.004	0.004
m_{H0}	0.001	6.13E-05	0.003	1.63E-04
m_{L0}	0.001	3.88E-05	0.002	1.33E-04
H_0	0.023	0.051	0.036	0.074
L_0	0.028	0.047	0.054	0.087
m	0.022	0.005	0.040	0.010
$t_{1/2}$	0.078	0.088	0.123	0.138

Table 3.2. Average parameter SI under normal (290) and hyperosmotic (450) conditions.

3.4.3 Hyperosmotic culture simulations

Figure 3.4 compares the experimental data [Wu et al., 2004] for cell growth, death, metabolism and antibody production under hyperosmotic culture conditions with the simulation results generated by the hybrid model. It is observed that under normal conditions the lag phase is non-apparent, in contrast with the significant lag phase observed under hyperosmotic culture conditions (Figure 3.4 a). Consequently, as an initial approximation based on the presented experimental data, a simple 24-hour lag phase has been implemented for hyperosmotic culture simulations during which it is assumed that there is little cell growth or antibody production. This assumption is reflected in the behaviour of the specific growth rate (Figure 3.4 b) where there is a step increase in its value from 0 to 0.018 hr^{-1} at 24 hours, the point at which significant cell growth and antibody production begins. Despite the basic nature of the above assumption, the simulated trends are in overall agreement with experimental data throughout the course of the culture. In addition, the specific death rate (Figure 3.4 b) and therefore the dead cell number, is well predicted by the hybrid model. The glucose consumption and lactate production (Figure 3.4 c) are also in good agreement with the experimental data.

With the observations derived from GSA, the values of key parameters have been modified systematically based on their relative sensitivity to antibody production (as indicated by the sensitivity indices), as the hybrid model is applied to hyperosmotic culture conditions. A summary of all parameter values used in the simulation of hyperosmotic culture conditions can be found in Appendix A. Of these parameters, the most significant changes involve the heavy and light chain transcription rates (S_H, S_L) and the initial translation rates ($T_{H,0}$, $T_{L,0}$). It can be seen that higher values for these parameters are required in order to accurately describe antibody production at hyperosmotic conditions (Figure 3.4d). However, the selected parameter values still fall within the recommended physiological ranges (S_H, S_L) or are within reported parameter value increases observed under hyperosmotic pressure conditions (T_H, T_L, $t_{1/2}$) [Lee and Lee, 2000]. Consequently, as demonstrated in Figure 3.4d the simulated antibody accumulation in the medium agrees well with the experimental values. The difference between simulated and experimental values at

each time point was less than 10%. These results indicate that the hybrid model predicts hyperosmotic culture behaviour relatively well.

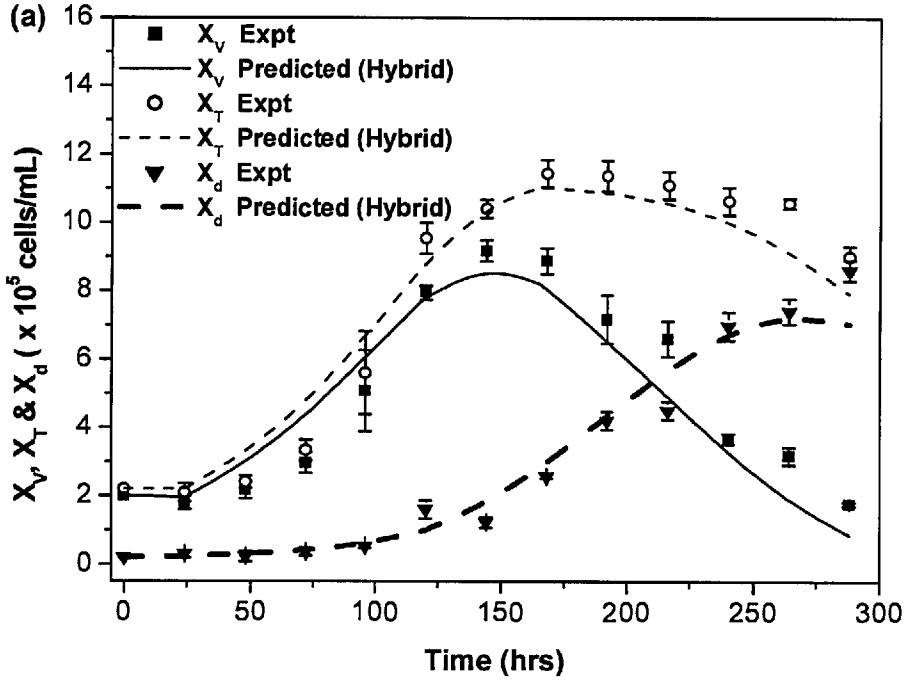
(a)
X_V Expt
X_V Predicted (Hybrid)
X_T Expt
X_T Predicted (Hybrid)
X_d Expt
X_d Predicted (Hybrid)
X_V, X_T & X_d (x 10^5 cells/mL)
Time (hrs)

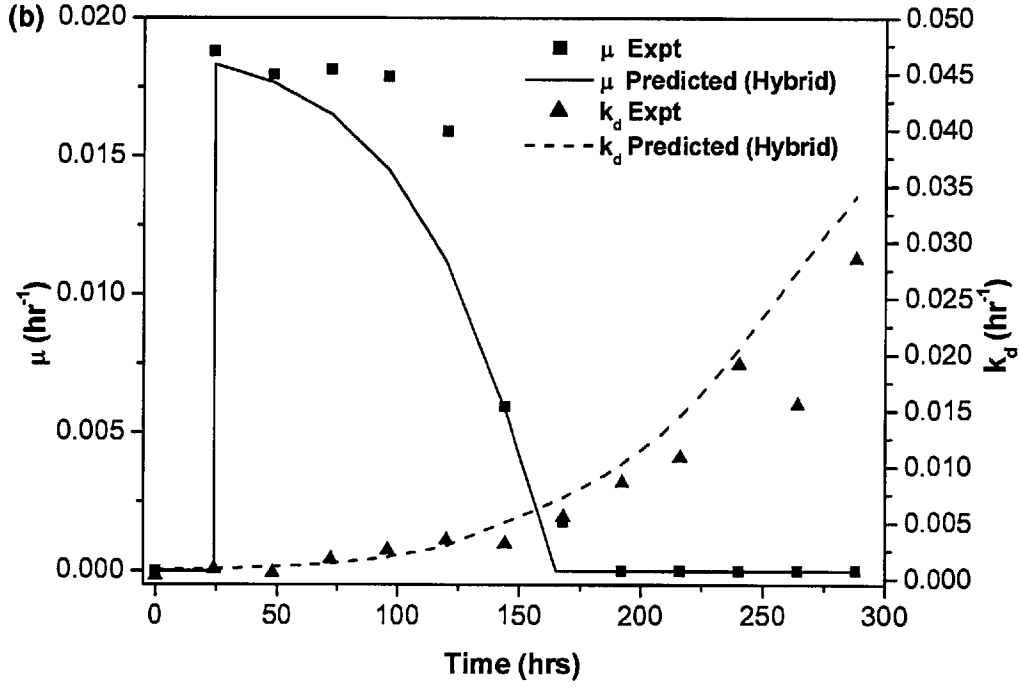
(b)
μ Expt
μ Predicted (Hybrid)
k_d Expt
k_d Predicted (Hybrid)
μ (hr^{-1})
k_d (hr^{-1})
Time (hrs)

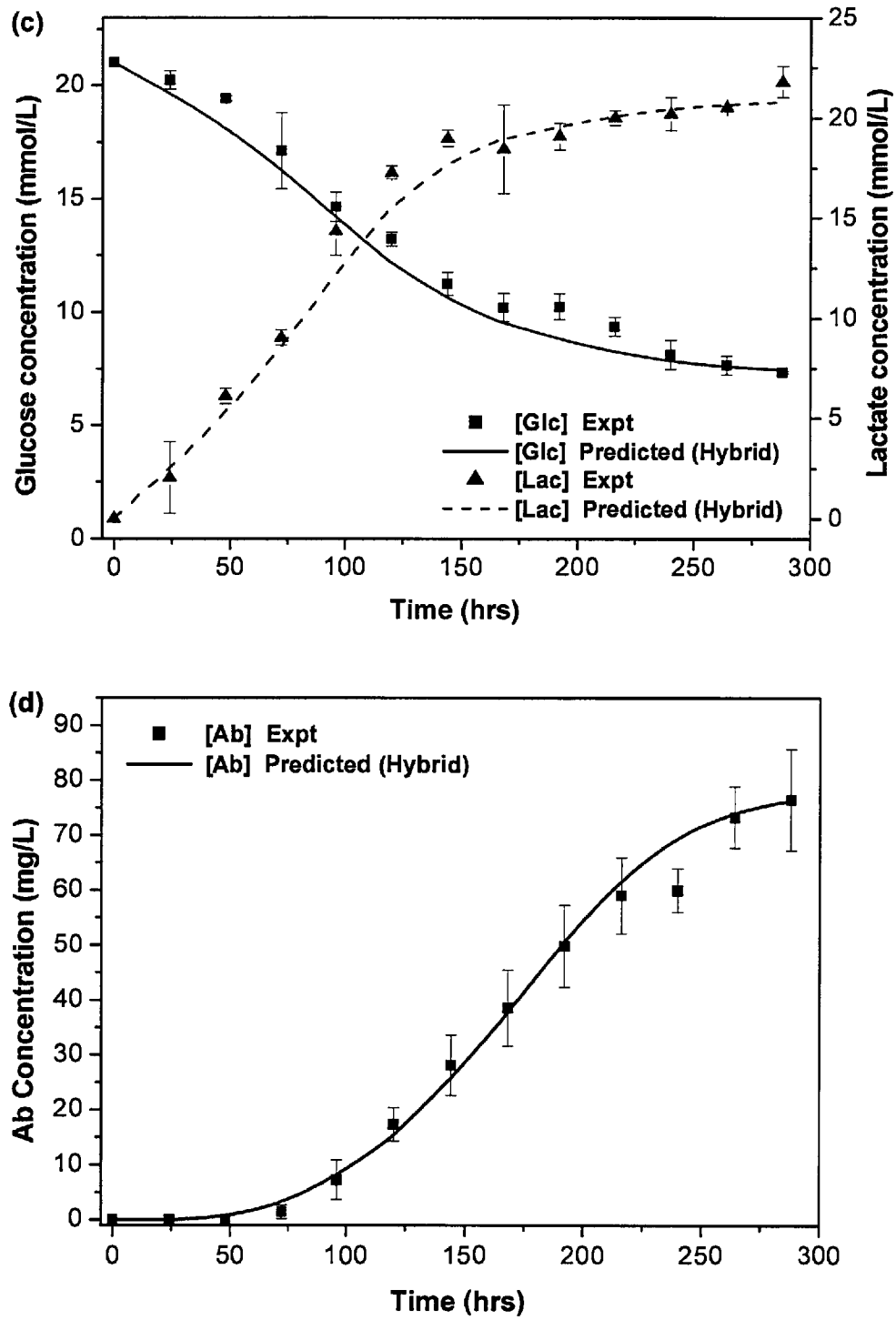

Figure 3.4. Comparison of hybrid model simulation results (Predicted) and experimental data (Expt) for GS-NS0 system under hyperosmotic pressure conditions (450 mOsm/kg) from reference [Wu et al., 2004]: (a) viable, total and dead cell numbers, (b) specific growth and death rates, (c) glucose and lactate concentrations in the medium and (d) antibody concentration in the medium.

3.5 Discussion

The key objective of this chapter was the development of a functional and tractable model that describes the antibody production process in GS-NS0 cells under normal and hyperosmotic culture conditions to within accuracy of ± 30%. The proposed hybrid model is unique to the GS-NS0 cell line and created a link between the metabolic processes in the cell and its antibody formation process. This represents an important advancement since previous models had either focused on the antibody production mechanism or cell metabolism. However, exclusion of cellular metabolism processes might result in the omission of potential effects of energy and precursor availability on the system [Sanderson et al., 1999], while a model based solely on cell metabolism tended to ignore the mechanistic details required to understand the antibody production process. The combination of an unstructured depiction of cell growth and metabolism with a structured representation of the intracellular antibody production mechanism allowed for relationships between metabolism, cell growth, death, and antibody formation to be described mathematically.

Hybrid model and SCM comparisons

Comparing the simulation results from the hybrid model with the results obtained from a complex, highly-detailed SCM indicate that both models predicted GS-NS0 cellular behaviour reasonably well. Nonetheless, two key differences in the predicted trends became evident. The first key difference was the use of differing expressions for the specific death and lysis rates. These expressions were responsible for determining the dead cell number, and hence the number of total cells in the culture. The specific death rate was better described by the hybrid model in an expression that was governed by the maximum specific growth rate and the accumulation of lactate in the medium. In contrast, the specific death rate in the SCM was correlated only to the specific growth rate, which appeared to result in differences between simulated and experimental trends, particularly during the later stages of the culture. It has to be noted that there are numerous correlations available in the literature for the specific death rate, including Michaelis-Menten type expressions [Glacken et al., 1989] and exponential type expressions [DiMasi and Swartz, 1995], some of which were correlated to specific growth rate and others that also involved waste metabolite

concentrations such as ammonia and lactate, or the concentration of rate-limiting substrates such as glutamine [Frahm et al., 2003; Portner and Schafer, 1996]. The wide variety of expressions, therefore, suggested that the specific death rate behaviour was likely to be cell line-specific, which in turn might explain the divergence in experimental and simulated values for the SCM that was originally derived for hybridoma cell cultures. In addition, the specific lysis rate was assumed to be constant in the SCM while it was correlated to the specific death rate in the hybrid model. The positive relationship in the hybrid model between the specific cell lysis rate and the specific death rate accounted for the effects of increasing toxicity of the medium. This led to a more accurate representation of the experimental data and was an improvement over the SCM.

The second difference corresponds to the prediction of glucose consumption and lactate accumulation rates. The SCM tended to predict trends that deviate from experimental observations as the culture progresses, despite prior adjustments for its glucose and lactate parameters. This observation highlights one of the main difficulties in extending the SCM to accurately predict cellular behaviour in other cell lines since it involves more than 350 parameters in order to describe the main intracellular metabolic processes as well as transmembrane transport of more than 50 components. As such, a vast amount of dynamic intracellular data, which at present is still difficult to obtain experimentally, would be required in order to allow for differences in the metabolic behaviour of different cell lines. In addition, it had been recently reported that just 37 out of the 350 parameters in the SCM were considered to be estimable from existing experimental data [Sidoli et al., 2005]. The practical difficulty involved in the accurate determination and analysis of parameter values for the SCM was an essential reason for the development of the simpler hybrid model, which focused particularly on the antibody production pathway. Unlike the SCM, the hybrid model had fewer than 30 parameters, half of which could be derived from existing experimental data. The remaining 13 parameters, which were involved in intracellular antibody formation and transport, could then be analysed in detail by performing GSA. The hybrid model could thus be seen as a successful compromise between the highly detailed structure of the SCM and the "black box" approach of unstructured models since it had the ability to correctly describe cellular and metabolic trends for GS-NS0 cells.

Global sensitivity analysis

GSA allows the incorporation of the entire parameter value ranges while providing quantitative results indicating the significance of each parameter [Saltelli et al., 2004]. This enables the compilation of a comprehensive overview of the individual parameter effects, as well as providing information regarding the existing degree of interaction between parameters. A time-dependent GSA can also identify any significant dynamic variations in SI_{ind} and SI_{tot} for model parameters. Previous research conducted [Kontoravdi et al., 2005; Sidoli et al., 2005] had shown that it was computationally inefficient to include a large number of model parameters in the GSA. In the former study for small size models, the less significant parameters were identified by GSA in the early exponential phase and grouped together in subsequent global sensitivity analyses at other time points. The latter study on the SCM by Sanderson [1997] involved carrying out a parameter perturbation study to determine the set of estimable and inestimable parameters before GSA was used to evaluate the two groups of parameters. Due to these considerations, the GSA in this study focused primarily on parameters within the structured antibody production mechanism, as actual experimental information on their values is scarce in comparison to the growth and metabolism parameters that have been experimentally determined for the GS-NS0 cell line.

The global sensitivity analysis identified parameters that appear to have a large impact on antibody production throughout the culture, as reflected by their consistently high sensitivity indices at all time points. These parameters included the heavy and light chain specific transcription and translation rates, which agreed with literature reports that stress the importance of the transcription [Fox et al., 2005; Lee and Lee, 2000; Yoon et al., 2003] and translation [Bibila, 1991; McKinney et al., 1995] steps in the production mechanism of recombinant proteins (including antibodies). This is in contrast to the time required for intracellular transport of the antibody molecule from the ER to the Golgi complex and subsequently to the extracellular medium, as reflected by the low sensitivity indices of $t_{1/2,ER}$ and $t_{1/2,G}$. The differences in sensitivity indices might be explained by the fact that the accumulation of intracellular IgG chains was mainly dependent on their production rate, regulated through the processes of transcription and translation. Subsequently, an increase in the speed of intracellular transport would lead to a depletion of the intracellular IgG pool.

Thus, the increased transport rate could not be sustained without a corresponding increase in transcription or translation rates. As a result, the effects of $t_{1/2,ER}$ and $t_{1/2,G}$ on increasing antibody production rates tended to be relatively small when compared to those of the transcription and translation parameters. In addition, certain parameters demonstrated a culture time-dependent behaviour following the sensitivity analysis. Specifically, a reduction in the sensitivity indices of the initial intracellular heavy and light chain values reflected their decreasing importance to antibody production as the culture progressed, which was biologically consistent. Early in the culture, the initial pools of heavy and light chains were the main intracellular source for antibody formation. However, as the culture progressed into the mid-exponential phase, the translational process became responsible for controlling the intracellular heavy and light chains concentrations; thus the importance of the initial heavy and light chains values decreased with culture time. Similarly, the half-life of heavy and light mRNA molecules is another example of parameters with a culture time-dependent impact on antibody production. The half-life of the mRNA molecules determines the degradation rate of mRNA in the cell. As the culture progressed and nutrients were used up, the basic components required as "building blocks" for mRNA production also decrease, subsequently causing the accumulation of mRNA molecules in the cell to decline. Minute changes in the mRNA concentration would therefore have a larger effect on antibody production under these conditions. As such, the value of the mRNA half-life had a more significant impact on antibody production towards the stationary and decline phases of the culture.

Extension of model to hyperosmotic conditions

Initially, attempts to extend the model to hyperosmotic culture conditions by modifying the unstructured model parameters in order to reflect the lower cell growth rate and higher metabolic rates proved to be insufficient in providing an accurate depiction of experimental antibody production rates. However, global sensitivity analysis yielded useful information regarding important parameters involved in the antibody production mechanism in GS-NS0 cells. These results were utilised in adapting the model parameters to hyperosmotic culture conditions. In Chapter 2, a number of hypotheses existing in literature regarding the possible

mechanisms of hyperosmolarity in improving antibody production were presented. Here, the changes in parameter values required to accurately reflect antibody production at hyperosmotic culture conditions are discussed in relation to these proposed hypotheses. Increasing the values of the specific transcription and translation rates under hyperosmotic pressure conditions was corroborated by the proposed theories of Oh et al. [1993] and Lin et al. [1999a]. Specifically, Oh and co-workers state that hyperosmotic pressure, together with butyrate treatment, induced transcriptional activation of mRNA due to the change of chromatin structure in the cell nucleus. This stimulation of transcription led to the increase in the amount of heavy and light mRNA chains, which in turn increased antibody productivity. Furthermore, the increase in specific translation rates is supported by the hypothesis proposed by Lin and co-workers [Lin et al., 1999a], which states that hyperosmotic pressure enhances the uptake of nutrients, such as glucose, resulting in an increase in ATP production rates. Translation is known to be an energy consuming process [Pestova and Hellen, 2000] and increases in ATP levels therefore resulted in higher heavy and light chain translation rates in the cells; thus the higher antibody productivity. Additionally, a study on hybridoma cells by Sun et al. also reported an overall increase in protein translation rates as a result of hyperosmotic culture conditions [Sun et al., 2004]. The simulation results under hyperosmotic pressure conditions also showed higher specific glucose consumption rates, as reflected in the higher maximum glucose consumption coefficient. This is consistent with Lin's hypothesis [Lin et al., 1999a]. In addition, the decrease in the value of the mRNA half-life under hyperosmotic culture conditions is supported by the findings of a study based on hybridoma cells [Lee and Lee, 2000]. The changes in key parameters, together with implementation of a lag phase, have enabled the hybrid model to capture the behaviour of extracellular antibody accumulation under hyperosmotic pressure conditions fairly accurately.

3.6 Conclusions

In this chapter, a hybrid model was developed and its validity in describing the cellular and antibody production processes for the GS-NS0 system successfully demonstrated.

Comparisons between the simulation trends of the SCM and hybrid models also highlighted the difficulties involved in the adaptation of a highly structured and complex model (SCM) for a different cell line, due primarily to the large number of inestimable model parameters involved. The GSA conducted on the hybrid model aided in the identification of parameters that heavily influence the antibody production process and established the time-dependent variation in the significance of certain parameters. The information gathered from the GSA was then used effectively to extend application of the hybrid model to hyperosmotic culture conditions. The GSA findings also highlighted the parameters in the model whose values significantly affect antibody production. Based on the proposed 10% error margin inherent in cell culture data [Sanderson, 1997], the key parameters involved in the antibody production process (as identified by average SI values greater than 0.1 from Table 3.2) are: the H and L mRNA transcription rates, S_H and S_L, the initial H and L chain translation rates, T_{H0} and T_{L0}, and the H and L mRNA half-lives, $t_{1/2}$. As a result, the subsequent experimental study on GS-NS0 cells under normal and hyperosmotic culture conditions were focused on the transcription and translation processes in the antibody production pathway. The details of the experimental study and its findings will be further described and discussed in Chapters 4 and 5.

Chapter 4

Hyperosmotic Effects on GS-NS0 Growth, Metabolism and Antibody Production

4.1 Introduction

In Chapter 3, a hybrid model describing cell growth, metabolism and antibody production was developed using existing experimental data pertaining to the GS-NS0 cell culture system under both normal and hyperosmotic culture conditions. Model analysis of the hybrid model using a global sensitivity analysis has indicated that parameters related to the transcription and translation processes in the antibody production pathway, in particular, have a significant impact on antibody production rates in GS-NS0 cells. The experimental study has, therefore, focused on evaluating the behaviour of IgG mRNA and polypeptide chain concentrations at normal and hyperosmotic culture conditions. Additionally, in order to assess some of the proposed mechanisms of hyperosmolarity on antibody production mentioned in Section 2.3.2, the cell cycle and energy state of the GS-NS0 cells under both normal and hyperosmotic conditions have also been studied. However, prior to investigating the intracellular aspects of mRNA and protein synthesis, the general characteristics of cell growth and death, basic metabolism and extracellular monoclonal antibody accumulation need to be addressed. The first part of this chapter includes a description of the above-mentioned trends, as derived from the batch culture experiments. In the second part of this chapter, the effects of hyperosmolarity on the cell cycle and its significance in improving

specific antibody productivity in GS-NS0 cells are discussed. Finally, the energy state of GS-NS0 cells under normal and hyperosmotic culture conditions is also assessed. Subsequently, Chapter 5 then focuses on evaluating the intracellular trends of IgG mRNA and polypeptide species with respect to culture phase, as well as assessing their contribution towards increasing antibody productivity at hyperosmotic conditions. Results regarding the stabilities of the heavy and light IgG mRNA molecules at the mid-exponential and early stationary phases, under both normal and hyperosmotic culture conditions are also discussed.

4.1.1 Normal and hyperosmotic conditions – a summary of main characteristics

Normal osmotic conditions in mammalian cell cultures range from 270 to 310 mOsm/kg in order to closely resemble the osmotic conditions in *vivo* [Bogner et al., 2004]. Increasing the osmolarity of the culture beyond this range has led to the improvement of specific antibody productivity in a number of cell lines, including hybridoma [Lee and Lee, 2000; Ozturk and Palsson, 1991b], CHO [Ryu et al., 2000; Ryu et al., 2001] and GS-NS0 cells. In the experimental study conducted by Wu et al. [2004], an increase in the osmolarity of the culture from 290 mOsm/kg to 450 mOsm/kg resulted in a 30% increase in the accumulation of total antibody product in the extracellular medium. In addition, hyperosmotic culture conditions have been characterised by a slower rate of cell growth for various cell lines. For instance, in the GS-NS0 study described above, a 35% decrease in maximum cell density and a shift in peak cell density from 96 hrs to about 150 hrs was observed. In an earlier study on the GS-NS0 cell line, Duncan et al. [1997] had also reported an 1.8 fold increase in specific antibody productivity as the osmolarity of the culture was raised from 275 mOsm/kg to 400 mOsm/kg. The authors also observed that cell growth was suppressed and cell viability in the exponential growth phase was reduced under hyperosmotic culture conditions. Additionally, a 2-fold increase in the uptake of glucose and a 4-fold increase in lactate production occurred as a result of hyperosmolarity.

Most studies on hyperosmotic culture conditions available in the literature, including the GS-NS0 studies described above, have employed the use of sodium chloride as the means of increasing culture osmolarity, as it is relatively cost-effective and readily available

[Ryu et al., 2001] compared to other more expensive substances such as sorbitol and betaine. Similarly, in this study, sodium chloride is the substance chosen for increasing the osmolarity of the culture. Batch cultures of GS-NS0 cells in 250 mL shake flasks have been grown at normal and hyperosmotic culture conditions of 290 and 450 mOsm/kg respectively and samples taken at different culture points for various analyses, as described in detail in Section 4.2.

4.2 Materials and methods

4.2.1 Cell culture

Cell line

The cell line used in this study is a GS-NS0 mouse myeloma designated 6A1 (100)-3, which has been kindly made available by Lonza Biologics (Slough, UK). The cell line was derived from a NS0 mouse myeloma, which was transfected with the glutamine-synthetase (GS) selection marker, thus enabling it to grow in glutamine-free medium. A chimeric IgG_4 antibody, cB72.3, which recognises the Tag-72 tumour marker in colorectal cancer is produced by the GS-NS0 cells.

Culture medium and maintenance

Culture medium used in the routine maintenance of GS-NS0 cells consisted of the following components: 200 mg/L calcium chloride, 0.1 mg/L ferric nitrate, 400 mg/L potassium chloride, 97.7 mg/L magnesium sulphate, 3700 mg/L sodium bicarbonate, 125 mg/L sodium phosphate, 4500 mg/L D-glucose, 150 mg/L glutamic acid, 150 mg/L aspatagine, 220 mg/L pyruvic acid, 7 mg/L each of adenosine, guanosine, cytidine and uridine, 2.4 mg/L thymidine and 4.5 mg/L MSX (all from Sigma, UK). The medium was also supplemented with 1X MEM amino acids solution, 2X MEM vitamins solution, 1000 mg/L pluronic acid solution 1% (v/v) penicillin-streptomycin solution, and 2.5% (v/v) Foetal Bovine Serum (FBS) (all from Invitrogen, UK). The addition of different amounts of sodium chloride (NaCl) to the medium was used to vary the osmolarity of the medium, as required.

Cells were cultivated either in 250mL Erlenmeyer shake flasks (Corning Incorporated, Corning, US) with a 50-60 mL working volume or in 1 L shake flasks (Corning) with a 250 mL working volume. The shake flasks were incubated at 37°C and agitated using an orbital shaker at 125 revolutions per minute (rpm) (Stuart Scientific, UK). Cultures were gassed with 5% CO_2 daily. Cells were routinely subcultured every 2 days with an inoculum density of 2×10^5 cells/mL.

Freezing and recovery of GS-NS0 cells in liquid nitrogen

Prior to conducting batch culture experiments, a cell bank had to be created so as to minimise variations in the cell characteristics caused by a difference in cell generation. All experiments were therefore conducted with cells from the same generation number (approximately generation number 60). The freezing of GS-NS0 cells was carried out as follows: cultures were first centrifuged for 5 minutes at 800 rpm to remove the supernatant. The cells were then resuspended in culture medium supplemented with 20% FBS and 10% dimethyl sulfoxide (DMSO, Sigma, UK) at a density of 1×10^7 cells/mL and aliquoted into 1.5 mL cryovials (Corning). The vials were stored at –86 C overnight before being transferred to a liquid nitrogen dewar. Cells were recovered by thawing the cryovial in a water bath at 37 C. The contents of the cyrovial were added dropwise to 10ml of culture medium at 37 C. The cell mixture was then centrifuged at 800 rpm for 5 minutes to remove the freezing agent, DMSO, from the cells. The cell pellet was then resuspended in culture medium at an inoculum density of 2×10^5 cells/mL.

4.2.2 Cell culture experiments

Normal and hyperosmotic batch culture experiments

Batch culture experiments were carried out in triplicates using 1 L shake flasks with a working volume of 250 mL at either normal osmotic conditions (290 mOsm/kg) or hyperosmotic conditions (450 mOsm/kg). Samples of approximately 1-2 mL were taken daily for the measurements of extracellular metabolite and antibody concentrations, as well as cell number and viability determination. Additionally, 1×10^6 cells from each culture are

collected for cell cycle analysis and 1-2 × 10^6 cells were collected for the analysis of intracellular energy nucleotide levels on a daily basis until the late stationary – early decline culture phase.

4.2.3 Extracellular analytical techniques

Cell number and viability estimation

Approximately 0.5 mL samples were removed from the shake flask cultures. Cell concentration was estimated using a haemocytometer and the dye exclusion assay employing 0.4% trypan blue solution (Sigma). Each sample was counted at least in duplicate and if the values did not agree to within 10% of each other, additional counts were carried out.

Metabolites analysis

The analysis of glucose, lactate, glutamate and NH_4^+ ion concentrations was carried out using the BioProfile 200 Analyser (Nova Biomedical, UK). Approximately 0.5 mL of culture supernatant was required for each assay.

Osmolarity measurement

The osmolarity of the cell culture medium was measured using a freezing point osmometer (Camlab). 100 μL of sample was required for each assay. The osmometer was calibrated at 0 mOsm/kg using distilled water and at 300 mOsm/kg with a 300 mOsm/kg standard solution (Camlab). The response of the osmometer has been reported to be linear between 0 and 25000 milliosmols and measurements to be accurate to within 0.5% [Bond, 2004].

Extracellular antibody concentration determination

The extracellular antibody concentration was determined using a sandwich-based Enzyme-Linked Immunosorbent Assay (ELISA). A 96-well microplate (Grenier BioOne, UK) was first coated with an anti-human gamma Fc antibody (Jackson immunoresearch, US) in a coating buffer (15 mM Na_2CO_3, 35 mM $NaHCO_3$, pH 9.6) at a concentration of 2 μg/mL overnight in a 4 C refrigerator. The coating solution was then removed and the wells blocked

with a solution consisting of the coating buffer with 0.5% (w/v) casein hammerstein (VWR) for 1 hour at room temperature. Subsequently, the wells were rinsed 3 times with 300 μL of washing solution (PBS with 0.05% Tween).

Known standard concentrations of the cB72.3 IgG antibody (kindly provided by Lonza Biologics, UK) and cell free supernatant samples diluted in sample-conjugate buffer (12.1 g/L Tris, 5.84 g/L NaCl, 2.0 g/L Casein Hammerstein (VWR) and 0.2 mL Tween) were added next to the wells (100 μL/well) and incubated for 1.5 hours at room temperature on an orbital shaker. Sample-conjugate buffer was also added to at least two wells to serve as negative (background) controls. The standards, samples and sample-conjugate buffer were discarded and the wells washed 3 times with the washing solution described above. An anti-human kappa chain Fab antibody fragment conjugated to horseradish peroxidase (Sigma) was then added at a dilution of 1:8000 (in sample-conjugate buffer) to each well (100 μL/well) and incubated for a further 1 hour with shaking at room temperature.

After the incubation period, wells were washed 4 times with the washing solution before substrate solution (100 μL/well) was added to the wells. The substrate solution consisted of a TMB tablet (1mg/tablet of 3,3',5,5'-Tetramethylbenzidine, Sigma), which was dissolved in 10 mL of 50 mM phosphate-citrate buffer (pH 5.0). Immediately prior to use, 2 μL of 30% (w/v) hydrogen peroxide solution was added to the mixture. The reaction was allowed to proceed in the dark at room temperature for 15 to 30 minutes before being stopped by the addition of 50 μL of 2.5 M H_2SO_4 solution to each well. The OD_{450} of each well was measured using an ELISA microplate reader (BioTek, US). OD_{450} values for standards and samples were normalised by subtracting the average OD_{450} reading of the negative control wells. A standard curve based on known concentrations of the IgG can then be plotted and used to derive the unknown concentrations in each supernatant sample. Each sample was assayed at least in quadruplicates.

4.2.4 Cell cycle analysis

A Beckman-Coulter Epics Altra (Beckman-Coulter, US) equipped with a 488 nm argon laser set at 15mW laser power was used to carry out cell cycle analysis for samples collected at normal and hyperomsotic culture conditions.

1 x 10^6 cells were collected daily from triplicate cultures under both normal and hyperosmotic conditions. The supernatant was aspirated after centrifugation at 800 rpm for 5 minutes and cells were fixed by the addition of 1 mL of 70% ice-cold ethanol dropwise to the cell pellet with constant mixing using a vortex. The fixed cells were stored at –20 C for up to 1 month before being analysed by flow cytometry. Prior to flow cytometric analysis, the fixing solution was aspirated and the cell pellet rinsed with 1 mL of cold (4 C) PBS. The PBS was then aspirated after centrifugation at 800 rpm for 5 minutes and 1 mL of propidium iodide (PI) staining solution consisting of 50 μg/mL of PI, 0.1% (w/v) of Ribonuclease A (Sigma) and 0.1% bovine serum albumin (BSA) (Sigma) in PBS was added to the cell pellet. The mixture was then incubated at room temperature in the dark for at least 30 minutes to allow for cellular DNA staining. In addition, unstained cell samples were used as negative controls.

Flow cytometric data was collected using an excitation wavelength of 488 nm and an emission wavelength of 610 nm (conditions suitable for analysis of DNA staining intensity by PI). A total of 20,000 events were collected for each sample. The dot plots generated were then gated to obtain histograms using the WinMDI Multicycler 2.8 software and further analysed using the Cylchred software, both available over the internet[1].

4.2.5 Intracellular energy nucleotides analysis – capillary electrophoresis

Extraction of nucleotides from cell samples

2 x 10^6 cells were collected from normal and hyperosmotic cultures in triplicate on a daily basis. The sample was centrifuged at 800 rpm for 5 minutes at room temperature and the culture supernatant aspirated. 950 μL of ice-cold 0.3 M perchloric acid (60% (v/v), VWR) solution and 7.5 μL of 1.5 mM guanosine monophosphate (GMP, VWR) stock solution (to a final concentration of 10 μM) as an extraction efficiency standard was added simultaneously to the cell pellet. The resulting mixture was then centrifuged for 5 minutes at 12,000 rpm and a temperature of 4 C. Subsequently, the supernatant containing the extracted nucleotides was

[1] Analysis software downloaded from Cardiff University webpage. Web address: http://www.cardiff.ac.uk/medicine/haematology/cytonetuk/documents/software.htm

pipetted into a new microcentrifuge tube and 170 μL of 2 M potassium hydroxide solution (VWR) was added to neutralise the solution. The mixture was then centrifuged for 10 minutes at 10,000 rpm and a temperature of 4 C to separate the precipitated potassium perchlorate salt ($KClO_4$) from the solution. The resulting supernatant was removed to a new microcentrifuge tube and stored at –20 C prior to analysis by capillary electrophoresis.

Capillary electrophoresis system

An analytical method based on capillary electrophoresis was developed for the quantification of the energy nucleotides ATP, ADP and AMP present in the cell extracts. The capillary electrophoresis system was a Hewlett Packard 3DCE (Hewlett Packard, UK) system with a fused silica capillary tube externally coated with polyimine (Composite Metal Services, UK) with an internal diameter of 100 μm and a length of 64.5 cm. The internal surface of the capillary was coated with bind-silane (3-(Trimethoxysilyl)propyl methacrylate, Sigma) by flushing it with a solution containing 10% (w/v) bind-silane dissolved in acetone (VWR) for 10 minutes at room temperature.

The capillary tube was fixed into a cassette maintained at 25 C so as to allow for the precise alignment of the capillary with the capillary detection window. The ends of the capillary were dipped into two reservoirs containing 100 mM of MES ((2-(N-Morpholino)ethanesulfonic Acid, VWR) containing 0.2% (w/v) of hydroxyethyl-cellulose (VWR). The distance from the cathode end of the capillary to the detection window is 56 cm and compounds passing through the capillary were detected as peaks in absorbance at a wavelength of 252 ± 10 nm. The peaks were then recorded as an electropherogram on the HP 3DCE chemstation by the data handling software.

Each sample was injected for 10 seconds using a vacuum injection pressure of 500 mbars at the inlet side of the capillary. A voltage of –30 kV was then applied across both ends of the capillary, causing the nucleotides to migrate at different rates from one end of the capillary to the detection window according to their charge. Each sample was analysed for 15-20 minutes and an electropherogram recording the absorbance peaks as each component passed through the detection window was generated.

Quantification of energy nucleotides through capillary electrophoresis

Solutions containing known concentrations of ATP, ADP and AMP (all from Sigma), ranging from 0.5 to 20 μM, were prepared as calibration standards. 20 μM of DNP-L-glutamic acid (DNP) (Sigma) was added as an internal standard to account for minute differences that might be present in the volume of each sample loading. The peaks corresponding to ATP, ADP and AMP were identified firstly by the comparison of the retention time (RT) of each component as recorded on the electropherogram. The appropriate peaks were further confirmed by comparison between the electropherogram generated by a sample spiked with known concentrations (50 μM) of the 3 nucleotides and one that is generated by a sample that was not spiked. Additionally, a solution containing 20 μM of the extraction efficiency standard, GMP mixed with 20 μM of DNP was also run in duplicate, and the resulting electropherogram used as a reference point (100% extraction efficiency).

The integrated area under each peak on the electropherogram was then calculated for the different standard concentrations and calibration curves were plotted and fitted by linear regression for ATP, ADP and AMP. The areas were normalised according to the integrated area under the DNP peak for each sample. Subsequently, each unknown sample was run in duplicate and the concentrations of ATP, ADP and AMP determined by comparison to the standard curves, after the normalisation and adjustment for extraction efficiency of each integrated area was carried out.

4.2.6 Statistical analysis

The error bars in the figures refer to standard deviations of triplicate experiments unless otherwise stated. 95% confidence intervals have also been used to compare the similarities between the cell populations of normal and hyperosmotic cultures. Single-factor ANOVA at a significance level of $p=0.05$ have both been used to assess whether the mean values of any two samples can be considered to be significantly different from each other.

4.3 Results and analyses

4.3.1 Cell growth and death characteristics

Hyperosmotic culture conditions are known to result in lower specific growth rates and decreased maximum cell densities when compared to normal culture conditions. In Figures 4.1 a and 4.1 b, the number of viable, total and dead cells in normal and hyperosmotic culture conditions are shown. It is observed that the average maximum cell density was decreased by approximately 25%, from 9.7×10^5 cells/mL to 7.3×10^5 cells/mL in hyperosmotic cultures relative to normal condition cultures (Figure 4.1 a). Both average values were confirmed to be different statistically (p=0.027), based on a single-factor ANOVA test carried out at the 0.05 significance level. Additionally, the total cell number under hyperosmotic conditions reached a value that was approximately 33% lower than cells under normal conditions. Figure 4.1 b also indicates that the number of dead cells increased at a slower rate and was consistently lower for hyperosmotic cultures in comparison to normal osmotic cultures apart from during the hyperosmotic lag phase. The trends in Figure 4.1 can be further analysed by examining the behaviours of the specific growth and death rates, as presented in Figures 4.2 a and 4.2 b respectively. From Figure 4.2 a, the average specific growth rate at the mid-exponential phase of hyperosmotic cultures was observed to be 0.014 hr^{-1}, which represented a 33% decrease when compared to a growth rate of 0.021 hr^{-1} achieved by cells under normal culture conditions. This behaviour was thus responsible for the lower viable cell numbers achieved by hyperosmotic cultures. Additionally, the specific growth rate under hyperosmotic conditions was also maintained at its exponential growth value over a longer time period, before decreasing at a slower rate than under normal osmotic conditions. These specific growth rate trends thus resulted in relatively longer exponential growth and stationary phases in hyperosmotic cultures (Figure 4.1 a). In Figure 4.2 b, the specific death rates for hyperosmotic cultures were observed to remain at relatively low levels (< 0.010 hr^{-1}) over a longer time period (192 hrs) in comparison to the death rates of cells grown under normal culture conditions (k_d started increasing at 144 hrs). This trend explains the comparatively lower number of dead cells in hyperosmotic cultures with respect

to normal osmotic cultures (Figure 4.1 b). In Figure 4.3, the percentage cell viability for both normal and hyperosmotic cultures are shown. It appears that there was an initial drop in the cell viability of hyperosmotic cultures during the lag phase, which implied that an adaptation period for the cells to adjust to higher osmolarity in the medium was required. The drop in cell viability was also reflected in the comparatively higher specific death rate (3.7×10^{-3} hr^{-1}) for hyperosmotic cultures relative to the normal cultures (1.7×10^{-3} hr^{-1}). It was also observed that hyperosmotic cell viability averaged approximately 78% during the exponential growth phase, which was significantly lower than the 86% for normal cultures ($p = 4 \times 10^{-9}$ from single-factor ANOVA test conducted at a significance level of 0.05). Figure 4.3 also shows clearly that the decrease in cell viabilities for hyperosmotic cultures was more gradual relative to normal cell cultures – in fact, the hyperosmotic cell viabilities were consistently higher than their corresponding normal osmotic values after 120 hours of culture time (normal and hyperosmotic cell viabilities were statistically analysed using single-factor ANOVA at all time points from 120 hours – all p values were less than 0.05). The above viability trend is in agreement with the aforementioned behaviour of both the specific growth rate (extended exponential growth and stationary phases) and the specific death rate (slower rate of increase), indicating that hyperosmotic conditions of 450 mOsm/kg resulted in an extended culture longevity for GS-NS0 cells.

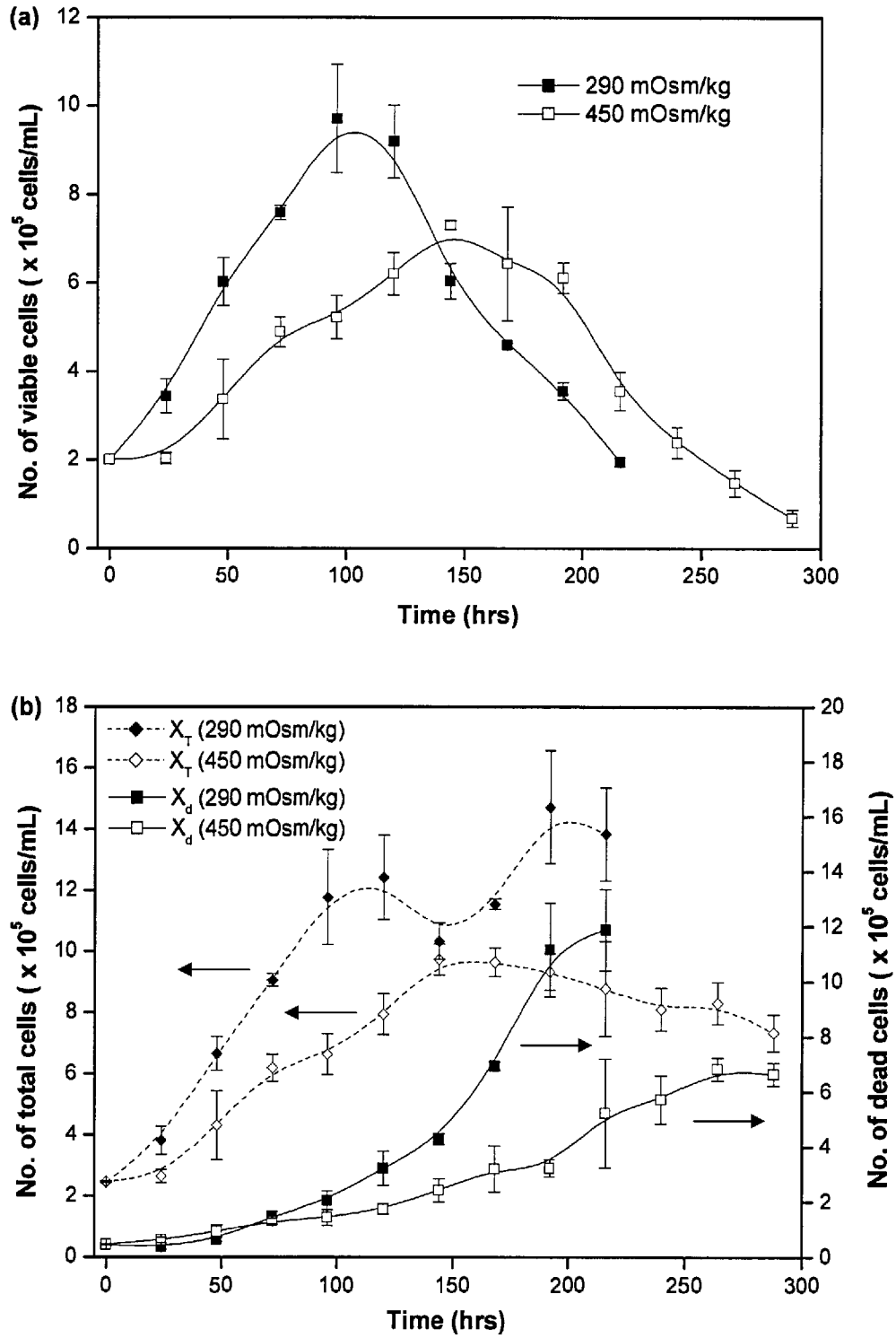

Figure 4.1. (a) Viable cell numbers and (b) total and dead cell numbers for normal osmotic (290 mOsm/kg) and hyperosmotic cultures (450 mOsm/kg).

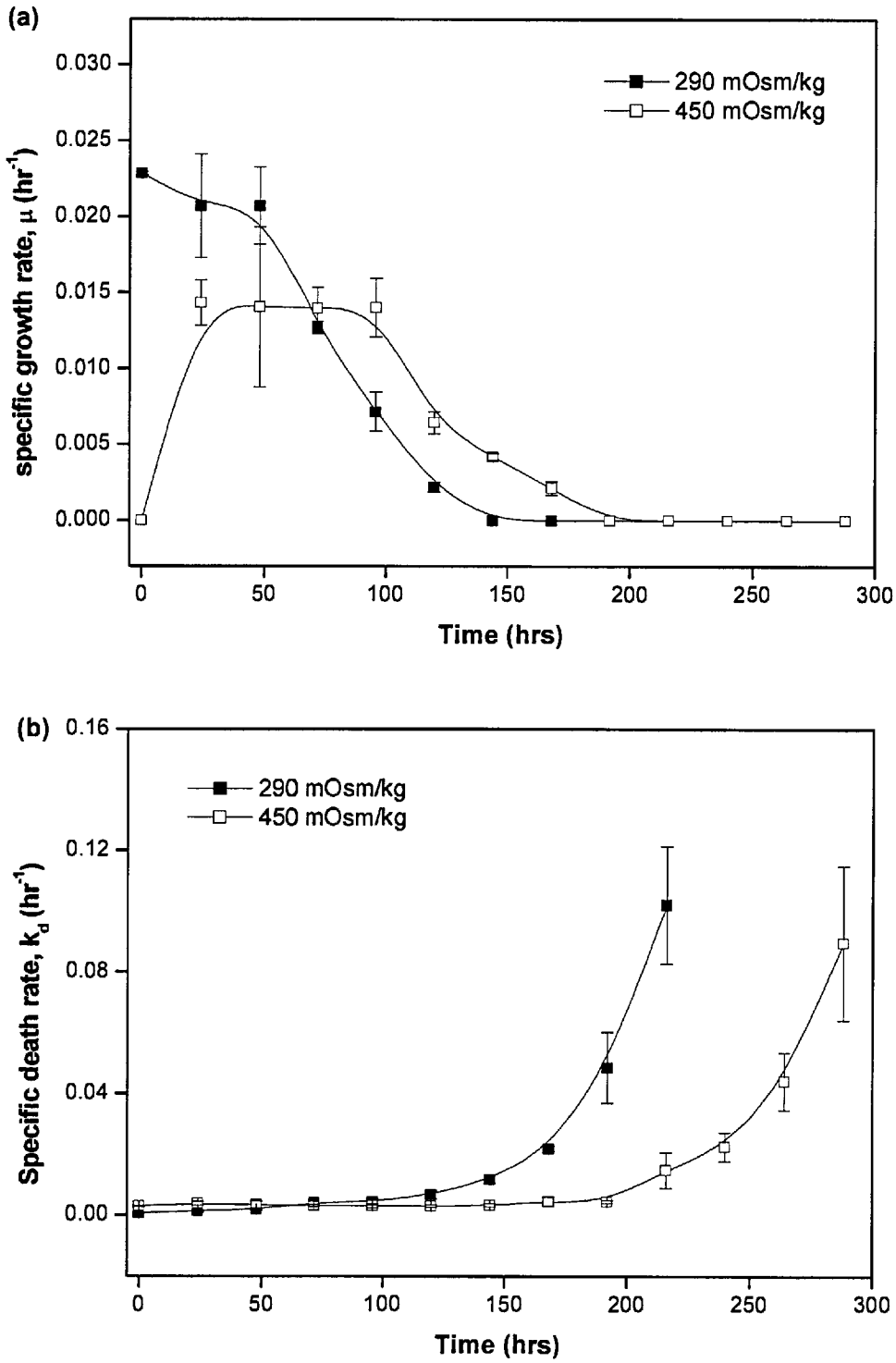

Figure 4.2. (a) Specific growth (μ) and (b) specific death (kd) rates for normal osmotic and hyperosmotic cultures.

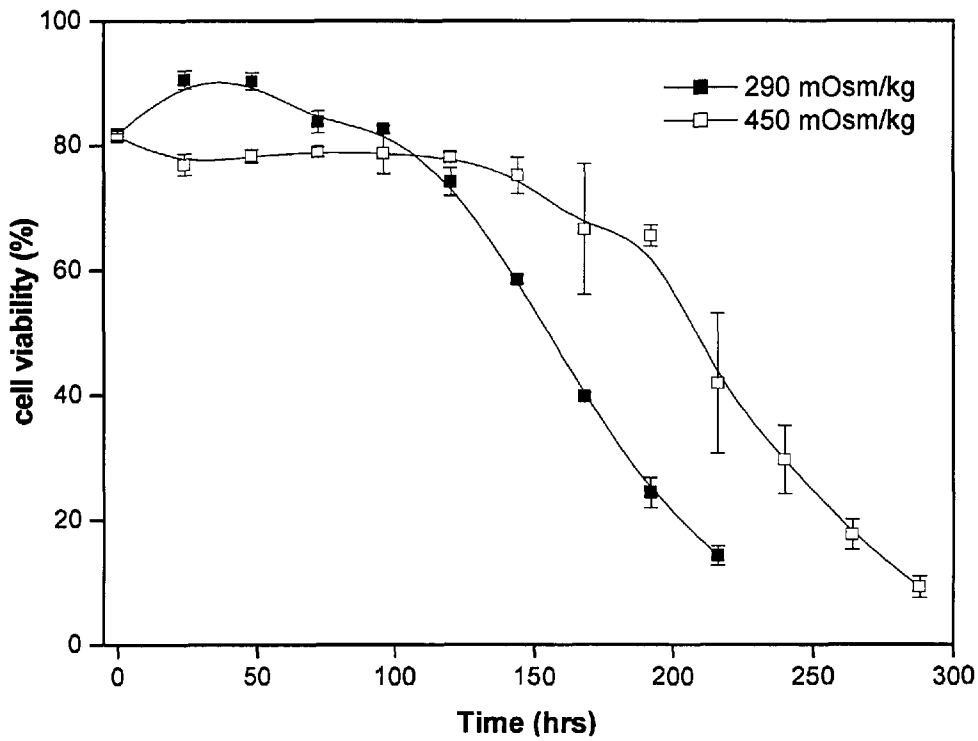

Figure 4.3. Percentage cell viability profiles under normal and hyperosmotic culture conditions.

4.3.2 Nutrient uptake and metabolite production

Figures 4.4 a to 4.4 c show the normal and hyperosmotic glucose, lactate and ammonium ion profiles respectively. In Figure 4.4 a, it can be observed that the glucose uptake rate was higher at the exponential growth phase for both culture conditions (steeper gradient) and subsequently decreased (gentle gradient) as the culture progressed. This trend is more clearly observed in Figure 4.5 a, which presents the specific glucose uptake rate as a function of time under both osmotic conditions. These specific glucose uptake rates were derived by first fitting the data points with polynomial expressions, then differentiating the equations with respect to time and finally dividing by the viable cell number (analogous to the differential method of calculating specific antibody productivity from [Yang et al., 1996]). It can be seen that the specific glucose uptake rate was higher for hyperosmotic cultures than normal osmotic cultures at the mid-exponential growth phase. However, the specific rates for hyperosmotic cultures dropped below the rates for normal cultures at the late-exponential to stationary phase. Figure 4.4 b shows the variation of lactate concentration in the medium under both osmotic conditions. The lactate production in hyperosmotic cultures seems to be similar to the production in normal cultures, up to 120 hours, before levelling out around 23 mM, which is slightly lower than the 26 mM produced under normal culture conditions. The relatively lower number of viable cells under hyperosmotic conditions suggests that lactate production rates are higher in hyperosmotic cultures. In order to substantiate this observation, the relationships between specific glucose uptake rate and the specific lactate production rate are presented in Figure 4.5 b; a linear relationship between both variables was approximated under both normal and hyperosmotic culture conditions. The specific yield of lactate from glucose can therefore be derived from the slopes of the curves. The calculated gradients indicate that that hyperosmotic cultures do indeed show a relatively higher specific yield (1.40) of lactate from glucose uptake, in comparison to the lactate yield at normal cultures (0.95). This behaviour suggests that there may have been a shift in glucose metabolism towards the lactate production pathway under hyperosmotic conditions.

From Figure 4.4 c, the final ammonium ion (NH_4^+) production appears to be slightly higher under hyperosmotic culture conditions. The variation in specific NH_4^+ production rate is more clearly seen in Figure 4.5 c. The specific NH_4^+ production rate increased to a

maximum at the mid-exponential phase before decreasing steadily in the stationary and decline phases under both osmotic culture conditions. While the normal condition-cultures had a higher maximum specific production rate during the mid-exponential phase, the specific rates were relatively lower than that of hyperosmotic cultures in the early stationary and decline phases. The observed trends for glucose uptake and lactate and NH_4^+ production are indications that hyperosmotic conditions lead to increased intracellular metabolic activity. However, the glutamate concentration, which has also been measured using the bioprofiler, do not show significant differences between normal and hyperosmotic cultures – under both osmotic conditions, the concentration decreased from 0.80 to a relatively stable range of 0.30 – 0.40 mM within two days and no observable correlation between glutamate uptake and ammonium ion production was deduced.

4.3.3 Antibody production in normal and hyperosmotic cultures

Hyperosmotic culture conditions have resulted in an increase in specific antibody productivity for various cell lines, as briefly mentioned in Section 4.1, which may or may not lead to an increase in the final antibody titre obtained, depending on the extent of suppression of cell growth. In this study, the antibody accumulation trends are shown in Figure 4.6. The figure indicates that the final antibody titre increased from 88 μg/mL to 157 μg/mL as the osmolarity was raised from 290 to 450 mOsm/kg. This represents an approximate increase of 78% and highlights the potential use hyperosmotic culture conditions in antibody product optimisation strategies.

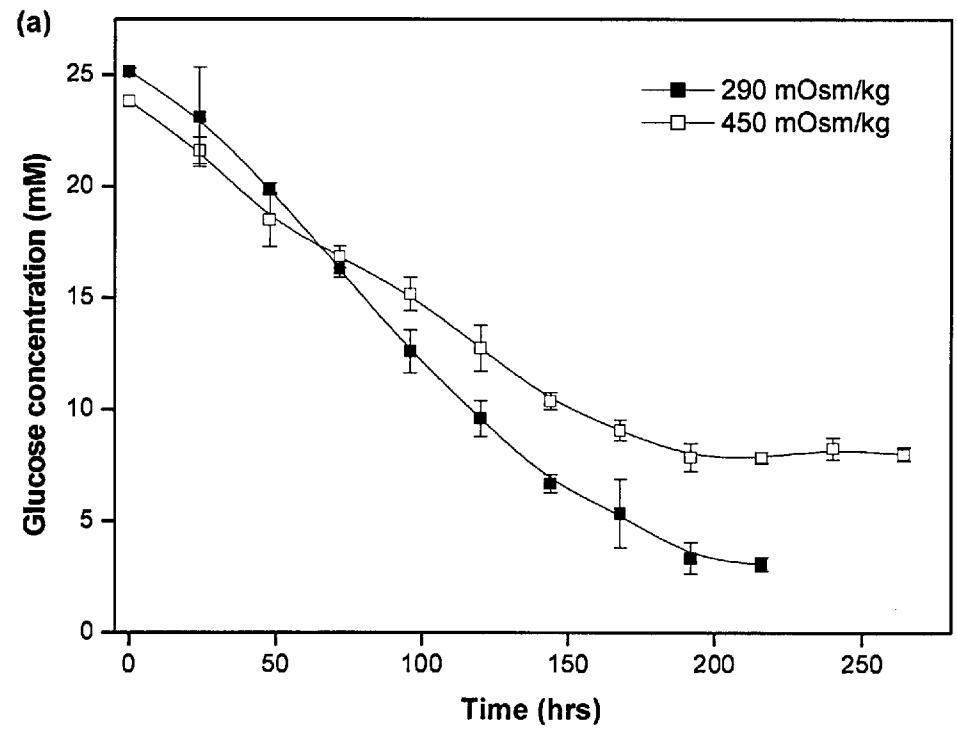
(a)
Glucose concentration (mM)
Time (hrs)
290 mOsm/kg
450 mOsm/kg
0
5
10
15
20
25
0
50
100
150
200
250

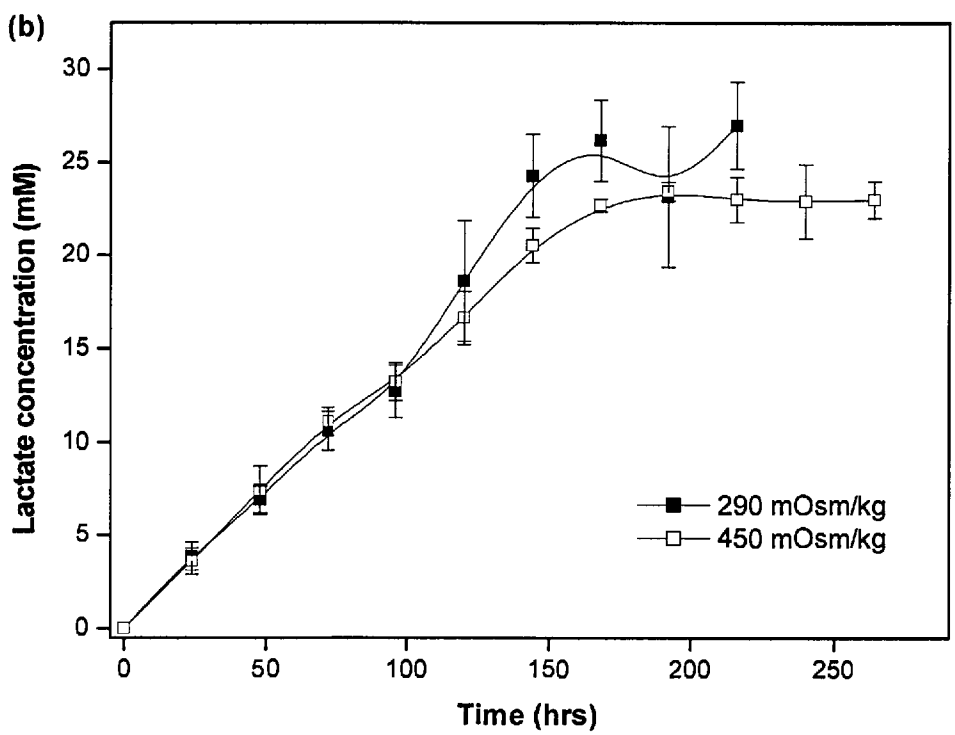
(b)
Lactate concentration (mM)
Time (hrs)
290 mOsm/kg
450 mOsm/kg
0
5
10
15
20
25
30
0
50
100
150
200
250

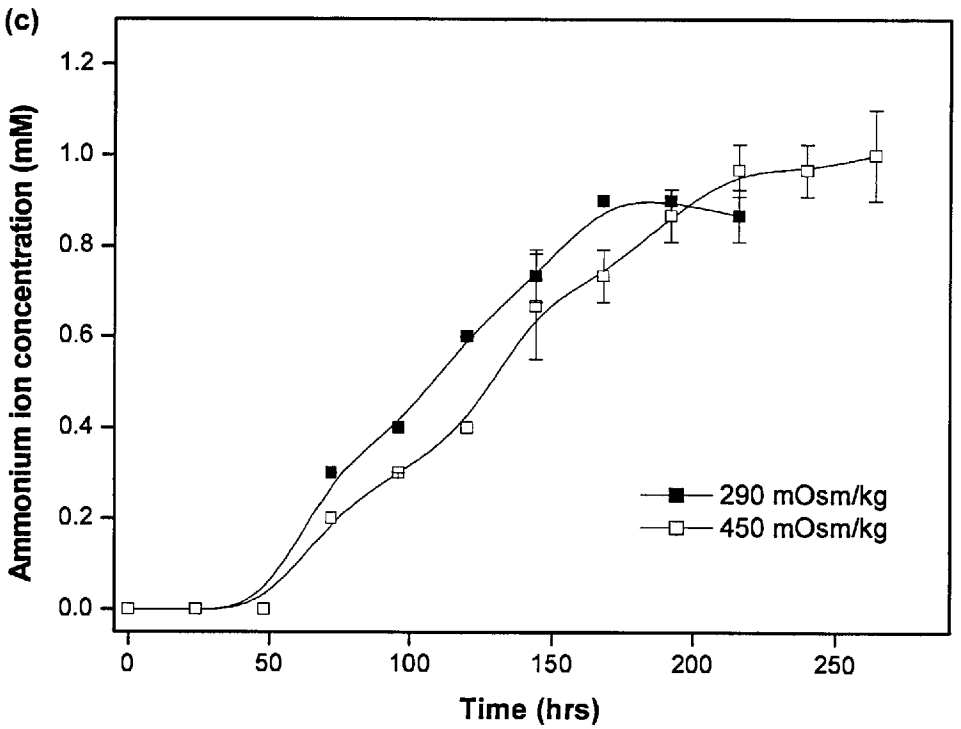

Figure 4.4. (a) Glucose, (b) lactate and (c) ammonium ion profiles under normal and hyperosmotic culture conditions.

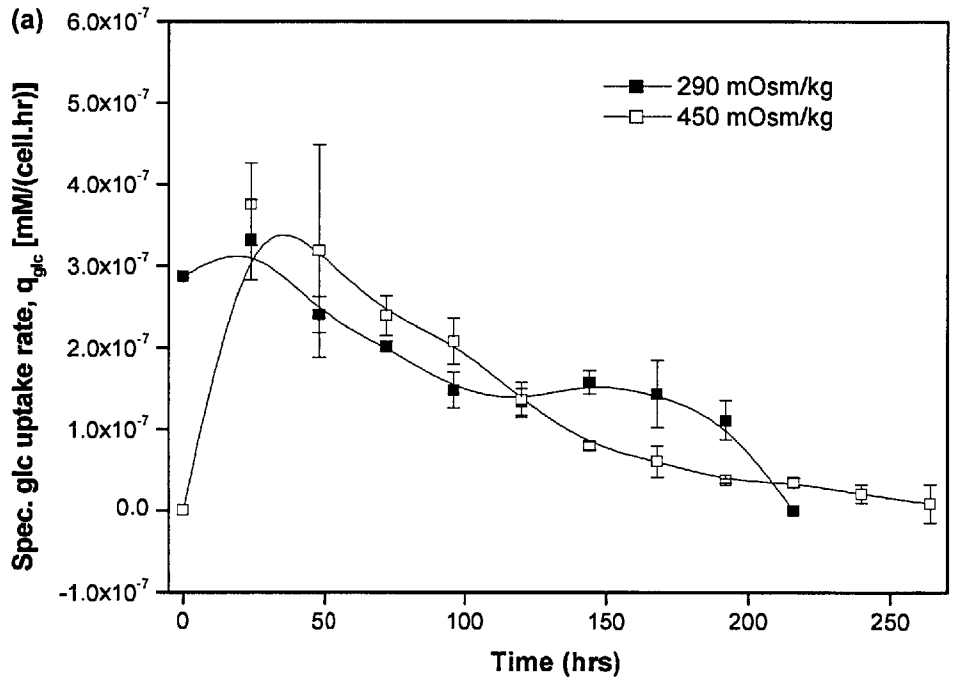
(a)
Spec. glc uptake rate, q_{glc} [mM/(cell.hr)]
6.0x10^{-7}
5.0x10^{-7}
4.0x10^{-7}
3.0x10^{-7}
2.0x10^{-7}
1.0x10^{-7}
0.0
-1.0x10^{-7}
290 mOsm/kg
450 mOsm/kg
0
50
100
150
200
250
Time (hrs)

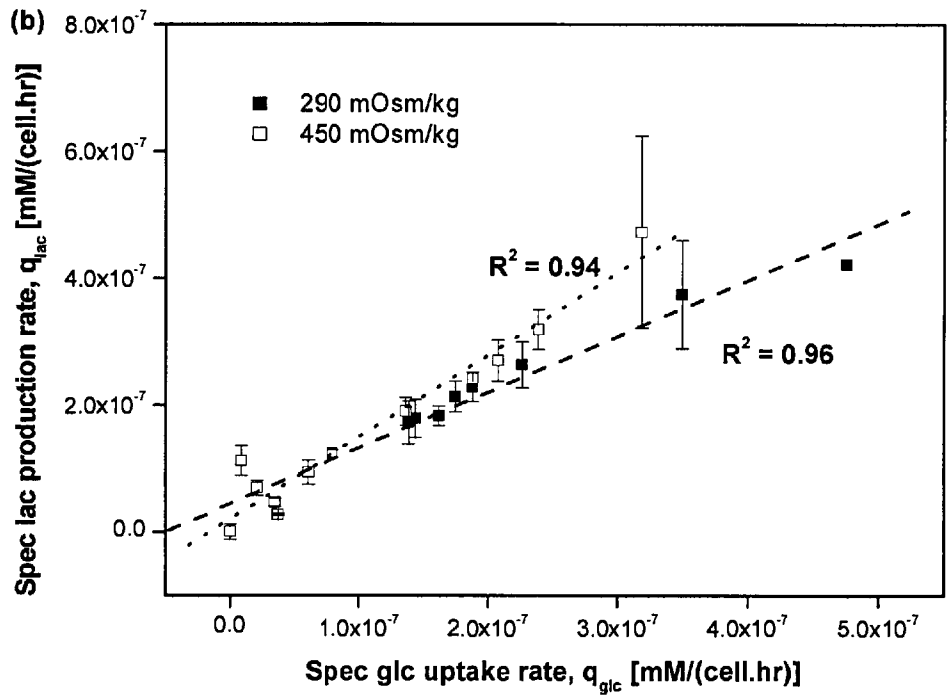
(b)
Spec lac production rate, q_{lac} [mM/(cell.hr)]
8.0x10^{-7}
6.0x10^{-7}
4.0x10^{-7}
2.0x10^{-7}
0.0
290 mOsm/kg
450 mOsm/kg
R^2 = 0.94
R^2 = 0.96
0.0
1.0x10^{-7}
2.0x10^{-7}
3.0x10^{-7}
4.0x10^{-7}
5.0x10^{-7}
Spec glc uptake rate, q_{glc} [mM/(cell.hr)]

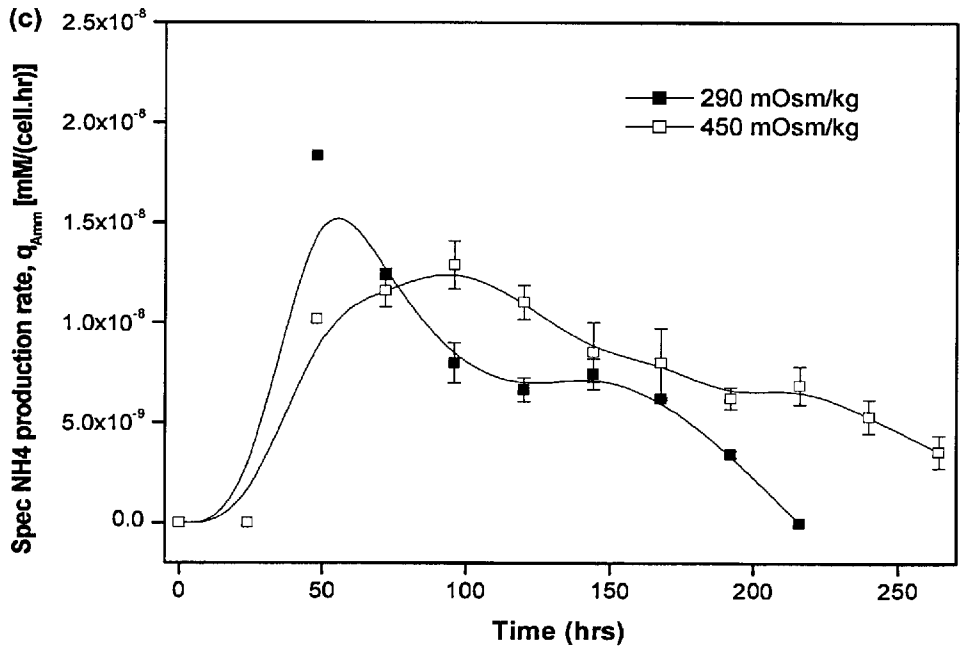

Figure 4.5. (a) Specific glucose consumption rates under both osmotic conditions, (b) relationship between specific lactate production rates and specific glucose consumption rates and (c) specific ammonium ion production rates under normal and hyperosmotic culture conditions.

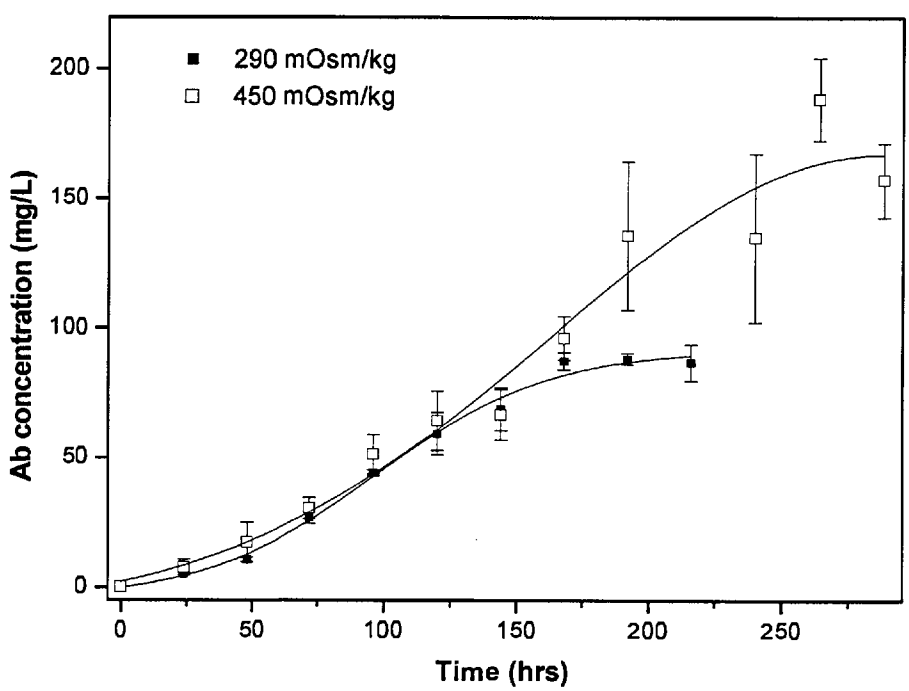

Figure 4.6. Extracellular antibody concentration profiles for normal and hyperosmotic culture conditions.

4.3.4 Cell cycle distribution in normal and hyperosmotic cultures

Having studied the general characteristics of GS-NS0 cell behaviour under normal and hyperosmotic conditions, an analysis was then carried out on the cell cycle distribution in normal and hyperosmotic cultures. Flow cytometry was used to analyse fixed cell samples that had been stained with PI, which enabled the DNA content in each cell to be determined. A histogram displaying the frequency of cells with varying amounts of DNA (as measured by the staining intensities) was obtained for each sample, a typical example of which is shown in Figure 4.7. The figure illustrates how the proportion of cells in the G0/G1, S and G2/M phases were determined from the generated historgram. Cells in the G2/M phase have replicated their DNA and are poised to divide, hence they possess twice the amount of DNA as cells in the G0/G1 phase. The G2/M peak seen in the figure should therefore be approximately at twice the channel number (x-axis) as the G0/G1 phase. Cells in between the two peaks are considered to be in the process of synthesising DNA and thus belong to the S phase of the cell cycle.

Hyperosmolarity, cell cycle arrest and effects on antibody productivity

One of the main reasons proposed in literature for the increase in specific antibody productivity at hyperosmotic cultures is through the process of cell cycle arrest. It is postulated that cell cycle arrest at hyperosmotic conditions results in a re-allocation of resources towards antibody production, thereby leading to improved antibody production rates in CHO cells [Ryu et al., 2001]. The validity of this theory for the GS-NS0 cell line will be tested by the results of this analysis.

The comparison between the percentage of cells in each phase of the cell cycle is presented in Figures 4.8 a and 4.8 b. In Figure 4.8 a, it can be seen that hyperosmotic conditions resulted in a comparatively higher proportion of cells in the G0/G1 phase, hence confirming that partial cell cycle arrest at the G1 phase had indeed taken place. The proportion of cells in this phase increased as the culture progressed into the stationary and decline phases, which corresponded with the decrease in specific growth rate and increase in specific death rate (Figures 4.2 a and 4.2 b) under both osmotic conditions. It can be

observed from Figure 4.8 b that the hyperosmotic cultures had a lower proportion of cells in the S phase than the normal cultures, which agreed with the lower specific growth rates observed under hyperosmotic conditions. The G2/M trend however, was not as clear – the hyperosmotic cultures started out with a lower proportion of G2/M cells in the lag phase, however during the exponential growth phase, the proportion of G2/M cells increased until the late-exponential phase before declining at a slower rate than normal condition cultures. This slower rate of decrease corresponded to the relative longevity of hyperosmotic cultures when compared to normal cultures, as mentioned in Section 4.4.1.

The results obtained confirm that hyperosmotic conditions partially induce cell cycle arrest, particularly in the G0/G1 checkpoint. The next step is therefore to evaluate whether the partial induction of cell cycle arrest actually leads to improved antibody production yields. In Figures 4.9 a and 4.9 b, the proportion of cells in the G0/G1 and S phases are shown with respect to the specific antibody productivities at various time points in the cultures. It is observed that two separate relationships between proportion of cells in the G0/G1 and S phases, and the specific antibody productivity, can be derived for normal and hyperosmotic cultures. A negative relationship was seen between the proportion of cells in the G0/G1 phase and specific antibody productivity, implying that a higher cell proportion in this phase resulted in a decrease in antibody productivity. Conversely, there was a direct relationship between the proportion of cells in the S phase and the antibody productivity for both normal and hyperosmotic cultures, indicating that antibody production was likely to be positively associated with growth in GS-NS0 cells. This observation is further substantiated by the positive relationship existing between the specific growth rate and specific antibody productivity under both normal and hyperosmotic conditions, as presented in Figure 4.9 c. Based on these findings, it appears unlikely that partial arrest of the cell cycle is the reason for increase in antibody productivity at hyperosmotic culture conditions.

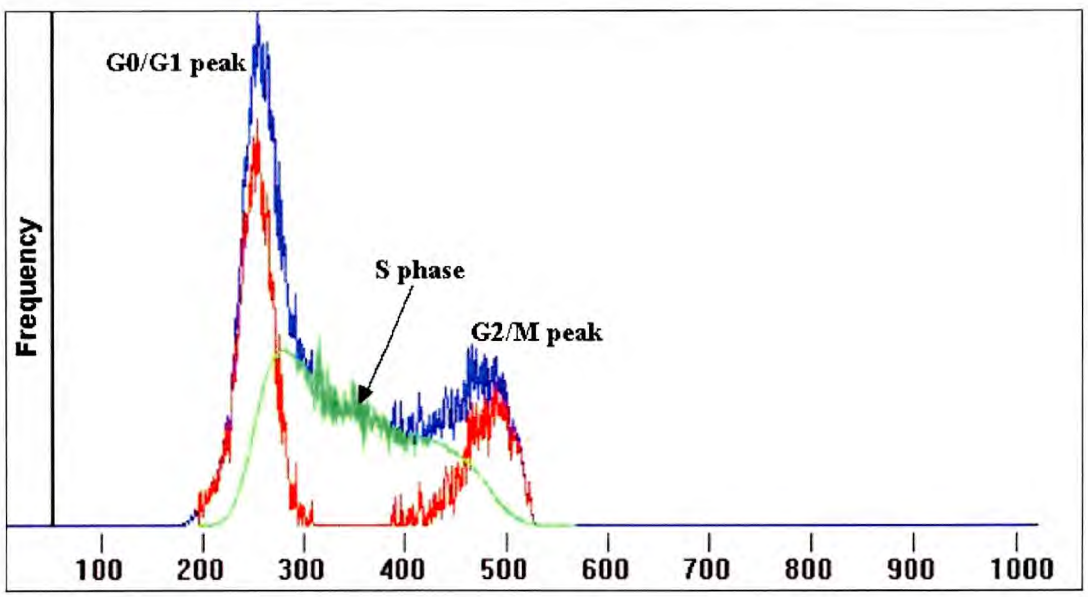

Figure 4.7. Example of a histogram (outlined in blue) displaying the frequency of cells with different staining intensities, as indicated by the channel number (x-axis). The histogram has been analysed using Cychlred software to determine the proportion of cells in the G0/G1 (first peak outlined in red), S (outlined in green) and G2/M (second peak outlined in red) phases of the cell cycle.

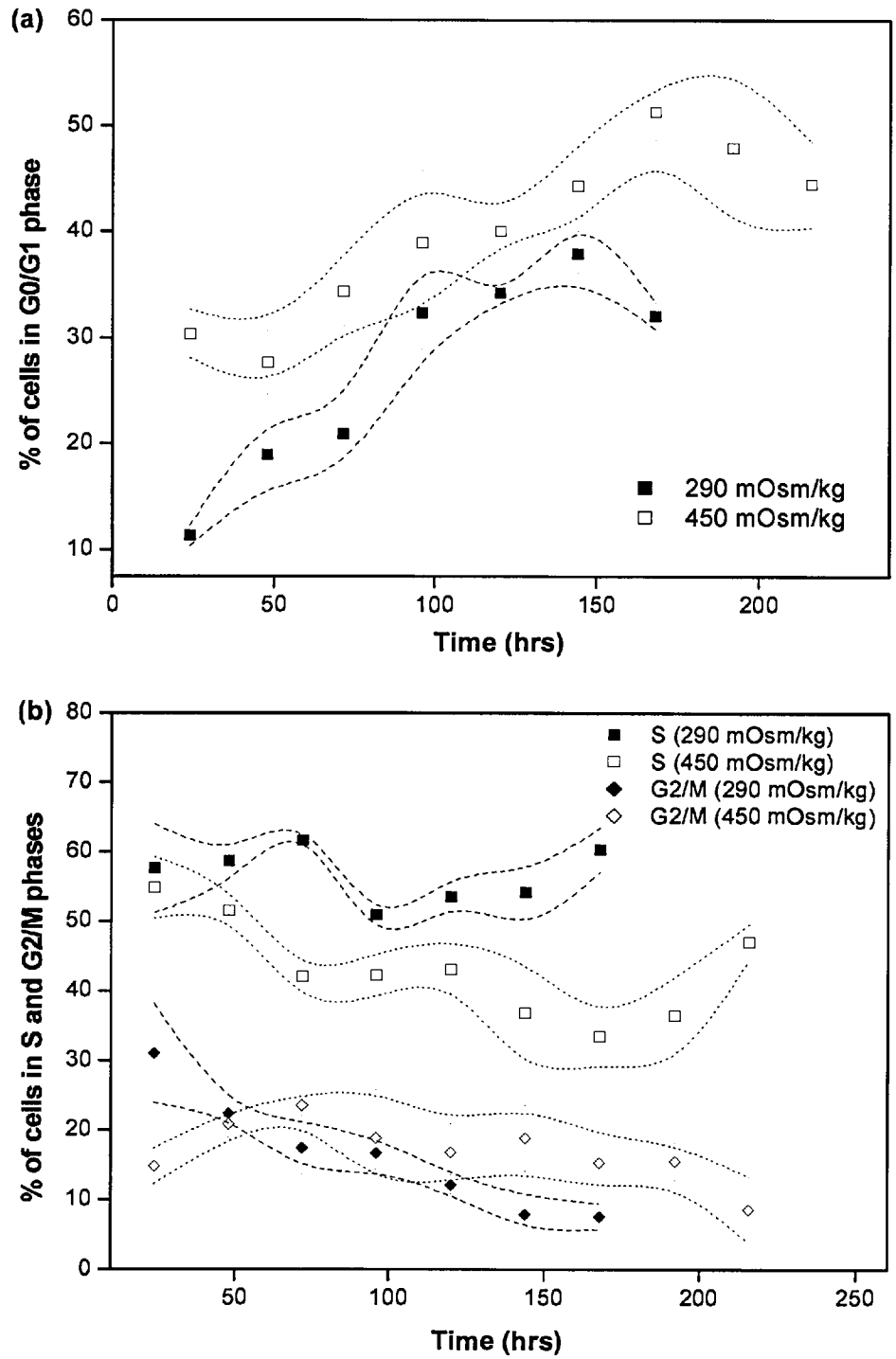

Figure 4.8. (a) Percentage of cells in the G0/G1 phase for normal and hyperosmotic cultures and (b) percentage of cells in the S and G2/M phases under normal and hyperosmotic culture conditions. The dotted lines for represent the 95% confidence intervals associated with each set of data points.

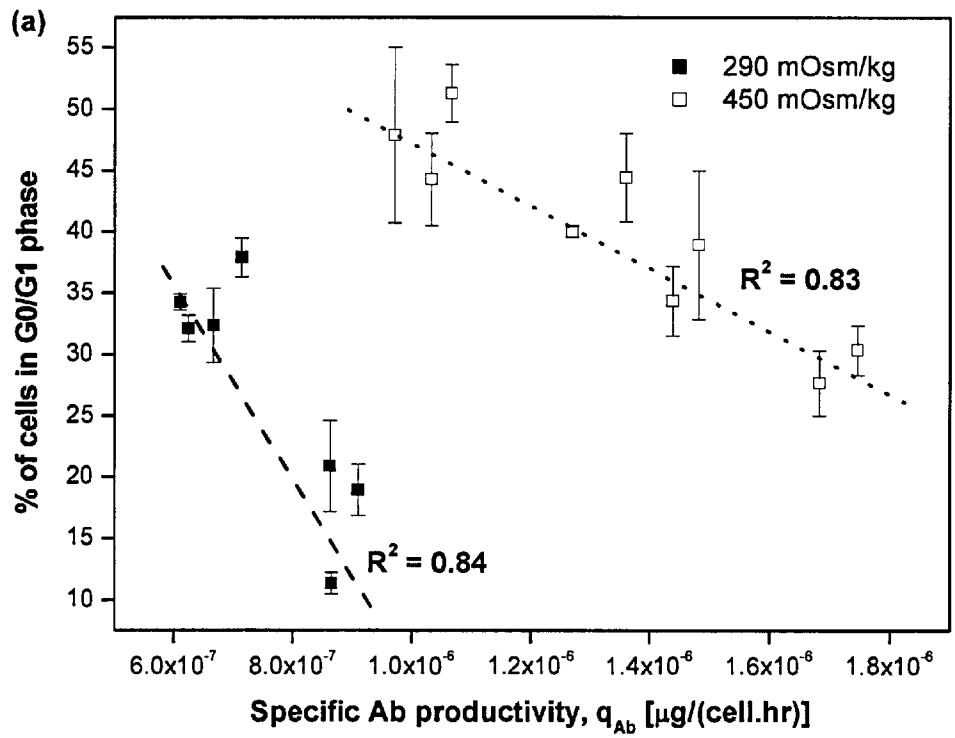
(a)
290 mOsm/kg
450 mOsm/kg
R^2 = 0.83
R^2 = 0.84
% of cells in G0/G1 phase
Specific Ab productivity, q_{Ab} [µg/(cell.hr)]

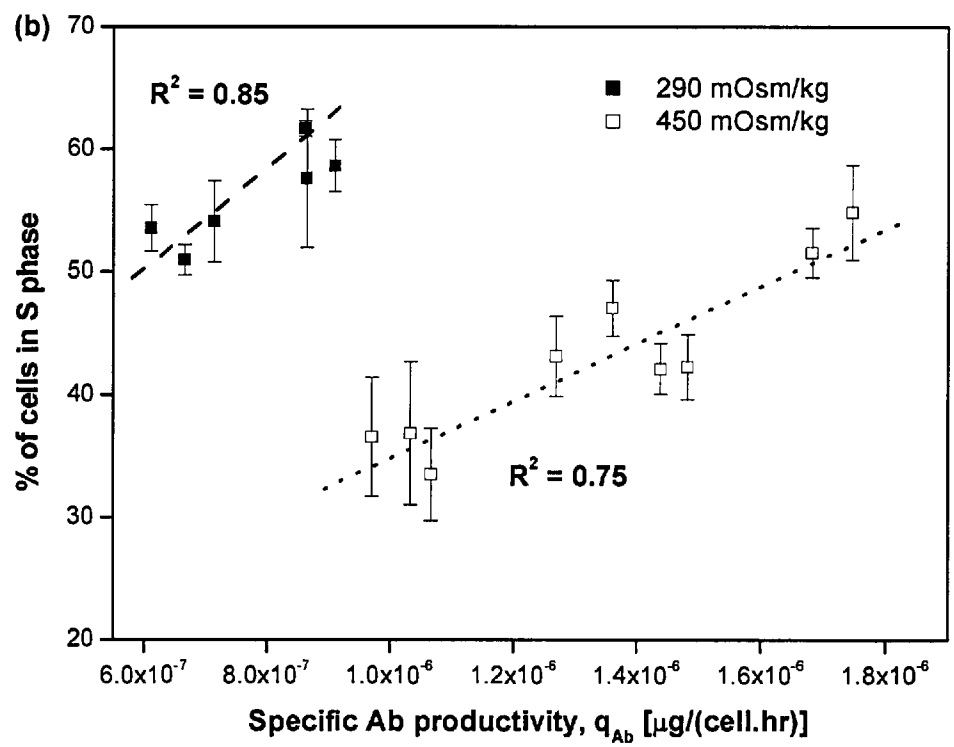
(b)
R^2 = 0.85
290 mOsm/kg
450 mOsm/kg
R^2 = 0.75
% of cells in S phase
Specific Ab productivity, q_{Ab} [µg/(cell.hr)]

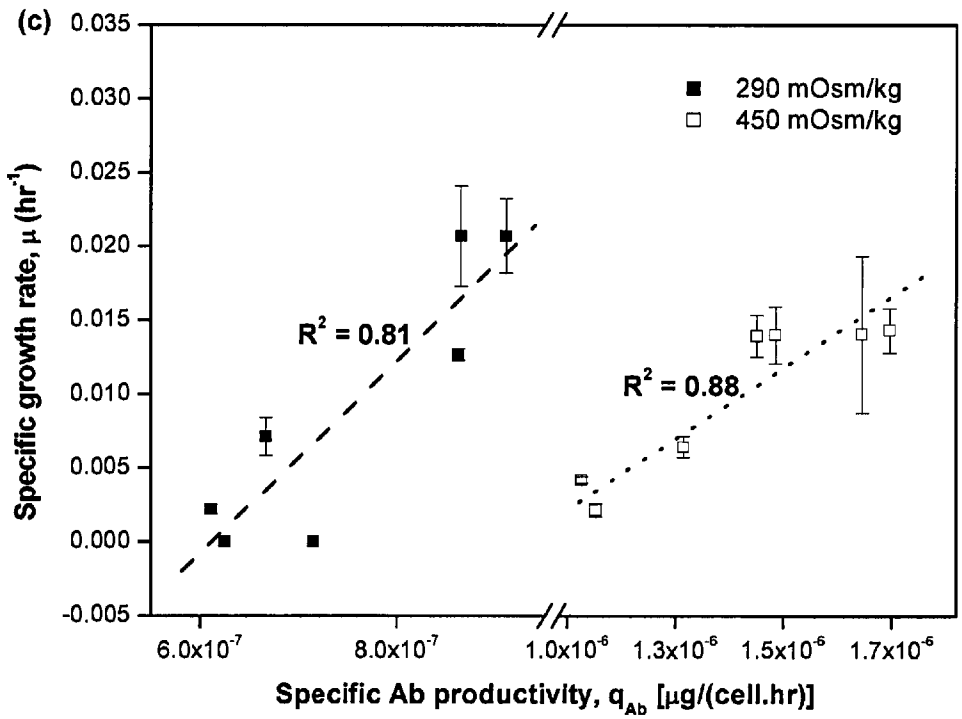

Figure 4.9. Percentage of cells in the (a) G0/G1 phase and (b) S phase with respect to specific antibody productivity under both normal and hyperosmotic conditions. (c) Relationship between specific growth rate and the specific antibody productivity for both osmotic conditions.

4.3.5 Energy state of GS-NS0 cells under normal and hyperosmotic conditions

Energy state parameters

The energy state of a cell can be assessed through the measurement of the energy nucleotide, adenosine tri-phosphate (ATP), as well as the derivation of the energy charge of the cell. The energy charge allows for a quantitative assessment of the energy levels in a cell and was first proposed by Atkinson [1968]. Based on the assumption that equilibrium of the adenine nucleotide pools is maintained, the energy charge can be defined as follows:

$$Energy\ Charge = \frac{([ATP] + 0.5\ [ADP])}{([ATP] + [ADP] + [AMP])} \tag{4.1}$$

where [ATP], [ADP] and [AMP] refer to the concentrations of adenosine tri-phosphate (ATP), adenosine di-phosphate (ADP) and adenosine mono-phosphate (AMP) respectively.

The value of the energy charge ranges from 0 to 1, where 0 represents a cellular state in which only AMP is present and 1 indicates that only ATP is present in the cell. A larger energy charge value is indicative of higher energy levels in the cell [Bibila, 1991]. In addition, the concentration of ATP in cells under normal conditions is reported to be in the range of 2-10 mM [Szewczyk and Pikula, 1998]; for example, in the hamster pancreatic cell line HIT-T1β, the intracellular ATP concentration was reported to be 5.2 mM [Niki et al., 1989].

Use of capillary electrophoresis in nucleotide measurements

Capillary electrophoresis has been chosen for the measurement of intracellular ATP, ADP and AMP concentrations due a number of reasons – firstly, the amount of sample required for analysis is relatively small compared to other methods such as high performance liquid chromatography (HPLC) (the amount of detected compound required in the sample is 100 times less in capillary electrophoresis [Ng et al., 1992]). Capillary electrophoresis methods also lead to reduced buffer consumption [Ji et al., 1999] and can result in shorter analysis times with the appropriate capillary and running conditions [Hsu et al., 1995; Kaulich et al.,

2003; Ng et al., 1992]. In addition, it is able to analyse the concentrations of all three nucleotides in a single run, unlike the use of fluorescent assays, in which each nucleotide has to be detected individually. Each electrophoresis run produces an electropherogram, an example of which can be seen in Figure 4.10. The ATP, ADP and AMP peaks are indicated in the figure, together with the extraction efficiency standard, GMP as well as the inverted peak which is representative of the internal loading standard, DNP-L-glutamic acid (DNP). The results obtained in this analysis were normalised to DNP and adjusted according to the extraction efficiency obtained in each sample run. The concentration of each nucleotide in unknown samples was then determined by comparing the area under the peak (AUP) to the respective standard curves constructed with known nucleotide concentrations. An example of the standard curves obtained for each data set is given in Figure 4.11.

Behaviour of energy parameters with specific growth rate and antibody productivity

Another key hypothesis regarding the mechanism of hyperosmolarity proposes that the increase in nutrient uptake leads to increased cellular energy levels and subsequently enhances IgG translation rates and specific antibody productivity [Lin et al., 1999a]. In order to test this hypothesis, the behaviour of ATP concentration and energy charge under normal and hyperosmotic conditions with respect to both specific growth rate and antibody productivity is presented in Figures 4.12 and 4.13. Firstly, as expected, the ATP concentrations under both osmotic conditions were positively correlated to the specific growth rates. The trends in Figure 4.12 a also indicate that the mid-exponential ATP concentration was in excess, hence, the decrease in specific growth rate in response to a fall in ATP concentration was comparatively smaller than in the stationary and decline culture stages. For instance, in hyperosmotic cultures – a drop in ATP concentration resulted in a less than proportionate decrease in specific growth rate initially, however, once the experimentally observed "threshold" ATP concentration (approximately 3 mM) was reached, the growth rate became very sensitive to slight decreases in the amount of ATP present. The same trend, although to a lesser extent, was also observed under normal culture conditions. To determine whether the ATP concentrations for normal and hyperosmotic culture conditions were significantly different with respect to growth, a single factor ANOVA and

two-tailed t-test were performed on both ATP data sets. Results of both tests indicate that the ATP values in both groups were not significantly different, implying that there was insufficient evidence to show that ATP concentrations were enhanced at hyperosmotic conditions. Figure 4.12 b shows the relationship between energy charge and the specific growth rate under both sets of osmotic conditions. In this graph, a distinct difference can be seen in the energy charge trends between normal and hyperosmotic cultures – at the same energy charge level, hyperosmotic cultures had a distinctly lower specific growth rate, which suggested that cells under hyperosmotic stress require a larger amount of energy to attain the same level of growth present under normal culture conditions.

From Figures 4.13 a and 4.13 b, the relationships between the energy parameters and specific antibody productivity can be determined. Figure 4.13 a indicates that a positive relationship existed between ATP concentration and specific productivity. However, two distinct positive relationships were derived for normal and hyperosmotic cultures, implying that specific productivities at hyperosmotic conditions were comparatively higher than those at normal culture conditions for any given ATP concentration. These trends also indicated that the increase in specific productivity at hyperosmotic culture conditions was probably not a direct result of increased energy levels in the cell. In Figure 4.13 b, a positive relationship between the energy charge and specific productivity was also apparent. Once again, the specific productivity at hyperosmotic conditions appeared to be relatively higher in comparison to normal culture conditions at the same energy charge level.

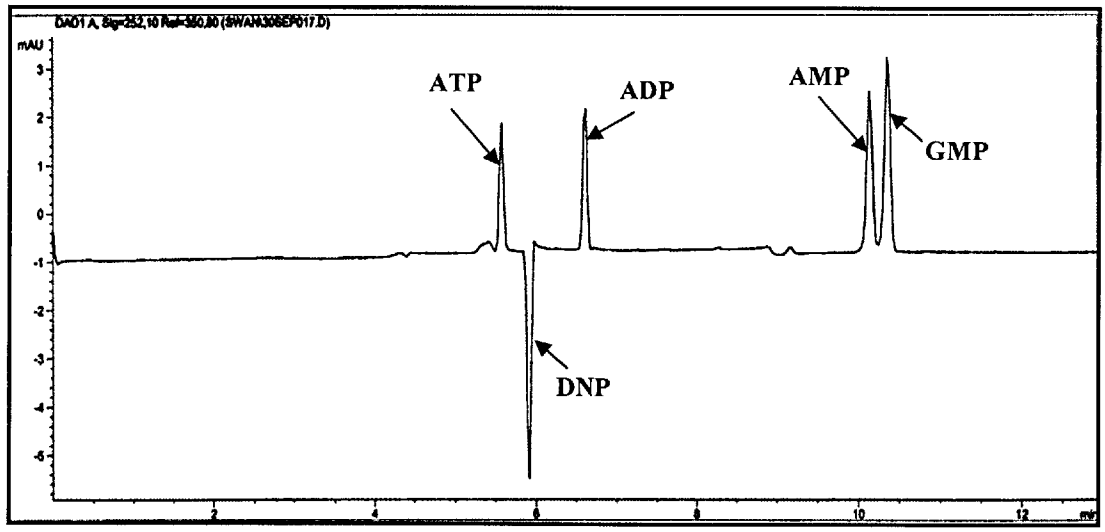

Figure 4.10. Example of an electropherogram obtained from the capillary electrophoresis analysis, with visible peaks representing ATP, ADP and AMP species. GMP is used as in extraction efficiency standard and the inverted peak represents the internal loading control, DNP-L-Glutamic Acid.

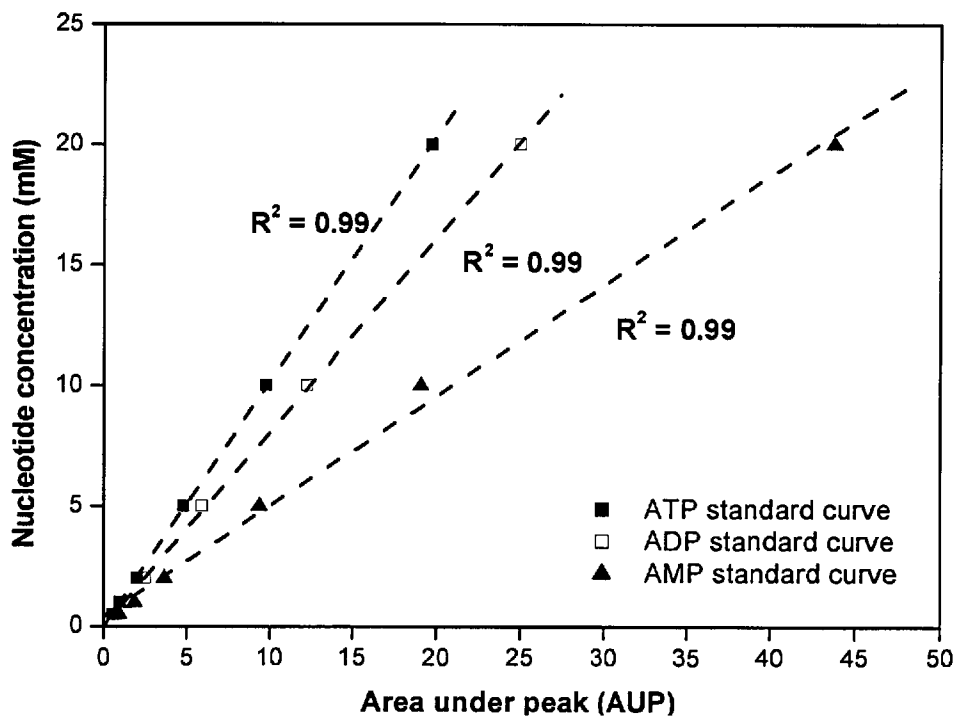

Figure 4.11. Example of standard curves derived for ATP, ADP and AMP with known nucleotide concentrations ranging from 0.5 to 20 mM. The standard curves were then used to determine ATP, ADP and AMP concentrations in cell sample extracts.

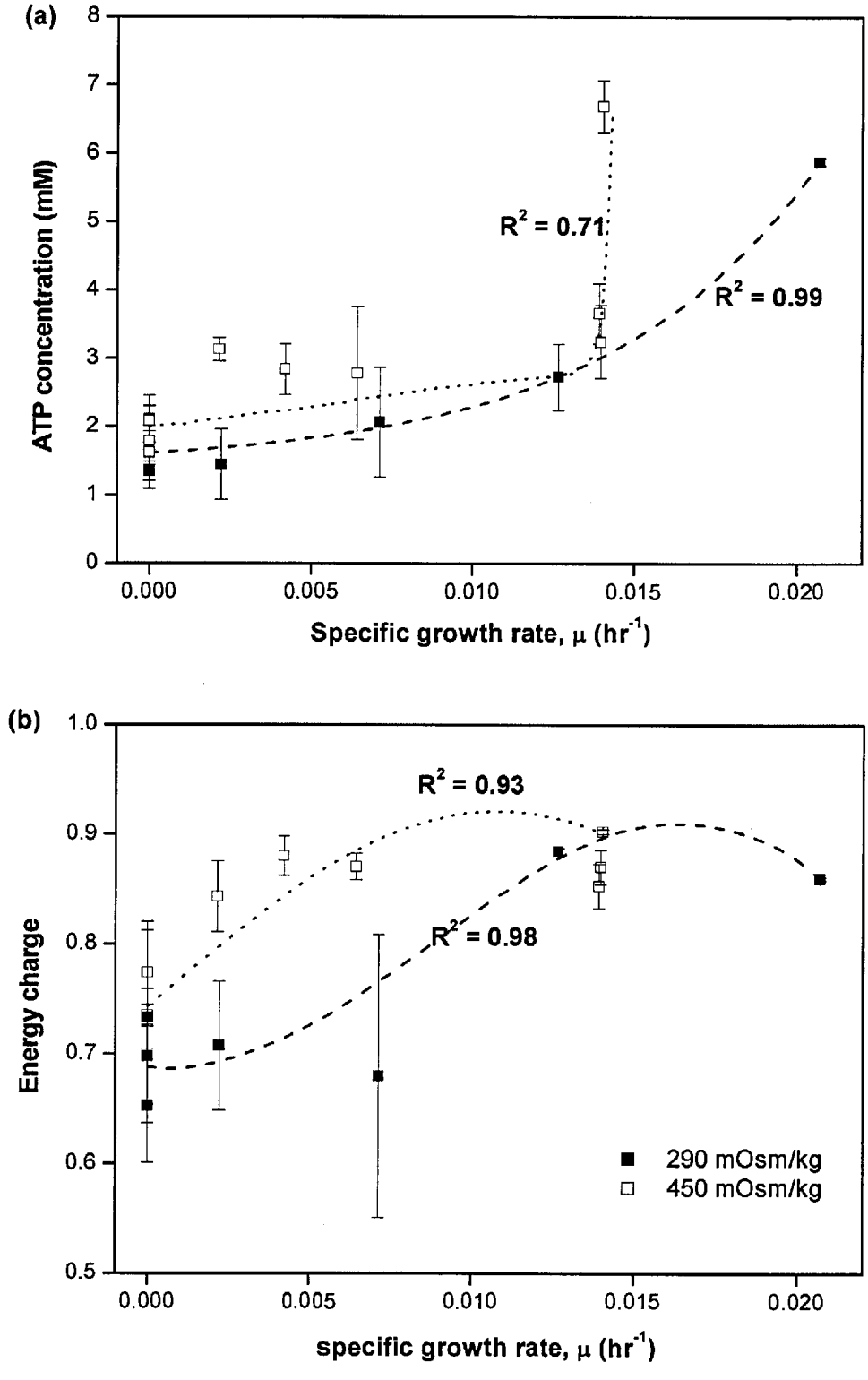

Figure 4.12. (a) ATP concentrations and (b) energy charge values with respect to specific growth rates under normal (290 mOsm/kg) and hyperosmotic (450 mOsm/kg) conditions.

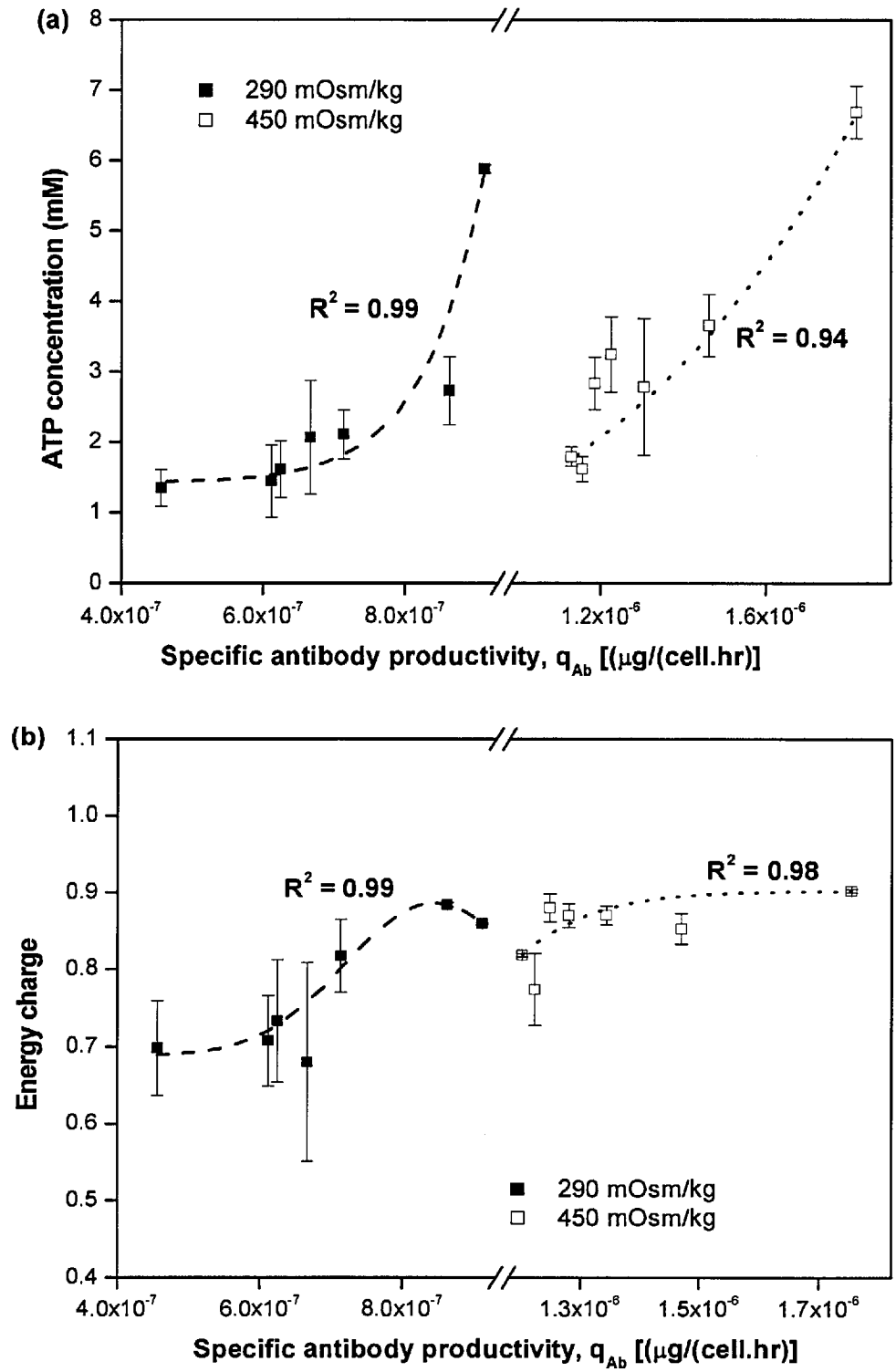

Figure 4.13. Behaviour of (a) ATP and (b) energy charge trends with respect to specific antibody productivity under normal (290 mOsm/kg) and hyperosmotic (450 mOsm/kg) culture conditions.

4.4 Discussion

In this chapter, the effects of hyperosmotic culture conditions on the aspects of growth, metabolism and extracellular antibody production for GS-NS0 cells have been studied. The resulting observations in terms of growth suppression and enhanced antibody production due to increased osmolarity are in agreement with previous studies conducted on the cell line [Duncan et al., 1997; Wu et al., 2004].

Extended culture longevity under hyperosmotic conditions

One of the key characteristics of GS-NS0 cells cultivated under hyperosmotic conditions is that of extended culture longevity. The relatively longer duration of hyperosmotic cultures can be attributed to longer mid-exponential and stationary phases due to a combination of a slower decrease in specific growth rates and a slower increase in specific death rate. The extension of culture longevity as a consequence of hyperosmotic conditions has been observed in previous studies on CHO [Ryu et al., 2001] and GS-NS0 cells [Wu et al., 2004]. The culture longevity is important at hyperosmotic conditions as it increases the duration of time available for the accumulation of antibody product in the medium and may partially compensate for the cell suppression effects caused by hyperosmolarity. In this study, the total antibody titre at hyperosmotic conditions (450 mOsm/kg) was substantially higher than under normal culture conditions. Antibody production trends indicated that the increase in final antibody titre could be attributed in large to the longer duration of the hyperosmotic culture. This is due to the fact that up until the 168-hour time point (towards the end of the normal condition culture), the total amount of antibody accumulated for both normal and hyperosmotic cultures were approximately the same; it was only after this time point that the main difference in total accumulated antibody concentration between the two osmotic conditions could be clearly discerned.

Relationships between hyperosmolarity, cell cycle arrest and growth suppression

The suppression of cellular growth under hyperosmotic culture conditions has frequently been attributed to the induction of cell cycle arrest in a number of mammalian cell lines,

including CHO [Ryu et al., 2001], hybridoma [Cherlet and Marc, 1999] and mIMCD-3 cells (murine inner medullary cell line) [Santos et al., 2003]. Hyperosmolarity induced by high concentrations of sodium chloride has been reported to induce DNA breaks, as well as prevent the repair of DNA damage in cells [Dimitrieva and Burg, 2005], thereby resulting in cell cycle arrest of damaged cells in the G0/G1 phase. In this study, a similar trend was observed in GS-NS0 cells under hyperosmotic culture conditions - the proportion of cells in the G0/G1 phase was significantly higher than in cultures under normal osmotic conditions, which supported the link between hyperosmolarity and the partial arrest of the cell cycle. Indeed, it appears that the proportion of cells in the G0/G1 phase under both osmotic conditions showed a negative correlation to the specific growth rate. For instance, the initial increase in specific growth rate as hyperosmotic cultures progressed from the lag to the mid-exponential phase was reflected in the slight decrease in the proportion of cells in the G0/G1 phase. The G0/G1 cell proportion then increased steadily as the cultures progressed from the mid-exponential to the stationary phase, reflecting the decrease in specific growth rates under both osmotic conditions, which further illustrated the inverse relationship between hyperosmotically- induced cell cycle arrest and cell growth rates.

It is also observed that the proportion of cells in the G2/M phase is consistently higher for hyperosmotic cultures when compared to normal osmotic cultures at time points beyond 72 hours into the culture. This phenomenon may have been due to a an arrest of a proportion of cells in the G2/M phase (in addition to G0/G1 cycle arrest), which had been previously observed in murine kidney cells after hyperosmotic induction by the addition of sodium chloride [Kultz et al., 1998].

Cell cycle arrest and enhancement of specific antibody productivity

In order to evaluate the hypothesis that the partial cell cycle arrest results in a redistribution of resources towards enhancing antibody productivity, the relationship between cell cycle behaviour and antibody productivity trends has also been analysed. Two key observations can be derived from the trends in the figures and will be discussed in detail in this section. The first important observation is concerned with determining the type of producers that GS-NS0 cells belong to. In a previous study conducted on hybridoma cell lines, Dutton et al.

[1998] had stated that cells could be classified according to four different types of producers based on the correlations between their specific productivity and specific growth rates. These four types include: (i) non-growth-associated producers, whose specific productivities remain unaffected by growth rates, (ii) growth-associated producers, whose productivities show a positive relationship with specific growth rates, (iii) negatively growth-associated producers, for which specific productivities increase when growth rates decrease and (iv) partially growth-associated producers, which show the characteristics of the first three producer types at different growth intervals.

Apart from the correlations between specific productivities and specific growth rates, the type of producer can also be inferred from relationships between specific productivities and the proportion of cells in different phases of the cell cycle. For instance, Fox et al. [2005] studied the effects of hypothermia on CHO cells and established that a positive relationship existed between the proportion of cells in the S phase and the specific antibody productivity values. As cells in the S phase were actively growing cells, the authors subsequently deduced that the cells were growth-associated producers. In our study, an increase in the proportion of cells in the S phase resulted in increased antibody productivity. Conversely, the antibody productivity had an inverse relationship with the proportion of cells in the G0/G1 phase (cell repair and "resting" phase), indicating that an increase in the proportion of arrested cells actually resulted in lower antibody productivity. In addition, a positive relationship was seen between the specific antibody productivity and the specific growth rate, further implying that antibody production in GS-NS0 cells was indeed growth-associated. It must be mentioned here that there had been suggestions that the increase in specific productivity could be attributed solely to an increase in cell size under hyperosmotic conditions [Lloyd et al., 2000], rather than being associated with growth charaacteristics. However, previous information related to the GS-NS0 cell size calculated at the mid-exponential phase [Wu, unpublished data] indicated that the percentage increase in cell volume was substantially less than the increase in antibody productivity at the mid-exponential phase (<30% increase in cell size compared to > 90% increase in q_{Ab}). Therefore, the increase in cell size is not likely to be the sole reason for the increase in specific productivities at hyperosmotic conditions.

The second point to note from the cell cycle and specific antibody productivities data is the fact that two separate correlations existed between the proportion of cells in each cycle phase and the specific antibody productivity under normal and hyperosmotic culture conditions. This implies that there was a shift in the cell cycle-specific antibody productivity relationship under hyperosmotic conditions, hence indicating that the increase in productivity is likely to be attributed to some other mechanism, rather than associated with changes in the cell cycle characteristics of hyperosmotic cultures. These deductions suggest that partial cell cycle arrest is unlikely to be a key reason for the improvement of antibody production rates under hyperosmotic conditions. Instead, the positive relationship between specific growth rate and antibody productivity seemed to imply that at hyperosmotic conditions, a reduction in cell growth suppression leading to improvements in the specific growth rates might actually lead to higher specific productivities. In the upcoming sections and the next chapter, other possible mechanisms through which hyperosmolarity may act will be further investigated so as to ascertain the cause of the increase in specific antibody productivities.

Hyperosmolarity effects on cellular metabolism and energy production processes

The trends of specific glucose, lactate and ammonium ion (NH_4^+) rates indicate that increases in metabolic rates were observed under hyperosmotic conditions. This increase is further corroborated by the gene expression analysis conducted by Wu [2006], who found an up-regulation in genes related to carbohydrate, nitrogen and energy metabolism, and glucose uptake under hyperosmotic culture conditions. In particular, the increase in specific glucose consumption at heightened osmolarity had been similarly observed in several previous studies on CHO [Takagi et al., 2000], hybridoma [Oh et al., 1995; Ozturk and Palsson, 1991b] and GS-NS0 cells [Duncan et al., 1997]. In addition, it was found that the lactate yield from glucose increased under hyperosmotic conditions, suggesting that a shift in glucose metabolism towards the production of more lactate from pyruvate was likely to have occurred. The shift could possibly reduced the proportion of pyruvate entering the TCA cycle and led to less efficient energy producing pathways – the theoretical yield of energy for the glucose to lactate pathway is only 8 moles of ATP per mole of glucose compared to the maximum theoretical yield of 36 moles ATP per mole glucose that can be produced by the

complete oxidation of glucose through oxidative phosphorylation. This metabolic shift towards less efficient energy pathways by hyperosmotic cultures had likely resulted in the similar cellular ATP concentrations being observed under both osmotic conditions. The observations are in agreement with results reported by Devin et al. [1996], who found a reduction in the oxidative phosphorylation efficiency (as given by [ATP]/[O] where [O] is the oxygen concentration) occurred under hyperosmotic conditions in the mitochondria of rat liver cells. Due to the reduced energy yield per mole of glucose, cells under hyperosmotic conditions at the exponential culture phase had to compensate by increasing the glucose consumption rate in order to generate the same amount of energy as cells under normal culture conditions. Duncan et al. [1997] also suggested that hyperosmotic cells might require comparatively higher maintenance energies, which agreed with our findings that a larger amount of energy had to be expended in hyperosmotic cultures so that the same growth rate present in normal cultures could be reached. The implications of the aforementioned metabolic and energy trends with respect to specific antibody productivities will be further discussed in the next section.

Energy metabolism and antibody productivity

In literature, the protein synthesis process is often affected by the availability of energy-providing substrates (in the form of nutrients) in the cell [Bibila, 1991]. The depletion of nutrients such as glucose and glutamine generally resulted in a decrease in protein translation rates [Dahn et al., 1993; Duncan and Hershey, 1987; Jorgensen and Tyers, 2004]. These reports signify that cellular energy levels may be a key factor in the determination of heavy and light IgG polypeptide chain synthesis rates. Additionally, it had been proposed by Lin et al. [1999a] that hyperosmotic conditions led to an increase in specific ATP production rates, which in turn resulted in heightened translation rates, hence improving specific antibody productivities. In this study, a positive relationship was derived between the energy levels in GS-NS0 cells and the specific antibody productivity, indicating that the availability of energy did indeed play an important role in the determination of antibody production rates, particularly at lower ATP concentrations (experimentally observed to be less than 3mM/cell). However, as discussed in the previous section, hyperosmotic conditions did not

lead to a significant increase in cellular ATP concentration due to the shift in metabolic processes towards less efficient energy producing pathways. Additionally, separate correlations had been obtained between ATP concentration and specific productivity for normal and hyperosmotic cultures. This implies that for any given ATP concentration, the specific productivities derived under normal and hyperosmotic conditions were different, suggesting that another determining factor was responsible for improving GS-NS0 antibody productivity under hyperosmotic conditions. Nevertheless, the positive correlation between specific productivity and ATP concentration highlights the possibility of further improving antibody productivities by increasing energy levels in the cell under hyperosmotic conditions. This may be achieved by firstly, the identification of the less efficient energy-producing pathways, and subsequently attempting to shift cellular metabolisms back towards the more efficient pathways; for instance, using a basal medium [Ryu and Lee, 1997] best suited to hyperosmotic conditions, as well as using a suitable nutrient feeding strategy may lead to more effective nutrient utilisation and an increase in cellular energy levels.

4.5 Conclusions

This chapter had focused on evaluating how the characteristics of growth and metabolism under normal and hyperosmotic conditions relate to antibody production rates in GS-NS0 cells. It was observed that hyperosmotic conditions lead to cell cycle arrest, which in turn reduced the specific growth rate of the cultures. However, GS-NS0 specific antibody productivity was found to be growth-associated, indicating that cell cycle arrest was unlikely to be the reason for the increased antibody productivity under hyperosmotic conditions. Additionally, relatively higher specific metabolic rates in hyperosmotic cultures did not result in a substantial increase in ATP concentration. Instead, a higher lactate yield from glucose indicated that there was a possible shift in metabolism towards less efficient energy production pathways at hyperosmotic conditions. As a result, the increase in glucose uptake rate was necessary to produce sufficient energy in hyperosmotically stressed cells to sustain growth and other cellular processes. Consequently, it was deduced that an increase in ATP

levels was not the key reason for the improvement of specific antibody productivity at hyperosmotic culture conditions.

Chapter 5

Behaviour of mRNA and Intracellular IgG Trends in GS-NS0 Batch Cultures

5.1 Introduction

In Chapter 4, two proposed hypotheses regarding the mechanism through which hyperosmotic conditions lead to improved specific antibody productivity were investigated – experimental results obtained subsequently indicated that neither cell cycle arrest induced by hyperosmolarity, nor an increase in cellular energy (ATP) levels, was likely to be responsible for increasing antibody productivity under hyperosmotic conditions in GS-NS0 cells. This chapter will focus on two key points: firstly, in order to identify the main reasons for hyperosmotic stimulation of antibody productivities and evaluate other existing hyperosmotic hypotheses associated with intracellular IgG synthesis, the behaviour of IgG mRNA, polypeptide chains and IgG mRNA degradation rates with respect to time and osmolarity are studied experimentally. The second key issue involves the experimental estimation of the key parameters (specific transcription and translation rates, as well as mRNA degradation rates) previously identified by global sensitivity analysis of the hybrid model (see Chapter 3).

The experimental study involves the use of two main experimental techniques for the analyses of intracellular mRNA and polypeptide chain concentrations. Northern blotting is utilised in the determination of relative mRNA levels at different culture time points while

a Western blotting procedure involving SDS-PAGE gel electrophoresis under reducing conditions is used for the evaluation of total intracellular heavy and light IgG polypeptide species. A more detailed description of these techniques will be given in Section 5.2.

In Sections 5.1.1 to 5.1.3, currently known information obtained from various literature studies regarding the behaviour of total RNA, heavy and light IgG mRNA and polypeptide chain concentrations with respect to time and osmolarity are summarised.

5.1.1 Behaviour of RNA and mRNA concentrations with respect to culture time

In previous studies on the variation of total RNA with culture time for hybridoma cells, Ozturk and Palsson [Ozturk and Palsson, 1991a], Bibila [1991], and Sun et al. [2004] reported that RNA concentration decreases steadily as the culture progresses from the exponential to the stationary and decline phases. However, Leno et al. [1992] observed that the total RNA concentration initially increased until it reached a peak at the end of the exponential phase before decreasing to 34% of the maximum RNA concentration in the decline phase. The trends for heavy and light mRNA concentrations on a per cell basis have also been studied. Relatively constant concentrations of heavy and light mRNA molecules were detected throughout the exponential phase before decreasing in the later culture phases [Bibila, 1991]. In contrast, both mRNA species were reported to increase to a maximum towards the end of the exponential phase before declining in the stationary and decline phases by Leno et al. [1992]. Another study on hybridoma cells carried out by Zhou [2002] appears to agree with the above trends - heavy and light mRNA concentrations were shown to increase until near the end of the exponential phase, before declining in the stationary phase.

5.1.2 RNA and mRNA trends under hyperosmotic culture conditions

At present, there are relatively few studies that have evaluated RNA and mRNA trends under hyperosmotic culture conditions. Two major studies have been mentioned in Section 2.3.2: the study on KR12H-2 transfectomas conducted by Lee and Lee [2000], which analysed

differences in RNA and mRNA values for different osmotic culture conditions solely at the mid-exponential phase, as well as the study carried out by Sun et al. [2004], which focused on how inducing osmotic shock in cultures affect RNA and mRNA values. The first study found a 56% increase in the amount of total RNA when the osmolarity of the culture was increased from 285 to 425 mOsm/kg while heavy and light mRNA concentrations were increased by 322% and 340% respectively. In the second study, a slower rate of decline for total RNA was observed when the osmolarity of the culture was increased from 290 to 400 mOsm/kg in the mid-exponential phase (36 hours). As the osmotically stressed cells enter the stationary phase of the culture, the RNA content was 20% higher than in normal, unstressed cells at 72 hours and 50% higher at 84 hours into the culture. Additionally, the heavy and light mRNA concentrations for osmotically stressed cells were approximately 4 times higher than in normal cells during the stationary phase of the culture. From the above observations, it can be concluded that higher RNA and mRNA concentrations are expected in hyperosmotic cultures.

5.1.3 Intracellular heavy and light polypeptide trends under normal and hyperosmotic culture conditions

Total cellular protein levels have been observed to increase in the exponential growth phase before declining as the culture progresses into the stationary and decline phases [Jang and Barford, 2000]. This behaviour may be explained by the fact that the depletion of nutrients present in the medium tends to occur at the later cell culture stages, hence resulting in a reduction of intracellular amino acid pools available for protein synthesis. Additionally, hyperosmotic culture conditions have been reported to result in an increase in total cellular protein levels [Lee and Lee, 2000; Oh et al., 1995; Sun, 2000]. However, in a study on mouse plasmacytoma cells, Nuss and Koch [1976] found a drastic decrease in total protein levels as translation initiation was inhibited under hyperosmotic conditions.

The intracellular heavy and light polypeptide chain concentrations with respect to normal and hyperosmotic conditions have been studied by Sun et al. [2004]. The authors deduced that the heavy and light chain concentrations remained the same in hyperosmotic

cultures on a per μg protein basis, and suggested that any increase in polypeptide chain concentrations could be fully attributed to the overall increase in protein synthesis. On the other hand, Nuss and Koch [1976] reported that the translation of IgG polypeptide chains were preferentially enhanced at hyperosmotic conditions relative to the translation of other proteins, as seen from the following observations - while the addition of low levels of sodium chloride increased osmolarity and led to a 10-15% inhibition of protein synthesis, a 2-12% increase in the absolute amount of light polypeptide chains in comparison to normal culture conditions was measured. The authors also stated that light polypeptide chains appear to be more resistant to the inhibition of translation initiation by sodium chloride than heavy polypeptide chains, resulting in a higher light to heavy polypeptide chain ratio at increased osmotic conditions.

The aim of this chapter is to evaluate the behaviour of total RNA and cellular protein, as well as heavy and light mRNA and polypeptide chains with respect to both culture time and hyperosmotic culture conditions. In addition, the mRNA degradation rates for normal and hyperosmotic cultures are also studied at the mid-exponential and early-stationary culture phases.

5.2 Materials and methods

5.2.1 Normal and hyperosmotic batch culture experiments

For the purposes of RNA and intracellular IgG polypeptide chains analyses, duplicate batch shake flask cultures were grown under normal (290 mOsm/kg) and hyperosmotic (450 mOsm/kg) culture conditions. 1×10^6 cells were collected for IgG polypeptide analysis by gel electrophoresis and Western blotting. For RNA analysis, 7.5×10^6 cells were collected at 48, 96, 120 and 144 hours after the start of the culture, corresponding to the mid-exponential, stationary and decline phases in normal osmotic cultures. In cultures under hyperosmotic conditions, 5×10^6 cells were collected at 96 (mid-exponential phase), 144 (late-exponential/ early-stationary) and 216 hours (decline phase) from the beginning of the culture.

5.2.2 Determination of heavy and light chain mRNA half-lives

In order to estimate the half-lives of the heavy and light IgG chain mRNA molecules, duplicate shake flask experiments were carried out at normal and hyperosmotic culture conditions. At the mid-exponential and early stationary phases of each culture, cell transcription was blocked by the addition of 65 μM of the transcription inhibitor DRB (5,6 dichloro-1β-D-ribofuranosyl benzimidazole; Sigma) dissolved in 100% ethanol (VWR). The concentration was chosen as it had previously been reported to ensure near maximal inhibition of transcription [Bibila, 1991]. Subsequently, 5 x 10^6 cells were collected from each culture at various time intervals following the addition of DRB. To ensure that ethanol does not affect the mRNA degradation process, the same volume of ethanol was added to control cultures at the mid-exponential phase under both normal and hyperosmotic conditions. Samples consisting of 5 x 10^6 cells were then collected at 0, 4, 8 and 12 hours after ethanol addition. All RNA samples collected were subsequently analysed by agarose gel electrophoresis and Northern blotting (procedure described in Section 5.2.3).

5.2.3 Intracellular heavy and light chain mRNA analysis – Northern blotting

Preparation of total cellular RNA from GS-NS0 cells

The cell samples collected at different culture phases from normal and hyperosmotic cultures were centrifuged at 800 rpm for 5 minutes in order to aspirate the supernatant. The cells were then washed once with PBS and centrifuged again (same conditions as above) to remove the PBS solution. 600 μL of cell lysis solution (buffer RLT) from the Qiagen RNeasy mini kit for total RNA extraction (Qiagen, UK), supplemented with 6 μL of β-mercaptoethanol (Sigma), was added to each cellular sample and mixed thoroughly by pipetting vigorously and vortexing continuously for 1 minute. The samples were then stored at -86°C prior to RNA extraction.

RNA extraction from the lysed cell samples prepared above was carried out just before analysis by agarose gel electrophoresis. The samples were first thawed by immersing them in a 37°C water bath for 10 minutes to ensure that all salts within the samples were

dissolved. 600 μL of 70% ethanol (prepared in RNase-free water) was then added to the samples and mixed thoroughly by pipetting. 700 μL aliquots of each sample were applied successively to the RNeasy mini spin column supplied in the kit and centrifuged at 10,000 rpm for 15 seconds. The flow-through was discarded after each centrifugation step. Subsequently, the silica-gel membrane in the RNeasy column was washed by 700 μL of buffer RW1 and two successive washes of 500 μL of buffer RPE each. The columns were centrifuged at 10,000 rpm for 15 seconds and the flow-through discarded after each washing step. After the final washing step, the column is centrifuged at 10,000 rpm for 2 minutes to dry the RNeasy membrane. The RNeasy column was transferred to a new 1.5 mL microcentrifuge tube and 35 μL of RNase-free water (both tube and water supplied by RNeasy kit) was pipetted directly onto the silica-gel membrane. The tube was centrifuged for 1 minute at 10,000 rpm to elute the RNA collected by the membrane. The above elution step was repeated with 30 μL of RNase-free water to ensure all RNA on the membrane has been collected.

Total RNA quantification

5 μL of the RNA eluent collected in the previous section was diluted in 245 μL of RNase-free water and vortexed to ensure equal mixing. The absorbance of the 1:50 diluted sample was then measured using a UV spectrophotometer (CaryWin UV, Varian Inc, USA) at wavelengths of 260 nm (A_{260}) and 280 nm (A_{280}). The concentration of RNA is given by the following formula:

$$\text{RNA concentration} = 40 \times A_{260} \times 50$$
$$= 200 \times A_{260} \ \mu\text{g/mL}$$

The A_{260}/ A_{280} ratio provides an estimate of the purity of RNA with respect to contaminants that absorb in the UV and all sample ratios were determined to be > 1.8.

Sample preparation for agarose gel electrophoresis

10 μg of sample was mixed with 5 × RNA sample buffer in a 4:1 volume ratio, vortexed and heated at 65 C for 15 minutes. The samples were transferred immediately onto ice for 5

minutes before being loaded onto the gel. For 10 mL of 5 × RNA sample buffer, the composition was as follows: 80 μL 0.5 M sodium EDTA at pH 8.0, 750 μL of 37% formaldehyde (Sigma), 3.084 mL of formamide (VWR), 4 mL of 10 × MOPS ((3-(N-Morpholino)propanesulfonic acid) buffer (0.4 M MOPS (VWR), 0.1 sodium acetate (Sigma) and 0.01 M di-sodium EDTA (VWR)), 25 mg bromophenol blue (Sigma), 25 mg xylene cyanol (Sigma) and 2 mL of glycerol.

Agarose gel electrophoresis of RNA and transfer to nylon membrane

A 1.5% agarose-formaldehyde based gel was used to separate the RNA molecules according to their molecular weight. The composition of the gel was as follows: 1.5 g agarose (Invitrogen), 10 mL of 10 × MOPS buffer, 1.8 mL formaldehyde (Sigma) made up to 100 mL with DEPC-treated water (1 mL diethyl pyrocarbonate, (Sigma) in 1 L deionised water). The gel was allowed to cool for 1 hour at room temperature before being submersed in approximately 500 mL of 1 × MOPS buffer composed of the following components in DEPC-treated water: 10% (v/v) of 10 × MOPS buffer and 2% (v/v) of 37% formaldehyde solution (Sigma). The gel was allowed to equilibrate with the buffer for at least 30 minutes prior to sample loading. 5 μg of RNA per sample was loaded into each well and the gel was run at a constant voltage of 75 V for 2.5 hours.

After RNA separation was completed, the gel was rinsed in large quantities of nanopure water (Nanopure Diamond unit, Barnstead Thermolyne, USA) in order to remove formaldehyde, which inhibits RNA transfer to membrane, from the gel. The gel was then soaked for 40 minutes in 20 × SSC transfer buffer (3 M sodium chloride, 0.3 M sodium citrate tribasic dehydrate, both chemicals from Sigma) before the RNA was transferred to a nylon membrane (Nytran membrane, Schleicher and Schuell, USA) by downward capillary action for 1 hour and 15 minutes. The membrane was then rinsed with 2 × SSC and air-dried for 1 hour before being UV irradiated for 3 minutes to allow cross-linking to take place. Subsequently, the membrane was wrapped in Saran wrap and kept in a cool, dark place for further analysis by Northern blotting.

Membrane staining and Northern blotting of heavy and light chain mRNA

The membrane was first stained for 3-5 minutes in methylene blue solution consisting of 0.02%(w/v) methylene blue (Sigma) and 0.3 M sodium acetate. This allowed for the visualisation of the 18S ribosomal RNA band, which was then used as an equal loading standard. The membrane was photographed using an Olympus C-5060 camera (Olympus, UK) and the band intensities quantified by densitometry methods using the AlphaEaseFC software (Alpha Innotech Corp, USA). Subsequently, the membrane was destained in a solution comprising of 0.2 × SSC and 1% (w/v) SDS for 15 minutes.

Prior to prehybridisation, the membrane was rinsed briefly in 6 × SSC. The prehybridsation solution recipe was as follows: 5 × SSPE (0.75 M sodium chloride, 50 mM sodium phosphate monobasic (Sigma), 4 mM di-sodium EDTA), 5 × Denhardt's solution (50 × concentrate from VWR), 50% (v/v) formamide, 0.5% (w/v) SDS and 100 μg/mL denatured salmon sperm DNA (Sigma). 1 mL of prehybridisation solution was used for every 10 cm^3 of membrane. The prehybridisation solution was pre-warmed to 42 C before being added to the membrane. The membrane was then placed in an orbital shaking incubator at 42 C for 1 hour. Subsequently, heavy and light chain mRNA-specific biotin-labelled oligonucleotide probes (Operon, Germany) were added to the prehybridisation solution at a concentration of 25 ng/mL and the membrane incubated overnight at 42 C on an orbital shaker. The oligonucleotide probe sequences were kindly provided by Dr Mark Smales (Univ. of Kent, UK) and are as follows:

Heavy chain mRNA probe – 5' GGCAGTGCTGGAGGATTT 3' and

Light chain mRNA probe – 5' TGTGTGCCCGATCCACTGCCA 3'

After hybridisation, the membrane was washed twice in 2 × SSC solution with 0.1% SDS for 5 minutes each. It was then washed once in 0.2 × SSC with 0.1% SDS for an additional 5 minutes at 42 C. The membrane was then processed with the Nucleic Acid Chemiluminescent kit (Perbio, UK) following manufacturer's instructions. Briefly, the membrane was blocked for 15 minutes with the supplied blocking solution at room temperature before the streptavidin-HRP conjugated solution was added (66.7 μL per 20 mL blocking solution). The membrane was incubated with this solution for a further 15 minutes at room temperature. Next, the membrane was transferred to a new container, rinsed briefly

with the supplied washing buffer before being washed 4 times with the same washing buffer for 5 minutes each. The membrane was then equilibrated for 5 minutes in the equilibration buffer before excess solution was blotted off and the membrane placed on a piece of Saran wrap. The luminal substrate was mixed with the stable peroxide solution in equal volumes and the mixture poured evenly onto the surface of the membrane. The substrate was allowed to react with the HRP-conjugated molecules for 5 minutes before the membrane was wrapped in Saran wrap and exposed to Kodak BioMax Light film (Kodak, UK) for a time period ranging from 1 second to 1 minute. The relative intensities of the bands were once again quantified using the densitometry function available in AlphaEaseFC software and normalised using the 18S rRNA relative intensities.

5.2.4 Intracellular cB72.3 antibody analysis – SDS-PAGE and Western blotting

Separation of viable and non-viable cells from sample

1-2 x 10^6 cells were harvested daily by centrifugation at 800 rpm for 5 minutes and washed in ice-cold PBS. The PBS was aspirated and the viable cells separated from non-viable cells using the MACS® dead cell removal kit (Miltenyi Biotec, UK), according to manufacturer's instructions. Briefly, the cell pellet was resuspended in 100 μL of dead cell removal microbeads for 15 minutes at room temperature. A positive selection column of type MS was set up in the magnetic field of a MiniMACS® Separator and rinsed with 500 μL of the supplied binding buffer. The cell-microbead mixture was subsequently mixed with 500 μL of binding buffer and allowed to pass through the MS column. The effluent from the column was then collected as the live cell fraction. The column was further rinsed with 4 x 500 μL of binding buffer and the additional effluent collected to ensure all viable cells are selected. Finally, the effluent was centrifuged at 800 rpm for 5 minutes so that the binding buffer can be aspirated and the resulting cell pellet was stored at –20 C for further analysis.

Preparation of GS-NS0 cell lysates

Cell samples were retrieved from –20 C and resuspended in 125 μL of CelLytic™ M solution supplemented by 1% (v/v) protease inhibitor cocktail (both products from Sigma).

The solution is then incubated at room temperature on an orbital shaker for 15 minutes. Subsequently, the lysed cells are centrifuged at 18,000 x g for 15 minutes to pellet the cell debris. The protein-containing supernatant is then removed to a chilled microcentrifuge tube and stored at –86 C prior to gel electrophoresis and Western blot analysis.

Total protein quantification

The total amount of protein in each cell sample was determined using the BCA™ Protein Assay Kit (Perbio). The quantification method was based on the reduction of the Cu^{2+} ion to Cu^{1+} by protein in an alkaline medium. The Cu^{1+} ion was then detected via a colorimetric reaction with a reagent containing BCA. The resulting intensity of the colour change (from pale green to purple) could then be used to determine the amount of protein present in the sample. Bovine serum albumin (BSA) was utilised as the known protein standard in a series of 8 dilutions to create a calibration curve against which the protein concentration in the unknown cell samples was determined. The quantification procedure is briefly described as follows: the protein-containing supernatant derived in the previous section was first diluted 1:10 with deionised water. 8 dilutions of the BSA standard was then prepared in deionised water with concentrations ranging from 0 μg/mL to 500 μg/mL. 25 μL of each standard and unknown sample was pipetted into a microplate well in duplicate. 200 μL of the supplied working reagent (consisting of Cu^{2+} ions and BCA) was then added to each well, the plate was covered and incubated in an orbital shaking incubator at 37 C for 30 minutes. Following incubation, the plate was cooled to room temperature and the absorbance of each well measured on a microplate reader at a wavelength of 560 nm.

Sample preparation for SDS-PAGE

20 μg of each cellular sample as determined by the BCA protein assay, in addition to known concentrations of the purified cB72.3 antibody standard kindly provided by Lonza Biologics (UK) (ranging from 100 μg to 1000 μg) were prepared for loading onto each lane for SDS-PAGE. The samples and standards are topped up to 20 μL with deionised water and mixed with 20 μL of 2 x SDS-PAGE reducing sample buffer comprising of the following: 0.125 M Tris-HCl, 5% SDS, 20% (v/v) glycerol, 0.2 M DTT (Dithiothreitol from VWR, UK),

0.02% bromophenol blue at pH 6.8. The mixture was then heated at 100 C for 10 minutes to ensure that the proteins were denatured. Subsequently, the mixture was placed on ice prior to gel loading.

SDS-PAGE and transfer to nitrocellulose membrane

One-dimensional SDS-PAGE (based on the method of Laemmli, 1970) was carried out in a vertical mini-gel electrophoresis unit (Thermo Electron, US) at a constant voltage of 150 V for 65 minutes or until the bromophenol blue dye has migrated to the bottom of the gel. The separating gel acrylamide concentration was 10% and the size of each gel was approximately 9 cm width x 8 cm height x 0.75 mm thick. The following solutions were used in the separation and stacking gels: 10% separation gel – 7.25 mL of Protogel acrylamide mixture (National Diagnostics, USA), 3.8 mL of 2M Tris-HCl at pH 8.8, 0.4 mL of 10%(w/v) SDS, topped up to 20 mL with deionised water, stacking gel – 1.7 mL of Protogel acrylamide mixture, 625 □L of 2M Tris-HCl at pH 6.8, 100 μL of 10%(w/v) SDS, topped up to 10 mL with deionised water. The separation gel solution was mixed with 200 μL of ammonium persulfate (APS) and 40 μL of TEMED (N, N, N', N' tetramethyl-ethylenediamine) (both chemicals from VWR, UK) and immediately introduced between the glass plates and allowed to polymerise for about 20-30 minutes. 40 μL of APS and 30 μL of TEMED were then added to the stacking gel mixture prior to the solution being introduced on top of the polymerised separation gel. A tris-glycine based solution was used as the SDS-PAGE running buffer (14.4 g/L glycine, 3.0 g/L tris, 1.0 g/L SDS).

Following gel electrophoresis, the gel was carefully removed from the glass plates and soaked in 1 x transfer buffer (14.4 g/L glycine, 3.0 g/L tris, 1.0 g/L SDS, 10% (v/v) methanol) for 30 minutes to allow for equilibration of the gel. The proteins on the gel were then transferred onto a nitrocellulose membrane (Protran, 0.45 μm pore size, Schleicher and Schuell, USA) following the method of Towbin et al. (1979) using the C140 Mini Blot Module (Thermo Electron, USA). The electro-blotter was assembled based on the manufacturer's instructions and filled with ice-cold 1 x transfer buffer. It was set to run at a constant current of 70 mA for 40 minutes. Subsequently, the blotted membrane was air-dried

for half a day at room temperature before being wrapped in Saran wrap and stored in a cool, dry place prior to Western blot analysis.

Western blotting of heavy and light IgG polypeptide chains

The dried nitrocellulose membrane was firstly blocked for 10 minutes in a blocking solution containing 10% (w/v) non-fat milk powder (Marvel non-fat milk powder, Premier International Foods Ltd, UK) in PBS. The blot was then allowed to react with a horseradish peroxidase (HRP)-conjugated goat anti-human IgG(H+L) antibody (Jackson Immunoresearch, USA) at a dilution of 1:4000 for 2 hours at room temperature on an orbital shaker. Following the incubation period, the blot was rinsed once with PBS for 5 minutes, washed 3 times with PBS containing 0.1% Tween for 5 minutes each and rinsed once again with PBS for a further 5 minutes. Excess solution was carefully blotted off using 3 MM chromatography paper (Whatman, UK) before the ECL chemiluminescent substrate solution, which reacted with the HRP molecule (Amersham Biosciences, UK), was added to the membrane and further incubated for 1 minute with gentle shaking. The membrane was then blotted dry, wrapped in Saran wrap and exposed to Kodak BioMax Light film for a period of time ranging from 2.5 to 30 minutes. The heavy and light polypeptide chains targeted by the HRP-conjugated antibody would appear as dark bands on the film. The resulting intensity of each band was quantified using AlphaEase FC densitometry-scanning software.

In order to check for equal loading of protein in each lane, the blot was then stripped by rinsing it twice in large quantities of PBS solution containing 0.1% Tween for 15 minutes each . Subsequently, the blot was blocked with 10% (w/v) non-fat milk powder in PBS for 10 minutes and re-probed with a HRP-conjugated anti-GAPDH antibody (Santa Cruz, CA, US) at a dilution of 1:500 for 2 hours. The blot was then washed with PBS and PBS-0.1% Tween solution and detected using the ECL substrate solution and Kodak BioMax film as described above.

5.2.5 Statistical analysis

The error bars in all graphs refer to standard deviations of duplicate measurements from two individual experiments unless otherwise stated. Single-factor ANOVA and two-sample t-tests (assuming unequal variance) at a significance level of $p=0.05$ have both been used to assess whether the mean values of any two samples can be considered to be significantly different from each other.

5.3 Results and analyses

5.3.1 Total RNA behaviour with respect to time and hyperosmotic conditions

The total RNA behaviours with respect to culture time for normal and hyperosmotic cultures are presented in Figure 5.1. Under both culture conditions, the total RNA appeared to be relatively constant during the mid-exponential phase and subsequently decreased as the culture progressed towards the stationary and decline phases. Hyperosmotic culture conditions seemed to result in a slower rate of decrease of total RNA concentration with respect to time. In particular, at the interface of the exponential and stationary phases, an 8% decrease in total RNA concentration was observed in hyperosmotic cultures, as compared to the 19% drop in RNA concentration observed in normal cultures.

The total RNA concentration has also been shown as a function of specific growth rate in Figure 5.2. The trends in the figure indicate that a positive relationship exists between cell growth and the amount of intracellular RNA under both normal and hyperosmotic conditions. It is observed that with respect to specific growth rates, total RNA concentrations were relatively higher in hyperosmotic cultures than in normal cultures. This trend is similar to the experimental observations of Zhou [2002], whose results have been derived from literature and displayed in the same figure. Once again, heightened levels of RNA were seen under hyperosmotic culture conditions at a given specific growth rate.

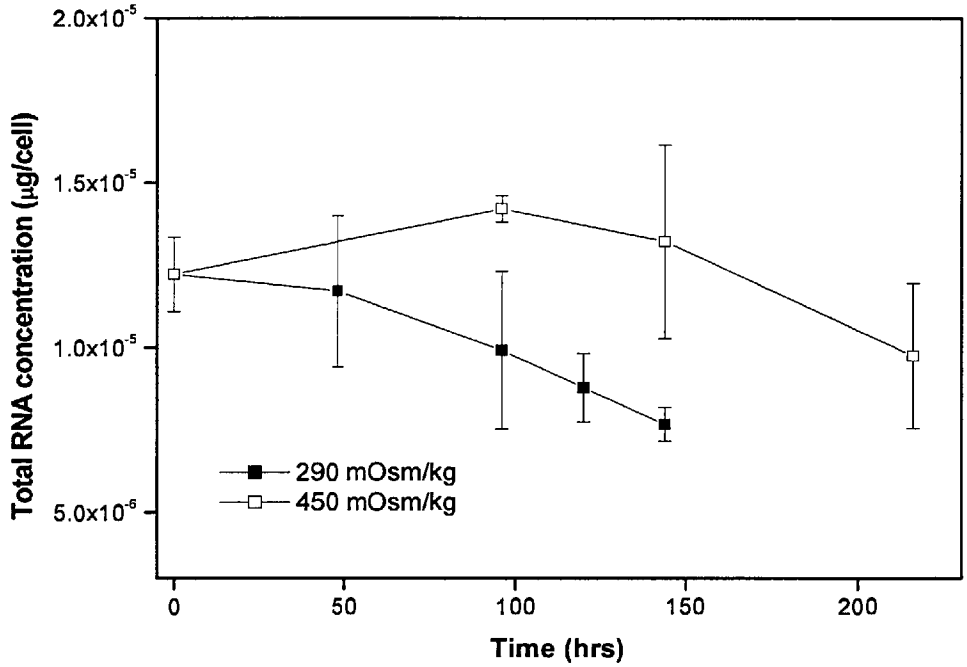

Figure 5.1. Variation of total RNA concentration at different culture time points for normal and hyperosmotic condition cultures.

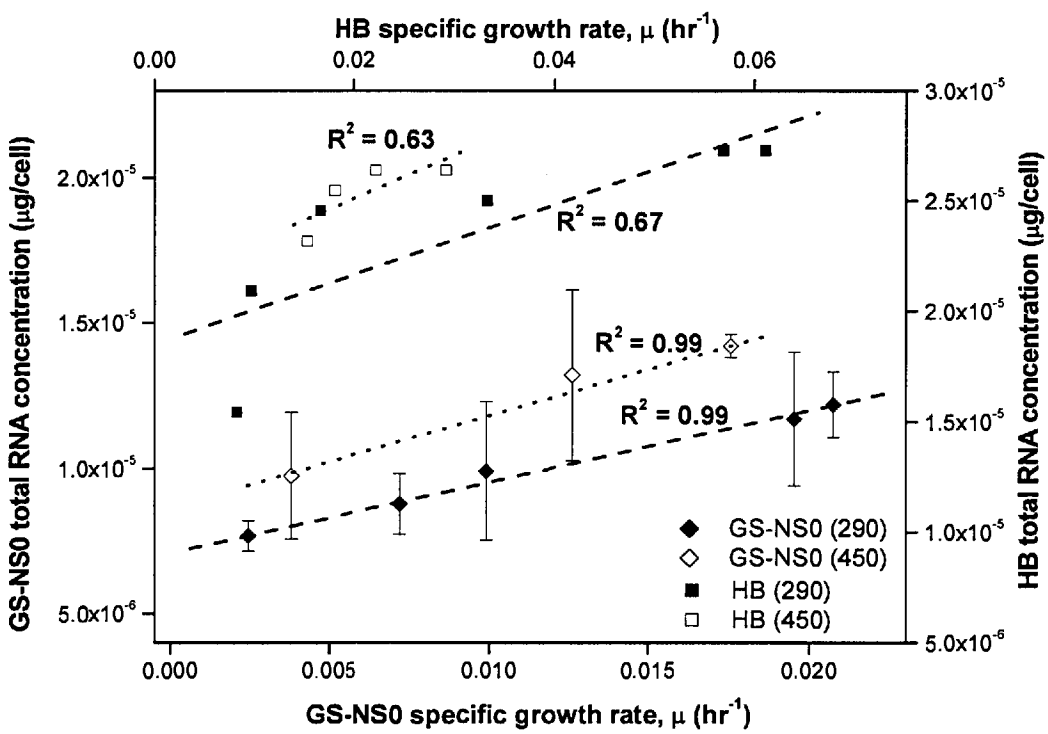

Figure 5.2. Relationships between total RNA concentrations and specific growth rates for both GS-NS0 cultures and hybridoma (HB) cells from experimental data derived from Zhou [2000]. Dotted lines represent the lines of best fit for each data set.

5.3.2 Heavy and light mRNA trends under normal and hyperosmotic conditions

Linearity of integrated intensity values

It is essential to first establish a relationship between the hybridisation signals of the heavy and light chain probes obtained from densitometry analysis and the amount of mRNA present on the blot before the densitometric value of each band on the blot can be compared. This relationship was determined by loading different known amounts of total RNA from a single sample onto a gel, and subsequently hybridising the membrane onto which the RNA was transferred. The bands on the membrane were then probed with the specific probe for either the heavy mRNA species or the light mRNA species and subsequently quantified using densitometry scanning, which calculated the integrated density value (IDV). Figures 5.3 a (heavy mRNA probe used) and 5.4 a (light mRNA probe used) show examples of the bands present on the Northern blots onto which total RNA amounts ranging from 1 to 12.5 μg, extracted from cells in the mid-exponential phase of a culture under normal conditions, were loaded. From Figures 5.3 b and 5.4 b, it can be observed that in both cases, within the range of intensity values, a linear relationship existed between the IDV and the total amount of RNA loaded for both the heavy and light mRNA probes. It is therefore possible to use the IDVs to determine and compare the relative amounts of mRNA present in each band, provided the IDV fall within the linear range studied.

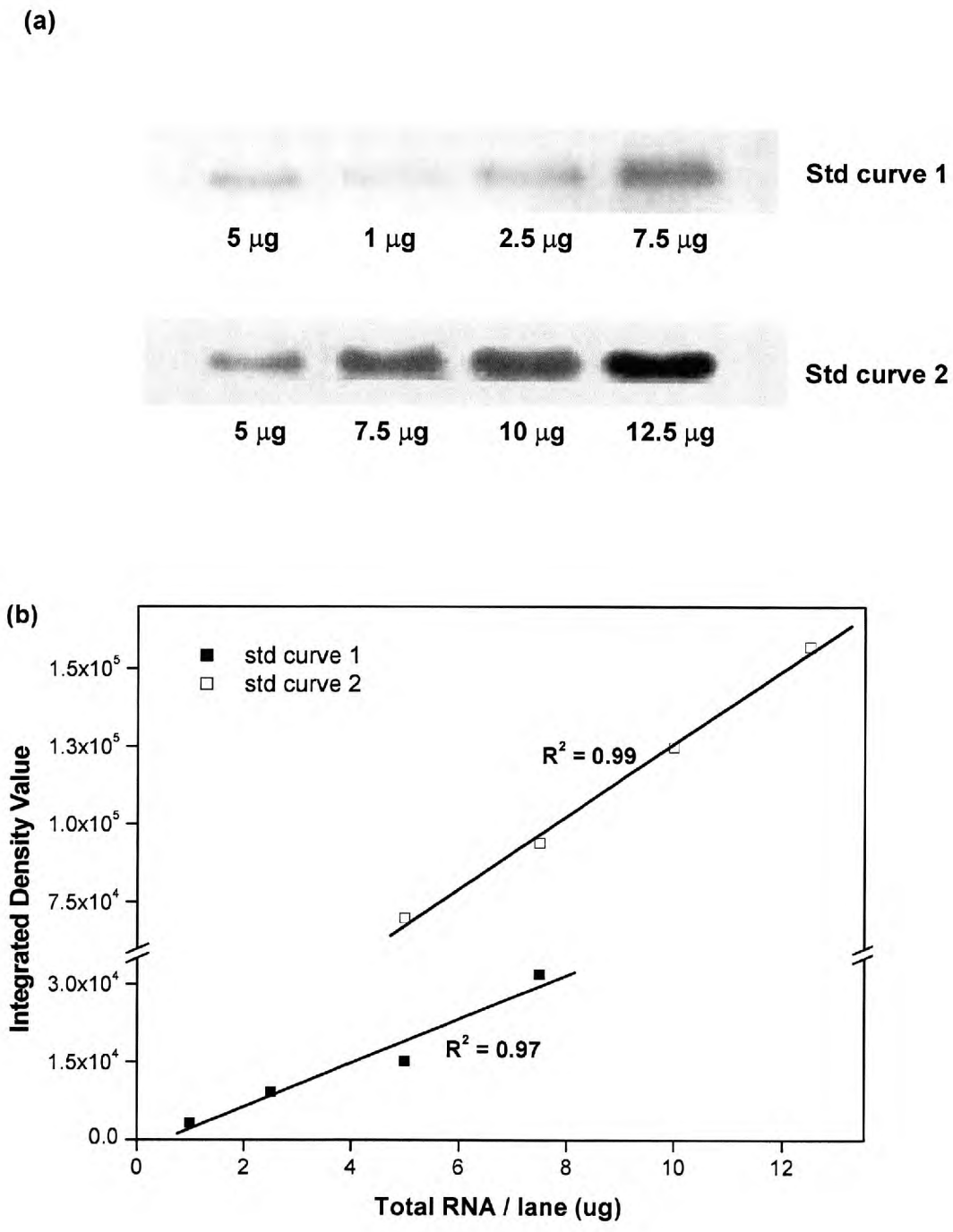

Figure 5.3. (a) Examples of two separate Northern blots probed with the specific heavy mRNA probe for total RNA concentrations ranging from 1 to 12.5 μg and (b) the linear relationships between the integrated density values obtained from densitometry scanning and total RNA (in μg) loaded on each lane of the gel using specific heavy mRNA probe.

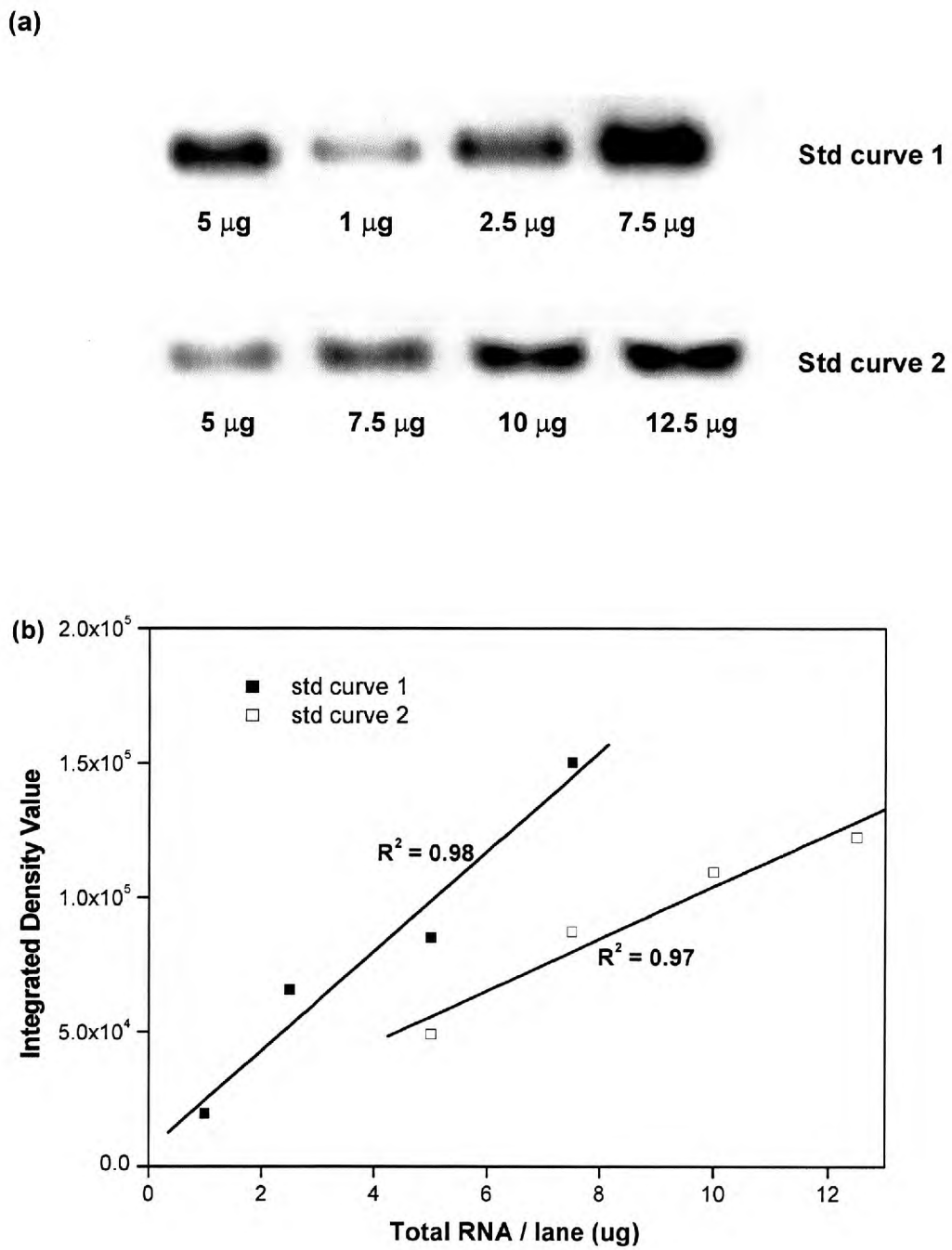

Figure 5.4. (a) Examples of two separate Northern blots probed with the specific light mRNA probe for total RNA concentrations ranging from 1 to 12.5 μg and (b) the linear relationships between the integrated density values obtained from densitometry scanning and total RNA (in μg) loaded on each lane of the gel using specific light mRNA probe.

Heavy and light mRNA behaviour under different osmotic conditions

The variations in heavy and light mRNA concentrations under normal and hyperosmotic conditions as a function of culture time are shown in Figures 5.5 and 5.6. Figures 5.5 a to 5.5 d represent the mRNA trends per μg of total RNA. It can be observed that in all four cases, the relative heavy and light mRNA concentrations per μg of RNA increased with respect to time until the decline phase of the culture, at which point the relative mRNA concentrations decreased. This indicated that the proportion of heavy and light mRNA in total RNA increased as the culture progressed, which in turn suggested that the heavy and light mRNA molecules were more stable compared to other mRNA species in the cell up till the stationary phase of the culture.

In Figures 5.6 a and 5.6 b, the mRNA values were determined on a per cell basis relative to the heavy or light mRNA concentration in the mid-exponential phase. In this representation, the decline in the amount of total RNA as the culture progressed counterbalanced the increases in the proportions of heavy and light mRNA molecules, resulting in fairly constant mRNA values until marked decreases of approximately 25 to 35% were observed in the early decline phase of the cultures. The trends are similar in both normal and hyperosmotic cultures.

Figures 5.7 a and 5.7 b show a comparison between the values for heavy and light mRNA species on a per cell basis for normal and hyperosmotic conditions at different culture phases. The mRNA values shown were relative to the heavy and light mRNA amounts at mid-exponential phase for normal osmotic cultures. It can be seen that there were comparatively higher concentrations of both heavy and light mRNA molecules in hyperosmotic cultures. Both the single-factor ANOVA and t-test analyses conducted at a significance level of 0.05 indicated that the relative mean heavy and light mRNA values for hyperosmotic cultures were significantly different from the mean mRNA values under normal culture conditions (with $p<0.05$). The ratio of mRNA values in hyperosmotic cultures and mRNA concentration in normal osmotic cultures remained relatively constant throughout the different culture phases, fluctuating between values of 1.5 and 1.7 for both heavy and light species.

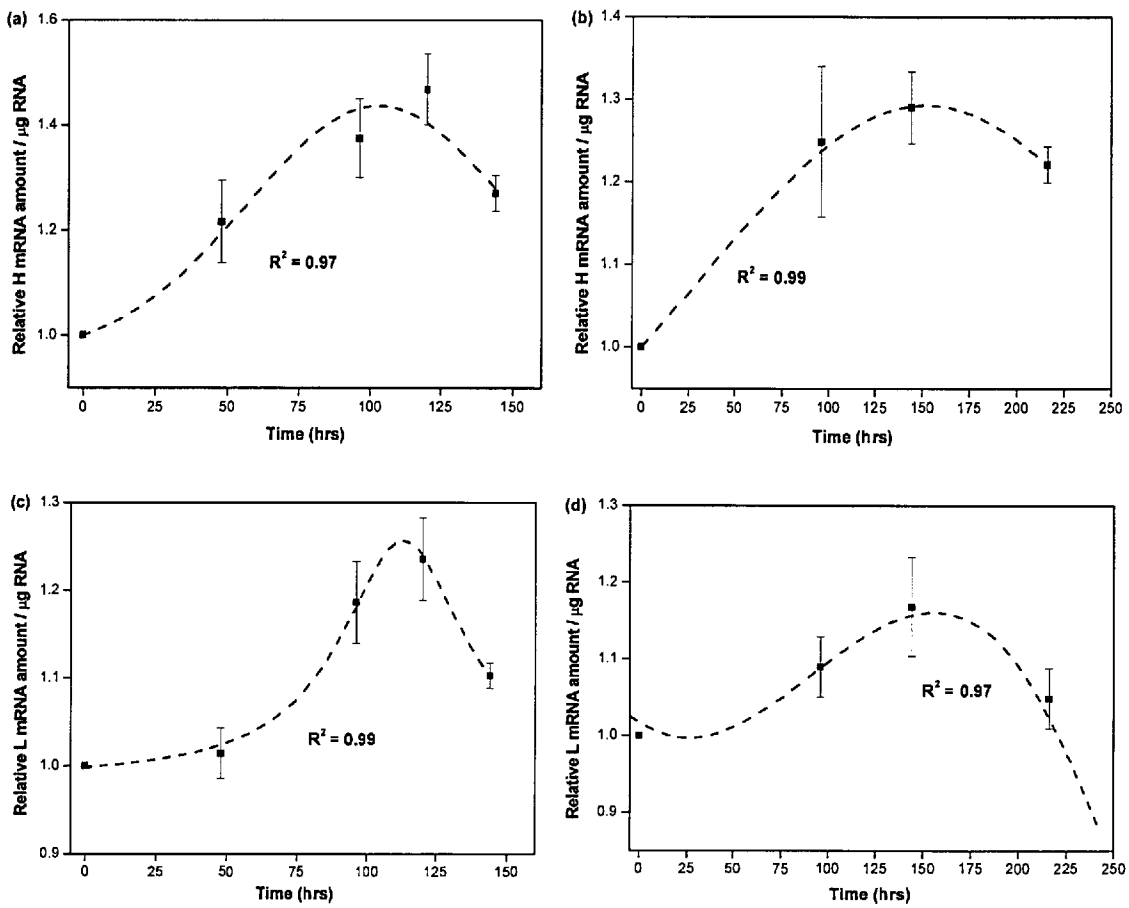

Figure 5.5. Relative mRNA amounts per µg of total RNA with respect to culture time (duplicate measurements from duplicate cultures) for (a) heavy mRNA species at normal osmotic and (b) hyperosmotic culture conditions as well as (c) light mRNA species at normal osmotic and (d) hyperosmotic conditions. Dotted lines represent the curves of best fit, with the R^2 value giving an indication of how good the fit is (R^2 values range from 0 to 1, with a larger value indicating a better fit).

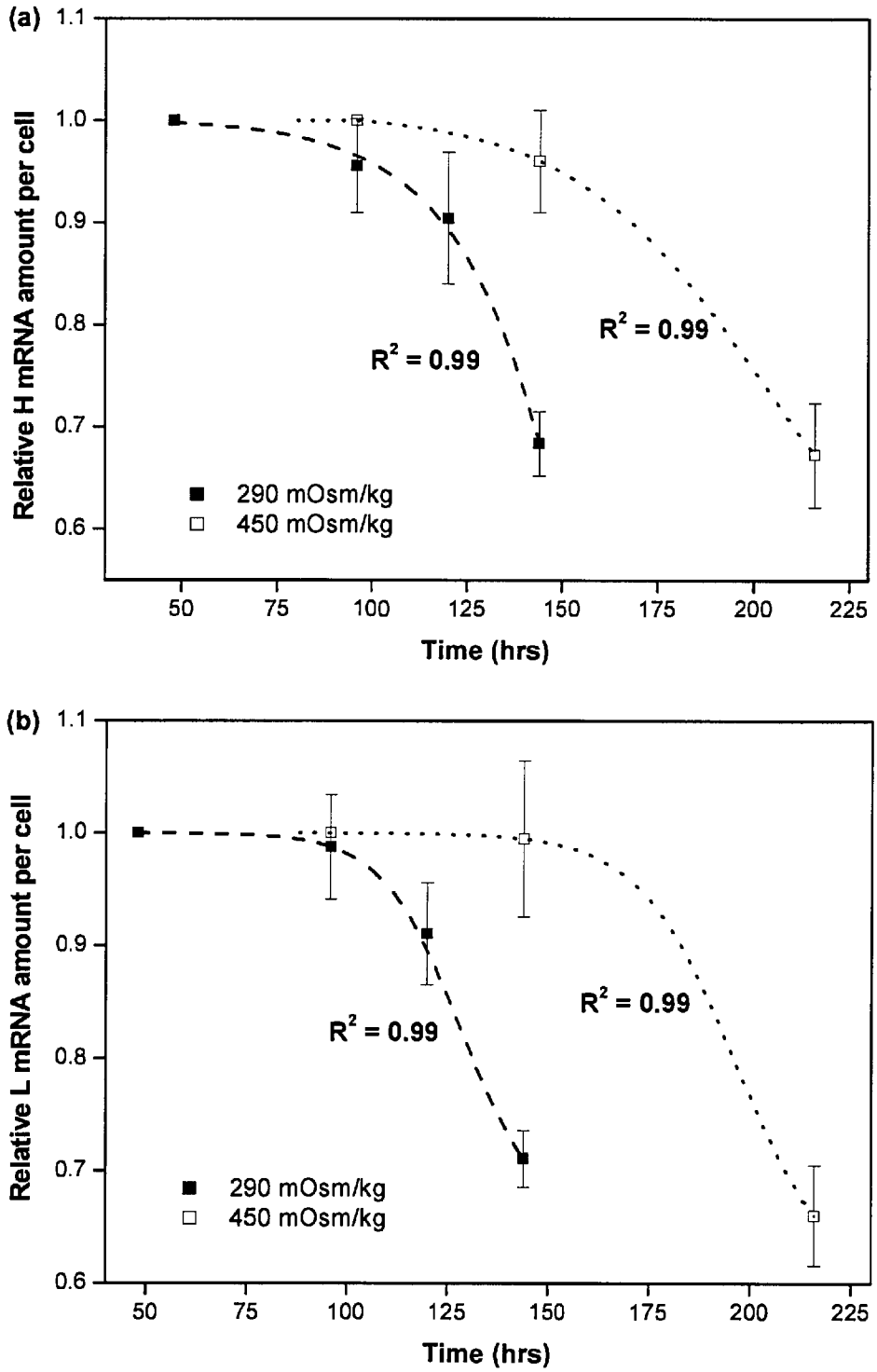

Figure 5.6. Relative mRNA amounts per cell with respect to culture time (from duplicate cultures) for (a) heavy mRNA species at normal osmotic and hyperosmotic culture conditions as well as (b) light mRNA species at normal osmotic and hyperosmotic conditions. Dotted lines represent the curves of best fit.

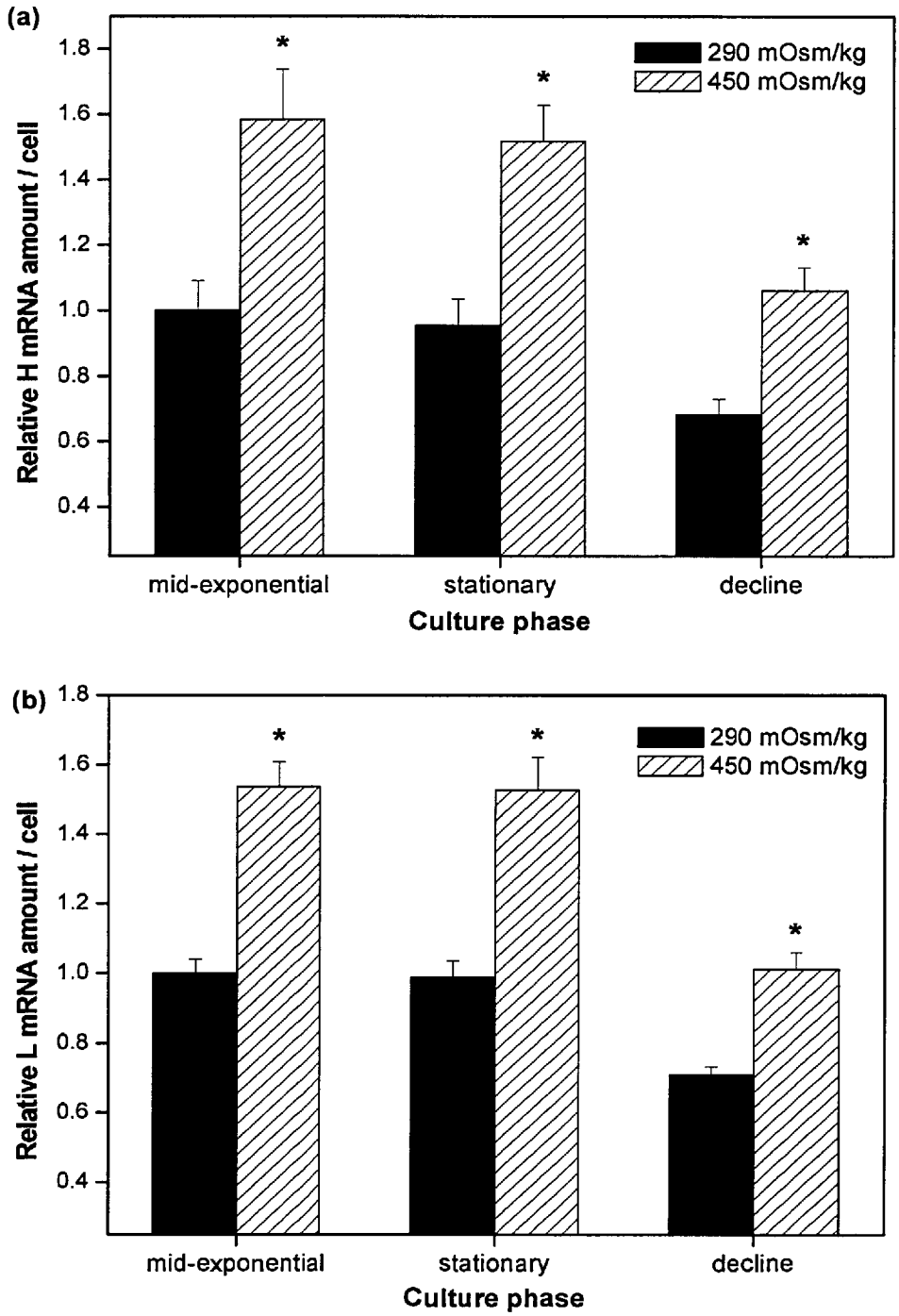

Figure 5.7. Relative mRNA amounts per cell with respect to culture time (from duplicate cultures) normalised by the mRNA concentration at mid-exponential phase (290 mOsm/kg cultures) for (a) heavy and (b) light mRNA species at different osmotic conditions.
(denotes values of $p < 0.05$ for both single-factor ANOVA and t-test analysis, indicating that the differences in the normal and hyperosmotic values are likely to be significant .)*

Heavy and light mRNA behaviour with respect to growth and antibody productivity

The relationships between heavy and light mRNA concentrations and the specific growth and antibody productivity are presented in Figures 5.8 and 5.9 respectively. In Figures 5.8 a and 5.8 b, a positive relationship was discerned between mRNA concentrations and cell growth. The figures also indicate almost parallel mRNA-cell growth relationships existed under normal and hyperosmotic conditions – for a given specific growth rate, the mRNA levels were found to be comparatively higher in hyperosmotic cultures. The heightened mRNA levels may be attributed to either a rise in mRNA transcription rates or an improvement in the stability of mRNA species at hyperosmotic conditions.

In Figures 5.9 a and 5.9 b, the relationships between heavy and light mRNA levels and the antibody productivity are analysed. It was found that mRNA levels show a positive correlation with the specific antibody productivity, reinforcing the findings from the global sensitivity analysis (GSA) conducted in Chapter 3, which identified both the transcription rates and mRNA half-lives as key influences on antibody production rates. Additionally, the relative mRNA levels at normal and hyperosmotic conditions appear to lie on the same curve, suggesting that the improved specific antibody productivities due to hyperosmolarity might be attributed to increases in mRNA levels.

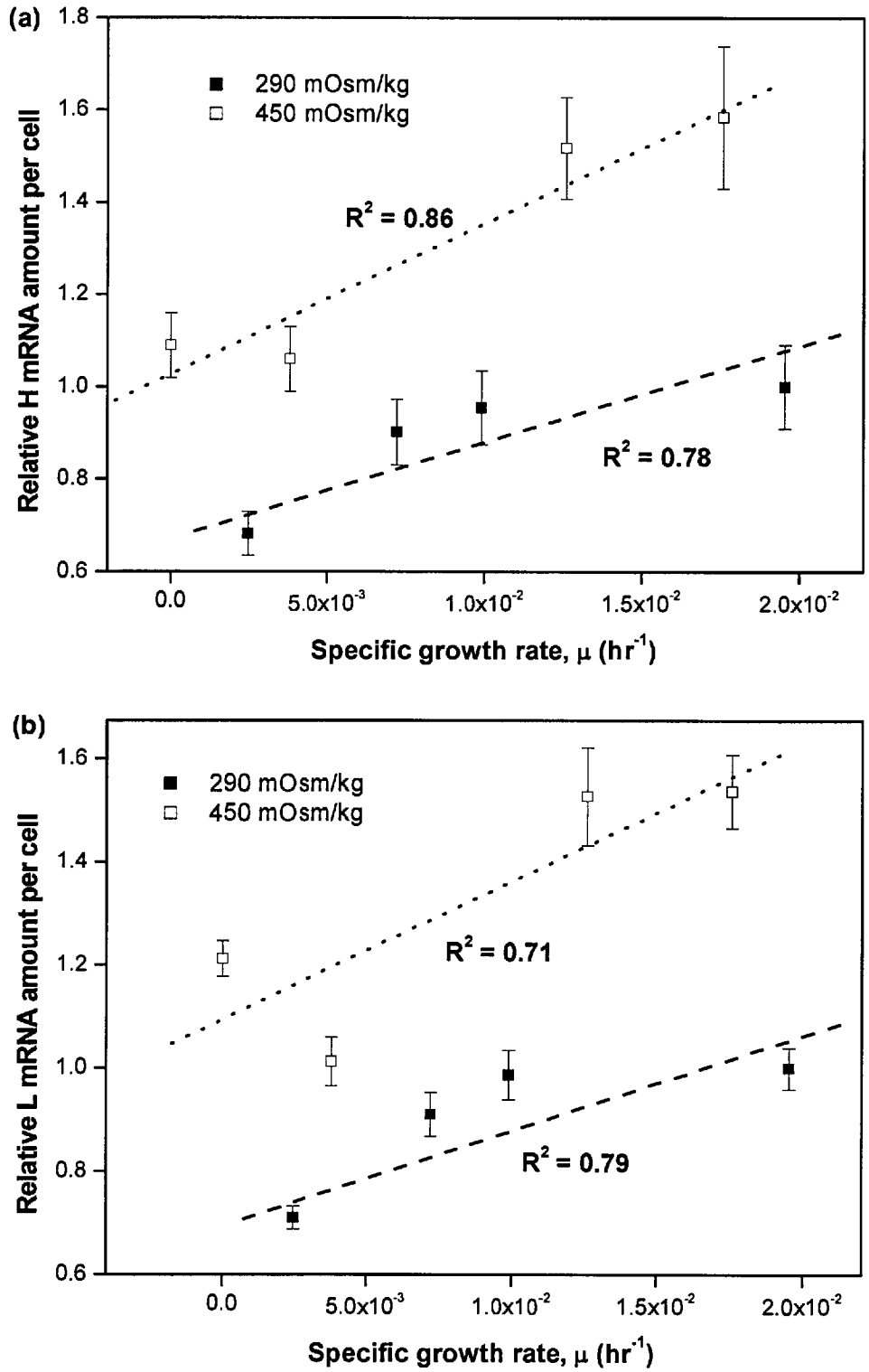

Figure 5.8. Relationships between the relative (a) heavy and (b) light mRNA concentration per cell with specific growth rates under normal and hyperosmotic culture conditions. Dotted lines represent the approximated linear relationships between the variables.

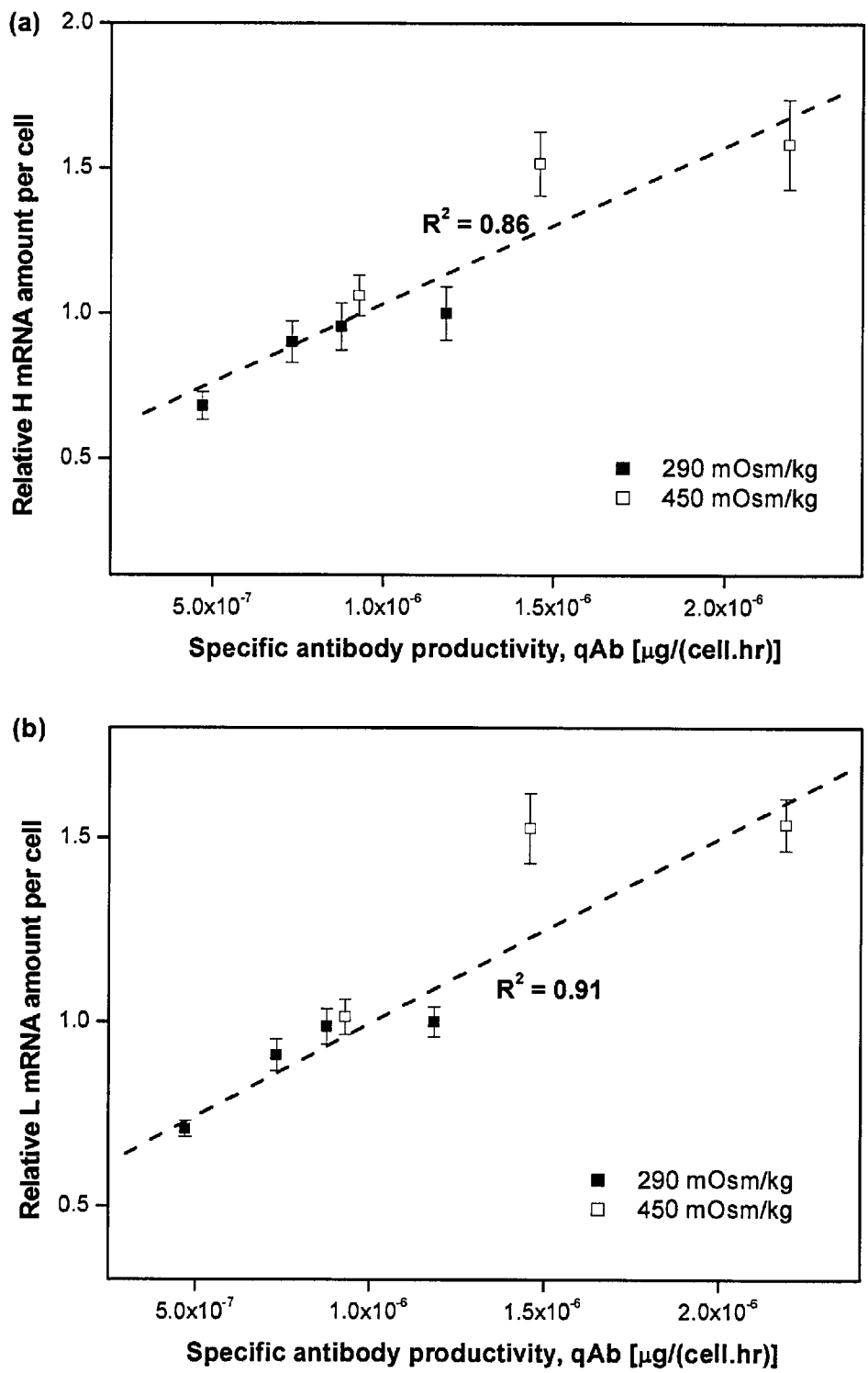

Figure 5.9. Relationships between the relative (a) heavy and (b) light mRNA concentration per cell with specific antibody productivity under normal and hyperosmotic culture conditions. Dotted lines represent the lines of best fit through the experimental data.

5.3.3 Degradation rates of heavy and light mRNA at different culture phases

Control ethanol cultures

The anti-transcription agent DRB, dissolved in ethanol, is used to inhibit transcriptional processes in the cell cultures. Prior to evaluation of the heavy and light mRNA degradation rates, ethanol was added to control cultures under normal and hyperosmotic culture conditions at the mid-exponential phase. Theses control cultures allowed us to ascertain that ethanol did not affect the degradation of mRNA molecules in any way. Samples were extracted from these control cultures at 0, 4, 8 and 12 hours after the addition of ethanol for cell number and mRNA levels analysis. Figure 5.10 a shows the viable cell concentrations of the control cultures, while the heavy and light mRNA integral intensity values, which were normalised to the intensities of the 18 S gene, as a function of time is presented in Figures 5.10 b and 5.10 c. It can be observed that no sudden drop in viable cell number was visible; although the number of viable cells in the hyperosmotic control cultures decreased slightly at 12 hours from 2.6×10^5 cells/mL to approximately 2.2×10^5 cells/mL. Similarly, the integral intensity values remained relatively constant for all cultures; however, at 12 hours after ethanol addition, apart from the heavy mRNA levels at 290 mOsm/kg, distinct decreases in the intensity values can be seen in the mRNA levels under both osmotic conditions (Figures 5.10 b and 5.10c). These results suggest that the effects of ethanol on heavy and light mRNA degradation were negligible up to a time point between 8 to 12 hours and indicate that the half-lives experiments should be completed in less than 12 hours after the addition of DRB dissolved in ethanol.

Half-lives determination of heavy and light IgG mRNA molecules

The half-lives of heavy and light IgG mRNA molecules were determined by conducting duplicate shake flask experiments at normal and hyperosmotic culture conditions. At the mid-exponential and stationary phases, 65 μM of DRB dissolved in ethanol was added to each culture to inhibit the transcription process. Samples were then collected at different time points to capture the degradation behaviour of the heavy and light mRNA molecules. For both normal and hyperosmotic cultures disrupted at the mid-exponential phase, cell

samples were collected at 0, 3, 7 and 10 hours following the addition of DRB. At the stationary phase, the cells were collected at 0, 3, 6 and 9 hours after the addition of DRB for normal osmotic cultures while for hyperosmotic cultures, cells were collected at 0, 2, 5 and 8 hours. All samples were run in duplicate on Northern blots and the IDV obtained were normalised according to the 18 S gene staining intensity. The intensity values in each case are presented in Figures 5.11 a and 5.11 b (mid-exponential phase) and 5.12 a and 5.12 b (stationary phase). As observed from the figures, a linear relationship could be approximated for each case and the half-lives were subsequently estimated using these linear relationships.

The half-lives of heavy and light mRNA molecules at mid-exponential phase were determined as 13.1 ± 2.1 hrs and 12.1 ± 1.5 hrs respectively for normal osmotic cultures. Hyperosmotic cultures appear to show faster mRNA degradation rates, with the half-lives of heavy and light mRNA species estimated at 9.0 ± 1.1 hrs and 9.0 ± 0.5 hrs respectively at the mid-exponential phase. In the stationary culture phase, the stability of the mRNA molecules is observed to have decreased for both normal and hyperosmotic cultures. Heavy and light mRNA molecules half-lives were derived as 8.5 ± 0.9 hrs and 8.2 ± 0.9 hrs respectively for normal osmotic cultures and determined as 6.6 ± 0.7 hrs and 5.9 ± 0.6 hrs respectively for hyperosmotic cultures. These values were compared using the both the single-factor ANOVA and unpaired two-tailed t-test at a significance level of 0.05, in order to identify any significant differences in the half-lives values with respect to mRNA species and culture conditions. A significance level of 0.05 was used to indicate how similar two sets of values are to each other. Table 5.1 summarises the p values for the various test sets carried out. From the table, the differences between heavy and light mRNA half-lives at the same culture phase and similar osmotic conditions were relatively insignificant ($p > 0.05$). However, the half-life values of both heavy and light mRNA at normal osmotic conditions were significantly different from the heavy and light mRNA half-lives at hyperosmotic cultures. Similarly, between culture phases, heavy and light mRNA half-lives were determined to be significantly different. These observations imply that hyperosmotic culture conditions did not lead to improved stabilities of the heavy and light mRNA species; instead, hyperosmolarity resulted in a higher rate of degradation of IgG mRNA species.

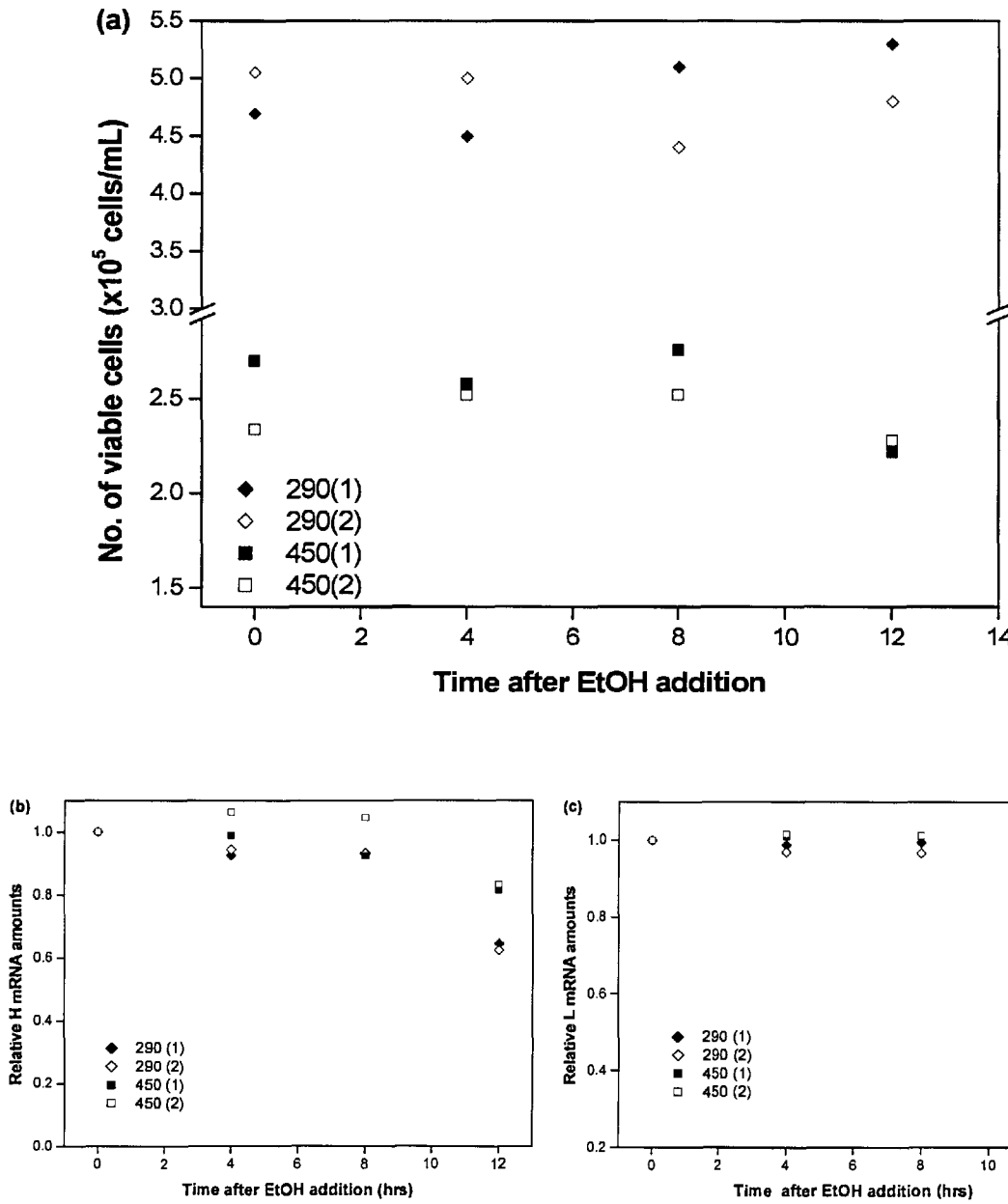

Figure 5.10 (a) Viable cell concentrations for control cultures and the (b) relative heavy mRNA and (c) relative light mRNA amounts at different time points after addition of ethanol.

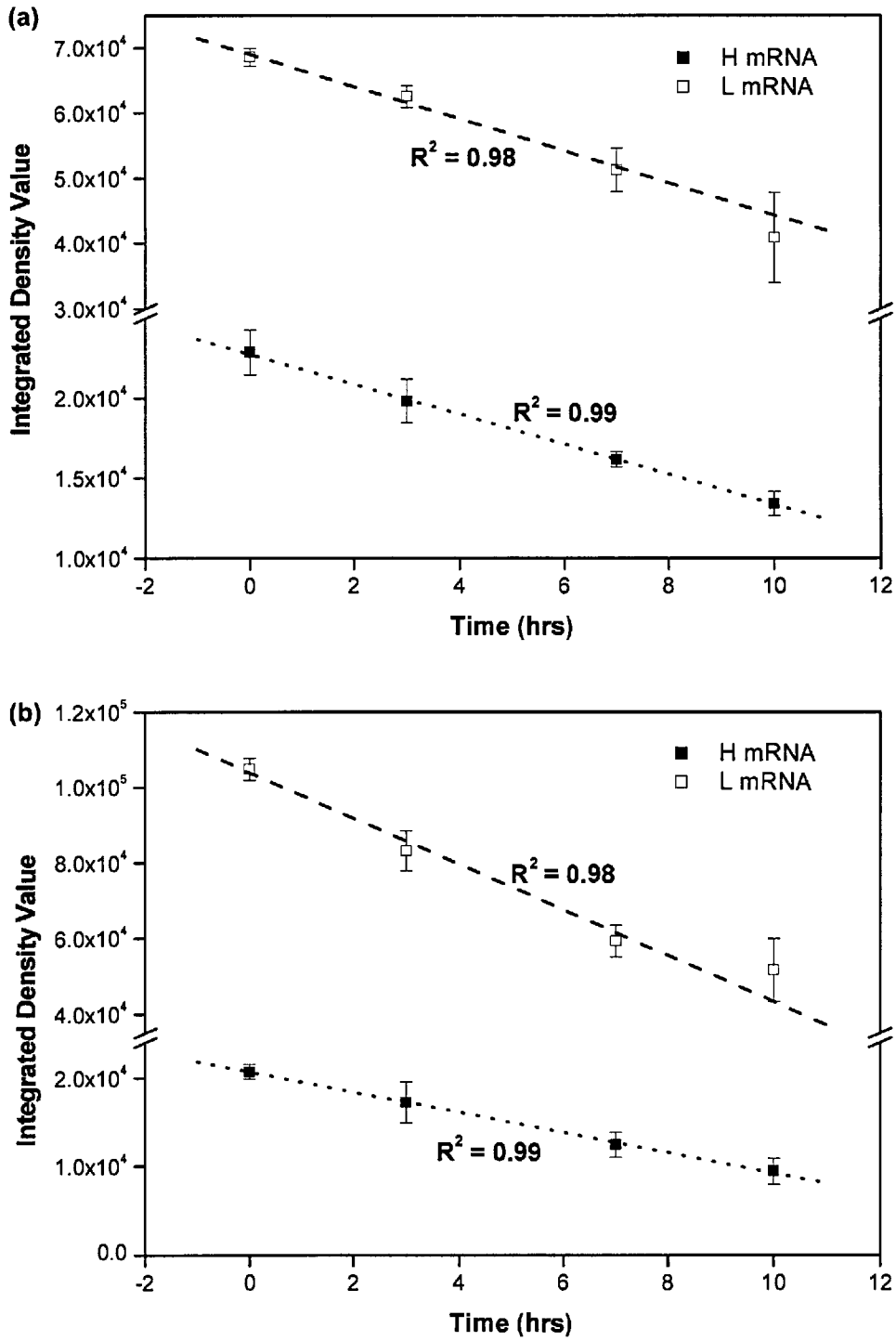

Figure 5.11. Integrated density values for heavy and light mRNA species at different time points after addition of DRB at the mid-exponential phase for (a) normal and (b) hyperosmotic cultures. Dotted lines represent the approximate linear relationships between the density values and time after DRB addition.

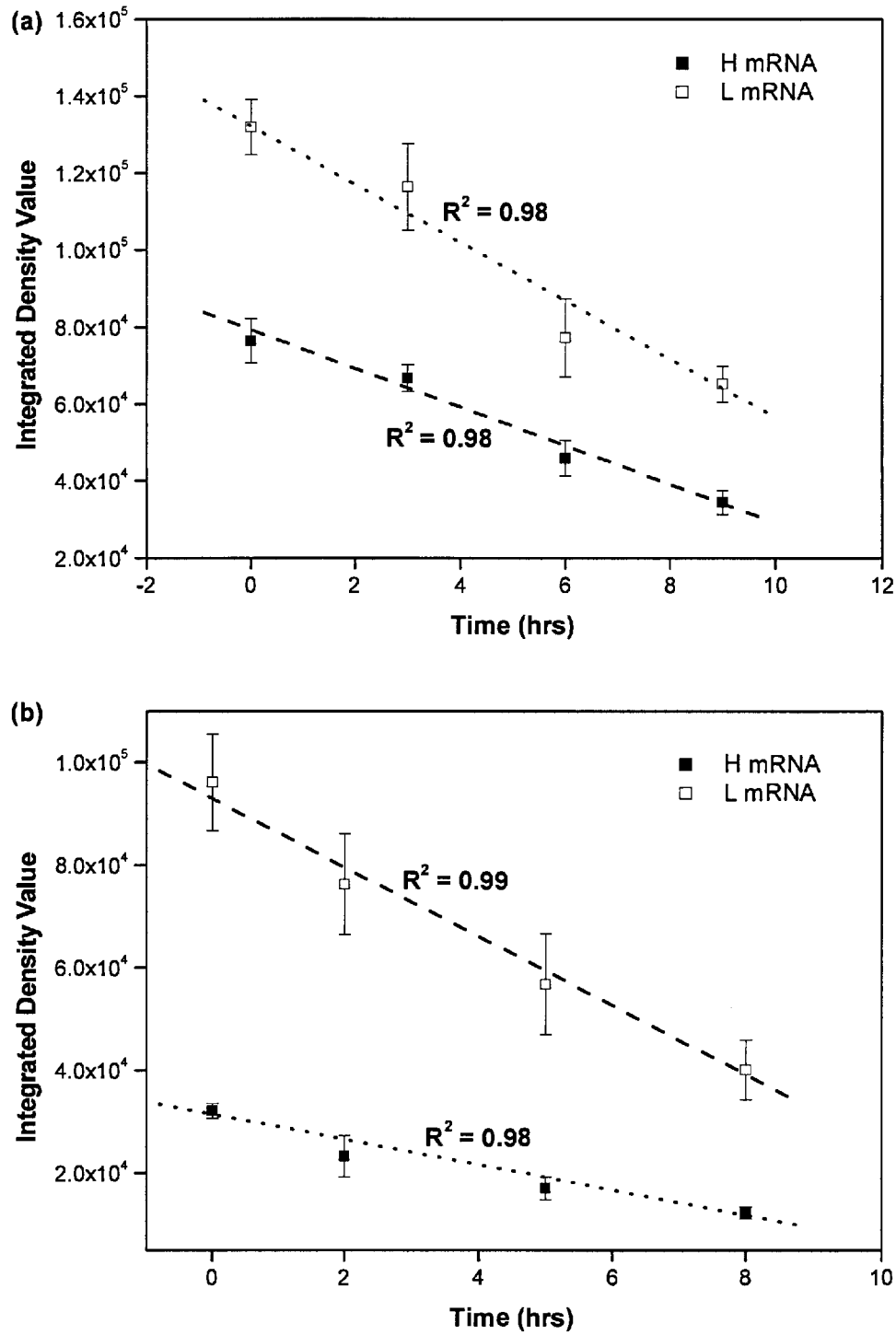

Figure 5.12. Integrated density values for heavy and light mRNA species at different time points after addition of DRB at the stationary phase for (a) normal and (b) hyperosmotic cultures. Dotted lines represent the approximate linear relationships between the density values and time after DRB addition.

Similarity of means between different species/culture phases	*ANOVA* ***p* value**	***t-test* *p value***
Mid-exponential Phase		
H and L mRNA (290)	0.50	0.50
H and L mRNA (450)	0.88	0.88
H mRNA (290 and 450)	7.0×10^{-3}	0.02
L mRNA (290 and 450)	0.02	0.02
Stationary Phase		
H and L mRNA (290)	0.62	0.62
H and L mRNA (450)	0.22	0.22
H mRNA (290 and 450)	7.0×10^{-3}	0.01
L mRNA (290 and 450)	0.01	0.01
Comparison Between Phases		
H mRNA (290)	4.3×10^{-3}	6.6×10^{-3}
L mRNA (290)	7.5×10^{-3}	0.02
H mRNA (450)	3.7×10^{-4}	4.0×10^{-4}
L mRNA (450)	9.9×10^{-3}	0.01

Table 5.1. Summary of p values for single-factor ANOVA and two-tailed t-tests for comparison of the similarity between means from various pairs of half-life data. ($p < 0.05$ indicate that the means of both species under analysis are significantly different.)

5.3.4 Total protein behaviour with respect to culture time and hyperosmolarity

In Figure 5.13 a and 5.13 b, total cellular protein trends at normal and hyperosmotic conditions with respect to time and specific growth rate are presented. While some variability exist in the experimental data obtained, a general decrease in total protein concentration as the culture progressed to the stationary and early decline phases could be deduced (Figure 5.13 a). This observation is corroborated by the trend shown in Figure 5.13 b, where total protein concentration declined following a decrease in the specific growth rate. The differences in total protein concentration with respect to hyperosmotic conditions were not particularly distinguishable – in Figure 5.13 a, there was a significant difference in total protein concentration between normal and hyperosmotic cultures only at 3 time-points. In Figure 5.13 b, particularly at specific growth rates less than 0.015 hr^{-1}, the total protein concentration at both osmotic conditions appear to overlap, suggesting that for GS-NS0 cells, hyperosmotic conditions did not result in a significant increase in overall protein synthesis.

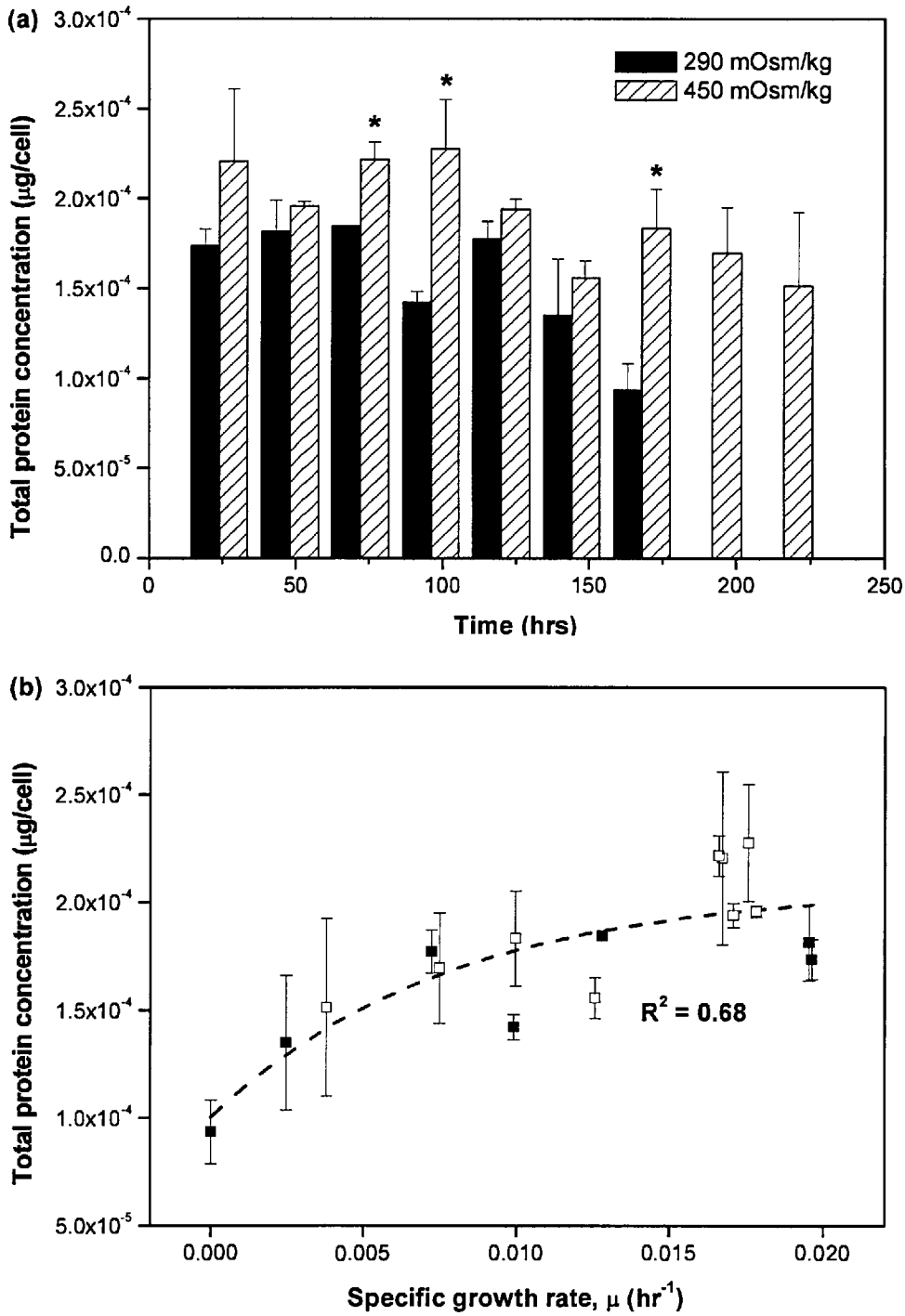

Figure 5.13. Total cellular protein concentration at normal and hyperosmotic conditions with respect to (a) culture time and (b) specific growth rates.(denotes $p<0.05$, indicating that the difference in normal and hyperosmotic protein concentration is statistically significant.) Dotted line represents curve of best fit for the experimental data.*

5.3.5 Heavy and light polypeptide chains behaviour in GS-NS0 cells

Linearity of integrated intensity values

Prior to the quantitative analysis of IgG polypeptide chain concentrations, a relationship had to be established between the integrated density value (IDV) and known concentrations of heavy and light chains. Known amounts of the cB72.3 antibody ranging from 100 to 800 ng/lane were processed through gel electrophoresis under reducing conditions and blotted with the HRP-conjugated anti-IgG (H+L) antibody capable of both heavy and light chain detection. Examples of the standard curves for heavy and light IgG polypeptides, together with the bands detected through Western blotting are shown in Figure 5.14 a and 5.14 b. The heavy and light chain amounts in Figure 5.14 b were calculated based on the following formula:

$$Amt\ i\ chains\ (g) = \frac{2 \times Amt\ H_2L_2\ (g) \times MW_i(daltons)}{MW_{H_2L_2}(daltons)} \qquad (5.1)$$

where i = heavy (H) or light (L) chain species, H_2L_2 refers to the number of completely assembled IgG molecule and MW is the molecular weight of each species in daltons. The above formula is based on the fact that two heavy and two light polypeptide chain molecules are used in the assembly of a complete IgG molecule.

The standard curves in Figure 5.14 b indicate that linear relationships between the IDV and heavy and light chain amounts could be approximated over the given range of density values. The amount of heavy and light chains in an unknown sample (obtained from the mid-exponential phase of a normal-condition culture) processed on the same blot could therefore be quantified by comparing the IDVs of the unknown sample to the standard curves. A standard curve for the equal loading standard, GAPDH, was also derived by loading 10 to 60 ng of total protein onto individual lanes and subsequently blotting with an HRP-conjugated anti-GAPDH antibody (Figure 5.14 c). The linear relationship between GAPDH IDV and sample concentration in Figure 5.14 d shows that GAPDH density values could be used to normalise the IDVs obtained from heavy and light chain bands.

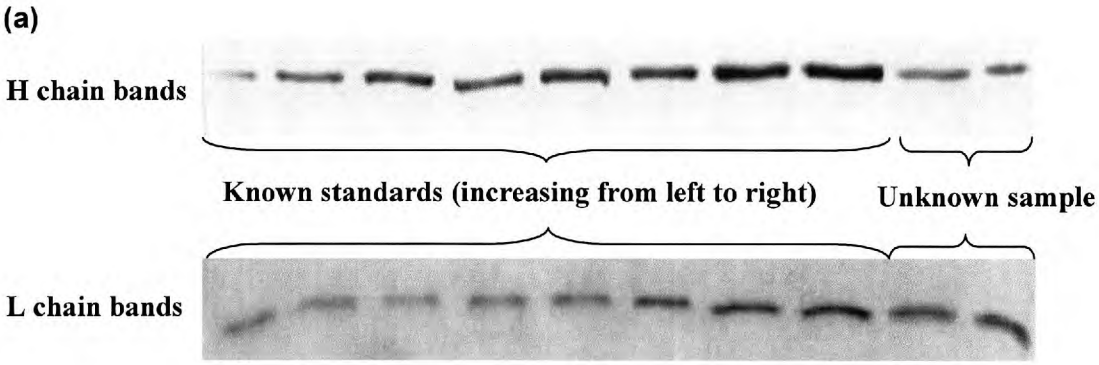
(a)
H chain bands
Known standards (increasing from left to right)
Unknown sample
L chain bands

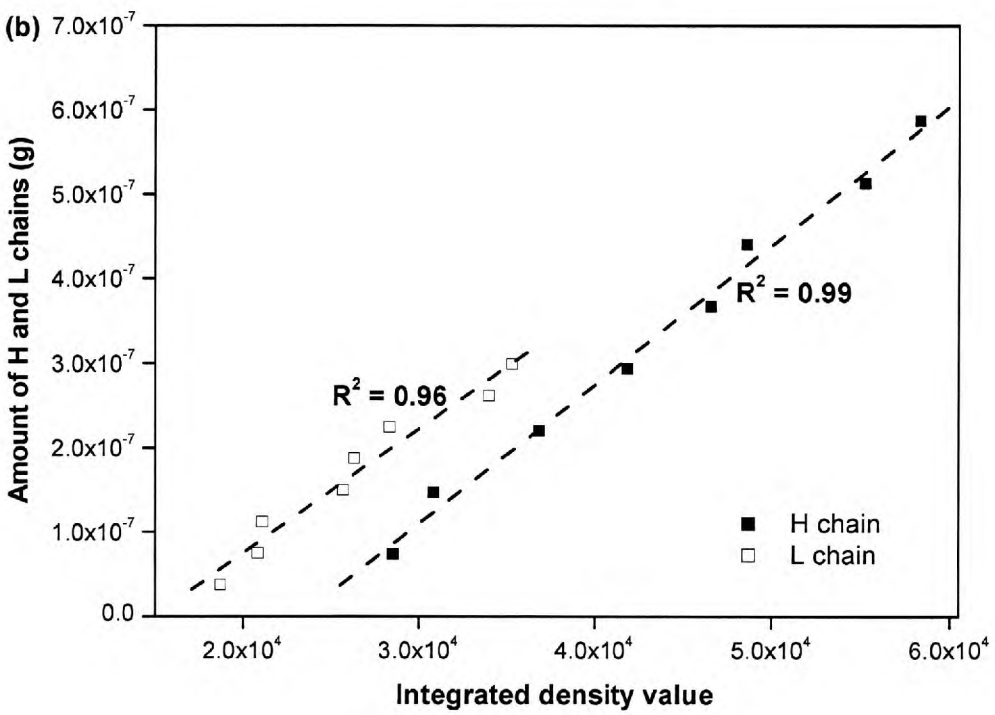
(b)
Amount of H and L chains (g)
7.0x10-7
6.0x10-7
5.0x10-7
4.0x10-7
3.0x10-7
2.0x10-7
1.0x10-7
0.0
2.0x10^4
3.0x10^4
4.0x10^4
5.0x10^4
6.0x10^4
Integrated density value
R2 = 0.96
R2 = 0.99
H chain
L chain

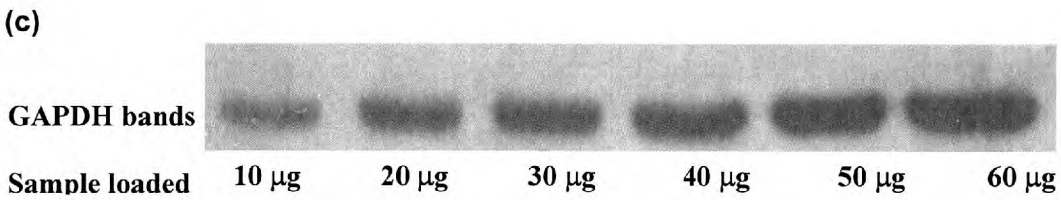

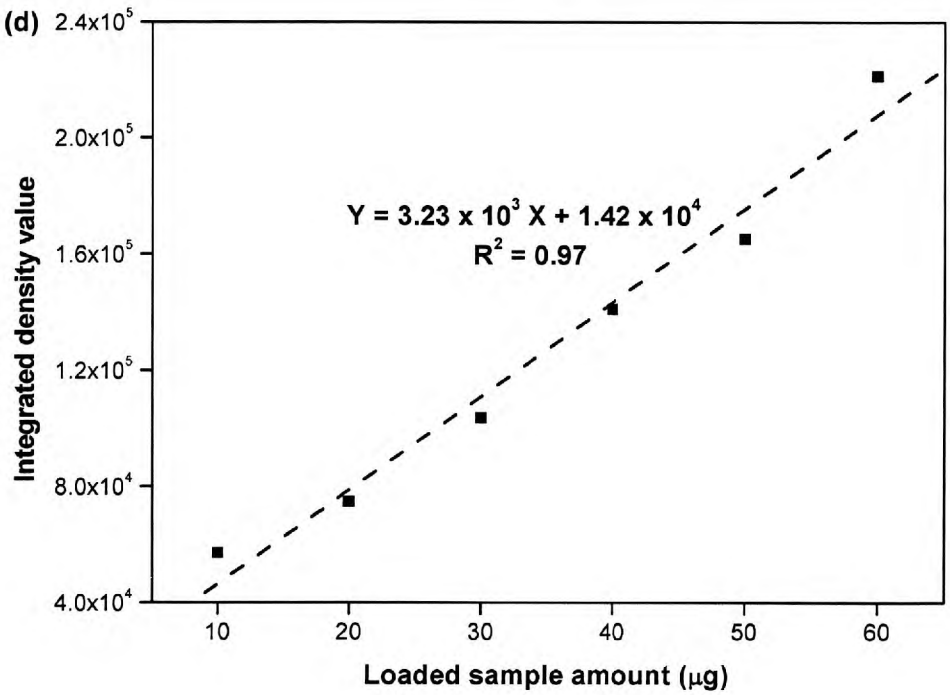

Figure 5.14. (a) Western blot bands depicting known concentrations of heavy and light polypeptide chains in each lane (equivalent to 100 ng – 800 ng cB72.3 antibody standard) and (b) the corresponding standard curves obtained by quantifying the bands using densitometric methods. (c) Western blot bands depicting 10 to 60 μg of the same cell sample and (d) the corresponding curve relating the IDV to the amount of sample loaded onto each lane. Dotted lines represent the approximate linear relationships between the IDV and amount of polypeptide chains or loaded sample. Note that reducing conditions were used for all Western blots obtained.

Heavy and light chain behaviour with respect to culture time and hyperosmolarity

The total intracellular heavy and light polypeptide chain concentrations were analysed on a daily basis for both normal and hyperosmotic culture conditions until the early decline phase of the culture. The resulting trends are displayed in Figures 5.15 a and 5.15 b. A couple of key points can be inferred from these figures: firstly, there seemed to be a higher concentration of light chains in comparison to heavy chains throughout the culture under both osmotic conditions. Secondly, the heavy and light chain trends with respect to time appeared to mirror the specific antibody productivity trends for both normal and hyperosmotic conditions. This implies that antibody productivity was likely to be dependent on the IgG polypeptide concentrations in the cell. The relationship between specific productivity and polypeptide chain concentrations will be further analysed in the next section.

The variation in heavy and light chains with respect to normal and hyperosmotic conditions is presented in Figures 5.16 a and 5.16 b. At 24 hours, the heavy polypeptide chain concentration appeared to be slightly higher in normal cultures compared to hyperosmotic cultures while the light chain concentrations seemed to be comparable. Beyond 24 hours, however, the heavy and light chains quantities under hyperosmotic conditions became larger in comparison to normal culture conditions. The trends can be explained by the fact that the hyperosmotic cultures were in the lag phase at 24 hours, during which there was comparatively little antibody production, while cells under normal culture conditions were already in the exponential growth phase and actively producing the antibody product. Subsequently, the hyperosmotic culture entered the exponential growth phase, thereby stimulating the antibody synthesis process and resulting in the increase of heavy and light chain concentrations. Another key observation was that the light chain concentrations appeared to show a relatively larger increase at hyperosmotic conditions as compared to the heavy chain concentrations, suggesting that light chain synthesis could have been more preferentially enhanced than heavy chain synthesis with respect to total protein synthesis rates. This possibility will be further discussed in Section 5.4.

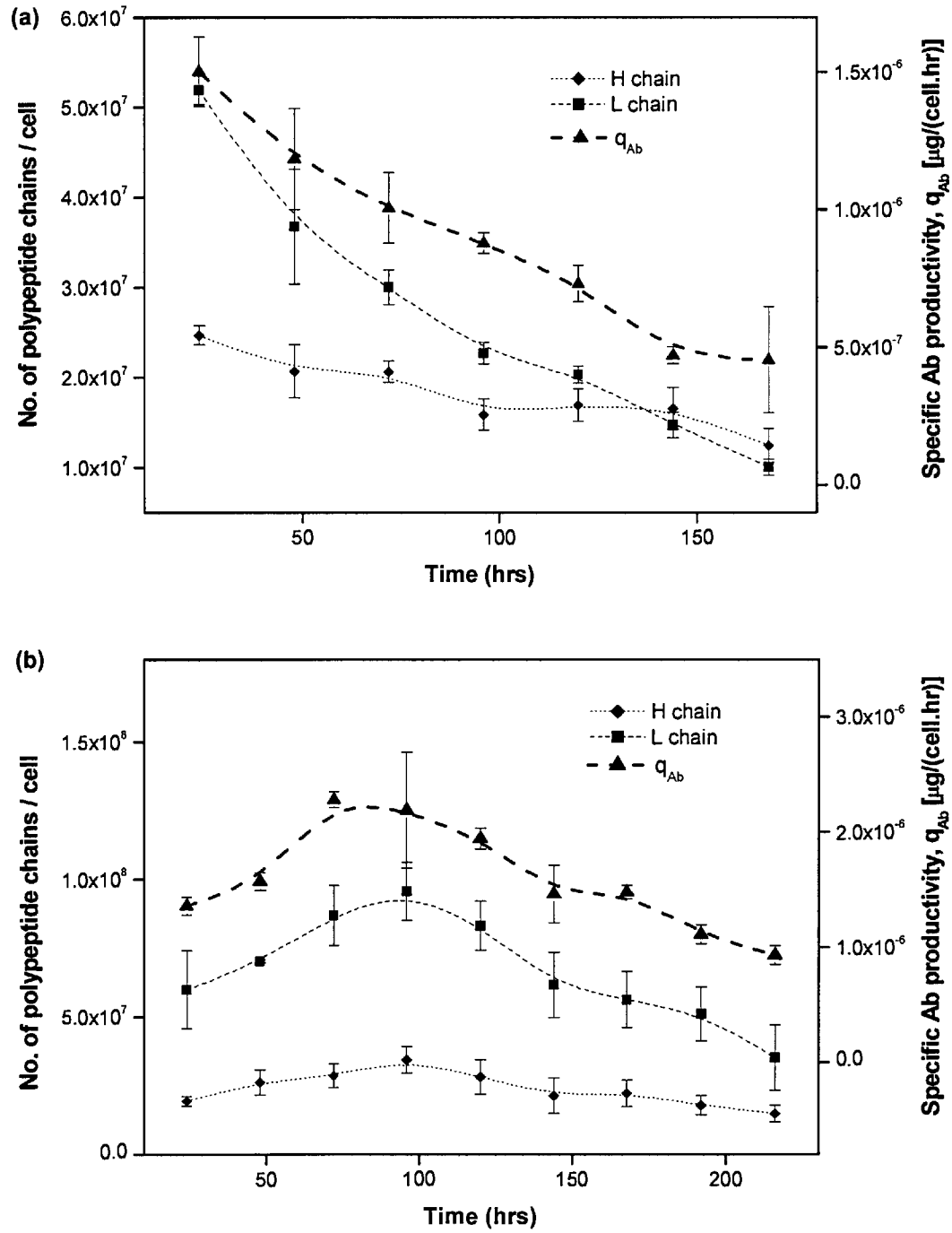

Figure 5.15. Heavy and light chain polypeptide trends with the corresponding time-dependent specific antibody productivity behaviour at (a) normal and (b) hyperosmotic culture conditions.

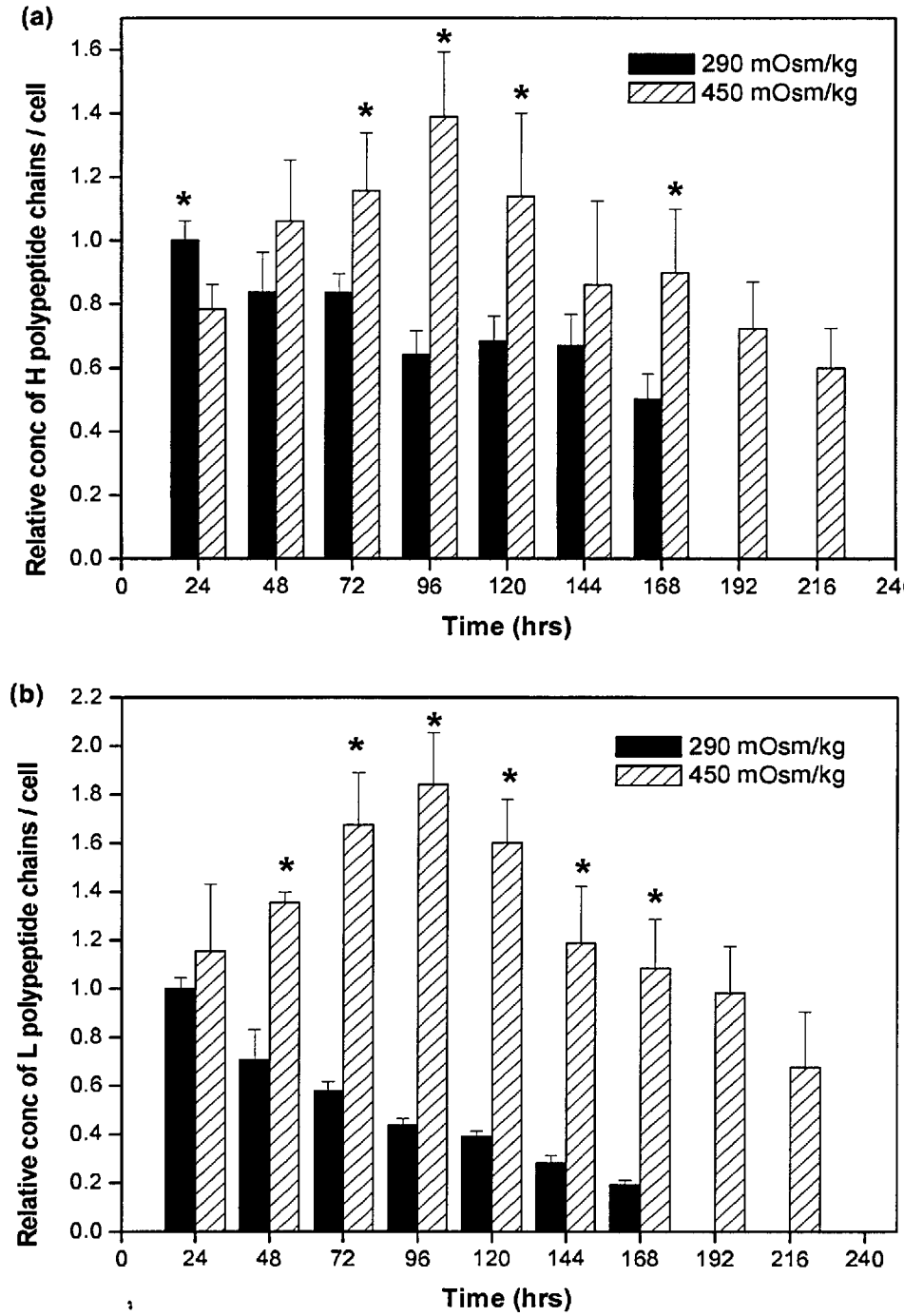

Figure 5.16. Relative concentrations of (a) heavy and (b) light polypeptide chains at normal and hyperosmotic conditions normalised to the polypeptide chain concentrations at 24 hours in normal osmotic cultures.(denotes $p<0.05$, based on both ANOVA and t-tests, indicating that the polypeptide chain concentrations for normal and hyperosmotic cultures at a particular time point are significantly different from each other.)*

Heavy and light chain behaviour with respect to growth and antibody productivity

The heavy and light chain trends with respect to specific growth rate and specific productivity has been ascertained in Figures 5.17 and 5.18. In Figures 5.17 a and 5.17 b, positive relationships are seen between polypeptide chain concentrations and the specific growth rate. While the heavy chain concentrations were only slightly elevated at hyperosmotic conditions with respect to specific growth rate, the increase in light chain concentrations as more distinct, once again suggesting that overall synthesis of light chains was more elevated under hyperosmotic conditions than heavy chains. Figures 5.18 a and 5.18 b indicate that a positive relationship existed between polypeptide chain concentrations and specific antibody productivity, confirming the observations made in the previous section regarding the similarity between the polypeptide chain trends and the specific antibody productivity trends. The positive association between these two variables implies that IgG translation rates are likely to be a key determinant of antibody production rates throughout the culture duration. In addition, it is observed that the polypeptide concentrations derived from normal and hyperosmotic cells appeared to lie on the same curve, indicating that the same correlation can be used to describe the heavy and light chain behaviour with specific productivity under both osmotic conditions.

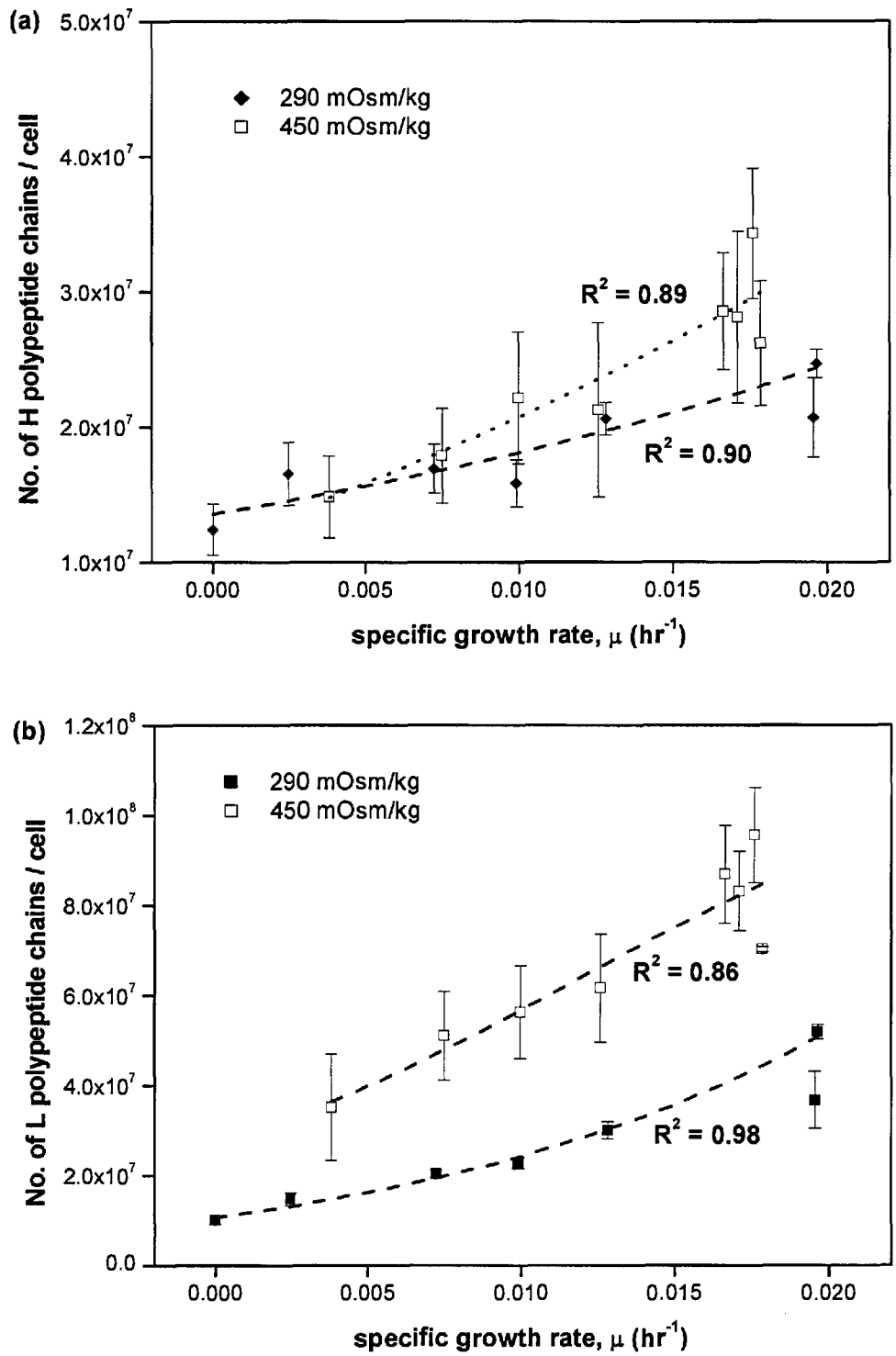

Figure 5.17. Relationships between (a) heavy and (b) light polypeptide chain concentrations and the specific growth rate under normal and hyperosmotic conditions. Dotted lines refer to best fit curves for each data set.

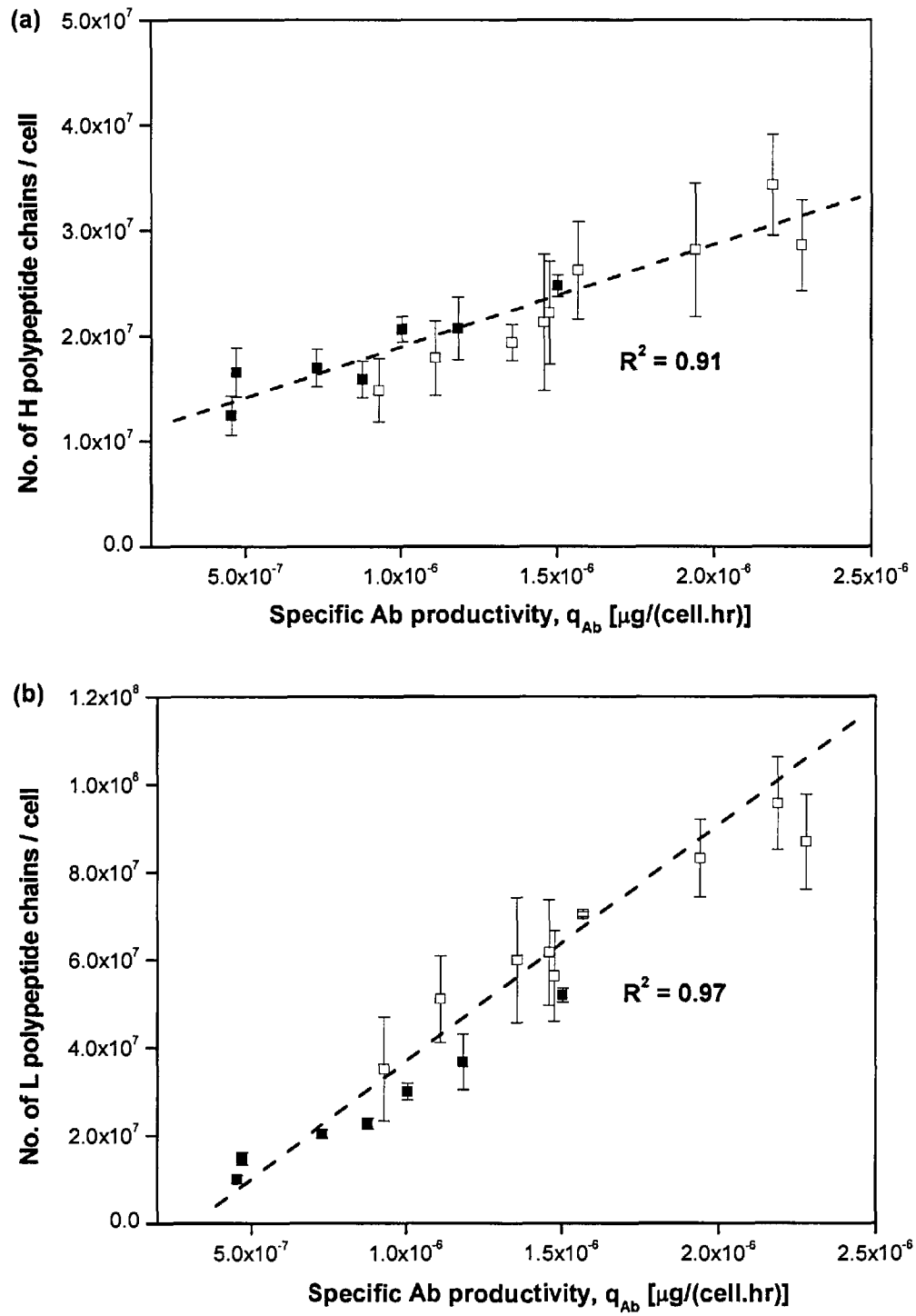

Figure 5.18. Relationships between (a) heavy and (b) light polypeptide chain concentrations and the specific antibody productivity under normal and hyperosmotic conditions. Dotted lines refer to best fit curves for each data set.

5.3.6 Estimation of parameters from experimental study

One of the key aims of the intracellular study of mRNA and polypeptide chains trends under normal and hyperosmotic conditions is to derive estimates for the key parameters identified by the global sensitivity analysis (GSA), as described in Chapter 3. The key parameters included the specific transcription and translation rates for heavy and light chain species, as well as the half-lives of heavy and light mRNA molecules. The half-life values already have been derived by Northern blot analysis in Section 5.3.3 previously. In this section, the estimation of the specific transcription and translation rates will be discussed.

Determination of specific transcription rates

The accumulation of heavy and light mRNA molecules in the cell is dependent on three key factors: the specific transcription rate, the mRNA degradation rate, as well as the dilution by growth term, as shown by Equations (3.11) and (3.12) from Chapter 3. The general form of the equation is shown below:

$$\frac{dm_i}{dt} = S_i - k_i m_i - \mu\, m_i \tag{5.1}$$

where i refers to heavy or light mRNA species, m_i represents the mRNA concentration, S_i is the specific transcription rate of mRNA and k_i refers to the mRNA degradation rate.

The mRNA degradation rates (k_i) are derived from the mRNA half-lives ($t_{1/2,i}$) using the following expression:

$$k_i = \frac{\ln 2}{t_{1/2,i}} \tag{5.2}$$

By rearranging equation (5.1), an expression for the specific transcription rate can be obtained:

$$S_i = \frac{dm_i}{dt} + k_i m_i + \mu\, m_i \tag{5.3}$$

In a previous study on hybridoma cells conducted by Lee and Lee [2000], the authors had estimated the specific transcription rates for heavy and light mRNA species, based on the assumption that mRNA concentrations remain relatively constant during the mid-exponential culture phase. This assumption appeared to be valid for GS-NS0 cells,

based on the experimental mRNA trends shown in Figures 5.6 a and 5.6 b. As a result, the accumulation term, $\frac{dm_i}{dt}$, could therefore be ignored at the mid-exponential culture phase. Estimates of the specific transcription rates (S_i) of mRNA molecules under normal and hyperosmotic conditions were thus determined by the simplified version of Equation 5.3:

$$S_i = k_i m_i + \mu\, m_i \tag{5.4}$$

As only the relative amounts of mRNA molecules was determined in the experimental study, typical values for actual heavy and light mRNA concentrations during the mid-exponential phase were obtained from a study on myeloma cells conducted by Wallach and Laskov [1980]. Heavy mRNA concentration was assumed to be 2.0×10^4 molecules per cell while light mRNA concentration was 3.0×10^4 molecules per cell. The relative mRNA values at normal and hyperosmotic conditions were derived from Figures 5.7 a and 5.7 b, while the mRNA degradation rates were calculated from the half-life values reported in Section 5.3.3. The resulting estimated specific transcription rates are shown in Table 5.2, where it can be deduced that hyperosmotic conditions of 450 mOsm/kg resulted in approximately a one-fold increase in both heavy and light mRNA transcription rates.

Transcription rates	Heavy mRNA	Light mRNA
Normal (290 mOsm/kg)	1450	2300
Hyperosmotic (450 mOsm/kg)	3000	4360
Ratio [(450 mOsm/kg)/(290 mOsm/kg)]	2.07	1.89

Table 5.2. Estimated specific transcription rates for heavy and light mRNA molecules at normal and hyperosmotic culture conditions (3 significant figures).

Culture phase	T_H (290)	T_H (450)	Ratio T_H (450/290)	T_L (290)	T_L (450)	Ratio T_L (450/290)
Mid-exponential	491	575	1.17	320	421	1.31
Stationary	364	392	1.08	234	263	1.13
Early decline	338	337	1.00	212	229	1.08

Table 5.3. Estimated specific translation rates for heavy and light polypeptide molecules at normal and hyperosmotic culture conditions (3 significant figures).

Estimation of specific translation rates

The estimation of specific translation rates is not as straightforward as the specific transcription rates derivation, due to the fact that specific translation rates do not remain constant throughout the culture. Consequently, these rates had to be calculated at each time point. In the experimental study, the measurement of total heavy and light polypeptide chains included not just the free heavy and light chains, but also the heavy and light chains found in the partially formed ([HL]) and fully formed intracellular antibody ([H_2L_2]) molecules. As a result, an intracellular mass balance for the total amount of heavy chains can be written as follows:

$$\underset{(1)}{\frac{d[H]_{total}}{dt}} = \underset{(2)}{\frac{d[H]}{dt}} + \underset{(3)}{\frac{d[HL]}{dt}} + 2\underset{(4)}{\frac{d[H_2L_2]_{ER}}{dt}} + 2\underset{(5)}{\frac{d[H_2L_2]_{G}}{dt}} \qquad (5.5)$$

Briefly, the above equation states that rate of accumulation of total intracellular heavy polypeptide chains **(1)**, is given by the summation of the accumulation rates of free heavy chains **(2)**, the intermediate HL **(3)**, and the fully formed H_2L_2 molecules in the endoplasmic reticulum (ER) **(4)** and the Golgi complex (G) **(5)**. The coefficient '2' is applied to the H_2L_2 concentration terms as each H_2L_2 molecule contains two heavy chains.

By combining equations (3.14), (3.16), (3.21), (3.23) and (3.25) from Chapter 3, and subsequently substituting unknown variables with measured quantities (the full derivation is given in Appendix B), the following expression is then obtained:

$$\frac{d[H]_{total}}{dt} = T_H m_H - \mu[H]_{total} - 2q_{Ab} \qquad (5.6)$$

A rearrangement of equation 5.6 results in the following:

$$T_H m_H = \frac{d[H]_{total}}{dt} + \mu[H]_{total} + 2q_{Ab} \qquad (5.7)$$

where T_H refers to the heavy chain specific translation rate, μ is the specific growth rate and q_{Ab} represents the specific antibody productivity; where q_{Ab} has units of [molecules/(cell.hr)]. A similar mass balance can be derived for describing the variation of the light polypeptide chain concentrations with time.

From equation 5.7, it can be noted that the translation rate term ($T_H\ m_H$) actually consists of two factors: the heavy chain specific translation rate and the heavy mRNA concentration. Using the mRNA values obtained in the study, the specific translation rates at various culture phases were estimated for normal and hyperosmotic conditions. A summary of these rates can be found in Table 5.3. It is observed that the specific translation rates for both heavy and light chains were higher at the mid-exponential phase of hyperosmotic cultures in comparison to normal osmotic cultures. However, the difference between normal and hyperosmotic specific translation rates was not sustained as the cultures approached the late-exponential and stationary culture phases. Another key observation from Table 5.3 to be noted is that the heavy chain specific translation rates were actually higher than the light chain specific translation rates, despite the larger intracellular pool of light chains under both normal and hyperosmotic conditions. It appears that the relatively higher light chain concentration compared to the concentration of heavy chains could be mainly attributed to the larger number of light mRNA molecules present in the cell.

5.4 Discussion

The aim of this chapter was two-fold: firstly, to study the behaviour of intracellular mRNA and polypeptide chain concentrations with respect to time under normal and hyperosmotic culture conditions, as well as to evaluate their relevance to antibody production rates. Secondly, the experimental results obtained have enabled estimates of the key parameters, previously identified through a GSA of the hybrid antibody production model, to be derived. Based on the experimental results, it was determined that hyperosmotic cells possessed higher levels of heavy and light mRNA molecules due to elevated specific transcription rates, which subsequently led to improved specific antibody productivities. A more detailed discussion on the findings is provided in the next few sub-sections.

Total RNA trends under normal and hyperosmotic conditions

The variation of total RNA concentration with respect to medium osmolarity had been studied in the past, with the general observation that hyperosmotic conditions tended to lead

to an increase the total cellular RNA content [Lee and Lee, 2000; Oh et al., 1995; Sun et al., 2004]. The results obtained from this study were in agreement with this trend, suggesting that an increase in RNA synthesis appeared to have occurred under hyperosmotic conditions. A possible reason for the higher RNA concentrations at hyperosmotic conditions had been proposed by Oh et al. [1995; 1993], who suggested that an increase in the available pool of "RNA building blocks" occurred under hyperosmotic conditions, thereby leading to higher RNA synthesis rates. The larger available pool of "building blocks", in turn, might have been a result of the increased uptake rates of nutrients observed under hyperosmotic conditions.

Influence of mRNA stability on IgG mRNA behaviour over culture time

The variation of IgG mRNA levels with respect to time could either be expressed per □g of total RNA or per cell. In particular, the former approach gave an indication of the relative proportions of heavy and light mRNA molecules in total RNA with respect to culture time. Using this approach, the proportions of heavy and light mRNA levels in total RNA were observed to increase as the culture progressed until the stationary culture phase, indicating that IgG mRNA molecules might be relatively more stable than other mRNA species over this culture period, despite the observed decrease in their half-lives under both normal (from 12.6 hrs to 8.4 hours) and hyperosmotic (9.0 hrs to 6.3 hrs) conditions. These findings agree with the mRNA trends reported by Bibila [1991], who also suggested that there might be a "preferential destabilisation" of non-IgG mRNA species as cultures progressed towards the stationary phase. In a study on MPC-11 cells, Schibler et al. [1978] also deduced that the heavy and light immunoglobulin mRNA species had relatively lower turnover rates when compared to other mRNA species. However, beyond the stationary phase, it appears that further decreases in the IgG mRNA half-lives must have occurred, eventually resulting in reductions of IgG mRNA proportions in total RNA in the decline phase. These observations highlight the importance of the heavy and light mRNA degradation rates in governing the variations in mRNA levels with respect to culture time, particularly in the stationary and decline phases. They also suggest that IgG mRNA degradation rates might exert an indirect influence on antibody production rates, through changes in the IgG mRNA levels. The next sub-section will thus focus on the major role that IgG mRNA levels play in the determination of specific antibody productivities throughout the duration of the culture.

Relationship between IgG mRNA levels and specific antibody productivity

The relationship between heavy and light mRNA levels with respect to specific antibody productivity has been a source of interest in previous studies, mainly conducted on hybridoma cells. However, there appears to be no general consensus regarding this relationship. Leno et al. [1992] noted that specific antibody productivity began to decrease during the mid-exponential phase despite increasing mRNA levels. The study found no real correlation between mRNA levels and productivity and it was conjectured that the regulation of specific antibody productivity occurred at a post-transcriptional stage of the production process. Sun et al. [2004] also mentioned that the changes in IgG mRNA levels did not match the changes in antibody production rates under both normal and hyperosmotic conditions. However, Lee and Lee [2000] found that the increase in specific productivity due to hyperosomlarity was likely to be a result of an increase in specific IgG transcripton rates, which had directly increased the heavy and light mRNA levels. In this study, a direct relationship was observed between mRNA levels and antibody productivity over the entire course of the culture, indicating that the factors influencing mRNA concentrations, including the specific transcription and mRNA degradation rates, played key roles in the determination of antibody production rates at all times. These observations are in agreement with the findings of the global sensitivity analysis (GSA) previously described in Chapter 3, which had shown that both the individual and total sensitivity indices (SI) of the specific transcription rates remain high throughout the culture, highlighting its perennial importance to antibody production. Additionally, the total SI values for IgG mRNA half-lives approximately doubled as the culture progresses from the mid-exponential to the stationary phase, which was a reflection of its growing influence on the antibody production process. Furthermore, the experimental study results showed that the same linear correlation between specific antibody productivity and mRNA levels could be applied for both normal and hyperosmotic conditions, thereby suggesting that the higher specific antibody productivities at hyperosmotic conditions could be attributed, at least in part, to the observed increases in heavy and light mRNA levels resulting from elevated transcription rates. This hypothesis is further discussed in the next sub-section, which considers the two factors governing intracellular mRNA levels under varying osmotic conditions.

Evidence of elevated transcription rates at hyperosmotic conditions

Based on the mass balance expressions describing the rate of accumulation of heavy and light mRNA molecules in the cell, it can be deduced that the two main determinants of mRNA levels are: (i) the specific mRNA transcription rate and (ii) the mRNA degradation rate. An increase in mRNA levels, therefore, can be attributed to either an increase in the specific transcription rate, or a decrease in the mRNA degradation rate, as reflected by a longer mRNA half-life.

However, results from the mRNA degradation experiments conducted in this study have shown that the half-lives of heavy and light mRNA molecules were distinctly shorter for cells cultured under hyperosmotic conditions (~ 9.0 hrs at mid-exponential and 6.2 hrs at stationary phase) when compared to normal-condition cells (~12.6 hrs at mid-exponential and 8.4 hrs at stationary phase). These findings imply that hyperosmotic conditions actually resulted in a destabilisation of mRNA molecules, making them more susceptible to mRNA degradation in comparison to normal osmotic conditions. Consequently, it is highly likely that the specific transcription rates of heavy and light mRNA molecules were elevated due to hyperosmolarity. The subsequent parameter estimation conducted in Section 5.3.4 showed that there was indeed an approximate one-fold increase in the specific transcription rates of both heavy and light mRNA molecules under hyperosmotic culture conditions. Similar observations had been made by Lee and Lee [2000], who reported a 37% decrease in half-lives of heavy and light mRNA molecules when osmolarity was increased from 285 to 425 mOsm/kg. The authors subsequently deduced that the transcription rates of heavy and light mRNA were significantly increased (by more than 400%) due to the rise in medium osmolarity.

It should also be noted that the estimated heavy (1450 molecules/(cell.hr)) and light mRNA (2300 molecules/(cell.hr)) transcription rates for normal osmotic cultures were comparable to values previously reported in literature. In a study using a myeloma cell line [Wallach and Laskov, 1980], the heavy and light mRNA transcription rates were determined to be 1020 molecules/(cell.hr) and 1440 molecules/(cell.hr) respectively. Schibler et al. [1978] also reported that the immunoglobulin mRNA transcription rates ranged from 20 to 60 molecules/min (1200 to 3600 molecules/(cell.hr)) for MPC-11 cells. The 2-fold increase

in IgG mRNA transcription rates under hyperosmotic conditions was less than the 400% increase reported by Lee and Lee [2000] in hybridoma cells, suggesting that the extent of transcription rates enhancement was probably cell-line specific. However, the hyperosmotic trancription rates estimated from this study were still within the physiological range derived from previous literature studies [Bibila, 1991; Schibler et al., 1978; Wallach and Laskov, 1980].

Total protein behaviour and cellular energy levels

Total protein concentration has been shown to vary positively with specific growth rates in cultures operating under both normal and hyperosmotic conditions. However, no distinct differences in the protein concentration could be discernable between normal and hyperosmotic cultures with respect to specific growth rates. This behaviour may be explained by the fact that protein synthesis is known to be an energy-intensive process [Bolster et al., 2002; Hucul et al., 1985]. As such, the total protein concentration is likely to be dependent on the availability of ATP in the cell. However, in this study, ATP levels had not been significantly elevated by hyperosmotic conditions, despite an increase in glucose uptake rates throughout the exponential phase. Although hyperosmotic conditions tend to increase the intracellular accumulation of amino acids and thus providing additional "building blocks" for protein synthesis [Oh et al., 1993, 1995], the relatively similar energy levels available in the cell under both osmotic conditions could have limited any possible increase in total protein levels.

Behaviour of heavy and light polypeptide chains in normal and hyperosmotic cultures

Having deduced that total protein concentrations are not elevated at hyperosmotic culture conditions, the behaviour of heavy and light polypeptide chain trends under normal and hyperosmotic conditions is subsequently analysed. Experimental results indicated that the concentrations of the IgG polypeptide chains were relatively higher at hyperosmotic conditions. Additionally, an abundance of light polypeptide chains in comparison to heavy polypeptide chains could be found in GS-NS0 cells under both osmotic conditions. This observation is in agreement with other studies on immunoglobulin production in mammalian cells [Laskov and Scharff, 1974; Whicher et al., 1987], which all reported an excess of IgG

light chain production in animal cells. A reason for this trend had been proposed by Schlatter et al. [Schlatter et al., 2005], who noted that excess light chains were required to minimise the accumulation of unfolded heavy chain polypeptides and increase the rate of antibody folding in the endoplasmic reticulum. This hypothesis is supported by findings from previous studies, which stated that light chains were necessary for the release of unfolded heavy chains from the immunoglobulin binding protein (BiP) and subsequently for facilitation of its folding process [Kaloff and Haas, 1995; Lee et al., 1999; Leitzgen et al., 1997].

Another important point to note is that positive relationships exist between the IgG polypeptide chain concentrations and the specific antibody productivities for both normal and hyperosmotic cultures. The fact that the same correlation could be deduced between the two variables under both osmotic conditions imply that the increase in polypeptide chain concentrations was likely to be responsible, at least in part, for the increase in antibody productivity at hyperosmotic conditions. Subsequently, estimates of the heavy and light chain specific translation rates were derived experimentally. The values were then used to determine whether the increase in antibody productivity could be attributed to improved specific translation rates. The resulting analysis reveals two interesting points: firstly, it is found that the heavy chain specific translation rates were generally higher than the light chain specific translation rates, despite the fact that the light polypeptide chains were present in larger amounts than the heavy polypeptide chains in the cell throughout the culture. This trait had also been seen in the study carried out by Bibila [1991], who derived higher specific translation rates for heavy polypeptide chains in comparison to light polypeptide chains, as more ribosomes were found to be present on the heavy chains. The observations imply that the elevated light chain concentrations were a result of the larger pool of light mRNA molecules present in the cell in comparison to heavy mRNA molecules rather than due to higher light chain specific translation rates. In addition, the estimated specific translation rates were also in general agreement with the range of values obtained from various literature sources – Shapiro et al. [1966] stated that the light immunoglobulin chain required approximately 30 seconds to synthesise (120 light chain molecules/(mRNA.hr)), while the heavy chain required 60 seconds (60 heavy chain molecules/(mRNA.hr)). Conversely, de Petris et al. [1970] calculated that each heavy mRNA molecule had 11-16 polyribosomes

while there were 4-5 polyribosomes present on each light mRNA molecule. Based on an average ribosome translation velocity of 7.2×10^4 ribonucleotides/(ribosome.hr) [Bibila, 1991], the specific translation rates of a 1.4kb heavy mRNA and a 0.7 kb light mRNA molecule was estimated to range from 580 to 850 molecules/(mRNA.hr) and from 400 to 510 molecules/(mRNA.hr) respectively. From the two examples above, it appears that there is a relatively large range of specific translation rates for immunoglobulin heavy and light chains in murine cells, which encompasses the estimated values obtained in this study.

The second interesting observation derived from this analysis concerns the relative specific translation rates of IgG polypeptide chains in normal and hyperosmotic cultures. It appears that in the mid-exponential phase, the specific rates were on average approximately 24% higher at hyperosmotic culture conditions, indicating that elevated specific translation rates did play a role in the improvement of antibody productivity levels. However, the extent of increase in the specific translation rates appeared to be relatively small in comparison to the approximate 100% increase seen in the specific transcription rate under hyperosmotic conditions. Furthermore, the differences between normal and hyperosmotic specific translation rates became smaller with culture progression. In fact, the ratio of hyperosmotic to normal spsecific translation rates (given by $T_H(450)/T_H(290)$ and $T_L(450)/T_L(290)$) decreased to almost 1.0 as the cultures entered the stationary and decline phases. These trends indicate that as the culture progresses, the positive effects that hyperosmotic conditions exerted on specific translation rates were not sustained. Instead, larger IgG mRNA concentrations at hyperosmotic conditions became the main reason for the increase in IgG polypeptide chain concentrations. Consequently, it can be deduced that the increase in specific antibody productivity under hyperosmotic conditions could be attributed mainly to an increase in specific transcription rates. The reduction in the ratios of specific translation rates [$T_H(450)/T_H(290)$ and $T_L(450)/T_L(290)$] to a value of 1 also implies that translation may become rate-limiting at the stationary and decline phases of cultures that are exposed to hyperosmotic culture conditions.

5.5 Conclusions

The two key goals of this chapter included both the evaluation of possible mechanisms through which hyperosmolarity improves specific antibody productivity, as well as the estimation of key parameters for the hybrid antibody production model. Both goals were met based on the analysis of the intracellular behaviour of IgG mRNA and polypeptide chains under normal and hyperosmotic conditions obtained from the experimental study. It was found that heavy and light mRNA levels under hyperosmotic conditions were relatively higher at all culture phases. This increase could be mainly attributed to an approximate 100% rise in the mRNA transcription rates in hyperosmotic cells, as the stabilities of mRNA molecules were not improved; indeed, mRNA molecules were less stable under hyperosmotic conditions, as shown by the lower mRNA half-life values obtained experimentally. The higher mRNA levels were also largely responsible for the increases in heavy and light polypeptide chain concentrations under hyperosmotic conditions. The estimated specific translation rates showed an average increase of only 24% during the mid-exponential phase for hyperosmotic cultures, based on the calculated heavy and light translation rate ratios [$T_H(450)/T_H(290)$ and $T_L(450)/T_L(290)$]. The ratios decreased in value as the culture progressed until a relatively similar translation rate was obtained in the stationary and early decline phases, indicating that IgG translation process might have become a rate-limiting step in hyperosmotic cultures beyond the mid-exponential phase. Finally, it was also determined that the increase in specific antibody productivities at hyperosmotic conditions was attributed mainly to the improvements in the specific transcription rates at a medium osmolarity of 450 mOsm/kg.

Chapter 6

Model Validation and Hyperosmotic Strategy

6.1 Introduction

In this chapter, the estimated parameter values for transcription, translation and mRNA degradation rates, first described in Chapter 5, are incorporated into the hybrid model. The validity of the updated model is verified and subsequently utilised to support a strategy to optimise GS-NS0 antibody production. This involves the induction of hyperosmotic conditions at different time points in the culture. The optimal hyperosmotic induction culture time is then derived based on simulation results of the hybrid model, described in further details in Section 6.3.2.

6.1.1 Product optimisation strategies involving hyperosmotic conditions

Hyperosmotic culture conditions have not been used widely in product optimisation strategies, as the trade-off between the induction of high specific antibody productivities and the suppression of cell growth often leads to a similar total antibody titre as normal conditions. However, there have been a number of studies conducted on overcoming the inhibitory cell growth effects caused by hyperosmolarity in literature. Cherlet and Merc [1999] reported that increasing the medium osmolarity in successive steps for a continuous culture allowed hybridoma cells to adapt to the increased osmolarity and resulted in 100% increases in total antibody titres at 370 and 400 mOsm/kg, in comparison to normal osmotic

conditions (335 mOsm/kg). A similar strategy was proposed by Lin et al. [1999b], who found that a gradual increase in osmolarity enabled hybridoma cells to recover from the osmotic shock. This led to total antibody titres that were higher than a culture grown solely under normal or hyperosmotic culture conditions.

The use of osmoprotectants in overcoming growth suppression under hyperosmotic conditions is one of the most well-studied in literature, with glycine betaine the most commonly used osmoprotective substance [Berg et al., 1991; Kim et al., 2000; Ryu et al., 2000]. However, all three studies, which were conducted on both hybridoma and CHO cells, concluded that while glycine betaine reduced the effects of growth inhibition at hyperosmotic conditions, its presence also eroded the increase in specific antibody productivity due to hyperosmolarity. The extent to which the specific productivity decreased was cell line dependent and could result in antibody titres that were not significantly enhanced. Other proposed strategies involving the alleviation of growth suppression included: the adaptation of cells to hyperosmotic conditions through successive subcultures [Oh et al., 1993], as well as the genetic modification of cells to over-express the anti-apoptotic family of Bcl-2 proteins [Kim and Lee, 2002]. The latter study found that overexpression of Bcl-2 proteins delayed the apoptotic effects of hyperosmolarity and resulted in a 200% increase in final antibody concentration at 522 mOsm/kg compared to values obtained under normal osmotic conditions and a 50% increase compared to a control culture (without Bcl-2 overexpression) conducted at 522 mOsm/kg.

More recently, a biphasic culture strategy for CHO cells was proposed [Kim et al., 2002]. The two phases in the culture involved initially culturing cells under normal osmotic conditions to allow for cell proliferation up to a certain cell density in the "growth phase" before increasing the medium osmolarity to enhance the specific antibody productivity in the "production phase" of the culture. This strategy had resulted in a 161% increase in final antibody titre when medium osmolarity was increased to 522 mOsm/kg from 294 mOsm/kg after 72 hours. However, an increase in medium osmolarity after 48 hrs did not result in a substantial increase in total antibody production relative to normal osmotic conditions. The varying results suggested that the time point at which hyperosmolarity was induced had an important effect on the final antibody titre. Subsequently, the hybrid model developed in

Chapter 3 has been used in an attempt to predict the optimal time point for the increase in media osmolarity. The simulation results attained are presented in the latter sections of this chapter.

6.2 Materials and methods

6.2.1 Hyperosmotic induction experiments

GS-NS0 cells (Lonza Biologics) were grown in 50 mL shake flask cultures at normal culture osmolarity with an inoculum density of 2×10^5 cells/mL. At 48, 72, 96 and 120 hours after inoculation, the osmolarities of duplicate cultures were increased to 450 mOsm/kg by the addition of 4 M sodium chloride (Sigma) solution prepared in standard medium in two 3-hour steps (290 mOsm/kg to 370 mOsm/kg, then to 450 mOsm/kg). Cell growth and viability was monitored daily, as previously described in Section 4.3.3, while the supernatant samples were collected and stored at -20 C for the determination of extracellular antibody concentrations.

6.2.2 Statistical analysis

In this chapter, the error bars in graphs represent the standard deviation of replicate experiments.

6.3 Results and analyses

6.3.1 Hybrid model validation

Based on the experimental results discussed in Chapters 4 and 5, estimates for the key parameters, as identified by the global sensitivity analysis (GSA), have been obtained and incorporated into the hybrid model. The key intracellular parameters estimated include the specific transcription rates, the mRNA degradation rates and the specific translation rates.

The resulting simulation trends for a number of variables under both normal and hyperosmotic conditions were then compared to the experimental results obtained (Figures 6.1 to 6.7).

Behaviour of heavy and light mRNA species

Figures 6.1 a and 6.1 b show the variation of experimental and predicted mRNA concentrations with respect to culture time. It is evident that the model was able to describe the behaviour of heavy and light mRNA species fairly well, indicating that the estimates of specific transcription rates and mRNA degradation rates were relatively accurate for both normal and hyperosmotic culture conditions. The mild increase in the initial mRNA concentrations observed under hyperosmotic culture conditions is due to the step increase in specific growth rate after the lag phase of 24 hours implemented in the model. In addition, the results also reflect the relatively higher mRNA concentrations observed under hyperosmotic conditions in comparison to normal conditions.

Specific translation rates and polypeptide chain concentrations

The previous model developed for antibody production by Bibila [1991] assumed that specific translation rates were a linear function of the total RNA content present in the cells. This correlation was based on the observations that specific translation rates were dependent on the number of polyribosomes present on each mRNA transcript. Since ribosomal RNA constituted 80-85% of total cellular RNA [Bibila, 1991], the specific translation rates were therefore assumed to vary proportionally with total RNA content. In the present model (hybrid), the same correlation has been adopted given the experimental results demonstrate that a positive relationship does exist between specific translation rates and total RNA levels. The simulated and experimentally derived heavy and light specific translation rate trends under both normal and hyperosmotic conditions can be observed in Figures 6.2 a and 6.2 b, plotted with respect to specific growth rate. The specific growth rate was chosen as a basis for comparison as it was also positively related to total RNA levels (see Chapter 5, Figure 5.2). The results indicate that there is a reasonably good agreement between predicted and experimentally derived values for the specific translation rates. Figures 6.3 a and b shows the

variation of total heavy and light polypeptide chain concentrations with respect to specific growth rate. For total heavy polypeptide chain concentrations, the predicted trends are in general agreement with experimental trends. However, a discrepancy can be seen in the total light polypeptide chain trends, especially under hyperosmotic conditions – the predicted trend appears to increase initially during the mid-exponential phase before remaining relatively constant while the experimental total light chain concentrations decreased with a decline in growth rates. However, it can subsequently be noted that the differences in the intracellular total light chain pool do not have a large impact on specific antibody productivity or total antibody produced (Figures 6.6 and 6.7).

Specific glucose and lactate metabolic rates

Figures 6.4 and 6.5 illustrate that the hybrid model is able to predict glucose uptake and lactate production rates relatively well under both normal and hyperosmotic conditions. As seen from these results, the specific glucose uptake rates are generally higher for hyperosmotic cultures in the exponential phase but decrease during the stationary and decline phases with respect to cultures under normal osmotic conditions. The glucose uptake trends are mirrored in the lactate production rates – the specific rates are higher for hyperosmotic cultures relative to normal osmotic cultures during the exponential phase but fall below normal-condition production rates during the stationary and decline phases.

Antibody production trends

The specific antibody productivity and total antibody concentration are shown in Figures 6.6 and 6.7. From Figure 6.6, it is observed that the experimental antibody productivity values are in relatively good agreement with values the predicted values, indicating that the hybrid model has succeeded in describing the intracellular antibody production process with some accuracy. The predicted antibody production trends shown in Figure 6.7 are in general agreement with experimental values, further supporting the validity of the hybrid model.

In addition, a summary of the parameter values used in the hybrid model under normal and hyperosmotic conditions have been provided in Table 6.1. A key point to note from the table is that, apart from the intracellular parameter values estimated in Chapter 5,

other intracellular parameters have all been maintained at their normal culture condition values.

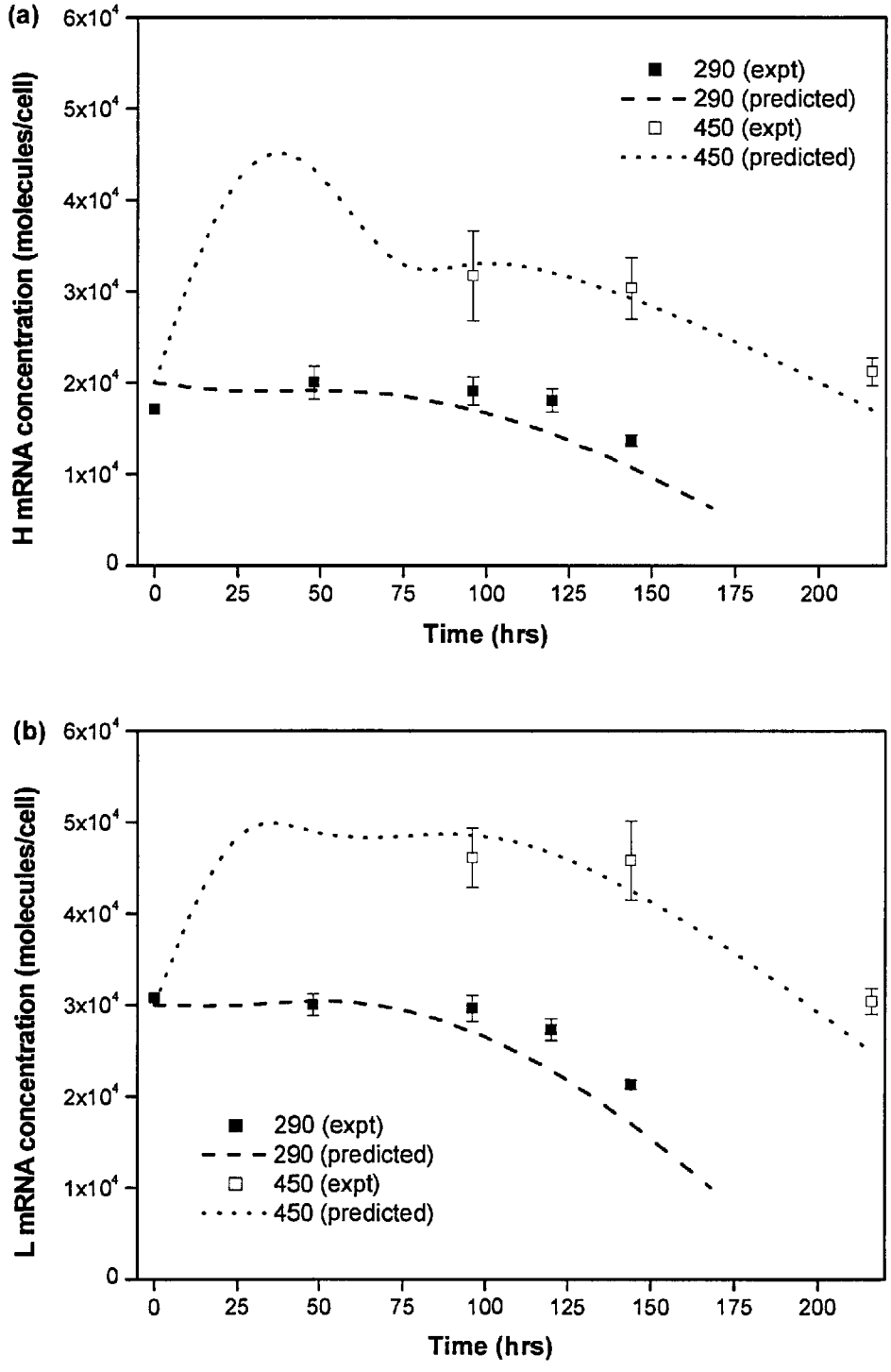

Figure 6.1. Hybrid model predictions with experimental results for (a) heavy and (b) light mRNA concentration profiles under normal (290 mOsm/kg) and hyperosmotic (450 mOsm/kg) culture conditions.

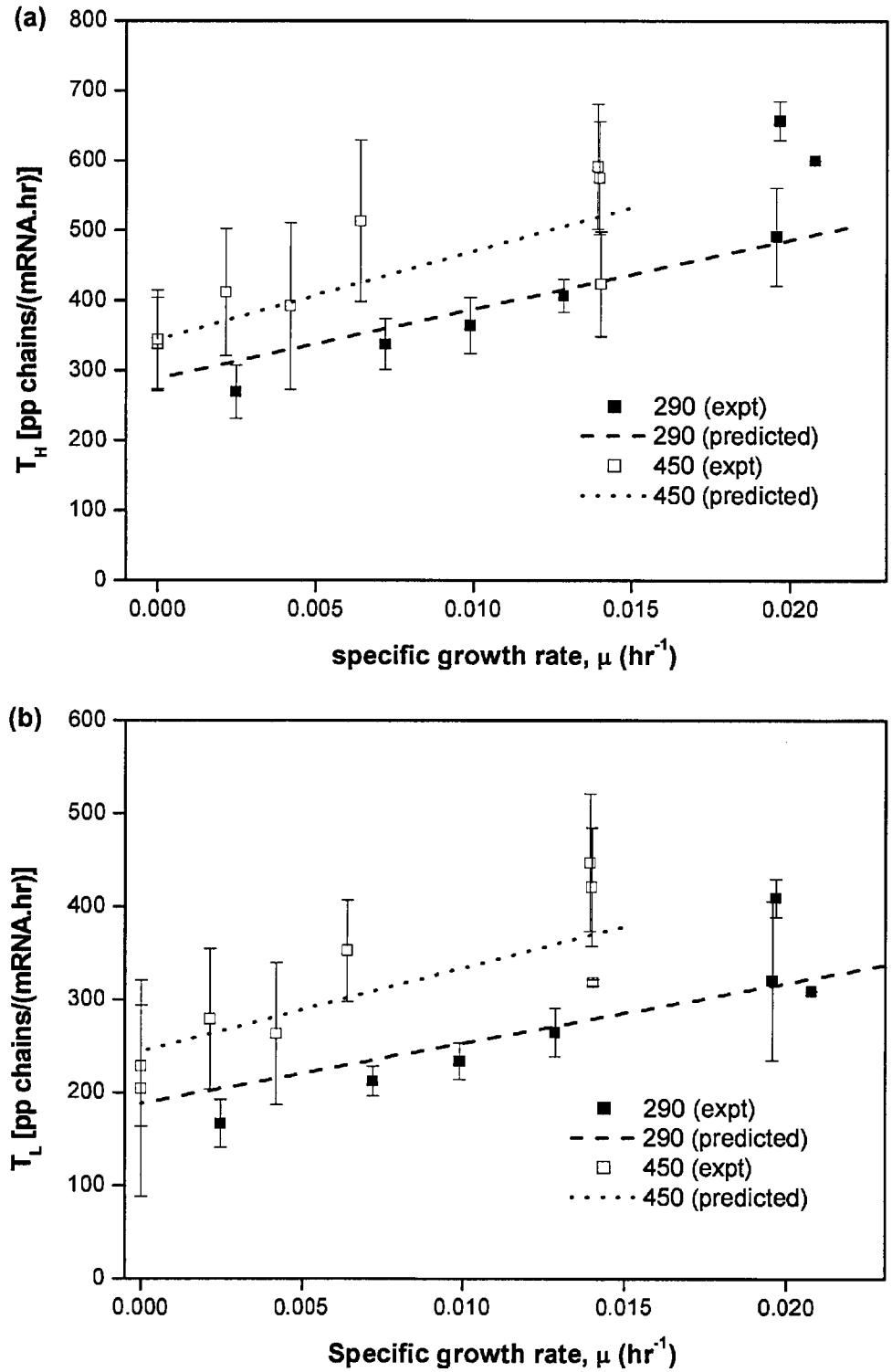

Figure 6.2. Hybrid model predictions with experimental results for (a) heavy and (b) light specific translation rates with respect to specific growth rates under normal (290 mOsm/kg) and hyperosmotic (450 mOsm/kg) culture conditions.

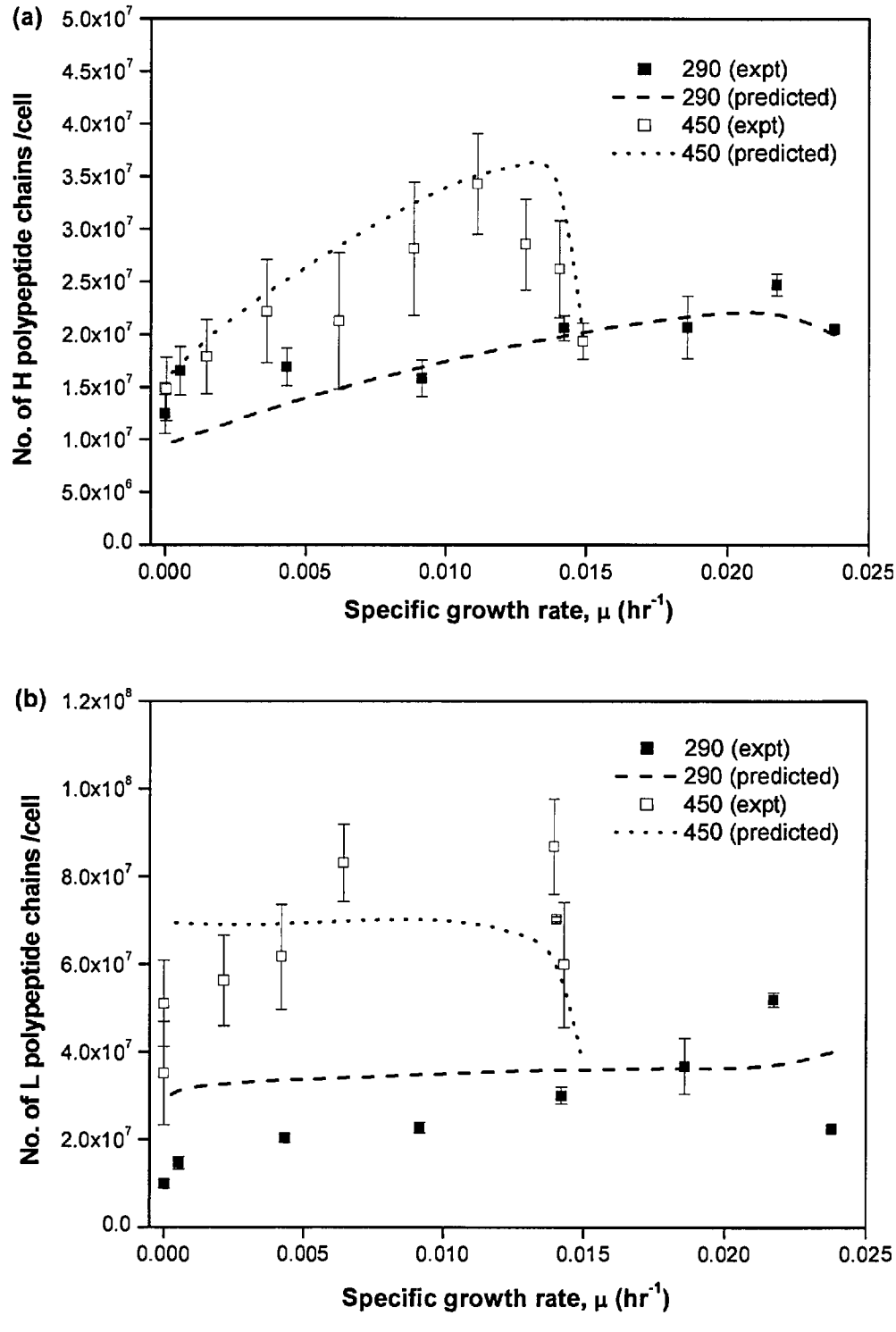

Figure 6.3. Hybrid model predictions with experimental results for (a) heavy and (b) light polypeptide chain concentrations with respect to specific growth rates under normal (290 mOsm/kg) and hyperosmotic (450 mOsm/kg) culture conditions.

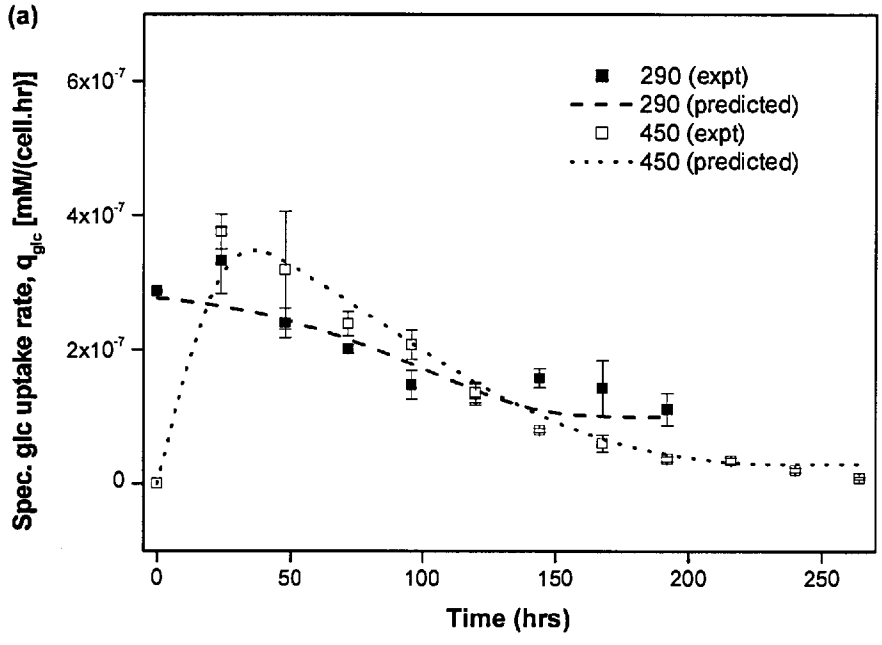

Figure 6.4. Experimental and predicted specific glucose uptake rates under normal (290 mOsm/kg) and hyperosmotic (450 mOsm/kg) culture conditions.

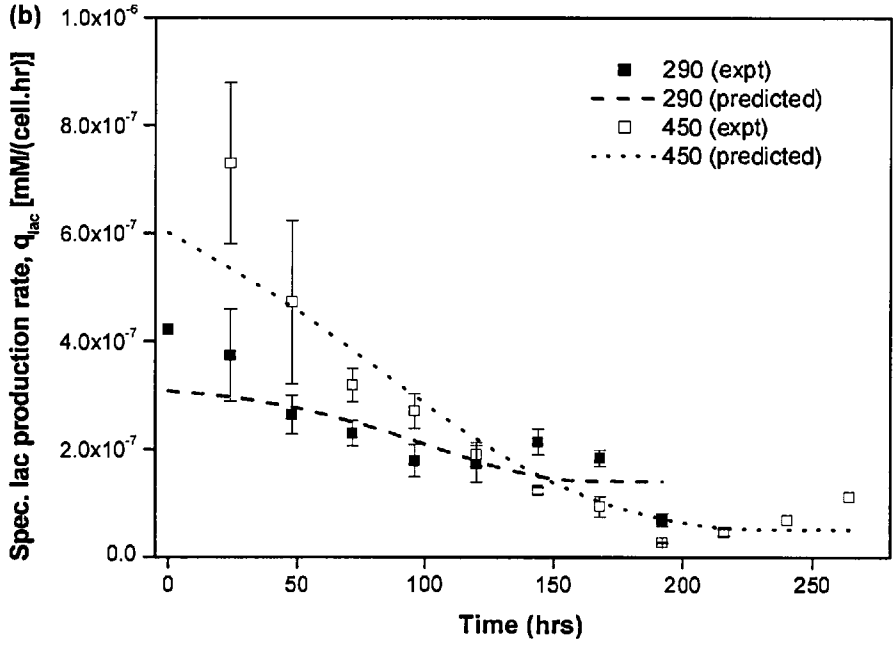

Figure 6.5. Hybrid model predictions with experimental results for specific lactate production rates under normal (290 mOsm/kg) and hyperosmotic (450 mOsm/kg) culture conditions.

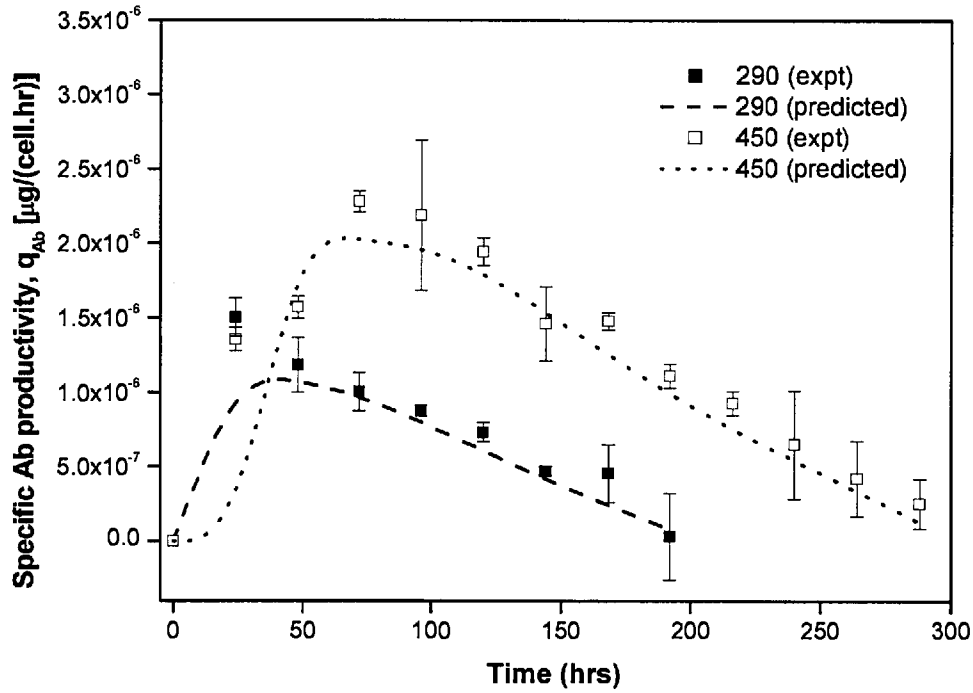

Figure 6.6. Hybrid model predictions with experimental results for specific antibody productivity under normal (290 mOsm/kg) and hyperosmotic (450 mOsm/kg) culture conditions.

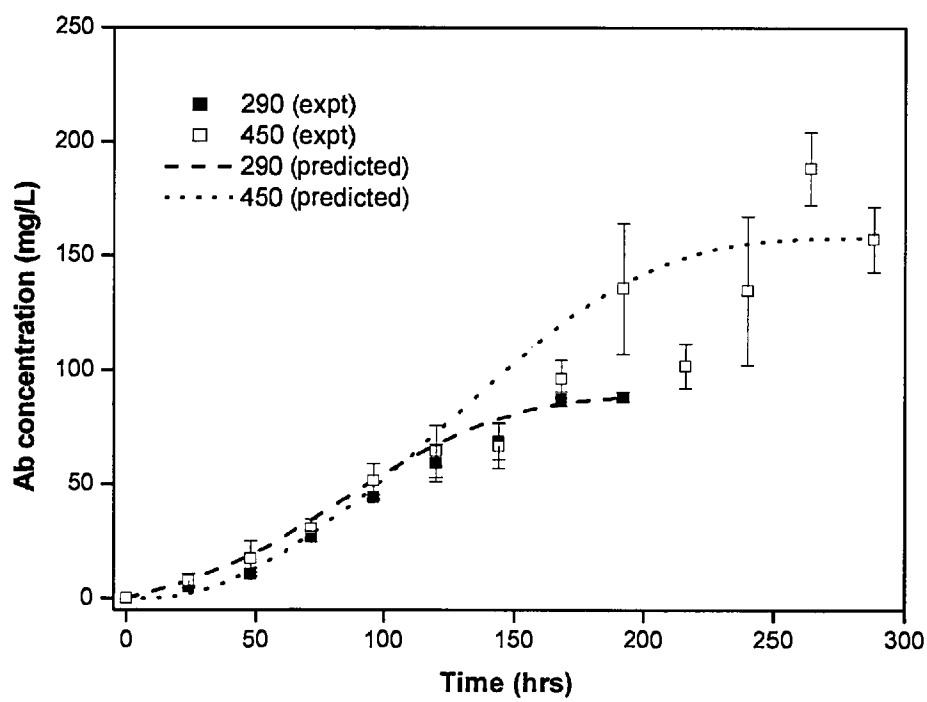

Figure 6.7. Hybrid model predictions with experimental results for antibody production trends under normal (290 mOsm/kg) and hyperosmotic (450 mOsm/kg) culture conditions.

Growth kinetics and metabolism parameters			
Parameter	Values used (normal condition)	Values used (hyperosmotic condition)	References
μ_{max}	0.33	0.023	This study
$[GLC]_{min}$	6.5	8.3	
$K_{d,l}$	5.0×10^{-4}	1.4×10^{-5}	
$K_{d,T}$	1.2×10^{-2}	9.7×10^{-4}	
$k_{l,1}$	0.030	0.025	
$k_{l,2}$	8.4×10^{-3}	2.2×10^{-3}	
K_{glc}	240	7.1	
$K_{glc,max}$	2.7×10^{-7}	1.3×10^{-5}	
$K_{glc,l}$	9.6	4.81×10^{2}	
m_{glc}	1.0×10^{-7}	3.0×10^{-8}	
m_{lac}	4.6×10^{-8}	1.1×10^{-8}	
$Y_{lac,glc}$	0.95	1.4	

Antibody formation and transport parameters				
Parameter	Reference values	Values used (normal)	Values used (hyperosmotic)	References
S_H	1200-3600	1450	3000	[Schibler et al., 1978; Wallach and Laskov, 1980]
S_L	1800-5400	2300	4360	[Bibila, 1991]
$T_{H,0}$	60-850	449	544	[de Petris, 1970; Shapiro et al., 1966]
$T_{L,0}$	120-510	293	386	[de Petris, 1970; Shapiro et al., 1966]
k_{HL}	-	1.5×10^{-6}	1.5×10^{-6}	-
k_{HL}/k_{HH}	11.5	11.5	11.5	[Percy et al., 1975]
$t_{1/2,ER}$	0.5-1	0.7	0.7	[Choi et al., 1971]
$t_{1/2,G}$	0.083-0.5	0.333	0.333	[Fries et al., 1984; Lodish, 1988]
$t_{1/2}$	2-14	12.6	9.0	[Wallach and Laskov, 1980]
$m_{H,0}$	2×10^4-4×10^4	2×10^4	2×10^4	[Potter, 1972; Wallach and Laskov, 1980]
$m_{L,0}$	3×10^4-6×10^4	3×10^4	3×10^4	[Bibila, 1991]
$[H]_0$	2×10^7 - 4×10^9	2×10^7	2×10^7	[Bibila, 1991]
$[L]_0$	2×10^7 - 6×10^9	2×10^7	2×10^7	[Bibila, 1991]

Table 6.1. Final parameter values for the hybrid model under both normal and hyperosmotic condition cultures.

6.3.2 Biphasic antibody production strategy with hyperosmotic induction

As described in Section 6.1, one of the proposed optimisation strategies involving the use of hyperosmotic culture conditions is the biphasic culture – during which cells are first allowed to proliferate until a certain cell density level is attained, before hyperosmotic conditions are induced so as to achieve the higher specific productivities associated with high osmolarity for the remaining culture period. Here, a strategy based on a trade-off between obtaining a high cell density at normal conditions and high specific antibody productivity at hyperosmotic conditions is proposed, in order to maximise the total antibody titre in the culture. The balance between both variables indicates that the optimal time point for hyperosmotic induction must be identified to achieve the highest increase in total antibody produced. In this study, the hybrid model is used to derive an estimate of the optimal hyperosmotic induction culture period, via a simple "switching" mechanism, in which the parameters are switched from their normal values to their values under hyperosmotic condition at different time points in the culture, ranging from 48 to 120 hours. The model predictions of total antibody produced at the end of each culture provides an indication of the best time point in the culture to switch to hyperosmotic culture conditions. Simulation results from the hybrid model suggests that the accumulation of total antibody product is maximum (182 mg/L) at approximately 72 hours into the culture, which represents an increase of approximately 100% from the antibody concentration derived under normal osmotic conditions and a 12% increase from total antibody produced under hyperosmotic (450 mOsm/kg) conditions. In comparison to the hyperosmotic conditions, the increase in the total antibody titre in the biphasic process appears to be less significant, however, this extra antibody titre required 25% less culture time.

To support the simulation study, further experimental work was undertaken. In brief, the procedure was as follows: duplicate cultures cultivated at normal osmotic conditions were hyperosmotically induced by the addition of sodium chloride to the culture medium at 48, 72, 96 and 120 hours into the culture. The resulting comparisons between experimental and predicted trends can be observed in Figures 6.8 and 6.9. Figure 6.8 shows the trends for final antibody titre achievable at different hyperosmotic induction time points. The optimal

hyperosmotic induction time point as predicted by the model appears to be consistent with experimental data – both trends demonstrate that the peak total antibody titre is achieved when hyperosmolarity is induced 72 hours into the culture. The experimental study appears to support the simulation work fairly closely, though there are variations at specific points; in particular at t = 72 hours.

Figure 6.9 shows the variations in the viable cell numbers (6.9 a and 6.9 b) and in the antibody concentration (6.9 c and 6.9 d). These results were obtained from the hyperosmotic shift points of 72 and 96 hours. From Figures 6.9 a and 6.9 b, it appears that the model does over predict the number of viable cells after the induction of hyperosmotic conditions. Here it is evident that the actual viable cell concentrations reach a lower maximum peak density and also show a steeper gradient during the decline phase than it is predicted by the hybrid model. Table 6.2 shows the predicted and experimental maximum cell densities obtained at the various hyperosmotic induction time points. The data suggests that the number of viable cells is consistently being overestimated by the model. In contrast, the simulated antibody accumulation profiles (figures 6.9 c and 6.9 d), which are dependent on the viable cell number, are in good agreement with the actual profiles attained from experimental methods, instead of being overestimated. Therefore, the data seems to imply that that the specific productivities of these hyperosmotically induced cultures are in fact higher than the values achieved under constant hyperosmotic conditions (solely hyperosmotic cultures inoculated at 450 mOsm/kg).

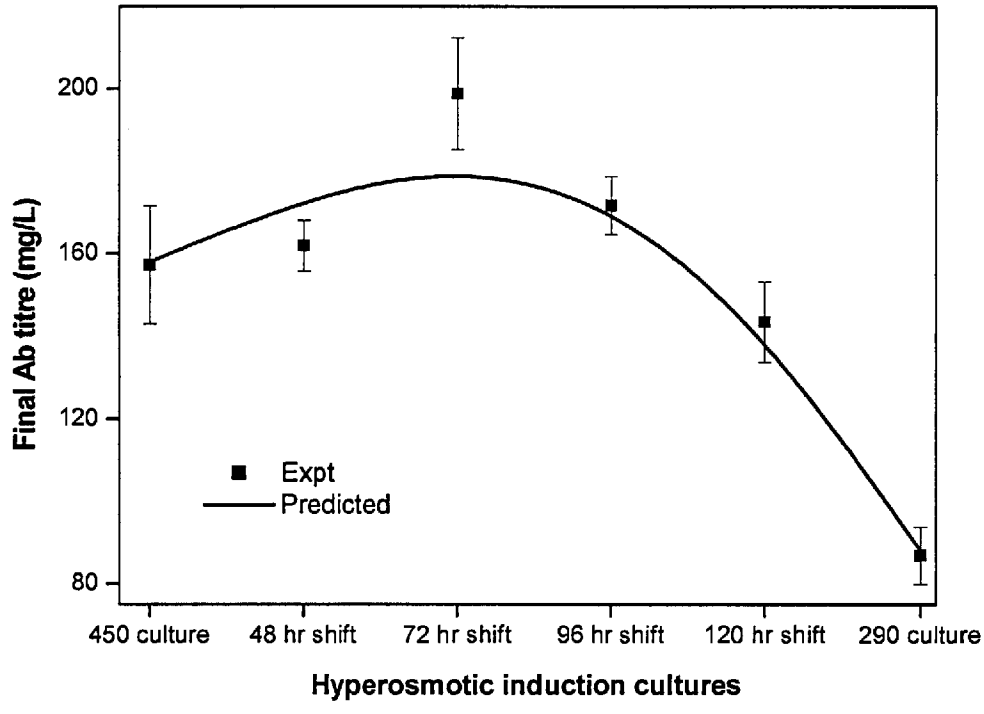

Figure 6.8. Predicted and experimental values of the final antibody titre achievable at each hyperosmotic induction time point.

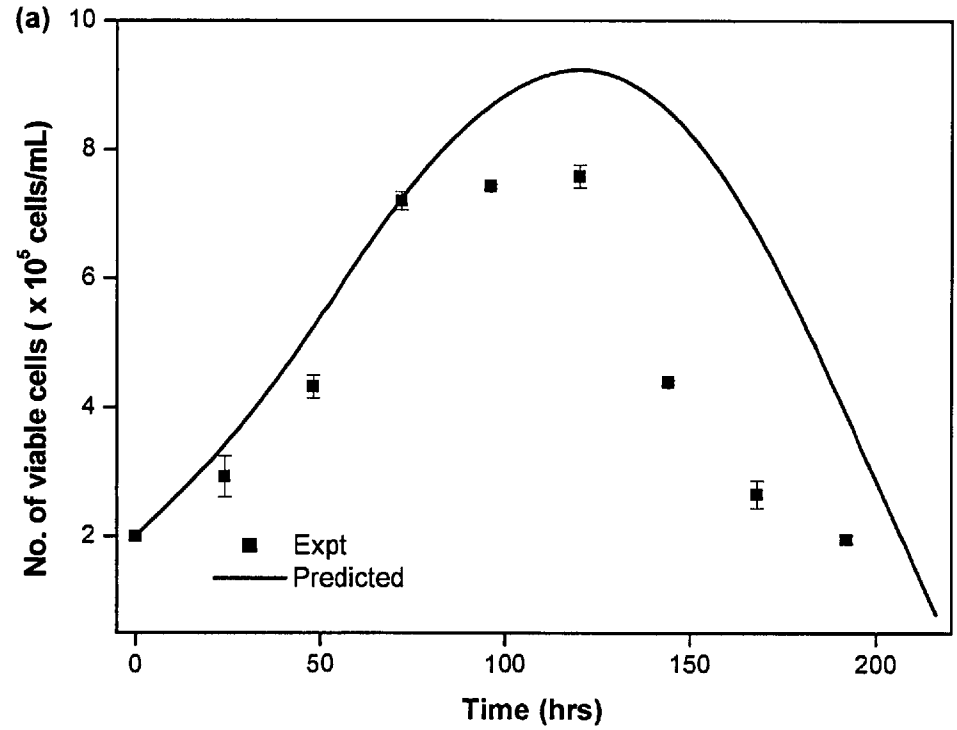
(a)
No. of viable cells (x 10^5 cells/mL)
Time (hrs)
Expt
Predicted
0
50
100
150
200
2
4
6
8
10

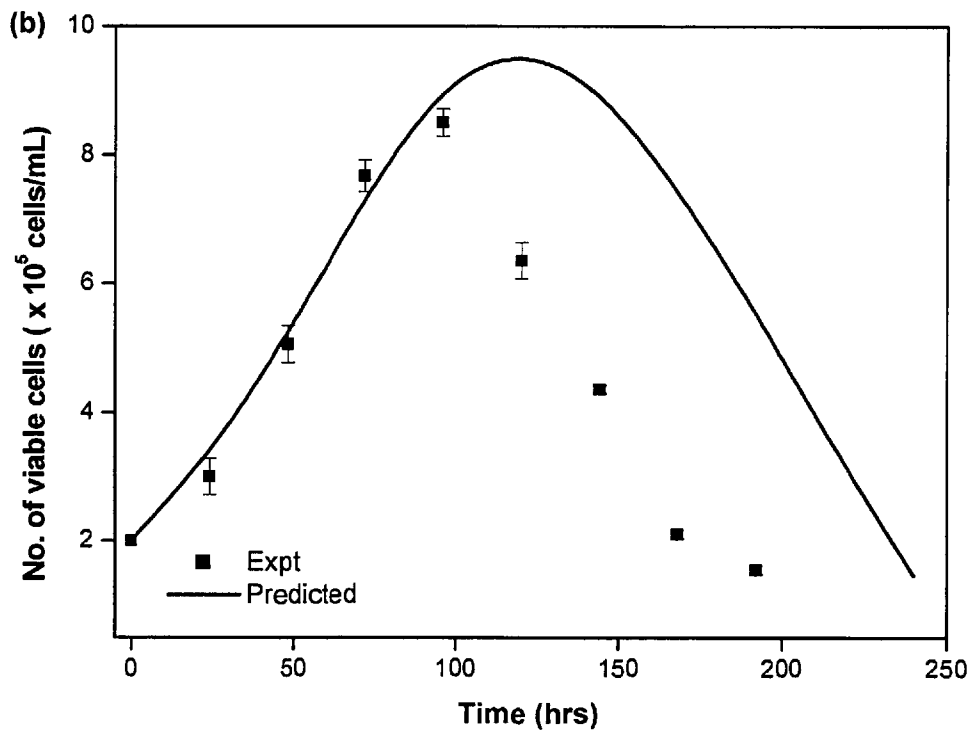
(b)
No. of viable cells (x 10^5 cells/mL)
Time (hrs)
Expt
Predicted
0
50
100
150
200
250
2
4
6
8
10

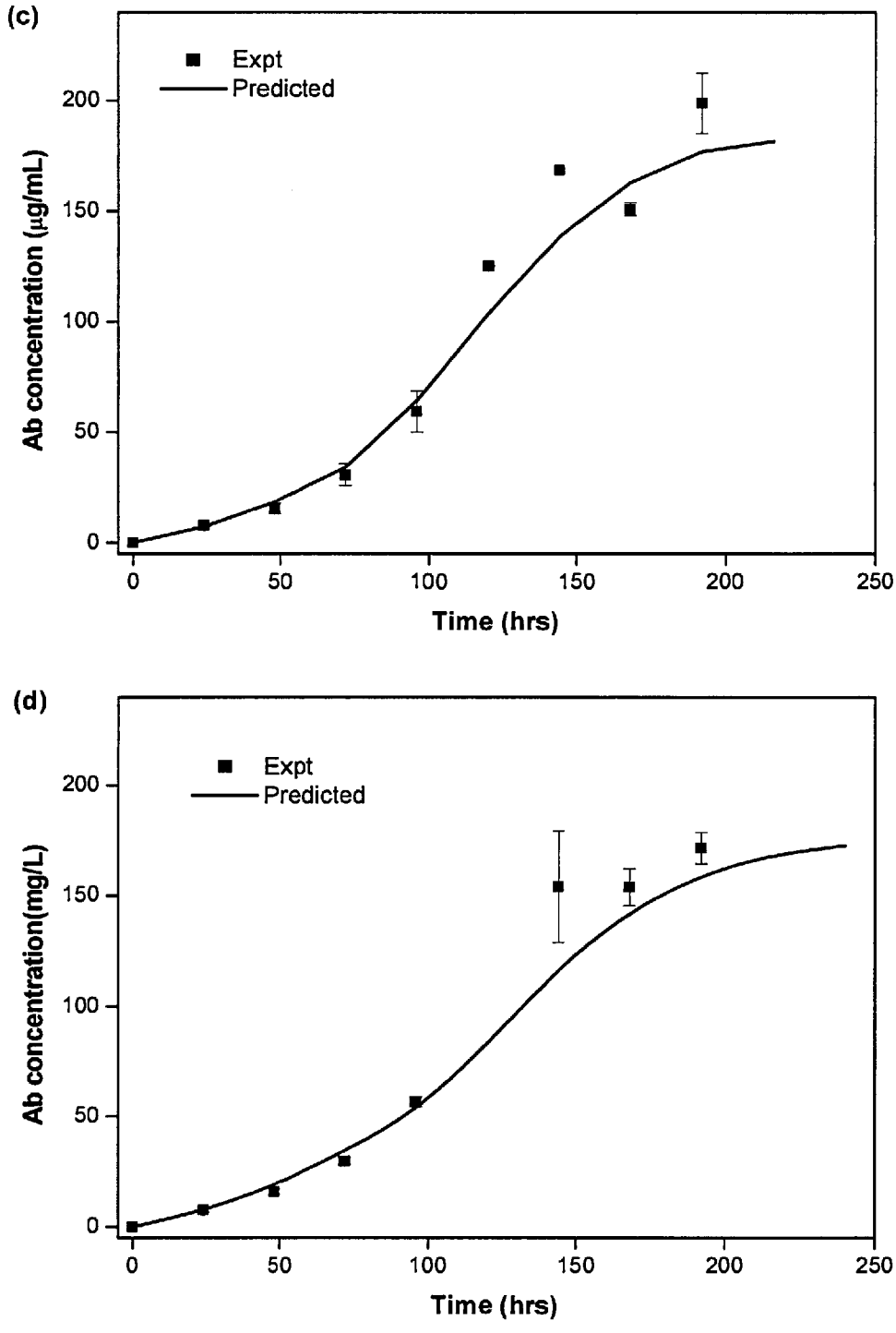

Figure 6.9. Predicted and experimental values of the viable cell concentration at (a) 72 hours and (b) 96 hours hyperosmotic induction time points, and predicted and experimental values of the antibody production profiles at (c) 72 hours and (d) 96 hours hyperosmotic induction time points.

Hyperosmotic induction time (hrs)	Max X_V (Predicted) (Cells/mL)	Max X_V (Experimental) (Cells/mL)
48	8.6×10^5	7.3×10^5
72	9.4×10^5	7.6×10^5
96	9.7×10^5	8.5×10^5
120	9.8×10^5	8.8×10^5

Table 6.2. Summary of predicted and experimental maximum cell densities for different hyperosmotic induction time points.

6.4 Discussion

Hybrid model validation

The ability of the hybrid model to predict growth, metabolism, intracellular and extracellular antibody production trends was assessed in Section 6.3.1. Based on the comparisons between experimental and predicted trends, it can be concluded that the model was relatively accurate in the depiction of the intracellular antibody production process, after key parameter values were estimated from the experimental study described in Chapters 4 and 5. It has also been noted that the only differences in intracellular parameter values were of the key parameters identified by the GSA conducted on the hybrid model (described in Section 3.4.2) while all other intracellular parameter values remained unchanged relative to normal culture conditions. This implies that the estimation of a small number of key parameters would be sufficient to accurately describe the intracellular antibody process and illustrates the effectiveness of the GSA in identifying the most influential parameters involved in the determination of antibody production rates and demonstrates how it has successfully guided the design of the subsequent experimental study.

Biphasic culture strategy

The hybrid model, under a simple "parameter switchover" strategy, was able to correctly predict the optimal hyperosmotic induction time point for a biphasic culture strategy. However, as identified previously, the model did consistently overestimate the number of viable cells present in the culture in comparison to the experimental data. The initial hypothesis of the biphasic culture resulting in an extended culture longevity due to hyperosmotic induction remained unconfirmed. The number of viable cells in biphasic culture experiments declined at approximately the same rate, or slightly even faster, than cultures solely grown under in either normal or hyperosmotic media. Similar trends were observed for the CHO cell line in biphasic culture experiments conducted by Kim et al. [2002]. In their study, the viable cell concentrations after the induction of hyperosmolarity (ranging from 370 to 522 mOsm/kg from a control osmolarity of 294 mOsm/kg) by the addition of sodium chloride after 3 and 4 days into the cultures were seen to decline at more rapid rates than the control cultures at normal osmolarities.

The variations in the viable cell number behaviour for hyperosmotically induced cultures in comparison to cultures grown solely under hyperosmotic conditions appear to imply that there are inherent differences in the growth characteristics of both culture types. For a newly inoculated culture in a hyperosmotic medium, a lag phase was initially observed, during which cells adjust to the increased osmolarity before proliferating actively (see Section 4.4.1). However, in cultures that had been hyperosmotically induced at a certain point during its progression, the sudden increase in medium osmolarity might have added to the stress caused by the accumulation of toxic metabolites and the reduction in nutrient levels. This might have resulted in a larger proportion of necrotic and apoptotic cell deaths compared to a culture originally inoculated at hyperosmotic conditions. G0/G1 cell cycle arrest was also likely to have been induced when the medium osmolarity was increased, further reducing the proportion of actively proliferating cells. In addition, the sharp decrease in the experimental viable cell numbers after hyperosmotic induction was particularly apparent for the 96- and 120-hour time-shift cultures, in comparison to the time-shift cultures at 48 and 72 hours, for which the viable cell numbers continued to increase for 1 to 2 days before declining. These observations suggest that hyperosmotic induction at a later culture stage was more likely to cause cell lysis through necrotic cell deaths, while induction at an earlier culture stage may cause cell apoptosis to occur. In general, the effects of apoptosis are not instantaneously visible and only become apparent after a period of time, which could explain the relatively rapid decrease in viable cell number after 1 to 2 days in the 48- and 72-hour time shift cultures. As the present model adopted a parameter "switchover" mechanism, it was not able to take into consideration the initial osmotic shock effects on normal osmotic cultures that were already in progression. Therefore, a possible modification to the hybrid model is the inclusion of an "osmotic shock" term, which takes into account the apoptotic and necrotic cellular effects of hyperosmotic induction. The use of an "osmotic shock" term is further discussed in Section 7.2.1.

The similarity in predicted and experimental antibody production results suggests that higher than expected specific antibody productivities might have been achieved after the induction of hyperosmolarity. The combined stress of hyperosmotic shock, the reduction in nutrient levels and the build up of toxic metabolites could have possibly led to further

overexpression of certain genes related to the antibody production pathway of the cells and subsequently caused the specific antibody productivity to increase by a larger than expected amount. For example, it is possible that genes related to the transcription of heavy and light mRNA molecules were expressed at a higher level due to hyperosmotic induction, particularly at a later culture stage in comparison to cultures inoculated at hyperosmotic conditions. Consequently, despite the over-prediction in viable cell number by the hybrid model, the experimental antibody production values were still comparable to the simulation results.

To take advantage of (i) the high cell density associated with normal osmotic conditions, (ii) the enhanced specific antibody productivity and (iii) the culture longevity observed at hyperosmotic conditions, the biphasic culture procedure needs further modifications. For example, increasing the medium osmolarity through a step-wise approach over a longer time period will allow the cells to adjust to the higher osmotic condition without triggering necrotic and apoptotic cell death mechanisms. The overall increase in the cumulative volumetric cell hour possible under this modified strategy is likely to result in further increases in total antibody titre.

6.5 Conclusions

This chapter presented the validity of the hybrid model utilised for the predictions of intracellular and extracellular variables related to growth, metabolism and antibody production. The updated model was then utilised to estimate the optimal hyperosmotic induction time in a biphasic culture strategy aimed at improving antibody production yields. Comparisons between predicted (model) and experimental results showed that the hybrid model correctly estimated the optimal induction time for hyperosmolarity. However, the simple parameter "switchover" mechanism resulted in an over prediction of viable cell number, as it did not take into consideration the possible growth and death effects caused by osmotic shock. Consequently, further advancement of the description of the initial hyperosmotic effects would lead to improvements in the predictive capability of the model. Finally, hyperosmotic induction of normal condition cultures resulted in specific antibody

productivity values which were relatively higher than solely hyperosmotic cultures. This was evident as the increase of the total antibody titre from 157 mg/L to 199 mg/L for the optimal hyperosmotically induced culture was achieved over a comparatively shorter time period (8 days for hyperosmotically induced culture compared to 12 days for culture inoculated in 450 mOsm/kg medium) relative to cultures solely grown at 450 mOsm/kg.

Chapter 7

Overall Conclusions and Future Work

The main goal of this thesis was to derive a better understanding of the antibody production process, as well as improving antibody production yields from GS-NS0 cells cultivated under both normal and hyperosmotic conditions. In the following sections, the overall conclusions obtained from the combined modelling and experimental study will be discussed and recommendations regarding future work will be provided.

7.1 Overall conclusions

The overall conclusions derived from the combined study can be divided according to the four main objectives mentioned in Chapter 1.

7.1.1 Development of hybrid model

In this study, a hybrid model consisting of both unstructured and structured elements was first developed based on existing GS-NS0 data pertaining to growth, extracellular metabolism and antibody accumulation in the medium. The model was constructed as a trade-off between the lack of detailed intracellular information characteristic of an unstructured cell culture model and the mathematical complexity associated with a highly structured model. The combined modelling approach provided a detailed description of the antibody production process, while still ensuring that the number of parameters was kept low

enough to allow for an in-depth model analysis. Additionally, the model also established a link between cell metabolic processes and the intracellular GS-NS0 antibody production process, which was generally absent in previous unstructured and structured models. Predictions from the hybrid model using parameters estimated from literature agreed well with existing experimental information and were comparable to the predicted trends obtained from an up-to-date single cell model developed by Sanderson [1997].

7.1.2 In-depth model analysis

The hybrid model was then subjected to a detailed model analysis using the Sobol' global sensitivity analysis (GSA) technique, which allowed for the identification of key model parameters with respect to antibody production, based on the computation of sensitivity indices. The sensitivity indices provided a quantitative measure of the relative effect that each parameter exerted on antibody production rates and were an indication of the importance of individual parameters to intracellular antibody synthesis. The key parameters derived from the GSA were those involved in the transcription and translation of heavy and light antibody molecules (S_H, S_L, T_{H0}, T_{L0}, $t_{1/2}$), of which their combined sensitivity indices (both SI_{ind} and SI_{tot}) represented more than 90% of the total value of all sensitivity indices. A representation of antibody production at hyperosmotic culture conditions was subsequently derived based on the GSA results as well as existing literature data on transcription and translation rates under hyperosmotic conditions in hybridoma cells. The GSA results also served as an important guide to the design of the experimental study of GS-NS0 cells under normal and hyperosmotic conditions, described in the next section.

7.1.3 Experimental investigation of hyperosmotic effects on GS-NS0 cells

The experimental study on GS-NS0 cells had two key goals. The first goal was to acquire estimates of the key parameters that were identified by the GSA under both normal and hyperosmotic conditions. Estimated values for specific transcription, translation and mRNA half-lives were successfully obtained from the cell culture experiments (detailed in Chapter

5) and subsequently incorporated into the hybrid model. The second goal was to identify the mechanism through which hyperosmotic conditions resulted in increased antibody productivities. A number of hypotheses proposed in literature regarding the mechanism of hyperosmolarity were thus assessed based on the experimental results obtained in this study. The first hypothesis involved the shifting of cellular resource utilisation from cell growth to antibody production as a result of hyperosmolarity-induced cell cycle arrest, thereby causing antibody productivities to increase. This hypothesis was found to be unlikely in the case of GS-NS0 cells, as analysis of cell cycle data with respect to specific productivities indicated that a positive correlation existed between productivity and proportion of cells in the S cell cycle phase, while a negative correlation was seen between productivity and the G0/G1 cell proportion. These results suggested that specific productivities in GS-NS0 cells were growth-associated and would improve further if the growth suppression at hyperosmotic conditions could be overcome.

Another frequently used hypothesis purports that the increase in nutrients uptake at hyperosmotic conditions results in higher energy levels, which increase overall protein translation rates and cause the rise in specific productivities. However, the experimental data derived showed that the increase in specific glucose consumption rates in the growth phase could be attributed to a metabolic shift in cells towards less efficient energy production pathways. Consequently, no significant rise in cellular energy levels was observed and total protein concentrations under hyperosmotic conditions were not significantly increased, thereby suggesting that this was not the key route through which hyperosmotic conditions influenced specific productivities.

The intracellular mRNA and IgG polypeptide chain analyses eventually indicated that the key reason for increased antibody productivities at hyperosmotic conditions was a result of heightened specific transcription rates, which was consistent with another hypothesis proposed by Lee and Lee [2000]. The authors suggested that the higher transcription rates were a result of the unbinding of histones from DNA at hyperosmotic conditions, which increased its accessibility to RNA polymerase, the enzyme responsible for mRNA transcription. The experimental findings also implied that the process of antibody production was likely to be rate-limiting at the translation step, particularly after the late-

exponential culture phase, as the increase in specific translation rates observed at the mid-exponential phase was rapidly reduced to the rates at normal osmotic conditions. The experimental estimates for the specific transcription and translation rates, as well as the mRNA half-lives were then incorporated into the hybrid model. Comparisons of the simulated and experimental trends for key intracellular and extracellular variables indicated that the hybrid model gave a fairly accurate description of the intracellular antibody production process in GS-NS0 cells.

7.1.4 Use of hybrid model in biphasic culture strategy

A biphasic culture strategy, consisting of a cell growth phase and an antibody production phase, was implemented on GS-NS0 cells, with the aim of increasing total antibody titre beyond the amount achieved by cultures grown solely at hyperosmotic conditions. The hybrid model was utilised based on a simple parameter "switchover" strategy to predict the optimal time point during the culture for hyperosmotic induction, at which total antibody titre would be maximum. The best hyperosmotic induction time point predicted by the model was subsequently validated experimentally as being 72 hours into the culture. The total antibody titre at this optimal time point was more than 200% higher than normal osmotic conditions. The value was also 12% higher than solely hyperosmotic cultures and was achieved in 8 days instead of the 12 days required by the latter. The results highlighted the potential use of hyperosmolarity in conjunction with other product optimisation parameters such as glucose and amino acid feeds.

7.2 Recommendations for future work

The combined modelling and experimental study has demonstrated that the implementation of hyperosmolarity results in a significant increase in total antibody production and highlights the potential use of modelling in the development of antibody product optimisation strategies. In this section, possible research directions are discussed, both with

regard to model improvement as well as the possibility of further elevating the total antibody titre achievable under hyperosmotic conditions.

7.2.1 Hybrid model improvements

The simple parameter "switchover" approach used on the hybrid model for the biphasic culture strategy enabled the optimal hyperosmotic induction time point to be determined. However, it was observed that the model constantly over predicted the number of viable cells present after hyperosmotic induction, as it did not take into account the probably shock effects caused by a sudden increase in osmolarity as the culture was progressing. A possible improvement to the model will be to introduce an "osmotic shock" factor, which will consider both cell cycle arrest and cell death through apoptotic and necrotic pathways. The introduction of such a factor can range from simply fixing the proportions of cells that become growth arrested or apoptotic (and necrotic), to the incorporation of cell cycle dynamics into the hybrid model. The latter approach will finally result in a population balance model, in which cells at the different cycle phases can be identified. In addition, the current hybrid model can also be adapted to study the effects of other environmental conditions, such as pH and temperature, on antibody production, as well as used to describe the behaviour of a fed-batch culture by the introduction of mathematical expressions describing the input of nutrient feeds and the removal of metabolites.

An improved model consisting of the above features will be likely to have potential process engineering applications as it can then be used to identify the range of operating conditions that leads to the global optimal, in terms of total antibody titre. It will therefore serve as a useful guide in the design of further experiments and allow process development to become more time- and cost-effective.

7.2.2 Hyperosmolarity and antibody production in GS-NS0 cells

It has been previously suggested that an increase in cell size under hyperosmotic conditions could be solely responsible for the increase in specific productivity. While this is unlikely to be true for this study (based on cell size estimation carried out by a previous study – see

section 4.4), a more detailed analysis into the relationship between cell sizes and specific productivities at different culture phases and different osmolarities would be beneficial in determining the extent to which the volume of cells actually affect antibody production.

In this study, the underlying reason for improvement in antibody productivity under hyperosmotic conditions has been attributed to an increase in the specific transcription rates. Additionally, experimental observations suggested that mRNA stability decreased under hyperosmotic conditions, while the increases in specific translation rates were relatively small and not sustainable compared to the increase in transcription rates. Possible strategies to improve antibody production yield further should therefore focus on a number of areas: firstly, methods to overcome the specific translation rate limits are likely to result in higher specific productivities. Secondly, increasing the stability of the mRNA molecules will result in higher intracellular IgG mRNA concentrations and possibly allow for further improvements in antibody productivities. Thirdly, strategies aimed at alleviating the cell growth suppression under hyperosmotic conditions will also lead to increased total antibody titre.

Increasing specific translation rates

In Section 4.1.3, it was found that hyperosmolarity did not increase cellular energy levels substantially despite an increase in specific glucose consumption. The higher yield of lactate per mole of glucose consumed suggested that cells had the tendency to shift to less efficient energy producing pathways at hyperosmotic conditions. The possibility of this hypothesis was substantiated by a similar observation made by Devin et al. [1995], who had reported a reduction in oxidative phosphorylation efficiency (given by [ATP]/[O]) at hyperosmotic conditions in the mitochondria of rat liver cells. A more detailed analysis of the metabolic pathway shift should therefore be carried out and the possibility of shifting the metabolic pathways of hyperosmotic cells towards more energy-efficient pathways should be investigated, as this may lead to increased ATP production and therefore a rise in total protein translation rates, which will then increase specific productivities. Subsequently, the combination of nutrient feeding strategies with use of hyperosmotic culture conditions will also contribute towards the achievement of higher specific productivities.

Another strategy to improve specific translation rates involves the overexpression of translation-inducing genes for hyperosmotically grown cells. For example, recent work has been carried out on creating an expression vector that led to enhancement of the mRNA translation of the transfected gene when incorporated in HeLa human fibroblast, CEM-A human T and 293 human embryonic kidney cells. This was achieved by the addition of a 5'-terminal post-transcriptional control element (PCE) onto the vector prior to cell transfection [Yilmaz, 2006]. The authors reported that the combination of PCE with the CMV IE transcription enhancer resulted in an 11- to 17-fold increase in protein yield for the various cell lines. The creation of such vectors will thus contribute greatly towards overcoming the upper limits of possible specific translation rates.

Improvement of mRNA stability

Another approach to increasing specific antibody productivities is to develop a strategy aimed at reducing the relative mRNA instability observed under hyperosmotic conditions and therefore increasing the number of mRNA transcripts in the cell. Currently, it is known that the determination of mRNA stability lies mainly in its 3' untranslated region (3'-UT), where the mRNA half-life is dependent on several factors [Ross, 1995]. One of the key determinants is the number of AU-rich elements (AURE) present in this region – the larger the number of AURE, the more unstable the mRNA becomes [Hollams et al., 2002]. Therefore, by changing the sequence of this 3'-UT region, it may be possible to improve the stability of IgG mRNA; for instance, it was found that β-globulin lacking AURE were four times more stable than those containing AURE [Ross, 1995]. Additionally, it is also known that a number of hormones, growth factors and ions affect mRNA stability; however, at present, very little is known about the mechanism through which they affect mRNA stability. While some of these factors (phorbol esters) appear to affect the half-lives of most mRNA molecules, other factors like estrogen stabilises some mRNA while simultaneously destabilising other mRNA in the same cell type. As such information becomes available, there may be more possibilities in improving the stability of mRNA to obtain higher specific productivities.

Reducing hyperosmotic induced cell suppression effects

Many strategies aimed at reducing the growth suppression effects of hyperomsolarity have been proposed over the years, as summarised in Section 6.1. However, these strategies tended to involve the trade-off between the reduction of growth suppression and achieving a high specific productivity. For instance, the addition of glycine betaine as an osmoprotectant reduced the suppression of cell growth but also resulted in a simultaneous decrease in specific productivities [Kim et al., 2000; Ryu et al., 2000]. Similarly, a gradual increase in osmolarity, while alleviating growth suppression, also resulted in a smaller increase in antibody productivities. A more long-term solution may be to overexpress genes that might reduce the growth suppression effect. At present, the only such approach to reducing cell growth suppression was to transfect cells with a protein belonging to the Bcl-2 family, which reduced apoptotic cell death in hybridoma [Perani et al., 1998] and CHO cells [Kim and Lee, 2000]. A similar approach can be used for the overexpression of genes which are known to participate in the repair of DNA damage caused by high sodium chloride concentration (for instance, Mre11, H2AX and Chk1) [Dmitrieva and Burg, 2005]. This strategy may help shorten the amount of time required for DNA repair to occur, thus leading to reduced G1 cell cycle arrest and improved growth rates in the culture.

Nomenclature

D	total variance for sensitivity indices calculation
$f(x)$	integrable function for sensitivity indices calculation
$f_i(x_i)$	ith order term in integrable function $f(x)$
[GLC]	glucose concentration (mmol L^{-1})
$[GLC]_{min}$	minimum threshold glucose concentration (mmol L^{-1})
[H], [L]	concentrations of free heavy (H) and light (L) chains in the ER (pp chain $cell^{-1}$)
[HL]	concentration of assembly intermediate species in the ER (pp chain $cell^{-1}$)
$[H_2L_2]_{ECM}$	antibody concentration in the medium (mg L^{-1})
$[H_2L_2]_{ER}$	antibody concentration in the ER (molecule $cell^{-1}$)
$[H_2L_2]_G$	antibody concentration in the Golgi complex (molecule $cell^{-1}$)
$K_{d,1}$	minimum specific death rate constant (hr^{-2})
$K_{d,T}$	specific death rate constant correlated to lactate concentration (L $mmol^{-1}$ hr^{-1})
$K_{D,XD}$	specific lysis rate (SCM) (hr^{-1})
k_{ER}	rate constant for antibody transport from ER to Golgi (h^{-1})
k_G	rate constant for antibody transport from Golgi to medium (h^{-1})
K_{GL}	substrate uptake constant for glucose phosphorylation reaction (μmol L $cell^{-1}$)
K_{glc}	Monod constant for glucose (mmol L^{-1})
$K_{glc,1}$	glucose consumption coefficient (mmol L^{-1})
$K_{glc,max}$	maximum glucose consumption coefficient (mmol L^{-1} $cell^{-1}$ hr^{-1})
k_d	specific death rate (hr^{-1})
$k_{d,max}$	maximum specific death rate (hr^{-1})
k_H, k_L	degradation rates of heavy and light chain mRNA molecules (hr^{-1})
k_{HH}	H-H chain assembly rate constant (cell $molecule^{-1}$ h^{-1})
k_{HL}	H-L chain assembly rate constant (cell $molecule^{-1}$ h^{-1})
$K_{I,LAC}$	Growth inhibition constant by lactate (SCM) (μmol L $cell^{-1}$)
$k_{l,1}$	specific lysis rate correlated to k_d (dimensionless)
$k_{l,2}$	apparent lysis rate at $k_d = 0$ (hr^{-1})
k_{lys}	specific cell lysis rate (hr^{-1})
K_{SDR}	specific death rate (SCM) (hr^{-1})

[LAC]	lactate concentration (mmol L^{-1})
m_{glc}	maintenance coefficient for glucose (mmol L^{-1} $cell^{-1}$ h^{-1})
m_{lac}	minimum lactate production rate (mmol L^{-1} $cell^{-1}$ h^{-1})
m_H, m_L	intracellular heavy and light chain mRNA concentrations (mRNA molecule $cell^{-1}$)
MW_{AB}	molecular weight of antibody (SCM) (g)
q_{glc}	specific glucose consumption rate (mmol L^{-1} $cell^{-1}$ h^{-1})
q_{lac}	specific lactate production rate (mmol L^{-1} $cell^{-1}$ h^{-1})
q_{Ab}	specific antibody production rate (mg L^{-1} $cell^{-1}$ h^{-1})
R_{Ab}	rate of antibody assembly in the ER (molecule $cell^{-1}$)
R_H, R_L	consumption rates of heavy and light chains in antibody assembly (chain $cell^{-1}$ h^{-1})
R_{HL}	production rate of antibody intermediate in ER (molecule $cell^{-1}$ h^{-1})
S_H, S_L	specific transcription rates of heavy and light chain mRNA (mRNA molecule h^{-1})
SI_{ind}	individual sensitivity index
SI_{tot}	total sensitivity index
T_H, T_L	specific translation rates of heavy and light polypeptide chains (pp chain (mRNA molecule)$^{-1}$ hr^{-1})
$t_{1/2}$	half-life of heavy and light chain mRNA molecules (hr)
$t_{1/2,\ ER}$	time required for 50% of antibody molecules to be transported from ER to Golgi (hr)
$t_{1/2,\ G}$	time required for 50% of antibody molecules to be transported from Golgi to extracellular medium (hr)
V_{CELL}	volume of cell (SCM) (μL)
$V_{M,AB}$	Michaelis-Menten maximum rate term for antibody formation (SCM) (μmol L $cell^{-1}$ hr^{-1})
$V_{M,CELL}$	Michaelis-Menten maximum rate term for cell formation (SCM) (μmol L $cell^{-1}$ hr^{-1})
$V_{M,GL}$	Michaelis-Menten maximum rate term for glucose phosphorylation (SCM) (μmol L $cell^{-1}$ hr^{-1})
$V_{M,GLN}$	Michaelis-Menten maximum rate term for glutamine conversion to glutamate (μmol L $cell^{-1}$ hr^{-1})

$V_{M1,PY}$	Michaelis-Menten maximum rate term for lactate formation (μmol L cell^{-1} hr^{-1})
$V_{M1,SER}$	Michaelis-Menten maximum rate term for Serine-Glycine exchange (μmol L cell^{-1} hr^{-1})
X_d	concentration of dead cells (cells mL^{-1})
X_T	total concentration of cells (cells mL^{-1})
X_v	concentration of viable cells (cells mL^{-1})
$Y_{lac,glc}$	yield of lactate from glucose (mmol mmol^{-1})

Greek letters

μ	specific growth rate (h^{-1})
μ_{max}	maximum specific growth rate (h^{-1})
Σ	summation term
$\int$	integration function

Subscripts

i,j,n,s	any integer equal to or larger than 1

References

Alberts, B., Bray, D., Lewis, J., Raff, M., Roberts, K. and Watson, J. D. (1994). *Molecular Biology of the Cell* (3rd ed.). New York & London: Garland Publishing, Inc.

Atkinson, D. E. (1968). The energy charge of the adenylate pool as a regulatory parameter. Interaction with feedback modifiers. *Biochemisty, 7*: 4030-4034.

b2b conference flyer. (2004). *Strategies for monoclonal antibody therapy 2004: Therapeutic applications, products in clinical trials and future outlook.* Visiongain. Available: http://www.b2b-conferences.com/b2bsite/Site%20Folder/PDF_FILES/monoclonal%20SALES.pdf.

Babu, C. V. S., Yoon, S., Nam, H.-S. and Yoo, Y. S. (2004). Simulation and sensitivity analysis of phosphorylation of EGFR signal transduction pathway in PC12 cell model. *Syst. Biol., 1*: 213-221.

Bailey, J. E. (1998). Mathematical modeling and analysis in biochemical engineering: Past accomplishments and future opportunities. *Biotechnol. Prog., 14*: 8-20.

Barnes, L. M., Bentley, C. M. and Dickson, A. J. (2000). Advances in animal cell recombinant protein production: GS-NS0 expression system. *Cytotechnology, 32*: 109-123.

Batt, B. C. and Kompala, D. S. (1989). A structured kinetic modeling framework for the dynamics of hybridoma growth and monoclonal antibody production in continuous suspension cultures. *Biotech. Bioeng. , 34*: 515-531.

Berg, T. M., Oyaas, K. and Levine, D. W. (1991). Betaine will protect hybridoma cells from hyperosmotic stress. *Biotechnol. Tech., 5*: 179-182.

Bibila, T. A. (1991). *A structured kinetic model for monoclonal antibody synthesis and secretion by mouse hybridoma cells.* Ph.D. Thesis, University of Minnesota.

Bibila, T. A. and Flickinger, M. C. (1991a). A structured model for monoclonal antibody synthesis in exponentially growing and stationary phase hybridoma cells. *Biotechnol. Bioeng., 37*: 210-226.

Bibila, T. A. and Flickinger, M. C. (1991b). A model of interorganelle transport and secretion in mouse hybridoma cells. *Biotechnol. Bioeng., 38*: 767-780.

Bibila, T. A. and Flickinger, M. C. (1992a). Use of a structured kinetic model of antibody synthesis and secretion for optimisation of antibody oriduction systems: I. Steady-state analysis. *Biotech. Bioeng. , 39*: 251-261.

Bibila, T. A. and Flickinger, M. C. (1992b). Use of a structured kinetic model of antibody synthesis and secretion for optimisation of antibody production systems: II. Transient analysis. . *Biotech. Bioeng. , 39*: 262-272.

Bibila, T. A. and Robinson, D. K. (1995). In pursuit of the optimal fed-batch process for monoclonal antibody production. *Biotech. Prog. , 11*: 1-13.

Birch, J. (2005). The importance of developing a high yield of product. *Presented at European Antibody Congress 2005*, Lyon, France.

Birch, J. R. and Racher, A. J. (2006). Antibody production. *Adv. Drug Del. Rev., 58*: 671-685.

Bogner, P., Sipos, K., Ludany, A., Somogyi, B. and Miseta, A. (2004). Steady-state volumes and metabolism-independent osmotic adaptation in mammalian erythrocytes. *Eur. Biophys. J., 31*: 145-152.

Bolster, D. R., Crozier, S. J., Kimball, S. R. and Jefferson, L. S. (2002). AMP-activated protein kinase suppresses protein synthesis in rate skeletal muscle through down-regulated mammalian target of rapamycin (mTOR) signaling. *J. Biol. Chem., 277*: 23977-23980.

Bond, J. E. (2004). *Investigation of the dynamic relationship between extracellular and intracellular pH in GS-NS0 cell culture*. Ph.D. Thesis, Imperial College London.

Butler, M. and Spier, R. E. (1984). The effects of glutamine utilisation and ammonia production on the growth of BHK cells in microcarrier cultures. *J. Biotechnol. , 1*: 187-196.

Cherlet, M., Kromenaker, S. J. and Srienc, F. (1995). Surface IgG content of murine hybridomas – Direct Evidence for variation of antibody secretion rates during the cell cycle. *Biotech. Bioeng., 47*: 535-540.

Cherlet, M. and Marc, A. (1999). Hybridoma cell behaviour in continuous culture under hyperosmotic stress. *Cytotechnology, 29*: 71-84.

Choi, Y. S., Knopf, P. M. and Lennox, E. S. (1971). Intracellular transport and secretion of an immunoglobulin light chain. *Biochemistry, 10*: 668-679.

Chu, L. and Robinson, D. K. (2001). Industrial choices for protein production by large-scale cell culture. *Curr. Op. Biotechnol., 12*: 180–187.

Chung, J., Zabel, C., Sinskey, A. J. and Stephanopoulos, G. (1997). Extension of Sp2/0 hybridoma cell viability through interleukin-6 supplementation. *Biotech. Bioeng. , 55*: 439-446.

Cowan, N. J., Secher, D. S. and Milstein, C. (1974). Intracellular immunoglobulin chain synthesis in non-secreting variants of a mouse myeloma: detection of inactive light-chain messenger RNA. *J. Mol. Biol., 90*: 691-701.

Cruz, P. E., Almeida, H. S., Murphy, P. N., Moreira, J. L. and Carrondo, J. T. (2000). Modeling retrovirus production for gene therapy. 1. Determination of optimal bioreaction mode and harvest strategy. *Biotechnol. Prog., 16*: 213-221.

Dahn, M. S., Hsu, C. J., Lange, M. P., Kimball, S. R. and Jefferson, L. S. (1993). Factors affecting secretory protein-production in primary cultures of rat hepatocytes. *Proc. Soc. Expt. Biol. Med., 203*: 38-44.

Dalili, M. and Ollis, D. F. (1988). The influence of cyclic nucleotides on hybridoma growth and monoclonal antibody production. . *Biotech. Lett. , 10*: 781-786.

Dalili, M., Sayles, G. D. and Ollis, D. F. (1990). Glutamine-limited batch hybridoma growth and antibody production: experiment and model *Biotech. Bioeng., 36*: 74-82.

de Petris, S. (1970). Electron microscopy of polyribosomes synthesizing immunoglobulin chains. *Biochem. J., 118*: 385-389.

de Tremblay, M., Perrier, M., Chavarie, C. and Archambault, J. (1992). Optimization of fed-batch culture of hybridoma cells using dynamic programming: single and multi feed case. *Bioprocess Eng., 7*: 229-234.

Devin, A., Guerin, B. and Rigoulet, M. (1996). Dependence of flux size and efficiency of oxidative phosphorylation on external osmolarity in isolated rate liver mitochondria: role of adenine nucleotide carrier. *Biochim. Biophys. Acta - Bioenergetics, 1273*: 13-20.

Dhir, S., Morrow Jr., K. J., Rhinehart, R. R. and Wiesner, T. (2000). Dynamic optimization of hybridoma growth in a fed-batch bioreactor. *Biotech. Bioeng., 67*: 197-205.

DiMasi, D. and Swartz, R. W. (1995). An energetically structured model of mammalian cell metabolism. 1. Model development and application to steady-state hybridoma cell growth in continuous culture. *Biotechnol. Prog., 11*: 684-676.

Dimitrieva, N. I. and Burg, M. B. (2005). Hypertonic stress response. *Mutat. Res., 569*: 65-74.

Dorner, A. and Kaufman, R. J. (1994). Thelevels of endoplasmic reticulum proteins and ATP affect folding and secretion of selective proteins. *Biologicals, 22*: 103-112.

Dorner, A. J. and Kaufman, R. J. (1990). Analysis of synthesis, processing, and secretion of proteins expressed in mammalian cells. *Meth. Enzymol. , 185*: 577-596.

Dorner, A. J., Wasley, L. C. and Kaufman, R. J. (1992). Overexpression of GRP78 mitigates stress induction of glucose regulated proteins and blocks secretion of selective proteins in chinese-hamster ovary cells. *EMBO J., 11*: 1563-1571.

Downham, M. R., Farrell, W. E. and Jenkins, H. A. (1996). Endoplasmic reticulum protein expression in recombinant NS0 myelomas grown in batch culture. *Biotech Bioeng, 51*: 691-696.

Duncan, P. J., Jenkins, H. A. and Hobbs, G. (1997). The effect of hyperosmotic conditions on growth and recombinant protein expression by NS0 myeloma cells in culture. *Genet. Eng. Biotechnol., 17*: 75-78.

Duncan, R. F. and Hershey, J. W. B. (1987). Initiation factor protein modifications and inhibition of protein synthesis. *Mol. Cell. Biol., 7*: 1293-1295.

Dutton, R. L., Scharer, J. M. and Moo-Young, M. (1998). Descriptive parameter evaluation in mammalian cell culture. *Cytotechnology 26*: 139-152.

Elliott, W. H. (1951). Studies on the enzymic synthesis of glutamine *Biochem. J., 49*: 106-112.

Enden, G., Zhang, Y. H. and Merchuk, J. C. (2005). A model of hte dynamics of insect cell infection at low multiplicity of infection. *J. Theor. Biol., 237*: 257-264.

Faraday, D. B. F., Hayter, P. and Kirkby, N. F. (2001). A mathematical model of the cell cycle of a hybridoma cell line. *Biochem. Eng. J. , 7*: 49-68.

Fox, S. R., Tan, H. K., Tan, M. C., Wong, S. C. N. C., Yap, M. G. S. and Wang, D. I. C. (2005). A detailed understanding of the enhanced hypothermic productivity of interferon-gamma by Chinese-hamster ovary cells. *Biotechnol. Appl. Biochem., 41*: 255-264.

Frahm, B., Lane, P., Markl, H. and Portner, R. (2003). Improvement of a mammalian cell culture process by adaptive, model-based dialysis fed-batch cultivation and suppression of apoptosis. *Bioprocess Biosyst. Eng., 26*: 1-10.

Frame, K. K. and Hu, W. S. (1991). Kinetic study of hybridoma cell growth in continuous culture. II. Behaviour of producers and comparison to nonproducers. *Biotech. Bioeng., 38*: 1020-1028.

Fries, E., Gustafsson, L. and Peterson, P. A. (1984). 4 secretory protiens synthesized by hepatocytes are transported from endoplasmic-reticulum to golgi-complex at different rates. *EMBO J., 3*: 147-152.

Fussenegger, M. and Bailey, J. E. (1998). Molecular regulation of cell-cycle progression and apoptosis in mammalian cells: Implications for biotechnology. *Biotechnol. Prog., 14*.

Galfre, G. and Milstein, C. (1981). Preparation of monoclonal antibodies: strategies and procedures In J. J. Langone & H. V. Vunakis (Eds.), *Methods in Enzymology* (Vol. 73, pp. 3-46): Academic Press.

Gething, M. J. and Sambrook, J. (1992). Protein folding in the cell. *Nature, 355*: 33-45.

Glacken, M. W., Huang, C. and Sinskey, A. J. (1989). Mathematical descriptions of hybridoma culture kinetics. III. Simulation of fed-batch bioreactors. *J. Biotechnol., 10*: 39-66.

Gonzalez, R., Andrews, B. A. and Asenjo, J. A. (2002). Kinetic model of BiP- and PDI-mediated protein folding and assembly. *J. Theor. Biol.*, *214* 529-537.

Gonzalez, R., Asenjo, J. A. and Andrews, B. A. (2001). Metabolic control analysis of monoclonal antibody synthesis. *Biotechnol. Prog., 17*: 217-226.

Goochee, C. F. and Monica, T. (1990). Environmental effects on protein glycosylation. *Bio/Technology, 8*: 421-427

Hauser, H. (1997). Heterologous expression of genes in mammalian cells. In Hauser H & Wagner R (Eds.), *Mammalian cell biotechnology in protein production* (pp. 3-32). Berlin: Walter de Gruyter.

Hayter, P. M., Kirkby, N. F. and Spier, R. E. (1992). Relationship between hybridoma growth and monoclonal antibody production. *Enzyme Microb. Tech., 14*: 454-461.

Horibata, K. and Harris, A. W. (1970). Mouse myelomas and lymphomas in culture. *Exp. Cell Res., 60*: 61-77.

Hsu, L. C., Constable, D. J. C., Orvos, D. R. and Hannah, R. E. (1995). Comparison of high-performance liquid chromatography and capillary zone electrophoresis in penciclovir biodegradation kinetic studies. *J. Chromatogr. B, 665*: 85-92.

Hucul, J. A., Henshaw, E. C. and Young, D. A. (1985). Nucleoside diphosphate regulation of overall rates of protein biosynthesis acting at the level of initiation. *J. Biol. Chem., 260*: 15585-15591.

Jacquez, J. A. (1998). Design of experiments. *J. Franklin Inst., 335B*: 259-279.

Jang, J. D. and Barford, J. P. (2000). An unstructured kinetic model of macromolecular metabolism in batch and fed-batch cultures of hybridoma cells producing monoclonal antibody. *Biochem. Eng. J., 4*: 153-168.

Ji, S., Chai, Y., Wu, Y., Yin, X., Liang, D., Xu, Z. and Li, X. (1999). Determination of ferulic acid in *Angelica sinensis* and *Chuanxiong* by capillary zone electrophoresis. *Biomed. Chromatogr., 13*: 333-334.

Jorgensen, P. and Tyers, M. (2004). How cells coordinate growth and division. *Curr. Biol., 14*: R1014-R1027.

Kaloff, C. R. and Haas, I. G. (1995). Coordination of immunoglobulin chain folding and immunoglobulin chain assembly is essential for the formation of functional IgG. *Immunity, 2*: 629-637.

Kaufmann, H., Mazur, X., Fussenegger, M. and Bailey, J. E. (1999). Influence of low temperature on productivity, proteome and protein phosphorylation of CHO cells. *Biotechnol. Bioeng., 63*: 573-582.

Kaulich, M., Qurishi, R. and Muller, C. E. (2003). Extracellular metabolism of nucleotides in neuroblastoma x glioma NG108-15 cells determined by capillary electrophoresis. *Cell. Mol. Neurobiol., 23*: 349-364.

Kim, M. S., Kim, N. S., Sung, Y. H. and Lee, G. M. (2002). Biphasic culture strategy based on hyperosmotic pressure for improved humanized antibody production in chinese hamster ovary cell culture. *In Vitro Cell. Dev. Biol. - Animal, 38*: 314-319.

Kim, N. S. and Lee, G. M. (2002). Response of recombinant chinese hamster ovary cells to hyperosmotic pressure: effect of Bcl-2 overexpression. *J. Biotechnol., 95*: 237-248.

Kim, T. K., Ryu, J. S., Chung, J. Y., Kim, M. S. and Lee, G. M. (2000). Osmoprotective effect of glycine betaine on thrombopoietin production in hyperosmotic chinese hamster ovary cell culture: Clonal variations. *Biotechnol. Prog., 16*: 775-781.

Kohler, G. and Milstein, C. (1976). Derivation of specific antibody-producing tissue culture and tumor lines by cell fusion. *Eur. J. Immunol. , 6*: 292-295.

Kontoravdi, C., Asprey, S. P., Pistikopoulos, E. N. and Mantalaris, A. (2005). Application of global sensitivity analysis to determine goals for design of experiments: An example study on antibody-producing cell cultures. *Biotechnol. Prog., In press.*

Kultz, D., Madhany, S. and Burg, M. B. (1998). Hyperosmolality causes growth arrest of murine kidney cells. *J. Biol. Chem., 273*: 13645-13651.

Lambert, N. and Merten, O. W. (1997). Effect of Serum-Free and Serum-Containing Medium on Cellular Levels of ER-Based Proteins in Various Mouse Hybridoma Cell Lines. . *Biotech. Bioeng. , 54*: 165-180.

Laskov, R. and Scharff, M. D. (1974). Independent synthesis of light and heavy chains. *J. Exp. Med., 140*: 1112-1116.

Lavric, V., Ofiteru, I. D. and Woinaroschy, A. (2005). A sensitivity analysis of the fed-batch animal-cell bioreactor with respect to some control parameters. *Biotechnol. Appl. Biochem., 41*: 29-35.

Lavric, V., Ofiteru, I. D. and Woinaroschy, A. (2006). Continuous hybridoma bioreactor: sensitivity analysis and optimal control. *Biotechnol. Appl. Biochem., 44*: 81-92.

Lee, M. S. and Lee, G. M. (2000). Hyperosmotic pressure enhances immunoglobulin transcription rates and secretion rates of KR12H-2 transfectoma. *Biotechnol. Bioeng., 68*: 260-268.

Lee, Y.-K., Brewer, J. W., Hellman, R. and Hendershot, L. M. (1999). BiP and immunoglobulin light chain cooperate to control the folding of heavy chain and ensure the fidelity of immunoglobulin assembly. *Mol. Biol. Cell, 10*: 2209-2219.

Leitzgen, K., Knittler, M. R. and Haas, I. G. (1997). Assembly of immunoglobulin light chains as a prerequisite for secretion. *J. Biol. Chem., 272*: 3117-3123.

Leno, M., Merten, O. W. and Hache, J. (1992). Kinetic studies of cellular metbolic activity, specific IgG production rate, IgG mRNA stability and accumulation during hybridoma batch culture. *Enzyme Microb. Tech. , 14*: 135-140.

Lewin, B. (2000). *Genes VII* (1st ed.). New York: Oxford University Press.

Lin, J., Takagi, M., Qu, Y., Gao, P. and Yoshida, T. (1999a). Metabolic flux change in hybridoma cells under high osmotic pressure. *J. Biosci. Bioeng., 87*: 255-257.

Lin, J., Takagi, M., Qu, Y., Gao, P. and Yoshida, T. (1999b). Enhanced monoclonal antibody production by gradual increase of osmotic pressure. *Cytotechnolgy, 29*: 27-33.

Linardos, T. I., Kalogerakis, N. and Behie, L. A. (1991). The effect of specific growth rate and death rate on monoclonal antibody production in hybridoma chemostat cultures *Can. J. Chem. Eng., 69*: 429-438.

Ljung, L. and Glad, T. (1994). On the global identifiability for arbitrary model parameterizations *Automatica, 30*: 265-276.

Lloyd, D., Holmes, P., Jackson, L. P., Emery, N. and Al-Rubeai, M. (2000). Relationship between cell size, cell cycle and specific recombinant protein productivity. *Cytotechnology, 34*: 59-70.

Lodish, H. F. (1988). Transport of secretory and membrane-glycoproteins from the rough endoplasmic-reticulum to the golgi - a rate-limiting step in protein maturation and secretion. *J. Biol. Chem., 263*: 2107-2110.

Lonza Press Release. (1998). *Lonza's glutamine synthetase expression system used in production of Hoffmann-La Roche's Zenapax ®.* Available: http://www.lonza.com/group /en/news/archive/news98/lonza3.html.

Lonza Press Release. (1998a). *Lonza's glutamine synthetase expression system used in production of Hoffmann-La Roche's Zenapax ®.* Available: http://www.lonza.com/group /en/news/archive/news98/lonza3.html.

Lonza Press Release. (1998b). *Lonza Biologics announces that MedImmune Inc.'s Synagis ™ becomes the second therapeutic monoclonal antibody to be produced using the glutamine synthetase expression system.* Available: http://www.lonza.com/group/en/news/ archive/news98/lonza1.html.

Mainwaring, D. O., Maxwell, A., Rendall, M. H., Blewett, J. M., Racher, A. J. and Wayte, J. R. T. (2002). Development of Improved Chemically Defined Mammalian Cell Fermentation Processes. . *Presented at 224th ACS National Meeting*, Boston, USA.

Malda, J., Rouwkema, J., Martens, D. E., le Comte, E. P., Kooy, F. K., Tramper, J., van Blitterswijk, C. A. and Riesle, J. (2004). Oxygen gradients in tissue-engineered PEGT/PBT cartilaginous constructs: Measurement and modeling. *Biotech. Bioeng., 86*: 9-18.

McKinney, K. L., Dilwith, R. and Belfort, G. (1995). Optimizing antibody-production in batch hybridoma cell-culture. *J. Biotechnol., 40*: 31-48.

Mercille, S. and Massie, B. (1998). Apoptosis-resistant NS/0 E1B-19K myelomas exhibit increased viability and chimeric antibody productivity under cell cycle modulating conditions. *Cytotechnology, 28*: 189-203.

Merten, O. W., Moeurs, D., Keller, H., Leno, M., Palfi, G. E., Cabanie, L. and Couve, E. (1994). Modified monoclonal antibody production kinetics, kappa/gamma mRNA levels, and metabolic activities in a murine hybridoma selected by continuous culture. *Biotech. Bioeng.*, *44*: 753-764.

Miller, W. M., Wilke, C. R. and Blanch, H. W. (1987). Effects of dissolved oxygen concentration on hybridoma growth and metabolism in continuous culture. *J. Cell Physiol.*, *132*: 524-530.

Miller, W. M., Wilke, C. R. and Blanch, H. W. (1988a). A kinetic analysis of hybridoma growth and metabolismin batch and continuous suspension culture: Effect of nutrient concentration, dilution rate, and pH. *Biotech. Bioeng., 32*: 947-965.

Miller, W. M., Wilke, C. R. and Blanch, H. W. (1988b). Transient responses of hybridoma metabolism to changes in the oxygen supply rate in continuous culture. *Bioproc. Eng.* , *3*: 103-111.

Miller, W. M., Wilke, C. R. and Blanch, H. W. (1989a). Transient responses of hybridoma cells to nutrient additions in continous culture: I. Glucose pulse and step changes. *Biotech. Bioeng., 33*: 477-486.

Miller, W. M., Wilke, C. R. and Blanch, H. W. (1989b). Transient responses of hybridoma cells to nutrient additions in continous culture: II. Glutamine pulse and step changes. *Biotech. Bioeng., 33*: 487-499.

Monica, T. J., Andersen, D. C. and Goochee, C. F. (1997). A mathematical model of sialylation of N-linked oligosaccharides in the trans-Golgi network. *Glycobiology, 7*: 515-521.

Monod, J. (1949). The growth of bacterial cultures. *Ann. Rev. Microbiol., 3*: 371-394.

Mutalik, V. K., Singh, A. P., Edwards, J. S. and Venkatesh, K. V. (2004). Robust global sensitivity in multiple enzyme cascade system explains how the downstream cascade structure may remain unaffected by cross-talk. *FEBS Lett., 558*: 79-84.

Ng, M., Blaschke, T. F., Arias, A. A. and Zare, R. N. (1992). Analysis of free intracellular nucleotides using high-performance capillary electrophoresis. *Anal. Chem., 64*: 1682-1684.

Niki, I., Ashcroft, F. M. and Ashcroft, S. J. H. (1989). The dependence on intracellular ATP concentration of ATP-sensitive K-channels and of Na,K-ATPase in intact HIT-T15β-cells. *FEBS Lett., 257*: 361-364.

Nuss, D. L. and Koch, G. (1976). Variation in the relative synthesis of immunoglobulin G and non-immunoglobulin G proteins in cultured MPC-11 cells with changes in the overall rate of polypeptide chain initiation and elongation. *J. Mol. Biol., 102*: 601-612.

Nyberg, K. A. (2002). Toward maintaining the genome: DNA damage and replication checkpoints. *Ann. Rev. Genetics, 36*: 617-656.

Oh, S. K. W., Chua, F. K. F. and Choo, A. B. H. (1995). Intracellular response of productive hybridomas subjected to high osmotic pressure. *Biotechnol. Bioeng., 46*: 525-535.

Oh, S. K. W., Vig, P., Chua, F., Teo, W. K. and Yap, M. G. S. (1993). Substantial overproduction of antibodies by applying osmotic pressure and sodium butyrate. *Biotechnol. Bioeng., 42*: 601-610.

Oyaas, K., Ellingsen, T. E., Dyrset, N. and Levine, D. W. (1994). Utilisation of osmoprotective compounds by hybridoma cells exposed to hyperosmotic stress. *Biotechnol. Bioeng., 43*: 77-89.

Ozturk, S. S. and Palsson, B. O. (1991a). Growth, metabolic, and antibody-production kinetics of hybridoma cell culture. 2. Effects of serum concentration, dissolved oxygen concentration and medium pH in a batch reactor. *Biotechnol. Prog., 7*: 481-494.

Ozturk, S. S. and Palsson, B. O. (1991b). Effect of medium osmolarity on hybridoma growth, metabolism, and antibody production. *Biotechnol. Bioeng., 37*: 989-993.

Pastor-Anglada;, Felipe, A., Casado, F. J., Ferrer-Martinez, A. and Gomez-Angelats, M. (1996). Long-term osmotic regulation of amino acid transport systems in mammalian cells. *Amino Acids, 11.*

Pendse, G. J. and Bailey, J. E. (1990). Effects of growth factors on cell proliferation and monoclonal antibody production of batch hybridoma cultures. *Biotech. Lett., 7*: 487-492.

Pendse, G. J., Karkare, S. and Bailey, J. E. (1992). Effect of cloned gene dosage on cell growth and hepatitis-B surface antigen synthesis and in recombinant CHO cells. *Biotech. Bioeng. , 40*: 119-129.

Percy, J. R., Percy, M. E. and Dorrington, K. J. (1975). A theoretical model for the covalent assembly of immunoglobulins. *J. Biol. Chem., 250*: 2398-2400.

Pestova, T. V. and Hellen, C. U. T. (2000). The structure and function of initiation factors in eukaryotic protein synthesis. *Cell. Mol. Life Sci., 57*: 651-674.

Petersen, J. G. L. and Dorrington, K. J. (1974). An in Vitro System for Studying the Kinetics of Intechain Disulfide Bond Formation in Immunoglobulin G. *J. Biol. Chem. , 249*: 5633-5641.

Portner, R. and Schafer, T. (1996). Modelling hybridoma cell growth and metabolism - a comparison of selected models and data. *J. Biotechnol., 49*: 119-135.

Potter, M. (1972). Immunoglobulin-producing tumors and myeloma proteins of mice. *Physiol. Rev., 52*: 631-719.

Potter, M., Appella, E. and Geisser, S. (1965). Variations in the heavy polypeptide chain structure of gamma myeloma immunoglobulins from an inbred strain of mice and a hypothesis as to their origin. *J. Mol. Biol., 14*: 361-372.

Potter, M. and Boyce, C. R. (1962). Induction of plasma cell neoplasma in strain BALB/c mice with mineral oil and mineral oil adjuvants. *Nature, 193*: 1086-1087.

Process Systems Enterprise Ltd. (2002). *gPROMS Introductory User Guide*. UK.

Provost, A. and Bastin, G. (2004). Dynamic metabolic modelling under the balanced growth condition. *J. Process Contr., 14*: 717-728.

Radisic, M., Malda, J., Epping, E., Geng, W., Langer, R. and Vunjak-Novakovic, G. (2005). Oxygen gradients correlate with cell density and cell viability in engineered cardiac tissue. *Biotech. Bioeng., 93*: 332-343.

Ramasamy, R., Munro, A. and Milstein, C. (1974). Possible role for the Fc receptor on B lymphocytes. *Nature 249*: 573-574.

Ransohoff, T. C., Mittendorff II, R. E. and Levine, H. L. (2004). Forecasting Industrywide Biopharmaceutical Manufacturing Capacity Requirements. *Advances in Large Scale BioManufacturing and Scale-Up Production, October issue.*

Reichert, J. M., Rosensweig, C. J., Faden, L. B. and Dewitz, M. C. (2005). Monoclonal antibody successes in the clinic. *Nature Biotechnology, 23*: 1073-1078.

Reitzer, L. J., Wice, B. M. and Kennell, D. (1979). Evidence that glutamine, not sugar, is the major energy source for HeLa cells. *J. Biol. Chem. , 254*: 2669-2676.

Robinson, A. S. and Lauffenburger, D. A. (1996). Model for ER chaperone dynamics and secretory protein interactions. *AIChE J. , 42*: 1443-1553.

Rodrigues, M. T. A., Vilaca, P. R., Garbuio, A., Takagi, M., Barbosa Jr, S., Leo, P., Laignier, N. S., Silva, A. A. P. and Moro, A. M. (1999). Glucose uptake rate as a tool to estimate hybridoma growth in a packed bed bioreactor. *Bioproc. Eng., 21*: 543-546.

Rullmann, J. A. C., Struemper, H., Defranoux, N. A., Ramanujan, S., Meeuwisse, C. M. L. and van Elsas, A. (2005). System biology for battling rheumatoid arthritis: Application of the Entelos Physiolab platform.

Ryu, J. S., Kim, T. K., Chung, J. Y. and Lee, G. M. (2000). Osmoprotective effect of glycine betaine on foreign protein production in hyperosmotic recombinant chinese hamster ovary cell cultures differs among cell lines. *Biotechnol. Bioeng., 70*: 167-175.

Ryu, J. S. and Lee, G. M. (1997). Influence of hyperosmolar basal media on hybridoma cell growth. *Bioproc. Eng., 16*: 305-310.

Ryu, J. S., Lee, M. S. and Lee, G. M. (2001). Effects of cloned gene dosage on the response of recombinant CHO cells to hyperosmotic pressure in regard to cell growth and antibody production. *Biotechnol. Prog., 17*: 993-999.

Sakaguchi, M. (1997). Eukaryotic protein secretion *Curr. Op. Biotechnol., 8*: 595-601.

Saltelli, A. (2000). What is sensitivity analysis? In A. Saltelli & K. Chan & E. M. Scott (Eds.), *Sensitivity Analysis* (pp. 3-13). Chichester: John Wiley & Sons, Ltd.

Saltelli, A., Tarantola, S., Campolongo, F. and Ratto, M. (2004). *Sensitivity analysis in practice.* Chichester: John Wiley & Sons, Ltd.

Sanderson, C. S. (1997). *The development and application of a structured model for animal cell metabolism.* Ph.D. Thesis, University of Sydney, Australia.

Sanderson, C. S., Barford, J. P. and Barton, G. W. (1999). A structured, dynamic model for animal cell culture systems. *Biochem. Eng. J., 3*: 203-211.

Santos, B. C., Pullman, J. M., Chevaile, A., Welch, W. J. and Gullans, S. R. (2003). Chronic hyperosmolarity mediates constitutive expression of molecular chaperones and resistance to injury. *Am. J. Physiol. Renal. Physiol., 284*: F564-F574.

Savage, A. (1997). Glycosylation: A Post-Translational Modification. In H. Wagner & R. Wagner (Eds.), *Mammalian Cell Biotechnology in Protein Production* (pp. 233-276). Berlin: Walter de Gruyter.

Schibler, U., Marcu, K. B. and Perry, R. P. (1978). Synthesis and processing of the messenger-RNAs specifying heavy and light chain immunoglobulins in MPC-11 cells. *Cell, 15*: 1495-1509.

Schiek, R. L. and May, E. E. (2005). Examining tissue differentiation stability through large scale, multi-cellular pathway modeling. *Nanotech 2005.*

Schlatter, S., Stansfield, S. H., Dinnis, D. M., Racher, A. J., Birch, J. R. and James, D. C. (2005). On the optimal ratio of heavy to light chain genes for efficient recombinant antibody production by CHO cells. *Biotechnol. Prog., 21*: 122-133.

Schneider, M., Marison, I. W. and von Stockar, U. (1996). The importance of ammonia in mammalian cell culture. *J. Biotechnol., 46*: 161-185.

Schroder, M., Korner, C. and Friedl, P. (1999). Quantitative analysis of transcription and translation in gene amplified chinese hamster ovary cells on the basis of a kinetic model. *Cytotechnology, 29*: 93-102.

Seifert, D. B. and Phillips, J. A. (1999). The production of monoclonal antibody in Growth-arrested hybridomas cultivated in suspension and immobilised modes. *Biotechnol. Prog., 15*: 655-666.

Shapiro, A. L., Scharff, M. D., Maizel Jr., J. V. and Uhr, J. W. (1966). Polyribosomal synthesis and assembly of the H and L chains of gamma globulin. *Proc. Natl. Acad. Sci., 56*: 216-221.

Shusta, E. V., Raines, R. T., Pluckthun, A. and Wittrup, K. D. (1998). Increasing the secretory capacity of Saccharomyces cerevisiae for production of single-chain antibody fragments. *Nat. Biotechnol., 16*: 773-777.

Sidoli, F. R., Mantalaris, A. and Asprey, S. P. (2004). Modelling of mammalian cells and cell culture processes. *Cytotechnology, 44*: 27-46.

Sidoli, F. R., Mantalaris, A. and Asprey, S. P. (2005). Toward global parametric estimability of a large-scale kinetic single-cell model for mammalian cell cultures. *Ind. Eng. Chem. Res., 44*: 868-878.

Simpson, N. H., Singh, R. P., Perani, A., Goldenzon, C. and Al-Rubeai, M. (1998). In hybridoma cultues, deprivation of any single amino acid leads to apoptotic death, which is suppressed by the expression of the bcl-2 gene. *Biotech. Bioeng. , 59*: 90-98.

Sobol', I. M. (2001). Global sensitivity indices for nonlinear mathematical models and their Monte Carlo estimates. *Math. Comput. Simulat., 55*: 271-280.

Sun, Z. (2000). *Cellular mechanisms of the hyperosmotic stress response of hybridoma cells.* Ph.D. Thesis, University of Toledo.

Sun, Z., Zhou, R., Laing, S., McNeeley, K. M. and Sharfstein, S. T. (2004). Hyperosmotic stress in murine hybridoma cells: effects on antibody transcription, translation, posttranslational processing, and the cell cycle. *Biotechnol. Prog., 20*: 576-589.

Suzuki, E. and Ollis, D. F. (1989). Cell cycle model for antibody production kinetics. *Biotech. Bioeng., 34*: 1398-1402.

Szewczyk, A. and Pikula, S. (1998). Adenosine 5'-triphosphate: an intracellular metabolic messenger. *Biochim. Biophys. Acta - Bioenergetics, 1365*: 333-353.

Takagi, M., Hayashi, H. and Yoshida, T. (2000). The effect of osmolarity on metabolism and morphology in adhesion and suspension chinese hamster ovary cells producing tissue plasminogen activator. *Cytotechnology 32*: 171-179.

Thorens, B. and Vassalli, P. (1986). Chloroquine and ammonium-chloride prevent terminal glycosylation of immunoglobulins in plasma-cells without affecting secretion. *Nature, 321*: 618-620.

Turanyi, T. and Rabitz, H. (2000). Local methods. In A. Saltelli & K. Chan & E. M. Scott (Eds.), *Sensitivity analysis* (pp. 81-99). Chichester: John Wiley & Sons, Ltd.

Tzafriri, A. R., Lerner, E. I., Flashner-Barak, M., Hinchcliffe, M., Ratner, E. and Parnas, H. (2005). Mathematical modeling and optimization of drug delivery from intratumorally injected microspheres. *Clin. Cancer Res., 11*: 826-834.

Umana, O. and Bailey, J. E. (1997). A mathematical model of N-Linked glycoform biosynthesis. *Biotech. Bioeng., 55*: 890-908.

Wallach, M. and Laskov, R. (1980). A high production-rate of translatable IgG messenger-RNA accounts for the amplified synthesis of IgG in myeloma cells. *Eur. J. Biochem., 110*: 545-554.

Waters, C. M., Oberg, K. C., Carpenter, G. and Overholser, K. A. (1990). Rate constants for binding, dissociation, and internalization of EGF: Effect of receptor occupancy and ligand concentration. *Biochemistry, 29*: 3563-3569.

Whicher, J. T., Wallage, M. and Fifield, R. (1987). Use of immunoglobulin heavy- and light-chain measurements compared with existing techniques as a means of typing monoclonal immunoglobulins. *Clin. Chem., 33*: 1771-1773.

Wieland, F. T., Gleason, M. L., Serafini, T. A. and Rothman, J. E. (1987). The rate of bulk flow from the endoplasmic reticulum to the cell surface. *Cell, 50*: 289-300.

Wu, M.-H. (2006). *The effect of osmotic pressure on GS-NS0 antibody production cell line.* Ph.D. Thesis, Imperial College London.

Wu, M.-H., Dimopoulos, G., Mantalaris, A. and Varley, J. (2004). The effect of hyperosmotic pressure on antibody production and gene expression in the GS-NS0 cell line. *Biotechnol. Appl. Biochem., 40*: 41–46.

Wu, P., Ray, N. G. and Shuler, M. L. (1992). A single cell model of Chinese hamster ovary cells. *Ann. NY Acad. Sci. , 665*: 152-187.

Wyeth Pharmaceuticals Inc. (2005). *Mylotarg® Label.* Available: http://www.wyeth.com/content/ShowLabeling.asp?id=119.

Yang, X., Oehlert, G. W. and Flickinger, M. C. (1996). Use of the weighted jackknife method to calculate the variance in the cellular-specific protein secretion rate: Application to monoclonal antibody secretion rate kinetics in response to osmotic stress. *Biotech. Bioeng., 50*: 184-196.

Yoon, S. K., Choi, S. L., Song, J. Y. and Lee, G. M. (2004). Effect of culture pH on Erythropoietin production by chinese hamster ovary cells grown in suspension at 32.5 and 37.0°C. *Biotech. Bioeng., 89*: 345-356.

Yoon, S. K., Song, J. Y. and Lee, G. M. (2003). Effect of low culture temperature on specific productivity, transcription level, and heterogeneity of erythropoietin in chinese hamster ovary cells. *Biotechnol. Bioeng., 82*: 289-298.

Zhang, J. and Su, W. W. (2002). Estimation of intracellular phosphate content in plant cell cultures using an extended Kalman Filter. *J. Biosci. Bioeng., 94*: 8-14.

Zhou, R. (2002). *Mechanisms of the increased antibody production in hybridoma cells in response to hyperosmotic stress*
Ph.D. Thesis, University of Toledo.

Zhou, W., Chen, C. C., Buckland, B. and Aunins, J. (1997). Fed-batch culture of recombinant NS0 myeloma cells with high monoclonal antibody production. *Biotech. Bioeng. , 55*: 783-792.

Zhou, Y. H. and Titchener-Hooker, N. J. (1999). Simulation and optimisation of integrated bioprocesses: a case study. *J. Chem. Technol. Biotechnol., 74*: 289-292.

Appendix A

Initial Parameter Values for Hybrid Model

The growth and metabolism parameters are presented in Table A.1 below while the intracellular antibody production and transport parameters are summarized in Table A.2 on the next page.

Parameter	Values used (normal condition)	Values used (hyperosmotic condition)	References
μ_{max}	0.125	0.023	[Wu et al., 2004]
$[GLC]_{min}$	8.2	9.62	
$K_{d,1}$	2.48×10^{-4}	1.89×10^{-5}	
$K_{d,T}$	4.70×10^{-3}	1.10×10^{-3}	
$k_{l,1}$	0.308	0.252	
$k_{l,2}$	2.84×10^{-3}	7.17×10^{-4}	
K_{glc}	46.1	2.81	
$K_{glc,max}$	3.08×10^{-7}	1.06×10^{-4}	
$K_{glc,1}$	1.94×10^{1}	4.56×10^{3}	
m_{glc}	3.16×10^{-8}	4.1×10^{-8}	
m_{lac}	5.91×10^{-8}	-4.5×10^{-8}	
$Y_{lac,glc}$	0.968	2	

Table A.1. Growth and metabolism parameters for the hybrid model under normal and hyperosmotic conditions.

Parameter	Reference values	Values used (normal condition)	Values used (hyperosmotic condition)	References
S_H	1200-3600	1500	2100	[Schibler et al., 1978]
S_L	1800-5400	2250	3150	[Bibila, 1991]
$T_{H,0}$	1020	1005	1640	[Bibila, 1991]
$T_{L,0}$	720	715	1123	[Bibila, 1991]
k_{HL}	-	3.8×10^{-10}	1.2×10^{-10}	-
k_{HL}/k_{HH}	11.5	11.5	11.5	[Percy et al., 1975]
$t_{1/2,ER}$	0.5-1	0.7	0.7	[Choi et al., 1971]
$t_{1/2,G}$	0.083-0.5	0.333	0.333	[Fries et al., 1984; Lodish, 1988]
$t_{1/2}$	2-14	9	6	[Wallach and Laskov, 1980]
$m_{H,0}$	2×10^4-4×10^4	2×10^4	2×10^4	[Potter, 1972; Wallach and Laskov, 1980]
$m_{L,0}$	3×10^4-6×10^4	3×10^4	3×10^4	[Bibila, 1991]
$[H]_0$	4×10^7 - 4×10^9	4×10^8	4×10^8	[Bibila, 1991]
$[L]_0$	6×10^7 - 6×10^9	6×10^8	6×10^8	[Bibila, 1991]

Table A.2. Antibody formation and transport parameters for the hybrid model under normal and hyperosmotic conditions.

Appendix B

Derivation of Mathematical Expression for Estimation of IgG Polypeptide Specific Translation Rates

The rate of accumulation of total intracellular heavy chain concentration is given by the sum of the rate of accumulation of all heavy chain-containing species:

$$\frac{d[H]_{total}}{dt} = \frac{d[H]}{dt} + \frac{d[HL]}{dt} + 2\frac{d[H_2L_2]_{ER}}{dt} + 2\frac{d[H_2L_2]_G}{dt} \quad \text{(D.1)}$$

Individual rates of accumulations of the right-sided terms in equation (D.1) are given below:

$$\frac{d[H]}{dt} = T_H m_H - \mu[H] - R_H \quad \text{(D.2)}$$

$$\frac{d[HL]}{dt} = R_{HL} - 2R_{Ab} - \mu[HL] \quad \text{(D.3)}$$

$$\frac{d[H_2L_2]_{ER}}{dt} = R_{Ab} - k_{ER}[H_2L_2]_{ER} - \mu[H_2L_2]_{ER} \quad \text{(D.4)}$$

$$\frac{d[H_2L_2]_G}{dt} = k_{ER}[H_2L_2]_{ER} - k_G[H_2L_2]_G - \mu[H_2L_2]_G \quad \text{(D.5)}$$

Additionally,

$$R_H = R_L = R_{HL} \quad \text{(D.6)}$$

Substituting the individual accumulation rates from equations (D.2) to (D.5) into equation (D.1) and rearranging, we obtain:

$$\frac{d[H]_{total}}{dt} = T_H m_H - \mu\{[H]+[HL]+2[H_2L_2]_{ER}+2[H_2L_2]_G\} - 2k_G[H_2L_2]_G \quad \text{(D.7)}$$

The total heavy chain concentration, $[H]_{total}$, is given by:

$$[H]_{total} = [H]+[HL]+2[H_2L_2]_{ER}+2[H_2L_2]_G \quad \text{(D.8)}$$

In addition,

$$k_G[H_2L_2]_G = \frac{1}{X_V}\frac{d[H_2L_2]_{ECM}}{dt} \quad \text{(D.9)}$$

where

$$\frac{d[H_2L_2]_{ECM}}{dt} = X_V q_{Ab} \quad \text{(D.10)}$$

Therefore,

$$k_G[H_2L_2]_G = q_{Ab} \quad \text{(D.11)}$$

Substituting equations D.8 and D.11 into equation D.7, the following expression is obtained:

$$\frac{d[H]_{total}}{dt} = T_H m_H - \mu[H]_{total} - 2q_{Ab} \quad \text{(D.12)}$$

Finally, the specific translation rate of heavy chains, T_H, can be estimated by rearranging equation D.12:

$$T_H = \frac{1}{m_H}\left(\frac{d[H]_{total}}{dt} + \mu[H]_{total} + 2q_{Ab}\right) \quad \text{(D.13)}$$

A similar expression for the light chain specific translation rate is obtained using the above derivation.